Progress in Energy and Combustion Science 97 (2023) 101072

Contents lists available at ScienceDirect

Progress in Energy and Combustion Science

journal homepage: www.elsevier.com/locate/pecs

A review of solar hybrid photovoltaic-thermal (PV-T) collectors and systems

María Herrando [a,b], Kai Wang [c], Gan Huang [b,d], Todd Otanicar [e], Osama Bany Mousa [f], Rafaela A. Agathokleous [g], Yulong Ding [h], Soteris Kalogirou [g], Ned Ekins-Daukes [i], Robert A. Taylor [f], Christos N. Markides [b,*]

[a] Fluid Dynamics Technology Group, I3A, University of Zaragoza, Zaragoza, 50007, Spain
[b] Clean Energy Processes (CEP) Laboratory, Department of Chemical Engineering, Imperial College London, South Kensington Campus, London, SW7 2AZ, UK
[c] Institute of Refrigeration and Cryogenics, Key Laboratory of Refrigeration and Cryogenic Technology of Zhejiang Province, Zhejiang University, Hangzhou, 310027, China
[d] Institute of Microstructure Technology, Karlsruhe Institute of Technology, Karlsruhe, Germany
[e] Department of Mechanical and Biomedical Engineering, Boise State University, Boise, USA
[f] School of Mechanical and Manufacturing Engineering, University of New South Wales, Sydney, NSW, Australia
[g] Department of Mechanical Engineering and Materials Science and Engineering, Cyprus University of Technology, Limassol, Cyprus
[h] Birmingham Centre for Energy Storage & School of Chemical Engineering, University of Birmingham, Birmingham, UK
[i] School of Photovoltaic & Renewable Energy Engineering, University of New South Wales, Sydney, NSW, Australia

A B S T R A C T

In this paper, we provide a comprehensive overview of the state-of-the-art in hybrid PV-T collectors and the wider systems within which they can be implemented, and assess the worldwide energy and carbon mitigation potential of these systems. We cover both experimental and computational studies, identify opportunities for performance enhancement, pathways for collector innovation, and implications of their wider deployment at the solar-generation system level. First, we classify and review the main types of PV-T collectors, including air-based, liquid-based, dual air–water, heat-pipe, building integrated and concentrated PV-T collectors. This is followed by a presentation of performance enhancement opportunities and pathways for collector innovation. Here, we address state-of-the-art design modifications, next-generation PV cell technologies, selective coatings, spectral splitting and nanofluids. Beyond this, we address wider PV-T systems and their applications, comprising a thorough review of solar combined heat and power (S–CHP), solar cooling, solar combined cooling, heat and power (S–CCHP), solar desalination, solar drying and solar for hydrogen production systems. This includes a specific review of potential performance and cost improvements and opportunities at the solar-generation system level in thermal energy storage, control and demand-side management. Subsequently, a set of the most promising PV-T systems is assessed to analyse their carbon mitigation potential and how this technology might fit within pathways for global decarbonization. It is estimated that the REmap baseline emission curve can be reduced by more than 16% in 2030 if the uptake of solar PV-T technologies can be promoted. Finally, the review turns to a critical examination of key challenges for the adoption of PV-T technology and recommendations.

1. Background and introduction

1.1. Context and motivation

The interest in and demand for alternative energy from renewable sources has continued to rise globally in recent decades, promoted by an increase in environmental awareness and the growing importance placed on sustainability, reducing energy consumption and the associated emissions and pollution. In 1992, the Rio Convention on Climate Change [1] established a framework for actions aimed at reducing fossil-fuel consumption and limiting the associated emissions. In 2015, over 190 countries signed a legally-binding agreement at the Paris Climate Conference [2] to keep the rise in the average global temperature below 2 °C (above 20th-century pre-industrial levels) [3]. To achieve this challenging target, a fundamental transformation of the global energy system is required, which has in fact been taking place in recent decades [4].

Renewable energy systems have been the main drivers and will continue to be essential for this transformation as they contribute to all objectives: promoting the security of supply while lowering energy costs, reducing emissions while driving growth and generating jobs through industrial development. A record 200 GW of renewable energy capacity was added in 2019. Renewable energy accounted for 27% of global electricity use and over 18% of the world's total energy consumption according to the latest REN21 report [5]. Solar energy remains

* Corresponding author.
E-mail address: c.markides@imperial.ac.uk (C.N. Markides).

https://doi.org/10.1016/j.pecs.2023.101072
Received 30 August 2021; Received in revised form 29 November 2022; Accepted 1 January 2023
Available online 12 April 2023
0360-1285/© 2023 The Authors. Published by Elsevier Ltd. This is an open access article under the CC BY license (http://creativecommons.org/licenses/by/4.0/).

Nomenclature

a-Si	amorphous silicon
AHP	analytic hierarchy process
ANN	artificial neural network
ASHP	air-source heat pump
AZO	aluminium zinc oxide
BIPV	building-integrated PV
BIPV-T	building-integrated PV-T
c-Si	monocrystalline silicon
CCHP	combined cooling, heat and power
CIGS	copper indium gallium selenide
CHP	combined heat and power
COP	coefficient of performance
CPC	compound parabolic collector
CPV	concentrated PV
CPV-T	concentrated PV-T
CSP	concentrated solar power
D	pipe diameter
DASC	direct absorption solar collector
DCMD	direct contact membrane distillation
DEC	desiccant cooling systems
DHW	domestic hot water
DNI	direct normal incident radiation
DSM	demand-side management
DX	direct expansion
E_g	band-gap energy
E_{th}	threshold for the onset of absorption
ETC	evacuated-tube collector
FF	fill factor
FPC	flat-plate collector
G	solar irradiance
GHI	global horizontal irradiation
GNP	graphene nanoplatelets
HCE	heat collection element
HDH	humidification-dehumidification
HP	heat pump
HVAC	heating cooling and air conditioning
I	electric current
IEA	international energy agency
ITO	indium tin oxide
IR	infrared
IX	indirect expansion
J_{01}	diode saturation current density
J_{sc}	cell short-circuit current density
k	Boltzmann constant
KPI	key performance indicator
LCA	life cycle assessment
LHS	latent heat storage
MD	membrane distillation
MED	multi-effect distillation
MWCNT	multi-walled carbon nanotube
NDC	national determined contribution
NePCM	nano-enhanced PCM
NSGA-II	non-dominated sorting genetic algorithm
O&M	operation and maintenance
ORC	organic Rankine cycle
PC	polycarbonate
PCM	phase-change material
pc-Si	polycrystalline silicon
PEM	proton exchange membrane
PMMA	poly(methyl methacrylate)
PTC	parabolic-trough collector
PV	photovoltaic
PV-T	PV-thermal
q	electric charge
REmap	renewable energy roadmap
RES	renewable energy systems
rev	reversible
RO	reverse osmosis
SAHP	solar assisted heat pump
SBS	spectral beam splitting
SH	space heating
SHC	solar heating and cooling
SHJ	silicon heterojunction
ST	solar thermal
SHS	sensible heat storage
T	temperature
TCOs	transparent conducting oxides
TCS	thermochemical storage
TES	thermal energy storage
TIM	transparent insulation material
TOPSIS	technique for order preference by similarity to ideal solution
TRL	technology readiness level
TW	Trombe wall
UFH	underfloor heating
USD	US dollar
UV	ultraviolet
V	voltage
V_{oc}	open-circuit voltage
W	distance between the pipes
W/D	width to pipe-diameter ratio
W&ASHP	water & air-source heat pump
WSHP	water-source heat pump

a small fraction of this total (below 2%) despite its fast growth compared to other renewable sources (solar thermal (ST) systems: 8% per year, photovoltaic (PV) systems: 37% per year, both on average since 2010 [6]). This growth has been made possible by the implementation of national policies that have supported renewable projects in Europe, and by the Chinese policy of subsidies for PV systems [5,7]. In 2019, the renewable energy sector employed 11.5 million people, among these 4.6 million were employed in the solar sector [8].

Solar energy is an abundant primary-energy resource, which can be exploited in cost-competitive and reliable ways for electrical power generation, either with PV technology or thermodynamic cycles in concentrated solar power (CSP) systems, as well as for heating or cooling purposes through ST systems. Some of the advantages of this renewable resource compared to others, e.g., wind, are its larger predictability on an annual basis and daily [9], the low degradation rate of the components of a solar installation during its lifetime which is generally 20–25 years [10,11], and that this technology rarely underperforms or fails. For example, long-term field data show that PV panels experience, on average, a power output loss of only 0.5% per year [12], and only 2% of the PV panels installed do not meet the manufacturer's warranty after 10 years [13].

The total worldwide power generation capacity of installed PV panels increased by 12% in 2019 and reached a record of 630 GW in total, while the thermal energy generation capacity of installed ST collectors amounted to 480 GW (thermal Watt) in 2019, with China accounting for almost 70% of the total solar thermal capacity [6,14], which corresponds to savings of about 140 million tons of CO_2 per year [6]. The PV market is driven by China, Japan and the US, and several

countries in Europe have an installed capacity that covers above 8% of the total demand (Italy 9%, Greece 8% and Germany 8%) [5], as a result of the strong incentives for solar electricity adopted in the recent years. As a consequence of this growth, the cost of PV panels has been falling, reaching an average selling price of PV panels of 0.38 USD/W_p (rated Watt peak) in 2019 [15,16], and it is becoming apparent that solar PV technologies will soon become one of the lowest-cost options for electricity generation. This technology has the potential not only of providing on-grid power, displacing fossil fuel consumption, but also PV panels can provide electrification in remote rural areas, particularly in developing countries, where there is no or limited access to the electricity grid. By the end of 2019, around 9.5 thousand mini-grids systems entirely or partly based on renewables were in operation together with small-scaled distributed standalone systems [17]. For instance, in China small-scale standalone PV systems substantially contributed to the progressive electrification of areas not yet interconnected to the main electricity grid [7].

The solar heat market represents a notable share of the global heating market, mainly in providing space heating (SH) and domestic hot water (DHW) [11]. Small-scale thermosiphon systems, which account for 60% of current ST systems, are facing market pressure from heat pumps (HPs) and PV systems. The global capacity of ST decreased by 6% in 2019 compared to 2018, driven by a market slowdown in China (new collector installations in China decreased by 8%) [6]. However, the number of large-scale (megawatt-scale) ST systems for industrial applications and district heating still keeps consistently growing in recent years. For example, the market of Denmark increased by 170% in 2019 owing to several newly installed large-scale solar thermal systems [6]. Compared to the PV market, the installation of ST systems in the EU has not experienced the same growth. For example, approximately 50 GW of PV panels and 15 GW of ST collectors were installed in Germany by 2019 [18]. This trend is attributed to the lack of incentives, financial support, education and knowledge [11]. The experience gained from ST installations in countries such as Cyprus, Greece and Austria, indicates the great potential of such systems for utilizing solar energy, and that this potential is still far from having been exploited.

Therefore, there is potential for the development and wider use of solar systems as they can help in the transformation of the worldwide energy system [19]. However, further investment in existing as well as in future solar technologies is necessary to reduce the costs and make these systems cost-competitive, as well as to ensure appropriate infrastructure [20,21], along with increased public awareness and support.

If solar generation should be deployed in a distributed nature, particularly in urban environments, then the amount of suitable space for solar installations will become increasingly scarce [22]. Therefore, to be competitive, the cost per unit of energy from solar technologies should be low and the energy generated per m^2 should be maximized. PV systems are widely used and there is a broad commercial offer available in the market. However, the limited conversion efficiency, the high PV cell temperature that can be reached, which damage the PV cells, and dust accumulation, are some of the barriers that hinder their potential. In an attempt to regulate the PV cell temperature, there has been important research in the last decades in the assessment of different cooling techniques [23]. This research gave rise to hybrid PV-thermal (PV-T) collectors, which generate both electricity and useful thermal energy from the same aperture area, and with overall (electrical + thermal) efficiencies that are much higher (reaching >70%) than separate standalone systems.

PV-T collectors can easily be integrated with other system components (energy conversion, energy storage, etc.) to provide both thermal and electrical energy outputs. For example, PV-T collectors can be easily integrated with economical hot water tanks for thermal storage, and with batteries for electricity storage. Thus, this technology appears as a particularly promising alternative, especially within a high-penetration scenario, and particularly in applications such as in the urban environment, where there are both thermal and electrical energy demands and the efficient use of limited space is essential. PV-T collectors can also be integrated with other types of solar collectors (i.e., PV panels or ST collectors) to adjust the ratio of heating and electricity supply, to meet specific demands [24]. The relevance and potential of PV-T collectors and their integration with other components to obtain new solutions in HVAC systems were underpinned by Task 60 "*Application of PV-T Collectors and New Solutions in HVAC Systems*", which run from 2018 to 2020, in the solar heating and cooling (SHC) Programme of the International Energy Agency (IEA) [25].

1.2. Physical considerations of PV-T collectors

The initial motivation for the development of PV-T technology was the possibility of using a heat transfer fluid to cool the PV cells in such collectors. However, the delivery of a thermal output at a useful (high enough) temperature [26] leads inevitably to a conflict in the design and operation of conventional PV-T collectors, as these can be operated at temperatures higher than those of PV panels in the same conditions. When the priority is electricity generation, the heat transfer circuit is kept at a low temperature to avoid an otherwise undesirable decrease in the electrical efficiency of the PV cells. This constraint limits the use of the thermal energy generated. Therefore, a trade-off is needed depending on the specific application and the environmental conditions [27]. This introduces challenges for the design and operation of PV-T collectors, and solutions to overcome this conflict have been proposed, e.g., through spectral splitting, amongst others, presented in Section 3.

The two main types of solar PV cell technologies considered for use in PV-T collectors are either based on crystalline silicon wafers or thin-film semiconductor materials deposited onto a glass or metal foil [28]. For a PV-T collector, the first significant difference is the fact that a c-Si PV panel is composed of a mosaic of discrete cells made from wafers whereas a thin-film module is made by patterning a large area of the semiconductor film. Superficially thin-film photovoltaics appears to lend themselves to PV-T collectors since, in principle, the PV cell could be deposited directly upon a thermally conductive heat exchanger. However, since silicon solar cells are manufactured as standard units that can be used interchangeably in regular PV panels and PV-T collectors, it is presently easier and cheaper to laminate c-Si cells to a heat sink rather than develop a bespoke process for depositing and patterning thin-film materials. This point becomes apparent when we consider the fabrication steps involved with each technology. In the case of c-Si, the process starts with processes developed for microelectronics to fabricate silicon wafers which are then processed into solar cells and then assembled into modules, usually by connecting the cells in series-connected strings, illustrated in Fig. 1(a). For a thin-film module, the process starts with the deposition of material onto a substrate (glass, metal foil, or polymer) which is then patterned using a laser to produce small strips of the active area, shown in Fig. 1(b). The patterning is necessary since the current density arising from a typical PV material is of the order 300 A m^2. The issue does not arise in silicon modules since the series-connected silicon cells naturally divide this large current density by a factor of ~30.

The spectral breath of sunlight places firm boundaries around the efficiency of PV power conversion but many of the losses in a standard PV cell can be recovered as thermal energy in a PV-T system. To indicate how much thermal and electrical energy is available we develop a simple model to quantify the losses.

Sunlight spans photon energies ranging from 0.4 to 4 eV and is plotted as a spectral flux b(E) in Fig. 2(a). An ideal semiconductor absorber with a band-gap E_g will selectively absorb sunlight with photon energies above that band-gap energy thereby promoting an electron from the valance band to the conduction band (Process 1 in Fig. 2 (b))

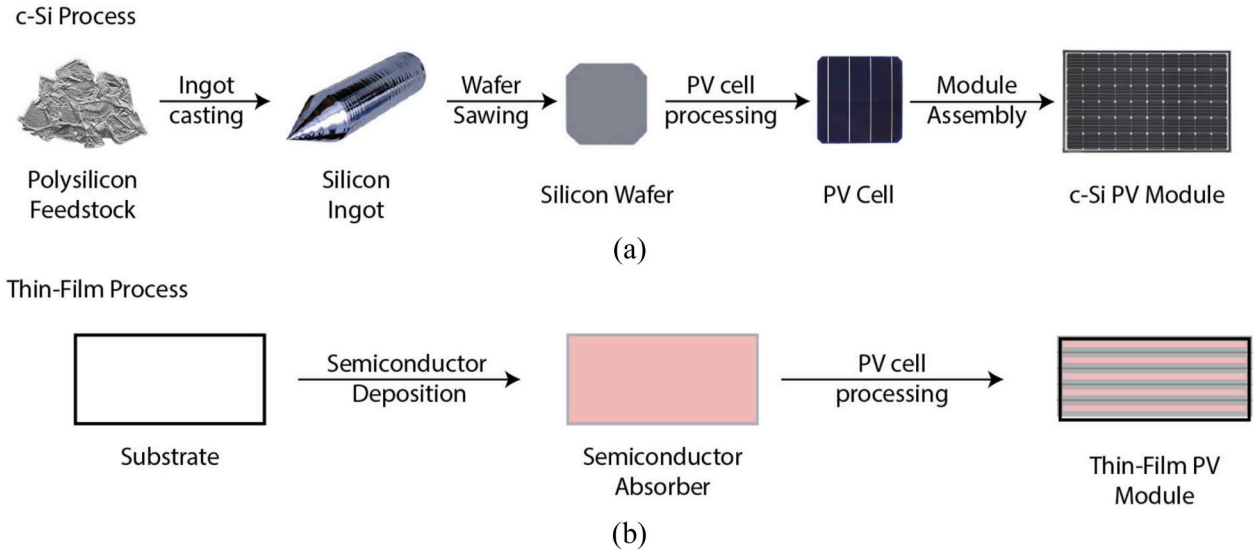


Fig. 1. Schematic diagrams showing the difference in fabrication processes for: (a) crystalline silicon solar cell; and (b) thin-film solar cell.

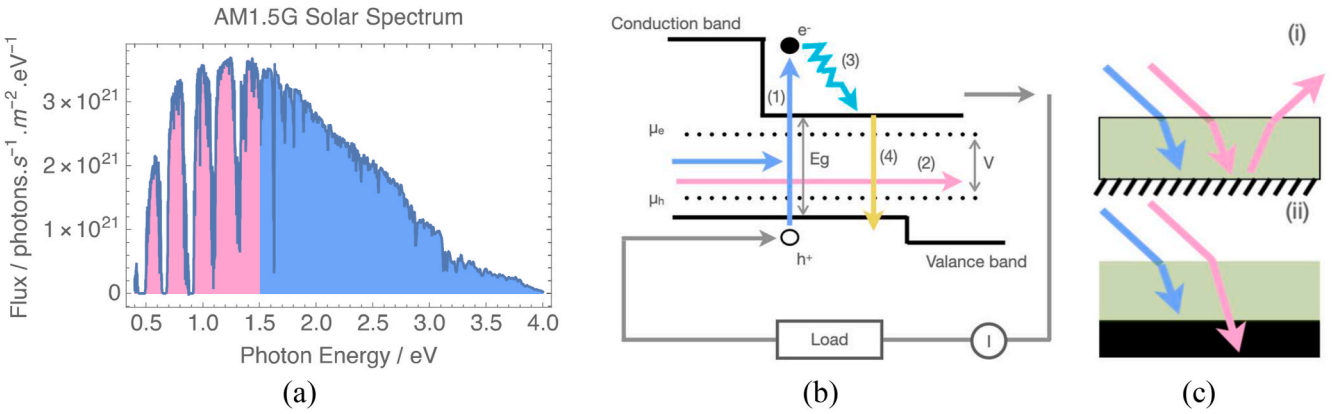


Fig. 2. (a) AM1.5G solar spectral flux b(E) plotted as a function of photon energy with an illustrative band-gap energy of 1.5 eV. (b) Schematic of a single junction solar cell of band-gap E_g showing four fundamental processes: (1) absorption of light above the band-gap energy (E_g); (2) transmission of light below the band-gap energy; (3) thermalization of excess energy; and (4) radiative recombination. (c) Two configurations for a PV device: (i) semiconductor absorber with rear mirror; and (ii) semiconductor absorber with the rear absorber.

while light below the band-gap energy will pass unabsorbed through the solar (Process 2 in Fig. 2(b)). For simplicity, in the example shown in Fig. 2(b) the excess photon energy (E_g) is imparted to the excited electron[1] that rapidly dissipates this energy through a thermalization process (Process 3 in Fig. 2(b)) to establish a thermal population of excited electrons. The occupation of electrons in the conduction band can be described by a quasi-Fermi level denoted by μc and a similar quasi-Fermi level denoted by μv for the holes. The separation of these quasi-Fermi levels results in the voltage (V) at the solar cell terminals which in turn drives current (I) through a load in the external circuit.

Two limiting cases for the solar cell configuration are shown in Fig. 2(c), in both cases the PV active photons are illustrated by the blue arrow while the pink arrow indicates sub-band-gap photons that are not absorbed by the semiconductor material. Most non-silicon solar cells correspond to Fig. 2(c–i) where the unabsorbed low-energy photons are reflected from the rear surface and leave the solar cell. Fig. 2(c-ii) shows a configuration where low-energy photons are absorbed by a separate thermal absorber. Uniquely silicon solar cells correspond to Fig. 2(c-ii) where the absorptivity of the solar cell is close to unity from UV through to the mid-IR hence completely extinguishing the solar [29,30].

Only the radiative recombination loss (Process 4 in Fig. 2(b)) is irrecoverable in a PV-T system. However, even in the radiative limit, it is a comparatively small fraction of the overall solar cell power-loss when operating at the maximum power-point [31]. Furthermore, in almost all solar cell semiconductor materials, parasitic non-radiative processes that operate in parallel to the radiative loss tend to be orders of magnitude larger, hence for a practical PV-T system recombination losses can be assumed to generate heat, rather than light. In the solar cell configuration shown in Fig. 2(c–i) the energy associated with the below-E_g loss (Process 2 in Fig. 2(b)) is lost from the solar cell however in the solar cell configuration shown in Fig. 2(c-ii), it results in the full absorption of the solar flux.

To illustrate the behaviour of two different solar cell types, we consider the limiting cases of silicon (E_g = 1.12 eV) and CdTe (E_g = 1.5eV) that correspond to the top-two solar cell terrestrial solar cell technologies manufactured by the capacity to date [32].

A simple model for the current (I) voltage (V) characteristic of a PV cell is:

$$I(V) = J_{sc}(E_g) - J_{01}\left(e^{\frac{qV}{kT}} - 1\right) \quad (1.1)$$

[1] This will arise if the effective mass of the electron is much smaller than that of the hole, a condition that is common in PV semiconductor materials.

where J_{sc} is the cell short-circuit current density, J_{01} is the diode saturation current density, q is the electronic charge and k is Boltzmann's constant. Assuming full absorption to the band-gap energy E_g and in the absence of reflectivity losses, the upper limit to the solar cell short-circuit current is given by:

$$J_{sc}(E_g) = q \int_{E_g}^{\infty} b(E)\mathrm{d}E \tag{1.2}$$

The thermal generation in a PV cell can be approximated by:

$$Q(V) = \int_{E_{th}}^{\infty} E\, b(E)\mathrm{d}E - V\, I(V) \tag{1.3}$$

where E_{th} is the threshold for the onset of absorption in the PV-T collector.

Taking illustrative examples of a CdTe solar cell ($E_{th} = E_g = 1.5$ eV, $J_{01} = 5.54 \times 10^{-13}$ A m^{-2}) and silicon solar cell ($E_{th} = 0$ eV, $E_g = 1.1$ eV, $J_{01} = 7.64 \times 10^{-10}$ A m^{-2}), the current–voltage characteristics, electrical power and thermal generation are plotted in Fig. 3.

The electricity generation potential of the PV cells is typically the primary energy output of PV-T collectors. In the two examples here, the IV characteristics of silicon and CdTe cells are broadly determined by their band-gap energy. The lower band-gap of silicon provides a larger current but smaller voltage compared to CdTe. The optimum band-gap energy for electrical power conversion is approximately 1.3 eV, which is between the band-gaps of CdTe and silicon [31]. The electrical power delivered by the two cells is broadly similar but the maximum power point for the CdTe cell sits at a higher voltage than the silicon.

All PV cell parameters are dependent upon temperature, hence the power that is delivered by a PV device is:

$$P(T) = V_{oc}(T)\, J_{sc}(T)\, FF(T) \tag{1.4}$$

The temperature coefficient of power (β_{Pmax}) is composed of the sum of three different coefficients:

$$\beta_{Pmax} = \beta_{Voc} + \beta_{Jsc} + \beta_{FF} \tag{1.5}$$

Of these temperature coefficients, the voltage coefficient (β_{Voc}) dominates the power loss with increasing temperature, owing to an increase in internal recombination rate with temperature. The temperature coefficient is weakly positive since the thermal expansion of the semiconductor lattice leads to a reduction in the electronic band-gap and hence marginally higher absorbed photon flux. The fill factor (*FF*) also has a weak dependence on temperature.

The temperature dependency of the fill factor depends largely on the cell voltage and any temperature dependency of series resistance R_s:

$$\frac{1}{FF}\frac{\mathrm{d}FF}{\mathrm{d}T} = (1 - 1.02FF_0)\left(\frac{1}{V_{oc}}\frac{\mathrm{d}V_{oc}}{\mathrm{d}T} - \frac{1}{T}\right) - \frac{R_s}{V_{oc}/I_{sc} - R_s}\left(\frac{1}{R_s}\frac{\mathrm{d}R_s}{\mathrm{d}T}\right) \tag{1.6}$$

In turn, the temperature dependency of voltage depends on the band-gap energy, the V_{oc} and an empirical parameter γ that accounts for the recombination mechanisms present in the solar cell [33]:

$$\frac{\mathrm{d}V_{oc}}{\mathrm{d}T} = -\frac{\frac{E_g}{q} - V_{oc} + \gamma\frac{kT}{q}}{T} \tag{1.7}$$

Overall, this gives a strong temperature coefficient dependency with band-gap energy (E_g). Cells with low band-gaps, such as Ge have large, negative temperature coefficients power, with silicon and other conventional PV materials having correspondingly smaller temperature coefficients. Therefore, from the perspective of achieving the smallest temperature coefficient, it is desirable to use a high-band-gap semiconductor. Since a high band-gap will leave many photons unabsorbed, these could be used in a thermal collector. It is also worth noting that in Eq. (1.6), the V_{oc} itself also affects the temperature coefficient.

From a wider PV-T perspective, however, the thermal generation potential of these collectors when using different solar cell technologies will also be of interest and this can be substantially different (refer back to Fig. 3(c) for the two cell types considered above). Under short-circuit and open-circuit, no electrical power is delivered, but since the silicon solar cell absorbs the full solar spectrum, the thermal generation equates to the incident solar energy. The CdTe device only absorbs light above the band-gap energy, giving substantially lower thermal generation. At the maximum power point, the thermal generation reaches a minimum, yet the silicon cell still delivers 750 W/m^2 at maximum power, while the CdTe cell only reaches 400 W/m^2. We will return to the current electrical and thermal performance of different PV-T collectors in Section 2 and the potential for improvement in Section 3.

1.3. Previous reviews

Almost all previous review papers on PV-T technology focussed on this technology at the collector level, reviewing various design and geometrical configurations based on different thermal management concepts. Older reviews focussed on air- or liquid-based PV-T collectors [34–36], while more recent ones also include concentrated PV-T (CPV-T) collectors [37], heat-pipe PV-T collectors [23,38–40], phase-change material (PCM)-based PV-T collectors [23,28,38–41], dual air–water PV-T and PV-T collectors with nanofluids [38,39,42,43]. Some of them review alternative structural designs [23,35,42,44], while others analyse the PV-T layers [44], and parameters that affect the performance of flat-plate PV-T collectors [45]. Other reviews analysed previous studies that discussed the design and cooling considerations aimed at improved collector performance [46], or reviewed studies that included environmental issues about PV-T systems [40] and analysed factors that affect PV-T collectors from an environmental point of view [47]. Others also include a review of the progress on practical PV-T applications [28,37,41], analysing the limitations and advantages of PV-T collectors [28]. Meanwhile, other reviews specifically focussed on liquid-based PV-T collectors [48], reviewing previous experimental and simulation studies of refrigerant-based and water-based PV-T collectors.

There are several reviews of solar cooling systems, mostly focussed

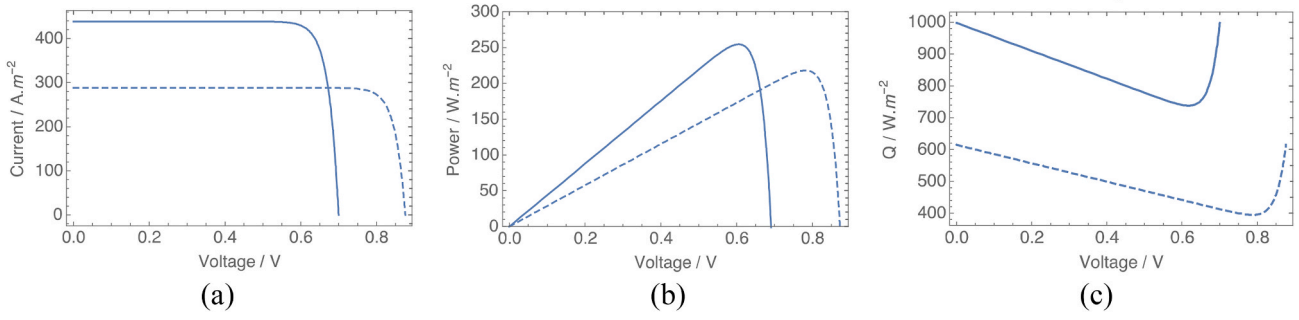


Fig. 3. Characteristic performance of solar cells made from silicon solar cell (solid line) and CdTe solar cell (dashed line) showing: (a) the IV characteristics; (b) electrical power; and (c) thermal generation.

on the integration of ST collectors, including flat-plate collectors (FPCs), evacuated-tube collectors (ETCs) and parabolic-trough collectors (PTCs), with thermally-driven cooling technologies, including ab/adsorption [49–59], desiccant [53–56,59], ejector/Rankine [54,55,59,60] or Stirling [59] systems. Some reviews also address PV panels integrated with HPs [49,51,53,55,59], Stirling or thermoelectric [59] systems, while a previous review of solar systems integrated with absorption HPs [57] includes a section on PV-T systems, but as a separate system from the HP (see Table 1).

Two recent reviews on solar heating and cooling (SHC) technologies report several alternatives for solar heating or cooling, without addressing combined heating and cooling technologies. One review focusses on solar thermal based on FPC/ETC or solar air collectors, or alternatively PV panels; air-based PV-T and water-based PV-T systems are briefly discussed as solar heating systems [61]. The second review covers solar thermal and electrical systems, electrical and thermal storage options, heat pumps and solar cooling alternatives, without specifically addressing PV-T collectors, but mentioning previous PV-T studies [62].

We have found very few review papers that specifically address PV-T collectors and wider systems for heating and/or cooling applications [63–65] (see Table 1). Amongst these, Guo et al. [63] focusses on PV-T façade and solar thermal (air/water) desiccant systems for cooling and dehumidification, while Alobaid et al. [64] review current developments of PV-T collectors integrated with absorption cooling systems. A recent paper [69] briefly reviews SHC systems by absorption and adsorption systems driven by solar thermal (FPC/ETC/PFC) or PV-T/CPV-T collectors, focussing on the modelling and simulation of polygeneration systems based con PV-T/CPV-T collectors for the provision of cooling, heating and power to buildings. Other studies review the integration of ST and PV-T collectors with solar assisted heat pumps (SAHP) for heating purposes [65–68], (a) analysing and comparing previous studies of PV, ST or PV-T collectors integrated air-source HPs [66], (b) reviewing mathematical models for SAHP systems and performance enhancements [67], or (c) specifically focussing on reviewing the performance, component details and of research progress of PV-T-SAHP systems [68,70]. However, none of the above [65–68] is specifically focussed on PV-T collectors, and none of them addresses other applications such as solar cooling, desalination, drying or hydrogen production.

Table 1
Summary of previous reviews.

		Ref.
Reviews at the PV-T collector level	Air-based	[23,28,34,35,38–43]
	Liquid-based	[23,28,43,48,34–36,38–42]
	CPV-T collectors	[37,43]
	Heat-pipe	[23,38–41]
	PCM-based	[23,28,38–41]
	Dual air–water	[38,39,42,43]
	Nanofluids	[38,39,42,43]
Review of PV-T structural designs		[23,35,37,42,44]
Review of PV-T concept, layers, parameters, modelling equations		[28,39,41,44–46]
Review of PV-T environmental issues		[40,47]
Review of practical PV-T applications		[28,37,41,43]
Reviews at the system level (heating and/or cooling applications)	PV-T façade and ST for cooling and dehumidification	[63]
	PV-T collectors + absorption cooling systems	[64]
	PV-T/CPV-T collectors + SAHP for heating	[65–68]
Solar cooling systems (not PV-T collectors)	Absorption/adsorption	[49–59]
	Desiccant	[53–56,59]
	Ejector/Rankine	[54,55,59,60]
	Stirling	[59]
PV panels integrated with HPs		[49,51,53,55,59]

1.4. Aim and contribution

This paper aims to provide a comprehensive overview of the state-of-the-art in PV-T collectors and of the wider solar-energy systems within which they can be implemented, and also to assess the local (at the end-user/building level) and worldwide energy and carbon mitigation potential of such systems.

In this review, we cover experimental and computational studies, identify performance enhancement opportunities and innovation pathways and, also, the implications of widespread deployment at the solar-generation system level. Specifically, we first proceed to classify and review the main types of PV-T collectors, including air-based, liquid-based, dual air–water, heat-pipe, building-integrated and CPV-T collectors (Section 2). This is followed by a presentation of techno-economic performance enhancement opportunities and pathways for collector innovation (Section 3). Here, we address state-of-the-art design modifications, next-generation PV cell technologies, selective coatings, spectral splitting and nanofluids. Beyond this, we include content with a particular focus on wider PV-T-based systems and their applications (Section 4), comprising a thorough review of solar combined heat and power (S–CHP), solar cooling, solar combined cooling, heat and power (S–CCHP), solar desalination, solar drying systems, and solar for hydrogen production. This includes a specific review of potential performance and cost improvements and opportunities at the solar-generation system level in thermal energy storage, component integration, control and demand-side management (DSM) (Section 5). Throughout the paper, we review research lines extending, importantly, to research gaps and opportunities to promote the technology readiness levels (TRLs) of important related elements of wider PV-T-based systems. Subsequently, a set of the most promising PV-T systems is assessed in a series of decarbonization scenarios to analyse the carbon mitigation potential of PV-T systems and how this technology could fit in various pathways for global decarbonization (Section 6). Finally, the review will turn to a critical examination of the future of PV-T technology and systems, including challenges, recommendations and main conclusions (Section 7).

2. Solar PV-T collectors

Most of the solar radiation absorbed by a PV cell is converted to heat (in fact, internal energy), increasing the temperature of the cell and decreasing its electrical efficiency [35,71–73]. To overcome this, solar cells can be cooled by a suitable fluid (gas or liquid) flow, decreasing their temperature and improving their efficiency, while producing a useful thermal output. The synergistic combination of the improved electrical output and the associated heat provision potential has motivated the development of hybrid PV-T collectors [35,71–73], which have emerged as holistic solar energy solutions that combine PV cells for electricity generation, coupled with a thermal absorber containing a heat transfer fluid for heat provision from the same collector [71,74–77].

PV-T collectors enable the generation and use of electricity onsite, so-called self-consumption, which is acknowledged as the cheapest way to generate energy with renewables while reducing the stress on the local grid [4,78]. PV-T collectors can be integrated with other technologies such as HPs or cooling systems [64,79], can be used for solar desalination [80,81], solar drying [82,83], or hydrogen production [84,85], and the excess electricity generated can be stored to be used later on [86–90]. Moreover, careful planning of the energy use via DSM is of key importance in the effective operation of the system [86,87], as detailed in Section 5.3.

There are several classifications of hybrid PV-T collectors depending on different factors: (a) the collector cover(s); (b) the type of PV

technology (amorphous silicon, a-Si, monocrystalline silicon, c-Si, polycrystalline Silicon, pc-Si, thin-film, multi-junction cells, etc.); (c) cooling method (active *vs*. passive); (d) the heat extraction medium (gas, liquid, dual, heat-pipe, thermoelectric); or (e) system structure (flat-plate, concentrated, building integrated).

There are different methods to cool the PV panel, and the optimum solution strongly depends on several factors such as the PV technology used, the concentration ratio (if any) and the weather conditions where the system is installed [23]. The two main cooling mechanisms are passive and active cooling. The former refers to technologies that minimize or extract the heat absorbed by the PV panel without additional power consumption. There are different options such as the integration on the rear PV panel surface of fins or other extruded surfaces made of high thermal conductivity metals such as aluminium or copper, to enhance heat transfer to the ambient; the use of PCMs or the use of heat pipes that efficiently transfer the heat through a boiling-condensing process. The main constraint of these alternatives is that the heat dissipation is limited by the contact area between the heat sink and the ambient [23,41].

Alternatively, active cooling systems extract the heat using different cooling fluids driven by fans in case of air or a pump when liquids are used. The cooling medium can be in the liquid or gaseous phase. The most common liquid used in flat-plate PV-T collectors is water or a mixture of water and glycol to avoid freezing. Meanwhile, air-based PV-T collectors provide a simpler solution to cool solar PV cells. For each of these types of PV-T systems, there are several designs of the thermal absorber, as shown in the following sections.

The potential of PV-T systems has been confirmed with simulations in reliable computational environments such as ANSYS Fluent, COMSOL, MATLAB, Modelica, Polysun, TRANSOL, and TRNSYS. However, despite their demonstrated potential, only a modest number of manufacturers are producing PV-T collectors and the market remains small [91,92]. A market survey was undertaken under Task 60 of the International Energy Agency (IEA), with 26 collector manufacturers and suppliers from 11 countries identified. The survey showed that most of the manufacturers focus on liquid-based PV-T collectors (48% uncovered PV-T collectors, 28% covered PV-T collectors, 4% vacuum tube PV-T collectors), while 12% manufacture air-based PV-T collectors and 8% CPV-T collectors [92].

Fig. 4 shows the performance of commercially available PV-T collectors, in terms of both thermal and electrical outputs. Note that the CPV-T options shown are low-concentrating ratios, without tracking. It should be highlighted that a specific norm for testing PV-T collectors is not available currently, so the thermal and electrical outputs are often stated at different conditions, and thus comparisons among different products are not straightforward. The thermal performance of PV-T collectors can be tested according to the standard ISO 9806:2017, but this has several limitations, as it is intended for ST collectors, so the electrical output is not considered. For the PV panel output, there is a standard procedure, following the methodology of the IEC 60904, and usually, this output is provided by the PV panel manufacturer. However, if PV cell performance is not characterized before its integration into a PV-T collector, it should be characterized accordingly when characterizing the PV-T collector, separately from the thermal performance characterization [93].

Fig. 5 shows a map of the same commercially available PV-T collectors in terms of the market price (as of 2020 when this data was collected) *vs*. their estimated thermal and electrical outputs. It is observed that, in general, water-based PV-T collectors have larger outputs (W/m^2) at a lower price (€/m^2).

By the end of 2019, a total PV-T collector area of 1,160,000 m^2 was installed, with a total thermal capacity of around 530 MW and a peak PV power of around 180 MW. In the European market, France is the market leader with an installed collector area of approximately 484,000 m^2, followed by Germany with around 112,000 m^2. Outside of Europe, Korea is the market leader with an installed area of ~280,000 m^2, followed by China with ~133,000 m^2 [6]. From the total installed thermal capacity, 57% corresponds to uncovered water-based PV-T collectors, 41% to air-based PV-T collectors and the remaining 2% to covered water-based PV-T collectors, while vacuum tube PV-T collectors and CPV-T collectors play only a minor role [92].

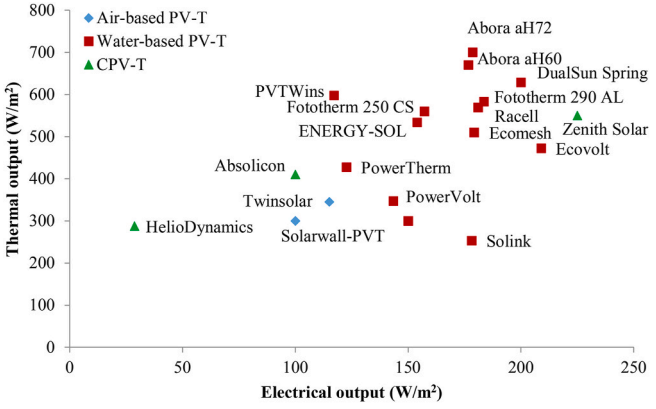


Fig. 4. Performance summary of a range of commercially available hybrid PV-T collectors (for which data was available) in terms of their thermal vs. electrical output (W/m^2), at STC (1000 W/m^2 and 25 °C).

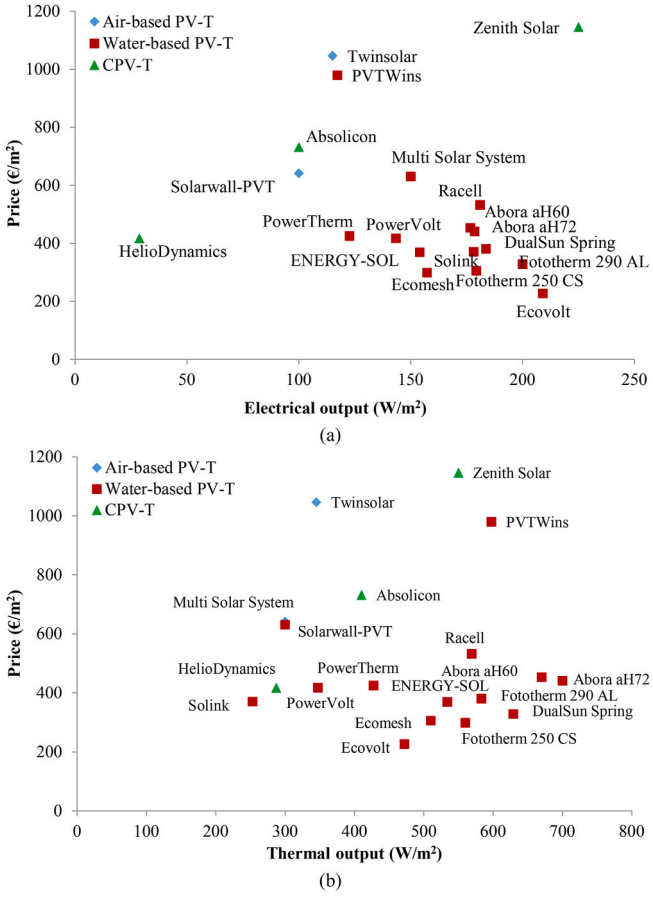


Fig. 5. Summary of a range of commercially available hybrid PV-T collectors (for which data was available), in terms of: (a) thermal; and (b) electrical output, with both plots showing cost (€/m^2) *vs*. output (W/m^2) as of 2020 when this data was collected.

2.1. Air-based PV-T collectors

In air-based PV-T collectors, air is selected as the working (or, heat transfer) fluid, and acts to regulate the temperature of the PV cells. The main applications of this type of collector are for ventilation and space heating, or air-preheating purposes, integrated into roofs and building façades [23,73], or installed as independent components on roofs [34], where the generated hot air can be used for drying, space heating or ventilation.

There are two main types of air-based PV-T collectors, namely flat-plate and CPV-T collectors. Flat-plate collectors are considered the most common and simple design [94]. Air-based PV-T collectors typically have a lower capital cost than liquid-based equivalents and are suitable for building applications in medium- and high-latitude regions. In low-latitude regions, the ambient air temperature during the day is high for almost half of the year, therefore limiting the application of air-based PV-T systems to a shorter period in terms of effective electricity production.

There are different configurations according to several factors. First, these systems can be classified depending on how the air flows through the system. Natural circulation is simpler and has lower costs than forced circulation, while the latter is more efficient. However, the energy necessary to drive fans decreases the net electricity gain of the system in forced circulation systems [71]. While liquid-based PV-T collectors need a restricted passage to allow the liquid flow near the PV cells' back surface (usually a pipe or conduit), the air is allowed to flow both at the back and over the front surfaces of PV cells in air-based PV-T collectors. This can be done with mechanical power, i.e., a fan, or the flow can be naturally driven by buoyancy forces. When air is flowing over the front surface of cells, an extra glazing layer is required to form a passage between the cells and the environment. Although this is beneficial from a thermal performance perspective, it is less effective concerning electrical performance, as it increases the operating PV cell temperature for the same conditions, and imposes an additional reflection loss to the incoming solar radiation.

According to Chow [35], we can discriminate between four main collector types, depending on the air channel configuration, with PV-T collectors having: a channel above the PV cells, a channel below the PV cells, the PV cells between single-pass channels, and double-glass designs (see Fig. 6). The most noticeable difference is the duct that brings the cold (ambient or recirculated) air towards the collector, usually at the bottom of the collector, and the duct that removes the hot air usually from the top of the collector. Sometimes recirculation is used, i.e., the air flows first over the PV cell's top surfaces and then directed underneath them before exiting the collector (Design (d) in Fig. 6). In this case, the inlet and outlet ducts are at the same end of the collector, usually the bottom one, reducing the height of the collector but also causing shading between subsequent rows.

Different conclusions have been drawn, for example, some studies conclude that double-pass designs (Design (d) in Fig. 6) outperform single-pass designs, while others conclude that Design (c) is the least consuming in terms of fan power [35]. Other investigators considered double-glass PV-T collectors [41], or the addition of a suspended metal sheet in the middle of the air channel to improve thermal performance [23].

In the comprehensive review of air-based PV-T systems with and without thermal storage by Tyagi et al. [95], it was concluded that air-based PV-T systems are particularly well-suited to crop drying and electricity production. Additionally, the application of PCMs for thermal storage in PV-T systems was mentioned.

Another review presented a broad classification of PV-T systems, an extensive list of important aspects of these systems together with suggestions for future work needed on the subject [96]. It was stated that air-based PV-T systems are most suitable for space heating applications in cold regions, since the ambient air temperature during the day is low most of the year, therefore eliminating the loss of effective electricity production while taking advantage of the collected heat from the PV-T collector for space heating.

The status and future perspectives of PV-T systems, in particular air-based PV-T systems, have also been reviewed [39,43]. According to Al-Waeli et al. [39], air-based PV-T collectors have general overall efficiencies (electrical plus thermal) ranging from 30% to 60%. Of this total efficiency, the electrical component associated with crystalline silicon PV cells is typically in the range of 15–20% at typical operating temperatures.

A review with attention to different solar cell technologies and recent techniques to improve such systems concluded that PV cells integrated with ST systems are self-sustained and more economical in rural areas [97].

A review focussing on the design of PV-T systems [46] highlighted the importance of nanofluids and nano-PCMs as alternatives or complementary to traditional cooling and storage solutions. From this analysis, it was concluded that cooling both sides of PV cells, with the employment of optical filtration using nanofluids, can result in significant improvements to the performance of a PV-T system. In addition, optimization of the cross-section of cooling channels and the use of honeycombs and nano-PCMs for storage and cooling purposes can provide better distribution of the thermal load. Guidelines for the appropriate selection of the channel depth, air flow rate and air distribution duct diameter optimization in PV-T collectors have also been studied [98].

An extensive study of the air cooling design and performance in a commercial air-based PV-T collector by natural flow is reported in Ref. [99], which suggests optimal configurations for PV-T solar systems. Other authors [100] investigated air-based PV-T collectors through modelling at steady-state conditions, to determine their thermal characteristics. Özakin and Kaya [101] studied an air-cooled channel in an air-based PV-T collector to consider the effects of fins added to the channel and to estimate the exergetic performance of the collector. A similar study [102] presented a combined theoretical and experimental investigation of such collectors. A glazed collector was also tested experimentally by Agrawal and Tiwari [103,104], who estimated a payback period for the system of 1.8 years and 16.5 tons of CO_2 emission avoidance.

The performance of four different air-based PV-T collector configurations with single-pass, double-pass and with glazing was studied by Slimani et al. [105], who concluded that the double-pass collector performs better in terms of overall daily energy generation. According to Hussain et al. [106], further work on efficiency improvements, cost

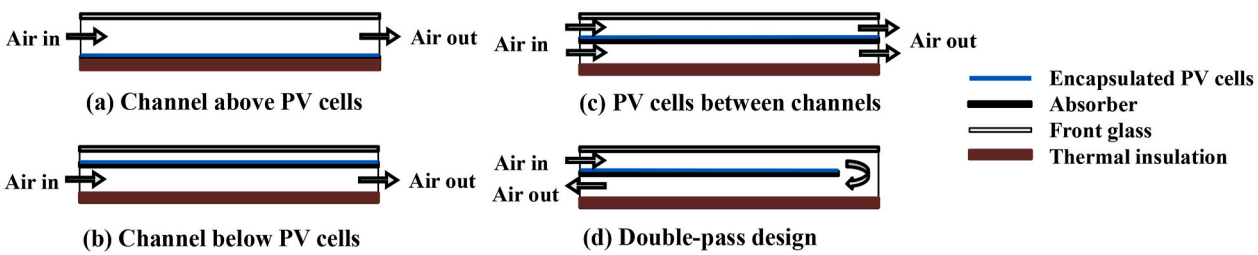


Fig. 6. Longitudinal cross-section of common air-based PV-T collector designs. Figure reproduced from Chow [35] with permission from Elsevier (Copyright 2009 Elsevier).

reductions and building integration of air-based PV-T collectors are necessary for good performance to be attained.

Several researchers have paid attention to various air-channel configurations. A theoretical analysis of air-based PV-T collectors [107] concluded that a glass cover improves the thermal efficiency of the system but reduces the electrical efficiency, in line with other similar work in the literature. It was additionally concluded that the solar radiation intensity, flow rate and channel depth are important parameters that influence the system performance. Another study focussing on the channel configuration with additional fins and metal sheets in the flow channel [99] concluded that the addition of fins and metal sheets in the channel can improve the system performance. Metal sheets in the channel were also investigated by Shahsavar and Ameri [108] (see Table 2).

A transpired collector with a transparent channel for air circulation was tested by Gholampour and Ameri [109]. Experimental validation of a model was performed with CFD modelling in Fluent, obtaining thermal system efficiencies of 45–55%. Other studies have used modelling to investigate the performance of air PV-T systems [100,113,117], or a combination of theoretical analyses, modelling and experimental investigations [113,114].

A summary of the different air-based PV-T collectors is provided in Table 2, addressing previous research on PV-T collectors with and without glazing, different arrangements of air channels, forced circulation by fans, adding fins in the air channel and size of the air channel. It can be concluded that double-pass PV-T collectors outperform single-pass designs, that glazed PV-T collectors have higher overall efficiencies than unglazed collectors, and that the use of metal sheets and fins in the air channel increases the thermal efficiency.

The most common air-based PV-T configurations have a high TRL of 9 (actual system proven in operational environment), with several manufacturers on the market, such as GSE and Sunovate, as detailed in the market survey undertaken under Task 60 of the IEA [25,92]. According to this survey, the French market is dominant, where almost all of the manufactured PV-T collectors are air-based PV-T collectors [92].

Table 2
Summary of research on air-based PV-T collectors.

System description	Location	Nature of work[a]	Thermal efficiency	Electrical efficiency	Ref.
Air-based PV-T collectors with and without glazing	Greece	Exp + Theo	60–70%	12–14%	[71]
Air-based PV-T collectors with flat transpired collector	Iran	Exp + Theo	45–55%	–	[109]
Open loop unglazed air-based PV-T system	Australia	Exp	28–55%	10–12%	[110]
Air-based PV-T collector with a 60-mm air layer and air pipes to collect heated air	South Korea	Exp	22%	15%	[111]
Air-based PV-T collectors with single-pass, double-pass and glazing	Algeria	Theo	44%	11%	[105]
Air-based PV-T collectors with fins and metal sheets in the channel	Greece	Exp + Theo	65%	10–11%	[99]
Glazed air-based PV-T collector	India	Theo	14%	11%	[112]
Air-based PV-T collector with fins	Australia	Exp + Theo	45–63%	8–9%	[113]
Air-based PV-T collector with a thin flat metal sheet suspended in the middle of the air channel	Greece	Exp + Theo	60%	12%	[114]
Air-based PV-T collector with a thin aluminium sheet suspended in the middle of the air channel	Iran	Exp	30–60%	6–9%	[108]
PV-T collector integrated with a glass-to-PV backsheet and glass-to-glass PV	Korea	Theo	48–52%	14%	[115]
Air PV-T collector with V-groove absorber	Germany	Exp + Theo	42%	10%	[116]

[a] Exp = experimental; Theo = theoretical.

2.2. Liquid-based PV-T collectors

Liquid cooling offers a better alternative to air cooling enabling to maintain the desired operating temperature of the PV cells with fewer temperature fluctuations together with more efficient use of the heat extracted, due to the higher thermal conductivity and better heat transfer coefficient [23,35,41,48]. The most common fluid employed is water, or a mixture of water-glycol to avoid freezing [23,37,48], although refrigerants capable to undergo phase change at relatively low temperatures have been used to integrate these collectors with HPs [23,28].

2.2.1. Water-based PV-T collectors

Water-based collectors are considered the most efficient type of PV-T technology for applications where water preheating is required all year long at locations with high solar input and high ambient temperature (low latitudes) [35,48,73,118]. In recent decades, significant research has been undertaken on this type of collector, giving rise to a large number of water-based PV-T system configurations, both in terms of materials and geometries [28,34,35,41,48]. Here it should be noted that this section considers both water and water-glycol mixtures as the heat transfer fluid without a specific differentiation. From the different designs found in literature, the main design concepts are [23,28,34,35,41,48,119] (see Fig. 7):

Copper is the most widely used material for several reasons, including primarily its high thermal conductivity. The most common PV-T collector design comprises a metallic sheet-and-tube absorber adhered to the rear of PV cells in which the liquid is circulated via forced convection through pipes connected in series or parallel (Design (a) in Fig. 7) [23,28,41,121]. Furthermore, the most common collector design features parallel pipes (Fig. 8) with diameters of 6–7 mm [122,123], 8 mm [121,122,124], 10 mm [27,71,125,126], 15 mm [74] (see Table 3); while serpentine arrangements are typically used in refrigerant-based PV-T collectors (see Section 2.2.2). Investigators have analysed serpentine water-based PV-T collectors with tube diameters of 10 mm [127] or 8 mm [128].

Table 3 summarizes the main outcomes of previous research on these types of configurations.

Alternatively, web-flow, direct-flow (also called parallel-pipes) or spiral-flow designs (Fig. 8) made of stainless steel have been also analysed by other authors [119,129]. The results show that, at an outlet temperature of 50–65 °C, the web-flow design performs the worst, with thermal efficiencies from 41% to 48% depending on the flow rate, the direct-flow design performs slightly better (46–54%), while the spiral-flow design performs the best, with thermal efficiencies of 58–68%, and the highest electrical efficiencies (13–14%), due to the lower PV cell temperature [129].

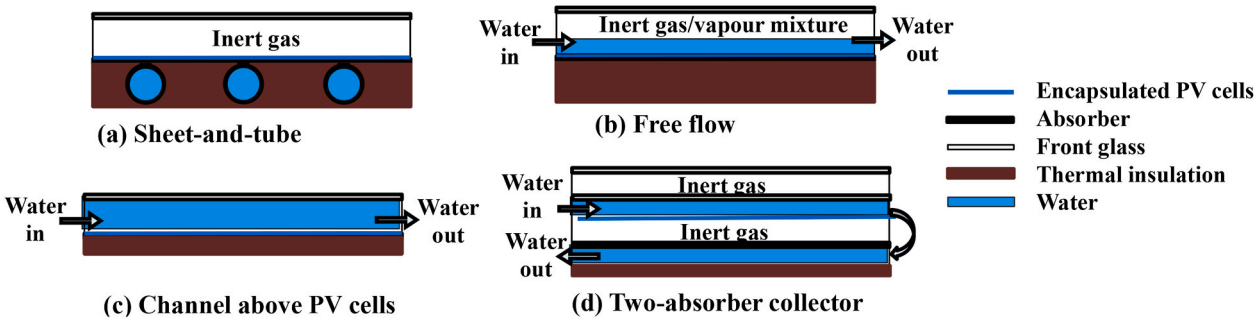


Fig. 7. Cross-section of some common water-based PV-T collector designs [35,36,120]. Figure reproduced from Aste et al. [36] with permission from Elsevier (Copyright 2014 Elsevier).

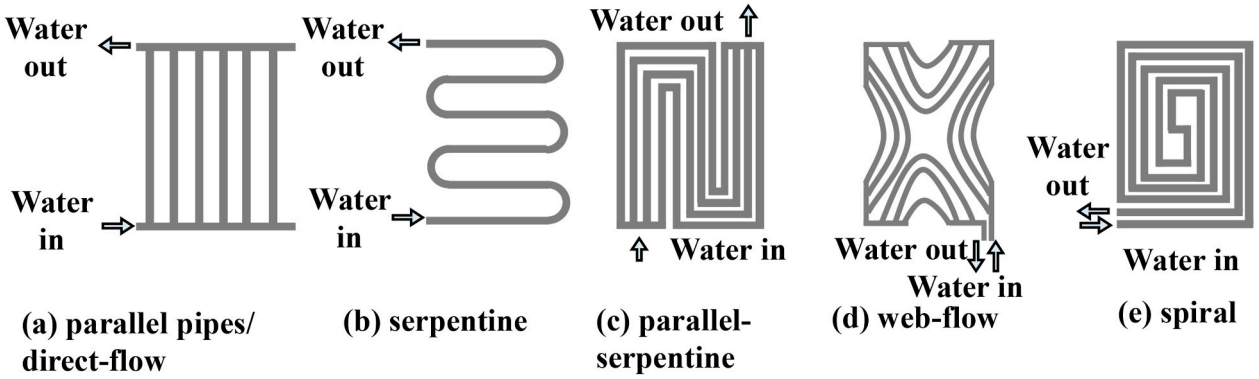


Fig. 8. Common sheet-and-tube cooling circuit designs [119,129].

Table 3
Summary of research work on water-based PV-T collectors.

PV-T design (Fig. 7)	Cooling circuit (Fig. 8)	Material/pipe diameter	Cover	Nature of work[+]	Fluid T_{out}	Thermal efficiency	Electrical efficiency	Ref.
(a)	(a)	Copper/8 mm	Uncovered	Exp	–	32%*	–	[121]
		Copper/8 mm	Single	Exp	–	39%*	–	[121]
		Copper/10 mm	Uncovered	Theo	30 °C	44%	14%	[126]
		Copper/10 mm	Single	Theo	31 °C	51%	13%	[126]
		Copper/10 mm	Uncovered	Exp	35–40 °C	51%[Ψ]	13%	[71]
		Copper/10 mm	Uncovered	Theo	–	52%[†]	10%	[120]
		Copper/10 mm	Single	Theo	–	58%[†]	9%	[120]
		Copper/10 mm	Double	Theo	–	58%[†]	8%	[120]
		Copper/10 mm	Single	Theo	–	79%[†]	9%	[132]
		Copper/15 mm	Single	Exp + Theo	–	71%[Ψ]	16%	[74]
		Stainless steel	Single	Theo	30 °C	32%[Ψ]	12%	[119]
		Stainless steel	Single	Theo	50 °C	54%[$]	13%[$]	[129]
		Copper	Single	Exp	60 °C	50%	16%	[133]
	(b)	Copper/8 mm	Single	Theo	–	55%[†]	–	[128]
		Stainless steel	Single	Theo	29 °C	23%[Ψ]	12%	[119]
	(c)	Stainless steel	Single	Theo	31 °C	34%[Ψ]	12%	[119]
	(d)	Stainless steel	Single	Theo	30 °C	29%[Ψ]	12%	[119]
		Stainless steel	Single	Theo	50 °C	48%[$]	12%[$]	[129]
	(e)	Stainless steel	Single	Theo	31 °C	35%[Ψ]	12%	[119]
		Stainless steel	Single	Theo	52 °C	55%	14%	[129]
(b)				Theo	–	64%[†]	9%	[120]
(c)				Theo	–	65%[†]	8%	[120]
(d)	Insulated			Theo	–	66%[†]	8%	[120]
	Non-insulated			Theo	–	65%[†]	8%	[120]
	Insulated			Theo	–	67%[†]	–	[130]
				Exp	–	70 ± 6%[†]	–	[130]

[+]*Exp = experimental; Theo = theoretical.* **Optical efficiency at real test conditions (G = 670–910 W/m^2; T_a = 38–39 °C, $T_{f,i}$ = 32–76 °C).* [†]*At zero reduced temperature.* [Ψ]*Optical efficiency.* [$]*Operating conditions: G = 800 W/m^2, flow rate = 0.04 kg/s, T_{in} = 39 °C.*

Each of the aforementioned configurations can be further divided depending on the number of covers (zero, one or two; see Table 3), whether an opaque or transparent PV panel is used or whether they have an additional transparent insulating layer between the channels (Design (d) in Fig. 7) [120]. Most of the studies apply the cooling water at the rear of the PV cells, with a reflective Tedlar layer in between, decreasing the efficiency of the heat extraction. There are several ways to overcome this problem, such as using a different layer (Tedlar-polyester-Tedlar)

with good electrical insulation and thermal conduction. However, this usually leads to a more complex design. The two-absorber PV-T collector (Design (d) in Fig. 7) uses a transparent PV laminate as a primary absorber and a black metal absorber as a secondary absorber, with water flowing in through the upper channel and then returning in the opposite direction through the lower one (underneath the PV laminate) [120,130]. PV cells receive most of the visible radiation as glass and water have high transmittance, and the infrared part of the solar spectrum is mostly absorbed by water, which also cools the solar cells preventing the decrease in efficiency due to an increase in the cell temperature [75]. The results show that this design achieves higher thermal efficiency than a single-cover sheet-and-tube PV-T collector (66% *vs*. 58% respectively at zero reduced temperature [120]; see Table 3), but the transparent PV laminates are more expensive and this design is heavier and more fragile due to the larger amount of glass required [120,130]. Another alternative is to let the fluid flow over the absorber (free flow panel, Design (b) in Fig. 7) [131], but the results show that evaporation strongly reduces the thermal efficiency and the condensate on top of the glass causes additional reflection, so the authors concluded that water is not an appropriate choice for this type of collectors [120].

Amongst the various thermal absorber configurations for PV-T collectors found in the relevant literature, those featuring parallel tubes (sheet-and-tube) are the most common [27,120,125,134–136], with high TRLs of 9. Most of the water-based PV-T collectors commercially available are based on thermally attaching mono-crystalline PV cells on top of flat-plate solar collectors [91,92,137–140]. According to the market survey undertaken under Task 60 [25,92], most of the PV-T manufacturers focus on liquid-based PV-T collectors, particularly on uncovered water-based PV-T collectors (48%), such as Caotec, DualSun, Fototherm, Meyer Burger, Racell, Solator, Solink; followed by covered water-based PV-T collectors (28%), such as Abora Solar, EndeF, Solvis; and vacuum tube PV-T collectors (4%), such as Naked Energy [92].

2.2.2. *Refrigerant-based PV-T collectors*

In refrigerant-based PV-T collectors, the PV-T collector usually acts as the evaporator of an HP [141], forming the so-called PV-T-SAHP [23,68]. Here, direct expansion evaporation coils are integrated underneath the PV cells (see Fig. 9), so when the refrigerant flows through the modules it evaporates at low temperatures (0–20 °C) [41,142], cooling down the PV cells. This allows the PV cells to operate at low temperatures and therefore achieve higher electrical efficiencies [143,144].

Typically these collectors have a serpentine design made of copper coils [146] of around 6–7 mm inner diameter [143,144,147–150], but there are also examples of copper parallel tubes of larger (10 mm) inner diameters [151] (see Fig. 9). Meanwhile, Mohanraj et al. [152] proposed to alternate circular tubes of 9.52 mm with equilateral triangular tubes of 12 mm to increase the heat transfer area and thus absorb more thermal energy. The results showed a 4–13% higher electrical efficiency and 4–9% higher evaporator heat gain compared to a circular tube configuration. Tsai [153] proposed a rooftop PV-T collector where multi-port copper tubes assembled in parallel are attached to the rear surface of the PV cells. In this line, a more recent work analysed a serpentine microchannel PV-T collector integrated into an opaque ventilated façade [154].

Alternatively, Xu et al. [142] proposed multi-port flat extruded aluminium tubes of 3.35 × 3 mm channels, increasing the contact surface, enhancing heat transfer and thus increasing the thermal efficiency by 6%. A similar design was proposed by Zhou et al. [155], where microchannel rectangular pipes (2 × 6 mm) are welded to the absorber plate of the PV-T collector (see Table 4). They concluded that this design improved heat transfer while reducing manufacturing costs due to the smaller size and weight. More recently, other authors have proposed a roll-bond design with serpentine aluminium coils as the PV-T collector evaporator [156,157]. In an attempt to reduce thermal losses, another study [158] proposed a glass vacuum tube PV-T collector, with a U-shape copper tube of 6 mm as the evaporator and a-Si PV cells. There are also examples of refrigerant-based CPV-T collectors, such as the one proposed by Xu et al. [159], where a multi-port flat extruded aluminium tube in a serpentine format acts as the evaporator of a low-concentrated PV-T parabolic collector (concentration ratio of 1.6).

Also in related work, the experimental study by Fang et al. [151] concluded that a refrigerant-based PV-T can improve the electrical efficiency by 24% relative to that of a conventional PV panel, due to the lower operating temperatures of the PV cells in the former. Similar results have been recently found by Vaishak and Bhale [149]. Several studies also concluded that the COP and the condenser heat capacity decrease with the increase in condenser water supply temperature [147,158].

Different refrigerants have been used as working fluids, such as R134A, R12, R22 [144,145,150,157,160], R410A [155], R600A, R407C [161] or R404A [68] (see Table 4). The performance analysis has shown that R12 and R22 outperform other fluids (e.g., can achieve a higher COP), but in turn, they have a negative environmental impact [162]. R134A is used in most of the reported studies [147,153,154,158,159,163], which has a similar performance to R12 and R22 [162], while it is more environmentally friendly [68]. Among the others, R410A is more efficient than R407C and R404A, and despite its lower (15–20%) performance than R134A [162], it has been identified as an ideal substitute because of its good chemical and thermal stability [68,155].

Previous research on refrigerant-based PV-T collectors has mainly focussed on: (a) analysing the influence of different design factors (top cover, PV cells, evaporation and condensation temperatures of the HP) on the system efficiencies [144,147,158]; (b) optimizing the collector design (geometrical shape, diameter size or packing factor) [145,164]; (c) analysing the experimental performance of the PV-T collector and its integration with an HP [144,149,151,153,157,160]; and (d) assessing the annual performance of the PV-T-SAHP system in one [149] or several [142] geographical locations.

Refrigerant-based PV-T collectors usually have larger electrical efficiencies than air- or water-based PV-T collectors, due to the lower operating temperature of the PV cells [37,41], but they have some disadvantages such as the high risk of refrigerant leakage [41], uneven refrigerant distribution in evaporation tubes [165,166], potentially

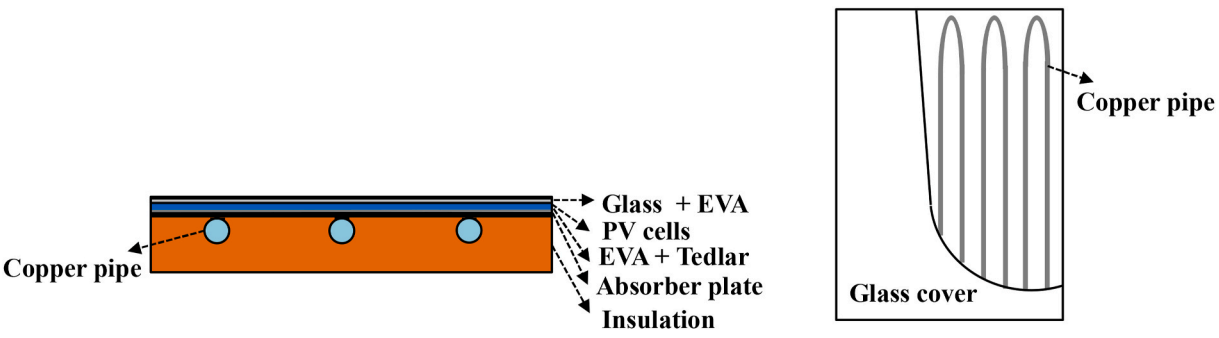


Fig. 9. Schematic of refrigerant-based PV-T collector [68,145].

Table 4
Summary of common refrigerants used in previous research on refrigerant-based PV-T collectors.

Refrigerant	System description	Nature of work[a]	COP[d]	Fluid T_{out}	Thermal efficiency	Electrical efficiency	Ref.
R134A	Uncovered, serpentine PV-T collectors (× 10), c-Si PV cells & 5 kW HP	Theo	–	–	42–60%	19%	[147]
R134A	Multi-port copper tubes, uncovered BIPV-T array; rated power 1 kWp & 200 L tank	Exp & Theo	–	–	–	–	[153]
R134A	Serpentine microchannel BIPV-T collectors	Exp	3.1 (max)	up to ~40 °C	–	9% (av.)	[154]
R134A	Glass vacuum-tube PV-T collector, U-shape copper tube (6 mm), a-Si PV cells	Exp	2.9–4.6	–	–	4–5%	[158]
R134A	Low-concentrating PV-T fixed truncated parabolic concentrators; multi-port flat extruded aluminium tubes	Exp	4.8 (av.)	20–30 °C	–	18%	[159]
R134A	Uncovered, serpentine PV-T collectors in a DX-SAHP system	Theo	5.9[c]	–	–	12%	[163]
R22	Uncovered, serpentine PV-T collectors, c-Si PV cells	Exp	10.4 (max), 5.4 (av.)	–	–	13%	[144]
R22	Roll-bond (× 4), serpentine aluminium coils PV-T collectors, 4.2 kW HP & 150 L heat storage tank, in a DX-SAHP system	Exp	6.2	–	–	12%	[157]
R410A	Microchannel rectangular pipes (2 × 6 mm), uncovered PV-T collectors in a DX-SAHP system	Exp	4.7 (av.)	up to ~35 °C	57%	15%	[155]
R407C	PV-T collectors & water-to-water HP in a DX-SAHP system	Theo	4.6–4.2	~12–30 °C[b]	32–49%	15–16%	[161]

[a] Exp: experimental; Theo: theoretical
[b] PV-T: panel temperature
[c] Yearly averaged COP
[d] av: average; max: maximum

induced degradation, delamination and UV degradation [68], or the need of a perfect seal in the refrigerant cycle to prevent air entering the system during operation [41]. Recently, Vaishak and Bhale [68] stated that some of these limitations might be overcome to some extent by heat-pipe PV-T collectors (see Section 2.3 for more details). The most common refrigerant-based PV-T configurations have a TRL of 7–8, consisting of a PV-T-SAHP system where the PV-T collector acts as the HP evaporator. However, according to the market survey of Task 60 [92], currently, there are no manufacturers of this type of PV-T collector.

2.3. Heat-pipe PV-T collectors

Heat pipes are highly efficient heat-transfer devices that have been widely used in various fields such as spacecraft and electronics cooling. Heat pipes have the advantages of high heat transfer rates, no moving parts, no energy consumption, and long service lifetimes, among others [167]. A typical heat pipe usually consists of two main sections: the evaporator and the condenser (see Fig. 10). The evaporator absorbs heat and evaporates the working fluid, which is then condensed in the condenser, releasing heat. Heat pipes have an ultra-high heat transfer effectiveness due to the phase change process. Considering the aforementioned advantages, heat pipes have been applied to PV-T collectors, specifically for the effective removal of waste heat in PV cells, and it is thought that heat-pipe PV-T collectors may have the potential to overcome some of the problems refrigerant-based PV-T collectors [41]. Fig. 10 shows a schematic of a heat-pipe PV-T collector. The heat pipe is tightly attached to the back side of PV cells to absorb residual heat. The heat is then transported through the heat pipe and recovered by a fluid at the condensation end of the heat pipe, which can then be delivered for downstream use. The heat pipe can be considered a heat-transfer medium with a very high thermal conductivity.

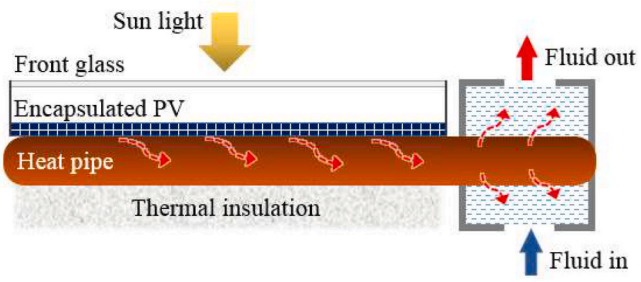


Fig. 10. Schematic of heat pipe PV-T collector.

Two main types of heat pipe have been applied to heat-pipe PV-T collectors, specifically microchannel flat heat pipes [168,169] and cylindrical heat pipes [170–172]. Fig. 11 shows a heat-pipe PV-T collector designed and tested by Pei et al. [173]. An array of cylindrical copper heat pipes was attached to the bottom of the PV cells, and the waste heat was removed and transported through the heat pipe array into the water box at the top of the panel. The system daily thermal efficiency increased from 45% to 55% as the heat pipe number increased from 5 to 15 [172]. The heat-pipe PV-T collector has an anti-freezing ability if the working fluid is selected appropriately and thus has a better performance in cold regions compared to conventional water-based collectors [173]. Low-boiling point refrigerants (e.g., R134A) can be used as working fluids in cold regions to overcome the freezing problem [170]. Due to

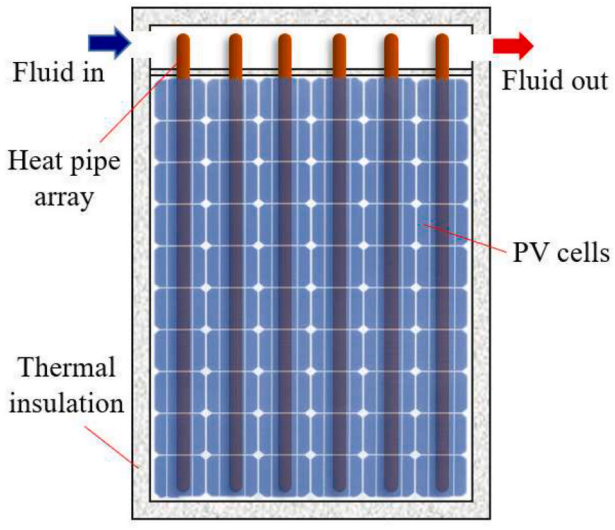


Fig. 11. *Structure of flat plate heat-pipe PV-T collector.* Figure reproduced from Pei et al. [173] with permission from Elsevier (Copyright 2011 Elsevier).

their high equivalent thermal conductivity, heat pipes maintain a uniform temperature distribution over the PV cells. The temperature difference between PV cells cooled by heat pipes was found to be less than 2.5 °C in the outdoor experiments of Wu et al. [174]. The performance of a heat-pipe PV-T collector with microchannel flat heat pipes in different seasons was investigated by Hou et al. [169], who found that the thermal efficiency was over 40% in summertime. Overall, the thermal efficiency of a heat-pipe PV-T collector strongly depends on its structure, the working fluid and the distribution of the heat pipe array, and typically varies from around 40% [169,172] to 60% [172,174,175].

Heat pipes are particularly effective at removing the high-flux waste heat in concentrated PV panels. In this context, the experimental results by Farahat [176] showed that the heat pipe delivered a more effective and reliable cooling for the concentrated PV panel compared to a conventional water cooling method. A concentrated heat-pipe PV-T system with a microchannel heat pipe was built and tested by Chen et al. [168], reaching thermal and electrical efficiencies of 55% and 15%, respectively, with the solar panel temperature at about 60 °C.

Attempts have also been made to convert recovered thermal energy from PV-T collectors into additional (secondary) electricity, e.g., using an integrated heat-pipe PV-T and thermoelectric generator (TEG) module design in which the condenser section of the heat pipe was directly contacted with the TEG [177,178]. In such applications, TEGs are in competition with organic Rankine cycle (ORC) power systems (discussed further in Section 4.1.1), Stirling engines, etc., whose efficiency and cost are both scale and temperature-dependent [179]. However, the economic viability of using a secondary power system to recover and convert excess PV-T thermal energy remains low at present, due to the inherently low efficiency of the secondary power system at temperatures below 100 °C, the added complexity and cost, and the alternative of generating additional electricity by increasing the total installed PV-T or PV area. In any case, experimental results showed that the PV cell temperature in the proposed PV-TEG-microchannel heat-pipe collector without insulation was 6 °C lower than that in the PV-only baseline panel (61.9 °C and 67.9 °C, respectively) after 1 h of operation, and that the electrical efficiency of the proposed hybrid collector without insulation was 12.2%, compared to the 12% of the PV-only panel. The TRL of this type of PV-T collector strongly depends on the specific configuration, with most of the configurations still at a TRL of 6–7. Currently, there is one UK manufacturer of vacuum-tube PV-T collectors [92].

2.4. Dual air–water PV-T collectors

Dual air–water PV-T collectors have appeared in an attempt to overcome the limitations of both air- and water-based PV-T collectors. These collectors are designed to operate either heating water (usually in periods of higher ambient temperatures) or heating air (mainly when the ambient temperature is low), depending also on the end-user needs. It is also possible to operate both heat extraction modes either under mild weather conditions or when both hot water and air are needed. Dual air–water PV-T collectors can achieve total efficiencies of about 55% and 70% for air and water heat extraction modes, respectively [73]. Different configurations have been studied [41,48,73], concluding that the best option is to have water channels in thermal contact with the PV cell rear surface and the air heat exchangers below it, also acting as thermal insulation [180], as shown in Fig. 12 [73,181].

Dual air–water PV-T collectors combine the advantages of water- and air-based collectors. To increase the amount of heat extraction using water, the number of water pipes can be increased, which is beneficial for the thermal efficiency but further increases the costs. Cost-effective fins or ribs can be added to the air channel to improve the heat transfer coefficient [73]. An experiment was conducted by Ji et al. [182] to investigate the real outdoor performance of a dual air–water PV-T collector in different working modes. The thermal efficiencies of the water-heating and air-heating modes at zero reduced temperature

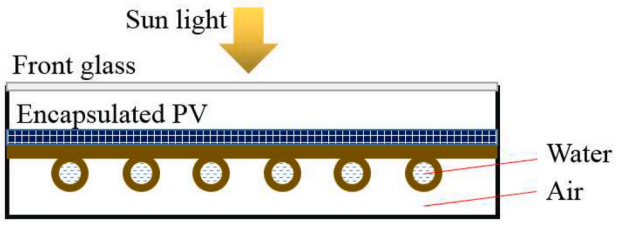


Fig. 12. Schematic of dual air–water PV-T collector [73,181].

reached 44% and 57%, while the electrical efficiency was around 10%. Ma et al. [183] added an additional air-flowing channel with fins above the PV cells. The air flowed through both the channels above and beneath the PV cells. The thermal efficiencies of the water-heating and air-heating modes reached 50% and 55%, respectively, while the electrical efficiency was not reported.

A noteworthy advantage of dual air–water PV-T collectors arises from their overall versatility, even though they are slightly more complex and expensive than typical water-based PV-T collectors. They can take advantage of the dual heat extraction to avoid freezing in cold climates, shifting to heat air when required. These systems can be used in houses, residential and office buildings, mainly for operation at low temperatures, providing a cost-effective solution with a flexible output [41,73]. This type of PV-T collector has a lower TRL of 6–7 with no manufacturers of this type of PV-T collector [92].

2.5. Building-integrated PV-T collectors

When PV cells are installed either on the facades or roofs of a building creating the external structure or skin of the building, they are referred to as building-integrated photovoltaic (BIPV) collectors. BIPV systems are used mainly to produce electricity, but also provide hot air for space heating, which is an added benefit. When the heated air is used to cover part of the building heating load, the system is called a building-integrated PV-T (BIPV-T) system.

By simultaneously serving as a building envelope material and a power generator, BIPV-T systems can offer savings in materials and electricity costs, thus reducing the use of fossil fuels and the relevant CO_2 emissions and offering an architectural enhancement to the building. Furthermore, PV panels can be integrated in such a way to provide additional functions like shading, active solar heating and lighting. The advantages of BIPV-T systems are many so they have attracted the interest of engineers and architects. In literature, a lot of successful projects are published from around the world. Most of these are applications for residential and commercial buildings. Recently, PV panels are produced as standard building products and a whole new market is created around BIPV-T systems [184]. As a BIPV-T panel is part of a building envelope it must be able to provide weather protection, thermal insulation and noise protection [185] and perform these functions without affecting the structural strength or integrity of the building. In addition to the electrical and thermal energy produced, BIPV-T may also allow daylight entry, through semi-transparent modules, thus providing the view of the outside environment so as the building occupants do not feel confined. An added important advantage of BIPV-T systems is that they can function as an attractive architectural element affecting positively the appearance of a building.

The idea of transforming buildings from energy users to energy producers is not new. Solutions involving the integration of PV cells into the building envelope appeared almost at the same time as the first PV panels entered the market. The first installation of a BIPV curtain wall façade appeared in Aachen, Germany in 1991 [186].

The need to increase the energy efficiency of buildings and reduce emissions are the main drivers for the continued uptake of BIPV-T products. Most countries promote such systems by funding part of the

installation costs and by providing attractive feed-in tariffs applicable to the use of BIPV products [187]. The present size of the global BIPV market is about 2.3 GW (or ~1% of the global PV market), with Europe constituting the largest market (42% of the global market) in particular due to attractive incentives in France, Italy and Germany [188]. The annual installed capacity of BIPV systems worldwide is expected to reach 32.3 GW by 2024 [189].

BIPV-T systems represent a favourable solution for clean electricity production combined with renewable cooling or heating while reducing the energy demand at the same time. It is estimated that air-based BIPV-T systems have the potential to reduce the primary energy required for heating and cooling from conventional systems by 30% [190], and in preheating applications where the fluid temperature is kept low, such as in combined PV-T-HP systems, the electrical output can be enhanced by 4–10% compared to an equivalent non-cooled PV system [191]. They should be applied to buildings usually after other energy-saving measures are taken and they should be economically examined in terms of their lifecycle cost, and not from their initial first cost because the initial expenditure is substantially reduced by the avoidance of the traditional building materials they replace. One important design consideration for BIPV-T systems is whether natural ventilation or mechanical ventilation is used to move the air in the gap between the PV cells and the wall or roof of the building.

In the case of solar façades with installed PV panels, the need for ventilated PV cladding is very important, otherwise, due to the high temperature reached by the PV cells, there will be a loss of efficiency and the development of undesirable heat gain to the building, which especially during the summer period could create extra cooling load. Unless provisions are not made to remove the hot air created between the PV cells and the wall of the building, the BIPV panels get warmer than the ones mounted in free air, consequently lowering more their electrical power output. To solve this problem, efficient ways to extract the heat by forced or natural fluid circulation have to be devised. There are a lot of studies trying to optimize the air gap between the PV cells back surface and the building element for air circulation, either by forced or natural flow, for cooling the PV arrays. Some studies on naturally ventilated systems are [192–201], and on mechanically ventilated systems [202–208]. Although the natural convection analysis of the BIPV systems seems complex and inconvenient, it is believed that it has many potentials and is worth better examination due to its advantages [196]. Moreover, various researchers studied the thermal effects in the air gap between the PV cells and the building wall [199,209–216] and numerous studies are focussed on the heat transfer analysis between the two skins [190,217–220].

PV cells for building integration are usually installed on flat or inclined roofs, on façades and as shading elements close to windows or even inside window glazing. According to a recent review [221], roof-mounted systems hold 80% of the BIPV market, and façade--mounted systems account for the rest of the installations. Roof-mounted systems include roof-integrated shingles, skylights, atria and roof panels, and façade-mounted systems include the shading systems, cladding and curtain walls.

One possible classification of BIPV-T systems has been provided in a recently published review [222], based on the application, while other studies provide alternative categorizations of BIPV-T systems based on the type of panels and their operation principles [223]. Recently, some authors presented a comparative review of the BIPV systems in selected EU countries, showing that Europe has been the leader in BIPV system development from 2014 to 2020 followed by the USA and Asia [224].

The need to develop more advanced BIPV-T system designs with improved performance has persisted over the years. Architects, engineers and users agreed that their preferences for the systems were relevant to the appearance of the systems and their performance. Thus, various design configurations were developed. Some of them are double-skin systems with air passing between the two skins for overheating prevention, transparent and semi-transparent PV panels [225–230], roof-integrated PV panels, replacing the conventional roof tiles called PV shingles, façade applications for curtain walls, glazing windows applications, and shading elements applications.

Schematics of the most used configurations of BIPV/BIPV-T systems are shown in Fig. 13 as given by Agathokleous and Kalogirou [231]. Fig. 13(a) shows a PV panel in full contact with a building wall. Various studies have examined this design and concluded that it is inefficient due to the overheating of both the PV panels and the building's interior spaces [207,232–237]. Fig. 13(b) shows a BIPV system that addresses these problems, by rejecting the heated air, while in Fig. 13(c) a BIPV-T system is shown that uses the heated air for space heating through an air duct in the ceiling. Fig. 13(d), (e), (f) and (g) show roof BIPV and BIPV-T systems; the first one rejects the heated air behind the PV panels and the other three, use the heated air for space heating with ducts or roof air circulation. Fig. 13(h) and (i) show BIPV applications with semi-transparent PV cells which provide indoor natural light as well. Other BIPV applications are the use of BIPV as shading elements and BIPV systems which are also used to provide hot water, connected with pumps and water tanks. Another work studied another configuration of the system named BIPV Trombe wall (BIPV-TW). These systems can provide heating/cooling and generate electricity simultaneously [238].

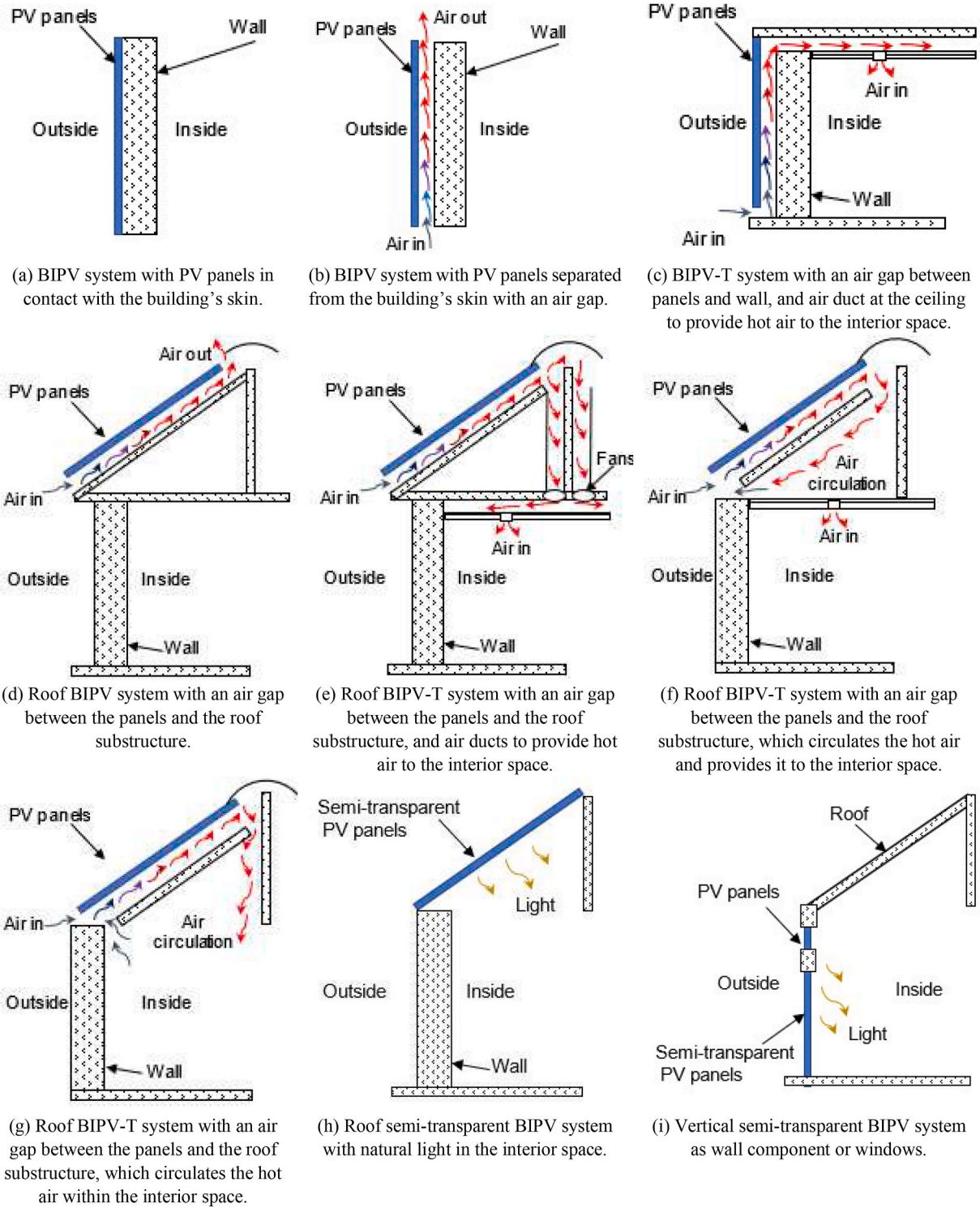
Another interesting configuration gaining attention recently is the use of PCMs for thermal regulation enhancement of BIPV-T systems [239]. A study where two PCMs were used on the thermal regulation performance of BIPV systems is given by Huang [240] where it is shown that the PV-PCM system with two types of PCM can maintain the PV cells at operating temperature closer to its characteristic value of 25 °C and thus lead to an improvement in solar-to-electrical conversion efficiency under variable diurnal insolation. The most used BIPV-PCM system in the market looks like the schematic representation of Fig. 14, which provides heat transfer enhancement in the interior, with radiation [231].

Various investigators have performed case studies, investigating real-size BIPV and BIPV-T applications or prototypes [241–253] and life cycle assessment of BIPV systems [247,254]. A considerable number of researchers have attempted to extend our knowledge of the behaviour of BIPV systems by investigating the flow, heat transfer and optical characteristics of the systems [187,255–257].

It is known that BIPV systems often reach higher temperatures than standalone systems and this leads to a performance drop. For this reason, accurate thermal modelling of BIPV systems is very important before their installation to evaluate their contribution to the reduction of building energy needs. In this context, several thermal modelling tools have been developed to estimate the operating cell temperatures of PV cells in BIPV systems because they directly affect the performance of the system.

Some studies [194,258] investigated the effect of the naturally ventilated air gap of vertical double-skin BIPV systems and provided correlations for the estimation of the convective heat transfer coefficients for the calculation of the heat transfer rate in the air channel. Friling et al. [206] performed mathematical modelling of the heat transfer dynamics of BIPV systems, showing that the heat transfer rate increases when forced ventilation velocity is increased which was more or less expected. Another study [259] presented the results of a simulation study performed in TRNSYS with the use of the existing types of TRNSYS for BIPV and BIPV-T systems considering only a forced ventilation system. Forced ventilation systems have also been investigated [260,261]. Bigaila et al. [260] performed an experimental study with emphasis on the cell temperature and the air gap heat transfer analysis whereas in another study Rounis et al. [262] investigated the wind effects and fan-induced suction in a multiple-inlet BIPV-T system.

There are also various studies on the performance of BIPV systems [225,245,263–267], which can be categorized into simulation modelling, experimental and case studies. The electrical and thermal efficiencies of BIPV systems depend on the type of PV used, on the climatic conditions as well as on the configuration of the system, the type of cooling method and the type of integration, among others. A comparison



(a) BIPV system with PV panels in contact with the building's skin.

(b) BIPV system with PV panels separated from the building's skin with an air gap.

(c) BIPV-T system with an air gap between panels and wall, and air duct at the ceiling to provide hot air to the interior space.

(d) Roof BIPV system with an air gap between the panels and the roof substructure.

(e) Roof BIPV-T system with an air gap between the panels and the roof substructure, and air ducts to provide hot air to the interior space.

(f) Roof BIPV-T system with an air gap between the panels and the roof substructure, which circulates the hot air and provides it to the interior space.

(g) Roof BIPV-T system with an air gap between the panels and the roof substructure, which circulates the hot air within the interior space.

(h) Roof semi-transparent BIPV system with natural light in the interior space.

(i) Vertical semi-transparent BIPV system as wall component or windows.

Fig. 13. Selected BIPV-T system configurations. Figure from Agathokleous and Kalogirou [231], used with permission from Elsevier.

between the different configurations in terms of efficiency is difficult to perform due to all these related parameters. Table 5 summarizes the main types of BIPV systems and shows efficiency estimations obtained in previous research. Based on these findings, it is concluded that the size of the air gap, the inclination angle of the collector, the height of the system and the type of PCM are critical parameters for the performance of BIPV systems. It can be generally concluded that BIPV systems with open-ended air channels have better cooling performance and thus higher electrical efficiency than the systems with closed air ducts, and that BIPV systems with PCMs have better thermal performance than the air-based BIPV systems due to the storage ability of the PCMs.

Yoo [274] performed a simulation for BIPV shading device optimization through parameter variation, studying the first practical application of a semi-transparent BIPV system in Korea. The performance of the system was investigated through long-term system monitoring and simulation modelling. Ghani et al. [276] estimated the PV cell conversion efficiency of BIPV-T systems using an artificial neural network, while another study [277] investigated the effect of roof configurations

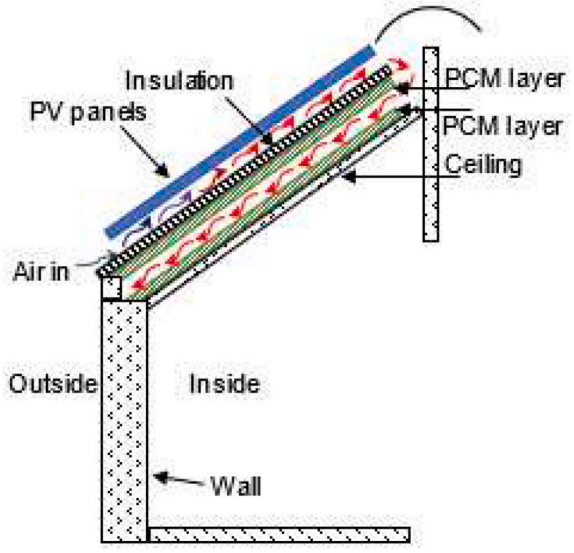


Fig. 14. BIPV-T system with PCM layers for heat transfer enhancement.

Table 5
Efficiencies of various BIPV systems from the literature.

System	Description	Thermal efficiency	Electrical efficiency	Ref.
Façade BIPV	PV panels in contact with the building skin	–	3–9%	[267]
Façade BIPV	With an air gap between the PV and the building outer skin	– 26%	11% 12%	[245] [193]
Façade BIPV	BIPV Trombe wall system	–	15%	[268]
BIPV-T curtain wall	BIPV curtain wall with air opening and air duct behind the PV	30%	13%	[269]
BIPV-T Wall	BIPV-T system with water-cooled wall	14%	13%	[270]
Roof BIPV-T	With an air gap and ducts for space heating	– 38% –	12% 9% 11–12%	[271] [272] [252]
Roof BIPV	BIPV system with water circulation	30%	17%	[273]
Semi-transparent BIPV	Semi-transparent PV panels for façade/roof applications	–	4–20%	[274]
BIPV-T-PCM	BIPV system with PCM layers for façade applications	– 61%	4–10% 8%	[267] [175]
Coloured BIPV	Sputter-coating based colour BIPV modules	–	16%	[275]

on the performance of BIPV systems. An experimental study of a low-cost passive strategy to improve the performance of BIPV systems was undertaken by Yang and Athienitis [278]. A performance evaluation of an air-based BIPV-T system with multiple inlets in a cold climate concluded that no more than four air inlets are needed to provide sufficient PV cell cooling [279]. Other investigators performed energy analyses and verification studies of BIPV cells in buildings with building information modelling, and the simulation results were compared to data measured over 3 years [280]. More recently, the performance of a BIPV-T system with PV cells installed at the optimum tilt angle and influenced by shadow was assessed [281], as was the performance of three types of BIPV-TW systems [238].

The influence of a BIPV system on the heating and cooling loads of the building with one-dimensional transient model analysis, for Tianjin, China, was analysed by Wang et al. [282]. A ventilated air gap BIPV system was compared to a non-ventilated system, close roof system and a conventional roof with no PV cells and no air gap. It was concluded that in summer the optimum system is the ventilated air gap which leads to higher conversion efficiency but in winter, the non-ventilated air duct is appropriate.

A real system investigation was also done by Aste et al. [283] in the first Italian BIPV project. The system was in operation for 13 years which is representative because it can be considered as about half of the supposed lifetime cycle of a PV system. The results obtained show that the PV plant analysed did not present a significant decrease in long-term performance. The measured performance ratio decay was just under 0.4% per year.

Azadian and Radzi [284] investigated the optimization assessment of the energy performance of a BIPV-T PCM system using genetic algorithms. The overall energy efficiency of the system was evaluated for winter and summer conditions adopting different utilization strategies, and optimized designs were identified. The thermal and electrical efficiencies were calculated, and the results showed that such systems can achieve a maximum overall efficiency of 64% in a winter configuration and 32% in a summer configuration.

Given the important benefits of BIPV systems, key factors that can influence their performance have been investigated as part of an effort to improve these systems. Such factors include the operating temperature, irradiation conditions, optical losses and changes to the solar spectrum. Additionally, although there is increasing uptake of installations, there are still some important barriers that affect their exploitation such as concerning feed-in tariff implementation, public acceptance and wider government support [231,285,286].

Some authors [272,287] have reported results from investigations in which water-based PV-T collectors were integrated within roofs, giving rise to roof-mounted water-based BIPV-T systems. They concluded that the electrical and thermal performance of these systems is affected by some key design parameters such as the fin efficiency, lamination requirements and the thermal conductivity between the PV cells and the supporting structure [287]. The results also showed better cost savings when these units use a natural circulation system, obtaining an estimated payback time of around 14 years in warm climate locations [272].

Another study on the effect of flow distribution on the PV cell performance in water-based BIPV-T collectors stated that parameters including the manifold-to-riser pipe ratio, array geometry, manifold flow direction and flow rate influence the flow distribution and PV cell efficiency [288]. The authors included several design recommendations for improved performance. More recently, significant energy conversion efficiency improvements to both the electricity generation and heat collection efficiency were reported with water-based BIPV-T collectors [289]. The energy yields of integrated water-based BIPV-T collectors using different façade orientations have been recently investigated [290], with results showing that the largest energy production is achieved on the South façade, while for maximum self-consumption it is recommended to split the BIPV-T collectors among the East, South and West façades. Other investigators analysed and compared the techno-economic performance of uncovered water-based BIPV-T collectors: roof-integrated and/or façade integrated *vs.* standalone PV-T collectors. They developed a model in TRNSYS and analysed the performance of the different integration alternatives for DHW, space heating and electricity provision in a multi-storey residential building located in different climates throughout Europe. The results showed simple payback times between 11 and 20 years depending on the climate, with lower payback times in Southern European cities [291].

Fig. 15 shows an application of dual air–water PV-T collectors in a built room, forming a BIPV-T system [292]. The PV-T collector was mounted on the south wall of the room, which can provide passive space heating on cold winter days and hot water during the warm seasons. The working mode can be easily switched between air-heating and water-heating modes in different seasons. On typical summer days, the thermal efficiency reached around 50% and the water tank temperature reached around 40 °C for the water-heating mode. The PV-T collector was

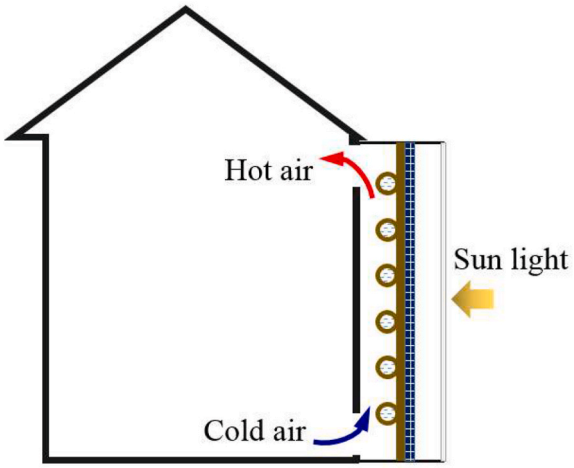


Fig. 15. Building-integrated dual air–water PV-T collector [292].

also able to reduce the cooling load of the room by 2% on summer days.

Alternatively, Zhao et al. [147] proposed a refrigerant-based PV-T collector directly integrated into the roof, which acted as the electricity generator and evaporator of an HP. They developed a computer model to analyse the influence of different factors on the system efficiencies and concluded that electrical efficiency remains almost the same under the variation range of evaporation temperatures, while lower evaporation temperature leads to higher thermal (and system) efficiencies.

2.6. Concentrated PV-T collectors

The difference between a concentrated PV-T (CPV-T) system and a CPV system with active cooling may be ambiguous. The authors take the view that the determination of whether any solar system that includes PV cells (whether concentrated or not) is or is not a PV-T system depends on whether the thermal energyrecovered from this system is utilized for a specific purpose, or rejected to the environment and/or the atmosphere. When the thermal energy is delivered as useful thermal output to an end-user in any application, either directly or indirectly via intermediate conversion, upgrading or storage, this can be considered a PV-T/CPV-T system, otherwise, it is a PV/CPV system with active (or passive) cooling.

CPV-T collectors increase the solar flux incident upon the solar cells, improving both the thermal and electrical outputs of the system, while at the same time the total PV area is reduced and replaced by low-cost reflectors; depending on the relative costs of these two components, this can lead to a reduction in the the system's capital costs (and, thus, payback time) [35,71,73,76]. However, especially when sun tracking is needed, they are more expensive than flat-plate collectors, as this complex mechanism introduces additional costs. Consequently, these systems are normally used when medium to high temperatures are required (usually over 100–150 °C), while for lower temperature applications flat-plate collectors appear as a better option [35,73].

CPV-T systems can use lenses or reflectors as concentrators, with lenses being more suitable due to their lower weight and material costs, although they cannot focus scattered light. Therefore, concentrators are normally limited to locations with clear sky weather. Generally, CPV-T systems use liquids (e.g., water, oil, molten salts) rather than air as a coolant because it is more effective, hence obtaining a higher electrical output [35,73].

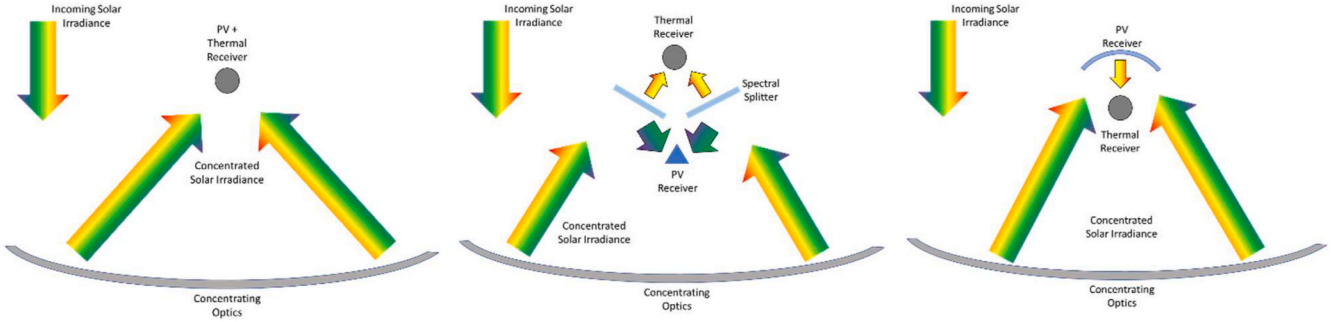
There are different CPV-T collector types, ranging from stationary flat-plate collectors with added reflectors and low concentrating ratio (solar concentrating ratio <2.5), to highly concentrating ratio units which require tracking, making roof integration difficult and significantly increasing maintenance costs [73,76]. Similarly, there are many types of solar tracking options and technologies, and a variety of tracker drive types, which have been reviewed in detail in previous work [293].

In general, CPV-T systems can be grouped into three broad categories: (a) systems with concentration onto a single receiver, where both the PV and thermal receiver are a combined, single unit and under concentrated sunlight; (b) spectrum splitting systems, where the incoming irradiation is split into two components that are delivered to distinct PV and thermal receivers; and (c) systems wherein the PV receiver acts as both a spectral splitter and concentrator. These configurations are shown schematically in Fig. 16.

Fig. 16(a) will result in the highest operating temperature of the PV cells and active cooling is required. In this configuration, achieving high working fluid temperatures results in exceedingly high PV cell temperatures, reducing cell efficiency. Fig. 16(b) reduces the PV cell working temperature by removing the incident spectrum that the PV cell cannot convert to electricity (or wavelengths of low conversion efficiency). This approach can potentially enable high PV cell efficiency and high thermal receiver working temperatures. Fig. 16(c) is a special case of (b) where the PV receiver acts as both a spectral filter and a concentrator. Such a configuration requires PV receivers with high reflectivity outside of wavelengths of absorption for the PV receiver and can also enable high thermal working temperatures. A significant challenge, however, arises in the comparison of such systems as the design with different levels of concentration, PV cell band-gap, and spectral splitting wavelengths (if used) all drastically impact performance. Additionally, this is further complicated by the design objective of the system, particularly concerning the desired operating temperature of the thermal receiver. The two primary metrics for assessing the performance are the overall efficiency and the fraction of energy collected from the thermal and PV receivers [294]. The biggest challenge in using the overall efficiency is in quantifying the relative values of the electrical and thermal energy outputs. While many approaches simply add the thermal efficiency to the PV efficiency, this oversimplifies the issue as higher temperatures may be required for a given thermal process. It is possible to assign weighting factors [295] to the thermal energy (although this is assumption driven) or to consider the conversion of all thermal energy to electrical energy (which may not be relevant for heat-driven needs). These metrics are useful for providing insights into the performance bounds of a variety of system configurations and are particularly useful for understanding the upper limits of efficiency, particularly with respect to the PV system [294,296]. Ultimately, this results in difficulty when comparing CPV-T systems, because differing operating temperatures, use cases, and designs can lead to significant variations in a defined efficiency.

In stationary applications, when the PV-T collectors are installed in a horizontal plane, part of the incoming solar radiation is not used, as it is incident on the horizontal surface free of PV cells which is left to avoid shading. To avoid this effect, some studies [71,73] proposed the installation of booster diffuse reflectors placed between the parallel PV-T collector rows. These reflectors consist of an aluminium sheet and give a nearly uniform distribution of the reflected solar radiation on the PV surface, increasing the solar input by about 50% maximum, which means a concentration ratio of about 1.5 [71]. The results showed that with this configuration it is possible to increase the electrical efficiency from about 25% to 35% compared to plain PV panels. Moreover, the use of these diffuse reflectors can offset the negative effect of the optical losses in the case of glazed PV-T collectors, achieving higher electrical and thermal efficiency. Thermal efficiencies of up to 80% and 75% for water and air extraction modes respectively have been reported [71,73].

In CSP systems, optical reflectors focus the solar radiation on channels that contain a heat transfer fluid. PV cells can be placed on the top of these channels, therefore providing electricity, while the fluid cools the PV cells, avoiding their decrease in efficiency due to an increase in temperature. In this line, some authors [297–299] have developed a low-concentration, linear, hybrid micro-concentrator collector for rooftop installation. Its main advantage is the replacement of expensive solar cells with inexpensive optics and tracking systems, consisting of



(a) CPV-T system with receiver comprised of both PV and thermal components

(b) CPV-T arrangement using spectral splitting where CPV and thermal receivers are spatially separated

(c) CPV-T where PV elements act as both spectral filter and concentrator element

Fig. 16. Schematics of the most common types of CPV-T collectors.

low-cost, ultra-light-weight Fresnel mirror arrays, which allow increasing the concentrating ratio to up to 20–30 ×, which is enough for the domestic market needs [297,298]. However, although the demands on optics, tracking systems, thermal management, and maintenance are considerably lower than for high-concentration CPV-T collectors, these collectors still have some drawbacks to enter the rooftop urban market, such as the need for lower maintenance, more reliability, easier operation and a more economical installation [297].

In higher concentration systems, more complex optics, tracking, and working fluids outside of water are necessary. Additionally, many of these systems use either spectral beam splitting (SBS), as recently reviewed [300], or spectral absorption filtering, also recently reviewed [301], to reduce the flux on the solar cells to limit the working temperature of the PV system. One approach of SBS is to use secondary mirrors to redirect light to a CPV-T system, as was proposed by Liu et al. [302], where a linear Fresnel mirror was coupled to a beam splitter to separate the spectrum. In their work, the visible light is transmitted through the beam splitter over wavelengths from 590 to 1082 nm to the receiver while the remainder was reflected to the thermal portion. Only modelling was conducted. Kandili [303] demonstrated a CPV-T system using parabolic dish concentrators where the light was focussed onto PV cells coated with an SBS mirror which reflects light to a vacuum tube. The system demonstrated a combined system efficiency of 7.3% (with 1.6 m^2 surface area under 720 W/m^2 of solar radiation).

A modelling study by Yu et al. [304] focussed on a retrofit for parabolic trough mirrors that replaces the traditional mirrors with PV cells and dichroic mirrors. Silicon hetero-junction cells were attached to a glass trough with dichroic mirrors covering the cells to reflect the wavelengths (shorter than 500 nm and longer than 1100 nm) to the heat collection element (HCE). The model demonstrated an energy output increase of 36% above that of a pure CSP system. Economic models predicted a 30% increase in the cost of the collector [304]. A large-scale experimental investigation of spectral beam splitting [305] developed a parabolic trough coupled to an organic Rankine cycle. Using vertical multi-junction solar cells and dichroic mirrors that intercepted 29% of the light from the trough, PV cell efficiencies of 29–30% were reported. Considering the full trough aperture area, the efficiency of the cells added in the retrofit was 3%. In an SBS demonstration using GaAs PV cells [306] that comprised a secondary mirror due to the high below-gap reflectivity, it was possible to create a secondary reflector comprised of the PV elements for increasing flux on the HCE. Another retrofit approach using the existing architecture of parabolic troughs coupled to a spectral splitter was demonstrated using SBS mirrors that reflected light onto a triangular receiver while transmitting the remainder of the light to the existing HCE [307].

The concept of spectral absorption was developed using a thin absorbing film filter as demonstrated by Stanley et al. [308]. PV cell efficiency was 3.6–4.0%, while the observed thermal efficiency was ~35% at working fluid temperatures of 120 °C, approaching the maximum working temperature due to the onset of flow boiling. This approach is unique in that it utilizes a solid film deployed in the liquid, but the vast majority of spectral absorption techniques employ volumetric absorption by deploying nanoparticles directly into the fluid. One of the first experimental demonstrations was by F. Crisostomo et al. [309] where various concentrations of silver nanodiscs in water were both the spectral filter and working fluid. A peak overall efficiency of 33% was obtained. An et al. [310] demonstrated a CPV-T system based on polypyrrole and water. The authors reported an overall efficiency (based upon temperature rise, not flowing fluid) at a peak of 25%, with a peak PV cell efficiency of 11%. This study was followed up with Cu_9S_5 nanoparticle suspended in oleylamine fluid with back contact c-Si solar cells [310]. The authors reported a peak total efficiency of 34% with the PV cell efficiency at 12% and the thermal efficiency at 23% with the temperature of the fluid exceeding 100 °C [311]. Otanicar et al. [312] was the first demonstration of a nanoparticle absorbing fluid in a CPV-T system where the working fluid was flowing and exceeded 100 °C [312]. The prototype system used a combination of gold and indium tin oxide nanoparticles suspended in Duratherm S to achieve thermal and electrical efficiencies of 61% and 4% respectively at a fluid working temperature of 110 °C.

3. Performance enhancement and pathways for collector innovation

According to previous reviews [28,35,129], the main bottlenecks for the widespread commercialization of PV-T collectors are the higher price compared to side-by-side solar systems (PV and ST collectors), public awareness, product standardization, warranties and performance certification, installation and training experiences. These studies concluded that more research is required on new and cost-competitive products, recognized testing procedures and standards, and demonstration projects. Special interest is given to the need of improving the electrical and thermal performance of liquid-based PV-T collectors [129], in particular to the research in the thermal absorber design and fabrication [41], material and coating selection, energy conversion and effectiveness, performance testing, system optimization and control and reliability [28].

The total energy output (electrical plus heat) of a hybrid PV-T collector depends on several factors, such as the configuration design and heat extraction arrangement employed; the solar irradiance, ambient temperature, and wind speed; and the operating temperatures of several important components. In most applications, the electrical output is the main priority, in which case the operating condition of the heat transfer arrangement is adjusted to optimize electrical performance. Specifically,

the cooling fluid in the heat transfer circuit is kept at a low temperature to avoid an otherwise undesirable decrease in the electrical efficiency of the PV cell [71,73–75]. Therefore, most PV-T systems deployed to date are aimed at delivering low-temperature heat (<40 °C) [22]. However, this constraint for the heat transfer fluid to exit the collector at low temperatures to allow higher electrical outputs imposes a limit on its posterior use for heating purposes.

It is believed that the PV-T technology can reach a considerably larger market if it was optimized to deliver thermal energy at 40–60 °C, as these are the delivery temperatures of DHW and space heating [22]. Nevertheless, if the system is designed to provide higher fluid temperatures at the PV-T collector outlet, then the electrical efficiency decreases [71,73,75,313]. Hence, a design conflict arises between the electrical and thermal performance of hybrid PV-T collectors, and a trade-off is needed depending on the end-user needs and the local solar and environmental conditions. This conflict, along with the higher costs of PV-T collectors compared to side-by-side PV panels and ST collectors, used to be the two main reasons why these systems are currently not as widely employed as separate, individual PV panels and ST collector equivalents [73].

The energy performance of a PV-T collector depends on the ability of the cooling fluid to extract heat from the collector. An ambitious strategy to boost the market uptake of this technology would be to optimize PV-T collectors to deliver thermal energy at higher temperatures (40–60 °C), whilst mitigating thermal and electrical losses, and ensuring collector reliability and longevity. To this end, the main performance enhancement pathways for collector innovation include: (a) increasing the heat transfer area and/or the heat transfer coefficient between the absorber plate/tubes and the cooling fluid [122,314]; (b) adapt the PV cell technology for its integration in PV-T collectors; (c) using solar selective coatings [314,315]; (d) using spectral splitting techniques; and (e) increasing the thermal conductivity of the working fluid using for example nanofluids [314]. The following sections address these pathways in detail.

3.1. Collector design modifications

Several design parameters influence the performance of a PV-T collector, including the fluid flow rate, the inlet temperature of the working fluid, the number of covers [28], the absorber thermal properties along with the quality of the thermal contact between the cooling fluid and the absorber [121], the PV cell packing factor [27] and the collector design (e.g., tube length, pipe diameter, width to pipe diameter (*W/D*) ratio) [48,122]. Fig. 17 shows an exploded view of a typical PV-T collector, with the different layers and the following sections summarize the main research studies that consider the aforementioned parameters.

3.1.1. Glazing

Several PV-T configurations exist for glazing (i.e., covering with transparent solid windows or plates) [28,120,317], specifically: uncovered, one, two (see Fig. 18) or more covers, along with different filling gases, honeycombs or transparent insulation materials (TIM), as well as evacuation [34].

The use of a cover (such as glazing) reduces thermal losses, thus increasing the thermal efficiency of the collector [121,318], but it also raises the PV cell temperature and the reflection losses, reducing the electrical efficiency [74,76,118]. A previous study concluded that a covered PV-T collector has almost double the thermal efficiency of an uncovered one, but the electrical efficiency drops by around 10% as shown in Fig. 19 [34]. Meanwhile, other studies have estimated that thermal generation increases by between 10% and 30% with the presence of a cover [71,319], while the electrical output decreases by 1–10% [120,319]. In more recent work, the same authors reported a decrease in the first-order heat-loss coefficient (a_1) from 7.07 to 2.17 W/(m^2 K) thanks to the addition of a glass cover, resulting in >30% efficiency at collector temperatures up to 75 °C [121]. However, the cover might also make the PV cells more sensitive to hot spots, and reflection losses and the higher PV cell temperature reduce electrical efficiency [76], by 10–20% reduction in electrical output, most notably at large solar incidence angles [121]. Similar findings were reported for a parallel-pipes PV-T collector made of aluminium alloy, with a thermal efficiency increasing from 44% to 51% with the glazing, while the electrical efficiency dropped from 14% to 13% when the PV cell temperature was around 38 °C [126].

Regarding the number of glass covers, the results of previous research concluded that although a sheet-and-tube collector with two covers has a slightly higher thermal efficiency at elevated water temperatures compared to a single-cover collector, its electrical efficiency deteriorates considerably due to the second cover [120,125]. Consequently, a good balance is needed between the increase in thermal and

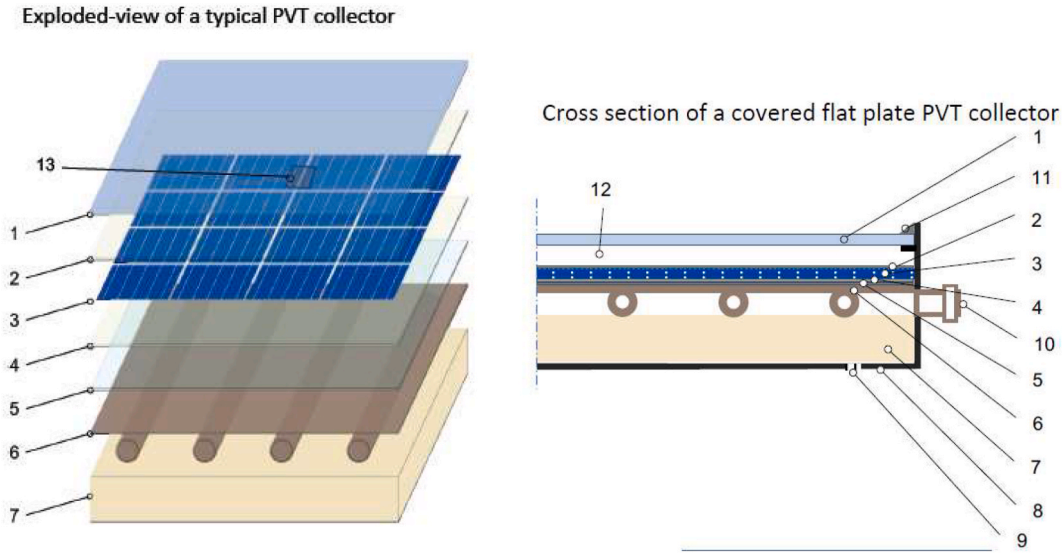


Fig. 17. Exploded view and cross-section of a common, sheet-and-tube PV-T collector design: (1) transparent cover (optional); (2) front cover of PV cells and encapsulant; (3) PV cells; (4) encapsulant; (5) backsheet/rear cover of PV cells and encapsulant (optional); (6) thermal absorber; (7) insulation; (8) casing; (9) air vent (optional); (10) fluid outlets; (11) sealing; (12) gap (optional, in covered collectors); and (13) junction box. Images reprinted with permission from the authors, Hadorn et al. [316].

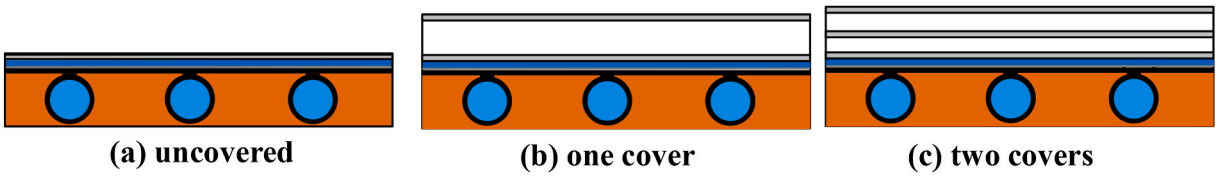


Fig. 18. Most common configurations for PV-T collector glazing. Figure reproduced based on Aste et al. [36] with permission from Elsevier (Copyright 2014 Elsevier).

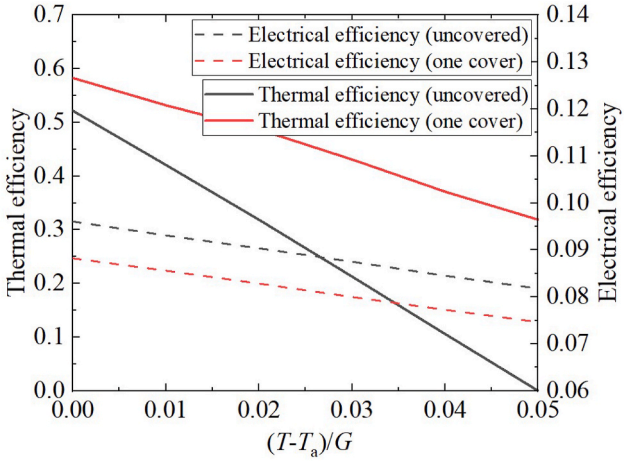


Fig. 19. Thermal and electrical efficiencies of uncovered and covered PV-T collectors (G is the solar irradiance in W/m^2). Figure reproduced based on Zondag [34].

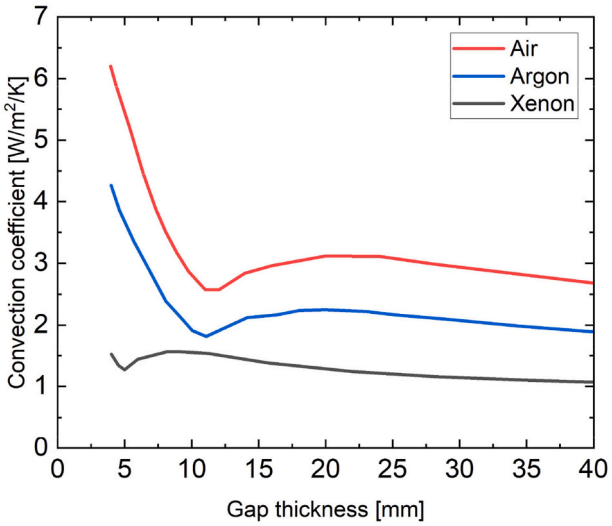


Fig. 20. Convection coefficients as a function of the thickness of the gap between the glazing and PV module for different gases. Figure reproduced based on Antonanzas et al. [317].

electrical efficiencies, being single-covered PV-T collectors an interesting option when a significant thermal output is needed [71], while the best exergy gain is found for uncovered PV-T collectors [28]. In the particular case of low-temperature water demand, the use of unglazed PV-T collectors is recommended for satisfying the demand year-round, with the hot fluid feeding the source of an HP [35,76].

Typical transparent covers are single glass sheets with a thickness of 3.2 mm [128,137,320] or 4 mm [122,317,321,322], due to their optical and mechanical properties. The glass is characterized by high transparency in the visible and near-infrared spectra, while it has an opaque behaviour for far-infrared wavelengths, as it is the radiation emitted by a hot surface. Meanwhile, the gap thicknesses should be thin enough to make use of the insulating properties of the filling gas, while preventing convective flows that would increase the thermal losses [36]. Different gap thicknesses have been considered in the literature: 5 mm [27], 10 mm [122,323], 20 mm [120,127,324], 25 mm [126,134,272,325] and even 40 mm [132]. A previous study analysed the impact of the gap thickness (from 4 to 40 mm) on the convection coefficient between the glazing and PV cells, as shown in Fig. 20. The minimum heat convection loss and maximum thermal efficiency are achieved for a thickness of around 11 mm when using air or argon as an encapsulant [317]. It is observed that the gap thickness has a small influence on the electrical efficiency because the optical efficiency is independent of the gap thickness.

In addition to performance in terms of efficiencies, the use of glazing results in higher stagnation temperatures, which can be useful for certain applications but critical for some PV panel encapsulants [76]. For instance, EVA experiences a deterioration in its mechanical properties and can become brown under UV exposure at 130 °C, reducing absorption [22]. An alternative encapsulant is silicone resin [34]. Another possibility is to remove entirely the PV panel glass cover and associated EVA, in an encapsulant-free PV-T collector [22]. The feasibility of this solution has been demonstrated in covered PV-T collectors with dry air as filling gas [326].

Recently, two innovative PV-T collectors with overheating protection were proposed to avoid excessive stagnation temperatures: venting the collector by opening ventilation channels beneath the thermal absorber, and a switchable film that controls the heat losses by adjusting the distance between the thermal absorber and the polymer film, which substitutes the front glazing. The experimental tests show promising results, reaching a maximum stagnation temperature of 102 °C and 87 °C with both alternatives respectively [327].

There are also different options for filling the spacing between the cover and the PV cells. Honeycombs have been proposed to suppress natural convention and thus reduce convective heat losses [34]. TIM materials have been successfully applied to ST collectors, and it is believed their translucent properties are sufficiently good not to appreciably degrade PV cell performance [34]. Alternatively, some investigators [107,317] studied different options for the gas encapsulated between the cover and the PV cells and concluded that the use of inert gases is particularly promising as the convective heat loss on the top surface is significantly reduced; in the case of argon, the heat transfer coefficient is close to 30% lower than the equivalent for air. This leads to an improvement in the overall heat loss coefficient of around 4.8% for argon.

3.1.2. *Thermal absorber*

As detailed in Section 2.2.1, the most widely studied thermal absorber configuration in water-based PV-T collectors is that of parallel copper tubes (sheet-and-tube), which is also the one used most commonly in commercially-available PV-T collectors [91]. In this configuration, the amount of heat that can be extracted, and thus the overall efficiency that can be achieved, depends upon the W/D ratio (where W is the distance between the pipes and D is the pipe diameter), the collector fin efficiency, and the tube bonding quality [34,72,125]. Consequently, several authors have made efforts to optimize the design of PV-T collectors by paying attention to these design aspects [120,122,125].

Huang et al. [313] studied sheet-and-tube collectors made of different materials, such as extruded sheet-and-tube aluminium or copper tubes attached with thermally conductive adhesive to an aluminium plate, concluding that their performance is not satisfactory. Alternatively, they designed a corrugated collecting plate made of polycarbonate material to improve heat transfer, and concluded, agreeing with other studies [125,328], that to enhance the energy performance of the PV-T collector, the absorber plate should be in direct thermal contact with the PV cells, using it as the base plate of the PV cells. Poor thermal contact results in poorer heat transfer and higher PV cell temperatures, which leads to poor electrical efficiency and, over longer periods, thermal degradation of the PV cells. Previous research reported that improvements to this thermal contact resulted in a 10 °C reduction in the PV cell temperature and thus a 6–8% increase in electrical efficiency [121].

The heat transfer between the cooling fluid and the thermal absorber can be enhanced by increasing the contact area and by creating turbulence. Concerning the former, some investigators added a graphite layer with several recesses to fit the serpentine tube, to enhance the heat transfer between the pipes and thus increase heat transfer [329], while for creating turbulence, in liquid-based PV-T collectors, twisted tapes, perforated tapes, wire coils, inserts/baffle plates, grooves, or internally finned tubes have been used [330]. However, surface modifications and turbulence promoters lead to higher pressure drops, thus increasing the pumping energy consumption [314]. Any heat transfer enhancement is only promising if the gain is larger than this parasitic power increase.

A better convective heat transfer between the coolant and the channels can also be achieved with reduced pipe diameter, D, and an increased number of channels per unit width (e.g., shorter W) [331,332]. In particular, when the W/D ratio decreases, the PV-T collector efficiency increases. The main limitation is the increase in costs and weight of the PV-T collector as the number of channels increases [36]. Typical values of the W/D ratio for sheet-and-tube collectors are 6–10. Alternatively, roll-bond absorbers with thin-film PV cells have been proposed (Design (b) in Fig. 21), increasing the number of pipes to 30, with a pipe distance of 0.02 m [333], along with aluminium roll-bond designs with fractal shape (FracTherm® heat exchanger) [334,335], reporting 87% of global efficiency in controlled conditions, with a maximum thermal efficiency >75% [334]. Similar results are found in another experimental analysis with a covered roll-bond PV-T collector, where 79% thermal efficiency was measured under PV cell operation, when the mean fluid temperature is equal to the ambient temperature, with a corresponding electrical efficiency of 8.7% [336].

He et al. [72] concluded that the collector fin efficiency and the tube-bonding quality (key design factors) can be improved using a flat-box design (Design (a) in Fig. 21). This design has been explored by several authors [72,122,134,313,337–341], with which the W/D ratio can be reduced to 1 when square channels are used [313], improving the fin efficiency and bonding quality, and thus significantly increasing the heat transfer area between the absorber plate and the cooling fluid.

Different channel sizes have been considered: 6 × 4 mm ($W \times H$) [313], 28 × 5 mm [342], 20 × 10 mm [343], or 10 × 10 mm [344], based on the results of a parametric analysis undertaken in previous research [339], which concluded that, to collect more than 90% of the energy, the collector should have a fluid layer thickness smaller than 10 mm. A numerical analysis showed that increasing the number of channels from 1 to 30 improved the thermal efficiency from 42% to 49%, while the PV cell temperature decreased from 51 °C to 46 °C, therefore increasing the electrical efficiency [345]. This was attributed to the increase in the heat transfer area, so more heat can be extracted [122,345]. In this line, the experimental results of a 20 × 10 mm covered flat-box design [343] showed daily average thermal efficiencies of 38–49% (higher in summer), and electrical efficiencies of 10–12% (higher in winter). More recent research by the authors [122] analysed 26 alternative thermal absorber designs, and the results showed that, for a constant flow rate, smaller channels lead to higher thermal efficiencies. This is attributed to the higher water velocity through the channels given the smaller hydraulic diameters, which leads to higher convective heat transfer coefficients. In particular, a flat-box design with 3 × 2 mm^2 rectangular channels appears to be a particularly promising alternative, achieving 4% higher optical efficiency and 15% lower linear heat-loss coefficient compared to a commercial copper sheet-and-tube PV-T collector, a while also lowering the weight (by 9%) and investment cost (by 21%) of the collector.

Alternatively, V-shaped grooves and/or honeycomb grooves (e.g., see Designs (c) and (d) in Fig. 21) have been proposed as means for increasing the heat transfer between the fluid and the PV layer [41,44,346]. An experimental analysis of a polypropylene honeycomb PV-T prototype showed optical efficiencies of 0.51 without electricity generation or 0.39 with electricity generation [346].

Some of these studies [72,134,337] considered extruded aluminium alloy as the thermal absorber material; while in others [122,313,338,339], polycarbonate (PC) was proposed to lower the cost and weight of the PV-T unit. The adoption of a copolymer absorber has several advantages such as a reduction in weight and thus easier installation, a simplified manufacturing process, and a lower investment cost [122,347]. In this context, several authors [35,344] concluded that some polymeric materials, such as PC, have several properties that make them an interesting option for PV-T collectors, such as low density, mechanical strength, no special surface treatment required, no corrosion, ease of manufacturing at mass production as there are fewer components to assemble, and lower production cost because the material is generally cheaper and the manufacturing time is reduced. Other advantages are the freedom they offer in terms of design, as they can acquire layouts that would be very difficult and expensive using conventional materials, and the possibility to bring economies of scale to bear through, for example, extrusion processes which allow mass-production of complex geometries in lengths of kilometres [348]. Furthermore, previous LCA results [349] indicated that polymeric solar collectors appear as best as regards climatic and environmental performance when they are expressed in terms of the IPCC 100a indicator and the Ecoindicator 99, H/A indicator, respectively.

Nonetheless, there are also some disadvantages associated with the use of polymeric materials [35,341], such as low thermal conductivity, large thermal expansion, and limited-service temperature. Specifically, the ideal polymer for this application should have the following properties: UV protection, high thermal conductivity, water-resistant and glycol-resistant, good thermal range of utilization (−10/+150 °C), good mechanical strength, and be chemically stable [338,339,344]. To overcome the low thermal conductivity, PV-T collector geometries can be optimized to ensure homogenous flow and maximize the contact area between the absorber and the heat transfer fluid [348]. Previous work [122] showed that a PC flat-box design with small channels (3 × 2 mm) experiences lower von Mises stress than a copper sheet-and-tube collector (<13% *vs.* 64% of the material's yield stress), which is attributed to the larger thermal expansion of the PC thermal absorber, so this type of polymeric PV-T collectors are not expected to suffer higher strains

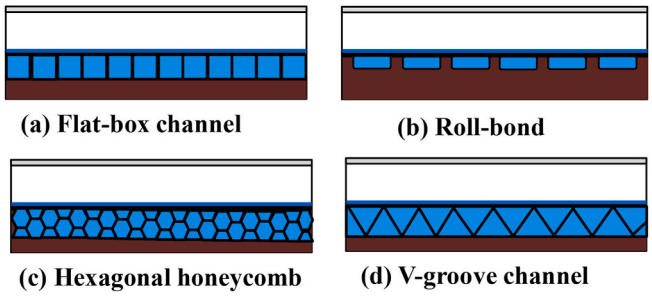


Fig. 21. Different structures of the thermal absorber to increase heat transfer [36,42,44]. Figure reproduced based on Pang et al. [42] with permission from Elsevier (Copyright 2020 Elsevier).

than copper PV-T collectors.

Loading the polymer with additives can also improve its thermal conductivity [350,351]. However, recent studies have concluded that the small improvement in the thermal performance of a polymeric flat-box PV-T collector might not outweigh the higher complexity and costs of loading the polymer with additives [122].

Another thermal absorber design proposed by Xu et al. [352] consists of two parallel thin flat-plate metal sheets, one of which is extruded by machinery mould to form arrays of mini corrugations, while the other one is attached beneath the PV cells. Both sheets are laser-welded together to form turbulent flow channels. The laboratory testing results showed that this PV-T collector can achieve an electrical efficiency of 17% and a thermal efficiency of nearly 65% at standard testing conditions (STC).

The best manufacturing process that would ensure the ideal thermal contact between the thermal absorber and the fluid is to laminate the whole package of the top cover, PV cells, and a flat absorber together in one step [353]. In this case, an electrically insulating foil can be interposed between the PV cell and the absorber in the lamination process, or an electrically insulating coating can be applied to the absorber's top surface [34]. Recent research showed that laminating the solar cells directly to a copper metal thermal absorber can reduce the thermal resistance by around 10% thanks to the effective heat transfer from the PV cells to the heat transfer fluid [354]. Another solution is to deposit the PV material directly on the absorber, with an insulating coating or galvanic separation between cells, as applied to the a-Si cells.

3.1.3. PV surface

The effective utilization of the surface area of a collector that is exposed to solar radiation is of primary importance and interest. When the PV cells are placed above the thermal absorber section to achieve high electrical performance, the presence of the cells leads to a reduction of the heat flux into the collector fluid circuit, reducing the thermal efficiency [132]. Previous studies [27,328,355] investigated the trade-off between larger coverage areas for increased electricity generation and smaller coverage areas when the priority is hot water production. The simulation results of a validated dynamic system model showed that the higher the covering factor and the glazing transmissivity, the better the overall performance [325].

Zakharchenko et al. [328] concluded that the solar PV cells area should be smaller than the absorber size, and that the PV cells should be located where the coolant enters the collector. This is due to the reduction of the heat flux to the solar collector when the PV cells are located above the absorber, thus reducing the collector's thermal efficiency. Furthermore, as the coolant/fluid's temperature increases, the rate of heat extraction from the PV cells. As a consequence, as the area covered with PV cells increases, the panel cooling decreases, impairing one of the core advantages of hybrid PV-T or conventional PV systems [328]. Other studies [355] concluded that depending on the user needs, PV-T collectors should be partially covered by PV cells when the priority is hot water production or fully covered when the priority is electricity generation. More recent research [27] concluded that for the case of the UK, complete coverage of the solar collector with PV cells leads to the coverage of a higher fraction of the annual electricity demand while maximizing the CO_2 emission savings. In addition, economic assessments of PV-T collectors with different covering factors showed that the lowest payback time and levelized production costs are achieved by fully covered collectors [91].

In summary, research to-date has shown that partially covered collectors can achieve better thermal efficiencies (with the PV cells located near the collector fluid inlet), while fully covered PV-T collectors enable maximum electricity generation but lower thermal yields. However, one should bear in mind that this trade-off is sensitive to the solar and environmental conditions at the geographical location of the installation, and that the overall preferred designs require that the relative value of the electrical and thermal outputs are known.

3.1.4. Phase-change materials

Increasing efforts are being made in the context of integrating PCMs with PV cells and modules. In early work, investigators considered the integration of PCMs with PV cells (PV-PCM) as a solution for limiting the temperature rise in BIPV systems [356]. If designed appropriately, PCMs can offer not only temperature reduction of PV cells, but also compact thermal storage with a stable temperature [357]. Previous work was extensively focussed on using PCMs only for the thermal regulation of PV cells [239], in which the electrical output is the sole design target [358]. The typical design of such PV-PCM systems is by integrating PCMs at the rear side of PV cells. The high thermal storage capacity of PCMs can shave the peak temperature of PV cells, leading to a more stable and flatter operation temperature, which is thus beneficial for efficiency and lifetime. Paraffin wax with melting temperatures around 25–35 °C has been extensively employed in PV-PCM systems [239,359–362]. It was reported that the peak temperature drop of PV panels can be as high as 20 °C [363,364], and an average electrical efficiency improvement of around 1–8% is attainable [365,366]. Other studies [367] used a water-saturated microencapsulated PCM layer as a passive thermal management medium for a BIPV panel. However, as the purpose of the above studies was to limit the temperature rise of PV cells, the phase-transition temperature of the applied PCMs was typically close to ambient temperature and thus the stored thermal energy was of low value.

More recently, researchers explored the possibilities of using PCMs for both electrical and thermal performance improvements of PV-T systems, forming the so-called PV-T-PCM systems. The design considerations of such systems are very similar to those in PV-PCM systems, but the desired phase-transition temperature could be higher to increase the usefulness of the collected heat. Studies observed that with an additional stable useful thermal output, the electrical efficiency of the PV-T collector can also be improved when integrating with PCMs. Some authors [368] proposed a PV-T-PCM hot water system. Numerical results showed that, by including an appropriate PCM in an optimized system, the PV cell output can be increased by typically 9% with an average water temperature rise of 20 °C. Experiments on PV-T-PCM collectors under clear sunny days at Mashhad (Iran) [369] showed that the electrical efficiency is improved by about 10% with additional thermal output at temperatures of 40–50 °C accounting for around 5.5 × the electrical output. In another work [370], it was found that the PV-T-PCM collector performed better in comparison with conventional PV-T collectors in terms of electrical efficiency, but the maximum thermal efficiency was slightly lower. Other authors [371] conducted experimental comparisons of a PV-T-PCM hot water system and a standard PV-T hot water system. Using fatty acid eutectic, capric-palmitic as the PCM, it was found that the PV-T-PCM system was able to maintain the water at a higher temperature for an extended period of time (by 100%).

Building-integrated PV-T-PCM collectors emerge as a promising technology for ventilation and space heating. A ceiling ventilation system integrated with a PV-T-PCM collector was proposed [372], where the air was used as the heat transfer medium between the PV cells and the two PCM layers. The indoor thermal comfort of the building was significantly improved with a maximum air temperature rise of 23 °C.

Low-temperature PCMs are typically characterized by their low thermal conductivity, which limits the heat transfer performance for charging and discharging heat, further influencing both the thermal and electrical performance of PV-T-PCM collectors. Adding nanoparticles with high thermal conductivity into a PCM enhances its heat transfer performance, forming the so-called nano-enhanced PCM (NePCM). Several studies have explored the performance potential of PV-T-NePCM using different nanoparticles, including SiC [373,374], graphene nanoplatelets (GNP) [375], Al_2O_3 [376,377], multi-walled carbon nanotube (MWCNT) [378], or CuO [379], as summarized in Table 6. Although the performance improvement of PV-T-NePCM collectors compared to PV-T-PCM, PV-T and PV panels varies in different studies and operation conditions, previous work demonstrated that adding nanoparticles into the PCMs can improve the thermal and electrical efficiencies, so this has

emerged as a promising direction.

In practice, the selection of the appropriate PCMs depends on many factors, including the desired temperature of thermal output, weather conditions, or weighting between electrical and thermal efficiencies. Trade-offs are always needed between the thermal and electrical outputs. It is estimated that PV-T-PCM collectors have a TRL of around 5–6 without any PV-T-PCM collector manufacturer yet. As the integration of PCMs increases the capital costs and system complexity of PV-T collectors compared to conventional PV-T collectors without PCMs, the cost-competitiveness of PV-T-PCM collectors needs to be improved to make them practically more attractive.

3.1.5. Aerogels

Aerogels are an emerging material in the field of PV-T technology that have been attracting significant attention in other research fields, such as building thermal-insulation windows [380], solar-thermal receivers [381], space launch applications [382]. Highly-transparent silica aerogels are a type of emerging thermal insulation material capable of reducing the heat loss of PV-T collectors [383]. Silica aerogel materials have low thermal conductivities and high transmittance (96% [383] and >80% [384], respectively). The highly-transparent aerogel layer is usually added on the top surface of a PV-T collector to reduce the heat loss with a slight impact on the electrical efficiency, as shown in Fig. 22. The modelling work by Wu et al. [385] shows that the heat loss of a PV-T collector covered with a 20-mm-thick silica aerogel layer is only 140 W/m^2 when the operating temperature is 70 °C, which is significantly smaller than that of a conventional covered PV-T collector (heat loss of 300 W/m^2). Therefore, the thermal efficiency of the aerogel-glazing PV-T collector is significantly improved, by 46%. The electrical efficiency of the aerogel-glazing PV-T collector is similar to that of a covered PV-T collector, as the transmittance of the aerogel layer is close to that of the glass layer (see Table 7). Overall, the exergy efficiency is improved by 17%, while the total cost of the aerogel-glazing PV-T collector is only 1.4% higher than the conventional covered PV-T collector [385].

An aerogel-glazed PV-T collector was built and tested by Weinstein et al. [383]. The 10-mm-thick aerogel layer had a solar-weighted transmittance of 96%, which is higher than the glass transmittance normally used for PV-T collectors, and low thermal conductivity (see Table 7), thus effectively reducing heat losses, especially at high operating temperatures. The compressive and flexural strength of the silica aerogel were around 3 MPa and 0.2 MPa, which is strong enough for PV-T applications. Comprehensive mathematical models of aerogel-glazed PV-T collectors were introduced by Du et al. [386] and Wen et al. [387]. It is expected that the rapid development of aerogel technology will promote the further development of high-performance PV-T technologies.

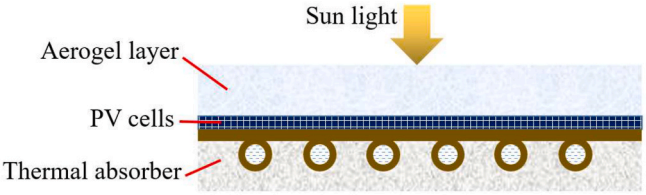


Fig. 22. Schematic of a PV-T collector covered with a highly-transparent aerogel layer [385].

Table 7
Properties of typical aerogels applied to PV-T collectors.

Aerogel material	Transmittance	Thermal conductivity (W/m K)	Thickness (mm)	Ref.
Silica	96%	0.055	10	[383]
Silica	87–96%	~0.03	10–40	[385]
Silica	N/A	0.02	50	[386]
Silica	N/A	0.02	10–70	[387]

3.2. Next-generation PV cell technology

The PV cells used in all current, commercially available PV-T collector products, but also more state-of-the-art collectors currently under development, are designed for PV (i.e., pure electricity-generation) applications, such that their optical and electrical designs (e.g., surface structure) and fabrication methods are optimized to maximize electrical generation without any consideration to thermal generation. This is beneficial for PV applications, but detrimental when used in PV-T collectors, as the thermal energy recovered (and, ultimately, delivered) by the latter will also have a value. Secondly, there is a further design conflict between the electrical and thermal performance of PV-T collectors, and a trade-off is needed depending on the end-user needs and the local environmental and economic conditions. Specifically, as mentioned in Section 1.2, the efficiency of PV cells decreases with temperature, so the cooling fluid of the PV-T collectors should be kept at a lower temperature when the electrical output is the main priority. This constraint for the heat transfer fluid to exit the collector at low temperatures imposes a limit on its posterior use for heating purposes. On the contrary, if the PV-T collectors are operated at higher fluid temperatures, then the electrical efficiency decreases. Therefore, there is a design conflict between the electrical and thermal performance of hybrid PV-T collectors, and a trade-off is needed depending on the end-user needs and the local solar and environmental conditions. In an attempt to solve this conflict, different types of next-generation PV cell technologies have been analysed for their integration in PV-T collectors,

Table 6
Summary of recent studies on PV-T-NePCM systems.

PCM	Nanoparticles	Year	Nature of work[a]	Performance improvement	Ref.
Paraffin wax	SiC (0–4 wt%)	2017	Exp	Thermal efficiency: 35%, 51%, 72%; electrical efficiency: 10%, 12%, 14% for PV-T, PV-T-PCM and PV-T-NePCM collectors, respectively	[373]
Paraffin wax RT24	SiC (0–4 wt%)	2018	Exp	Electrical efficiency: 13%, 8% for PV-T collectors and PV panels, respectively	[374]
Paraffin wax	GNP (20 wt%)	2020	Theo	Thermal efficiency: 13%, 39% at 70 °C; electrical efficiency: 13, 14% for PV-T and PV-T-NePCM collectors, respectively	[375]
Paraffin wax RT35	Al_2O_3 (0.04 vol%)	2021	Theo	The thermal and electrical efficiencies of the PV-T-NePCM collector reached 70% and 13%, which is 26% and 0.2% higher than the PV-T collector, respectively	[377]
Paraffin wax RT44HC	MWCNT (0.009 wt %)	2021	Exp	Maximum energy efficiency: 75%, 83%, 85%; maximum exergy efficiency: 10%, 11%, 13% for PV-T, PV-T-PCM and PV-T-NePCM collectors, respectively	[378]
Paraffin wax RT35HC	Al_2O_3	2021	Theo	Electrical efficiency: 13% for PV-T-PCM and PV-T-NePCM collectors; thermal efficiency enhanced by ~3%	[376]
Paraffin wax RT42	CuO (1 wt%)	2022	Exp	Thermal efficiency: 63%, 66%, 69%; electrical efficiency: 12%, 13%, 13% for PV-T, PV-T-PCM and PV-T-NePCM collectors, respectively	[379]

[a] Exp: experimental; Theo: theoretical

including innovative PV cell technologies, as detailed below.

3.2.1. Performance aspects

Silicon technologies hold the largest market share by a large margin (94% in 2019 [388]) with a large number of manufacturers mainly based in China, followed by cadmium telluride (CdTe) thin-film principally manufactured by First Solar, then copper indium gallium selenide (CIGS) principally manufactured by Solar Frontier.

Fig. 23(a) shows the relative power output ($P(T)$) for a series of different solar cell technologies, two variants of c-Si (the present market leader), CIGS, silicon heterojunction (SHJ) (a high-performance variant of c-Si), gallium arsenide (GaAs) and CdTe. All the cells lose power with increased temperature, but the degree to which power is lost depends on some fundamental cell properties that can help guide the choice of a PV-T system (see Section 1.2). Illustrative temperature dependencies for a silicon solar cell are shown in Fig. 23(b). The temperature coefficient of power (β_{Pmax}) is given by the gradient of the lines shown in Fig. 23(b).

Hence different silicon PV technologies can exhibit quite different temperature coefficients, indicated by the data shown in Fig. 24, where the SHJ cell achieves the lowest temperature coefficient due to an elevated cell voltage.

Some studies [28] concluded that the thermal performance of PV-T collectors based on c-Si cells is comparable to that of a-Si cells, while others [71,135]) obtained higher thermal efficiencies for water-based PV-T collectors with a-Si (~60% at zero reduced temperature) than for PV-T collectors with pc-Si (~55% at zero reduced temperature). Thin-film technologies, such as hydrogenated amorphous silicon (a-Si:H), appear as an interesting alternative thanks to their low manufacturing costs (about 1.5 USD/kW$_p$), low embodied energy per watt peak [393], less brittle and easiness to be attached to different surfaces including printable laminate. However, the electrical efficiency is lower (around 5–7%) [127,394] and it uses heavy metals that reduce its usage [395].

This shows that so far there are discrepancies about which PV cell type is better to use in a PV-T collector. It is believed that the choice should be made according to the specific end-user needs, being interesting the use of a-Si when high thermal efficiency is required, while when the main priority is electricity generation, pc-Si can be a more suitable option. Previous authors [328] concluded that the use of conventional PV cells is not appropriate for their integration in PV-T collectors as they have poor thermal conductivity in the rear surface which hinders the efficient heat extraction by the solar collectors. Hence, a modification of the commercial PV panel is needed to provide the collector with a good substrate material such as aluminium.

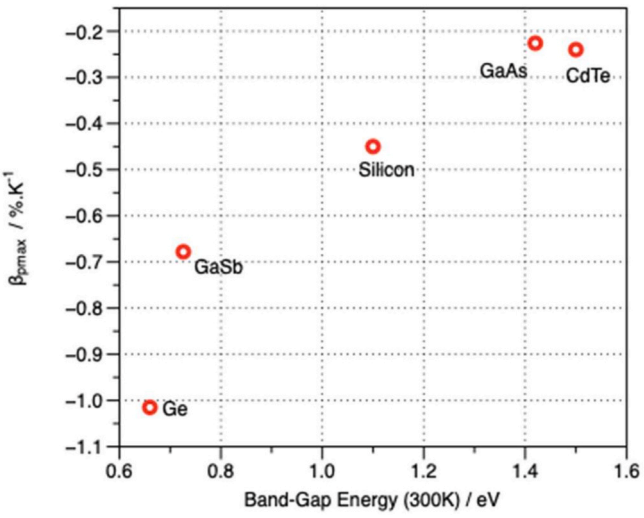


Fig. 24. Temperature coefficients of single-junction solar cells as a function of band-gap energy. Data from Refs. [389,390].

3.2.2. Tandem cells

A popular and nowadays well-understood means for augmenting the efficiency of a PV cell is to use several solar cells with different band-gaps to selectively absorb different parts of the solar spectrum. This preserves a larger fraction of the free energy in the incident sunlight and uniquely for PV-T collectors also offers the possibility of directing light that is unproductive for electrical power generation to a thermal absorber. Three configurations of this approach are shown in Fig. 25.

The monolithic and multi-terminal approaches make use of the property that a semiconductor becomes comparatively transparent for photon energies below the band-gap by cascading the band-gap energy from high energy to low naturally sorts photons into the appropriate sub-cells. In the case of the spectrum splitting configuration, the sorting of photons is achieved using a dichroic mirror, allowing long-wavelength photons to pass through while directing shorter wavelength photons to a suitable low band-gap solar cell.

To evaluate the performance of these two separate approaches we

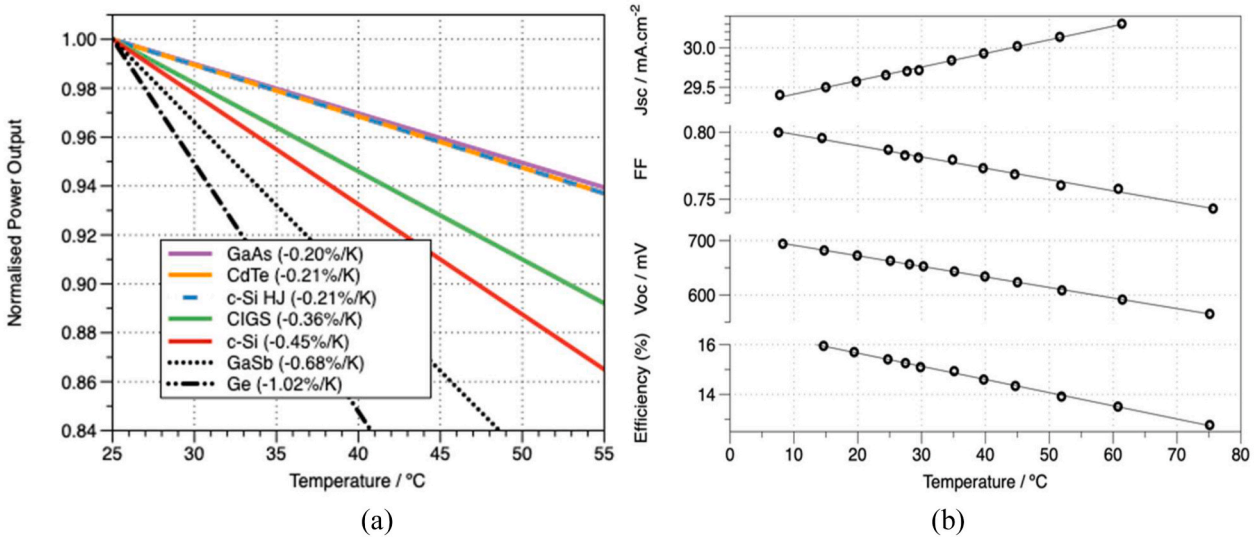


Fig. 23. (a) Relative power loss with temperature for different solar cell technologies. All lie between the boundaries shown by dotted lines of -0.1%/K and -0.5%/K; data from Refs. [389–391]. (b) Dependency of J_{sc}, FF, V_{oc} and efficiency for an early silicon PV cell; figure reproduced from Green [392].

note that Configurations (b) and (c) in Fig. 25 are geometrical permutations of the same approach and have similar limiting efficiencies. The only difference is that the opportunity for radiative coupling between sub-cells, whereby any radiative emission from the high-gap cell through Process (4) in Fig. 2(b) is lost in the case of the spectrum splitting Configuration (c) of Fig. 25, whereas it is transmitted into lower-lying junctions [396] in: (a) the monolithic; and (b) multi-terminal tandem configurations shown in Fig. 25.

The efficiency for monolithic and multi-terminal tandems is plotted in Fig. 26 along with the two limiting cases for the solar cell configuration depicted in Fig. 2(c): (i) where only light in the semiconductor is absorbed or (ii) where the full solar spectrum is absorbed. In these calculations, the cell is maintained at 300 K, hence only the thermal generation varies depending on whether solar absorption only takes place in the semiconductor (Fig. 26(i)) or the full solar spectrum is absorbed (Fig. 26(ii)). In the case of semiconductor absorption only (Fig. 26(i)), similar peak electrical efficiencies can be obtained with either high or low thermal generation. With full solar absorption (Fig. 26(ii)) the peak electrical efficiency will always coincide with the minimum electrical generation.

3.3. Selective coatings

Another way to enhance the energy performance of PV-T collectors is to maximize the solar irradiance harnessed through the application of coatings on the absorber surface [314,315]. Conventional solar thermal collectors are carefully engineered to have strong absorptivity for solar wavelengths yet minimal emissivity at the operating thermal wavelengths, typically >7 μm [397]. As discussed in Section 1.2, silicon PV cells have strong absorptivity from UV to mid-IR, but from wavelengths larger than 5 μm, the emissivity of the solar module is dominated by the module glass [29]. Fig. 27 shows the absorptivity and emissivity from a silicon PV panel with cover glass, unencapsulated, confirming the high emissivity at wavelengths where radiative loss at 60 °C will take place [22].

These losses can be mitigated by using low-emissivity coatings, similar to those used on energy-efficient windows [398]. Typically these coatings are made from transparent conducting oxides (TCOs) where reflectivity is high above the plasma frequency for example indium tin oxide (ITO) and aluminium zinc oxide (AZO) [399,400]. Applying an AZO film onto a double-glazed flat-plate collector achieved a thermal emissivity of 0.3 yet retaining a solar transmittance of 0.85 [401]. A more recent multi-layered coating achieved an emissivity of 0.13 and solar transmittance >0.8 [402]. TCOs have a much higher transmittance compared to silver-based coatings [401], typical films used in an efficient glazing are In_2O_3:Sn (ITO), TiO_2:Nb, ZnO:Al [403].

The consequences of controlling the PV-T collector emissivity are dramatic. Fig. 28 shows the projected annual thermal yield from different configurations of PV-T collectors with different thermal emissivities and module filling compared to a standard ETC. To reach high-temperature applications, such as air-conditioning using absorption chillers, achieving low emissivity is critical. The PV-T collector heat evacuation then becomes a critical factor to reduce convective thermal losses [22].

Optical coatings can also be used to control the colour of a PV panel, although this can only be achieved by reflecting what would otherwise be productive sunlight from the PV-T collector back towards the observer [404]. Normally, PV-T collectors are configured for optimum electrical and thermal outputs, but in the case of BIPV-T systems, the visual appeal of the system becomes an important consideration so impaired electrical and thermal performance might be tolerable [405].

3.4. Spectral splitting

The fundamental aim of spectral splitting technology is to harvest solar energy at its highest potential [406,407]. Thus, from a theoretical perspective, spectral splitting fundamentally shifts the goalpost from maximizing the energetic efficiency of a single element to maximizing the exergetic efficiency of the system. At the ideal limit (i.e., neglecting losses and costs), this would lead to a design where the solar spectrum would be split into an infinite number of bands with a corresponding number of receivers to optimally convert each band to useful energy, as indicated in Fig. 29. Neglecting losses, this type of system can approach 100% exergetic efficiency if all of the incoming solar energy were to be converted into electricity (e.g., with each receiver being a PV cell with a perfectly matching band-gap). In reality, of course, pursuing this approach would likely lead to very low exergetic efficiency since it would be plagued with optical and electrical losses. Additionally, converting the longest wavelengths of the solar spectrum into electricity is of dubious marginal benefit since the practical efficiency and open-circuit voltages of IR PV cells decreases considerably (i.e., germanium cells are ~15% efficiency and have an open circuit voltage of only ~500 mV [408]). Thus, rather than an infinite number, most of the proposed spectral splitting designs from the literature target 1 to 3 'splits' [409,410]. Additionally, in a PV-T beam splitting design, the longer wavelengths (e.g., >1.1 μm, longer than the band-gap of Si cells) are typically lumped together and sent to a thermal receiver.

Given the aim of maximizing exergetic efficiency, spectral splitting systems often (but not always) employ optical concentration to enable the thermal receiver to operate at higher temperatures (targeting higher thermodynamic quality thermal outputs) than would be possible

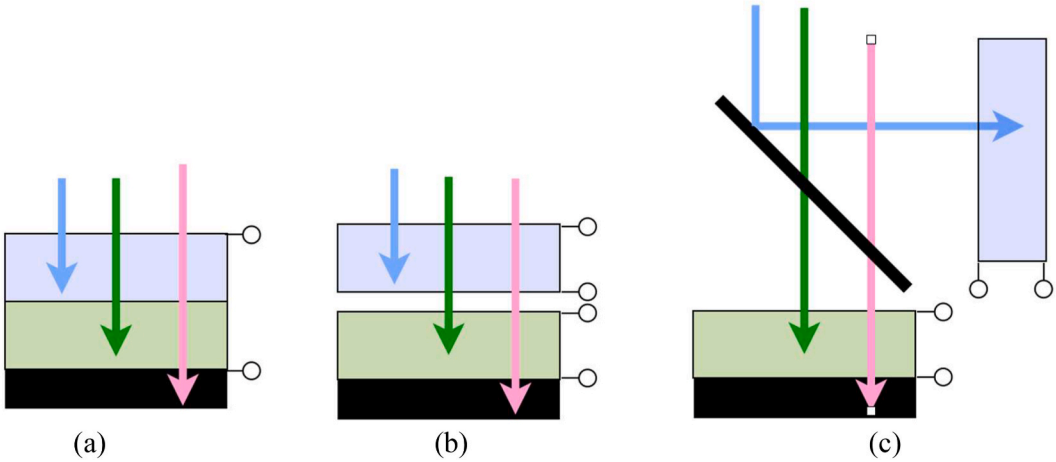


Fig. 25. Three configurations of a multi-junction solar cell: (a) monolithic series-connected tandem; (b) multi-terminal mechanical stack tandem; and (c) spectrum splitting.

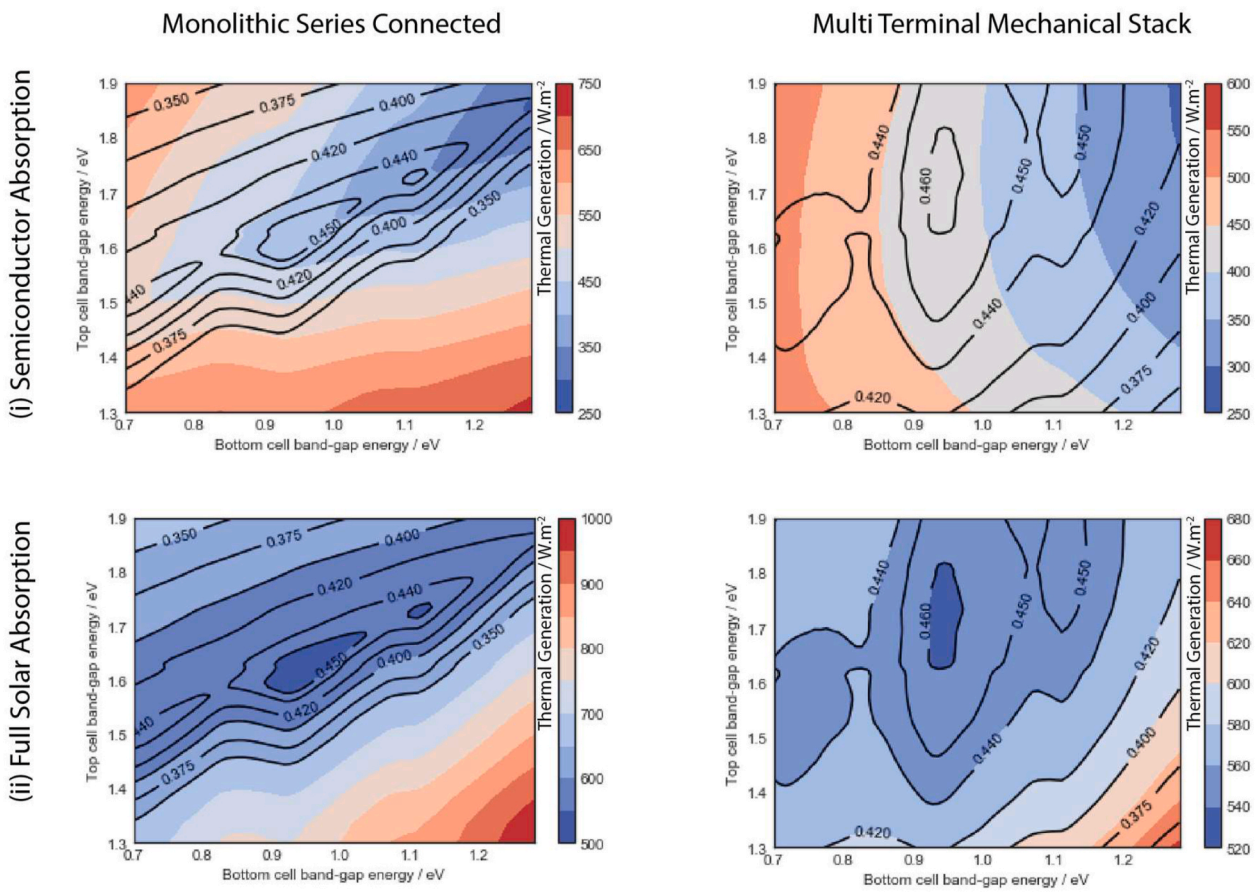


Fig. 26. Limiting iso-efficiency contour plots showing four permutations of monolithic or multi-terminal mechanical stack double junction solar cells. The plots are overlayed with the thermal generation that takes place either in the case of: (i) semiconductor absorption only; or (ii) full solar absorption.

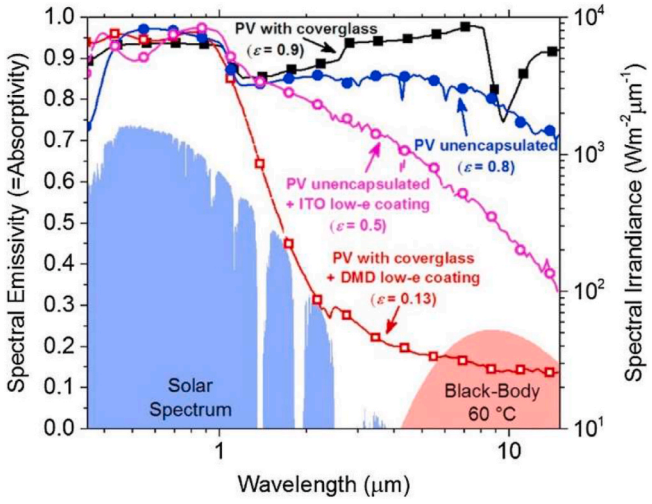


Fig. 27. Experimentally measured emissivity data for different permutations of a PV cell with and without module cover glass and low-emissivity coatings. Reprinted from Mellor et al. [22] under the Creative Commons Attribution 4.0 International (CC-BY 4.0) license.

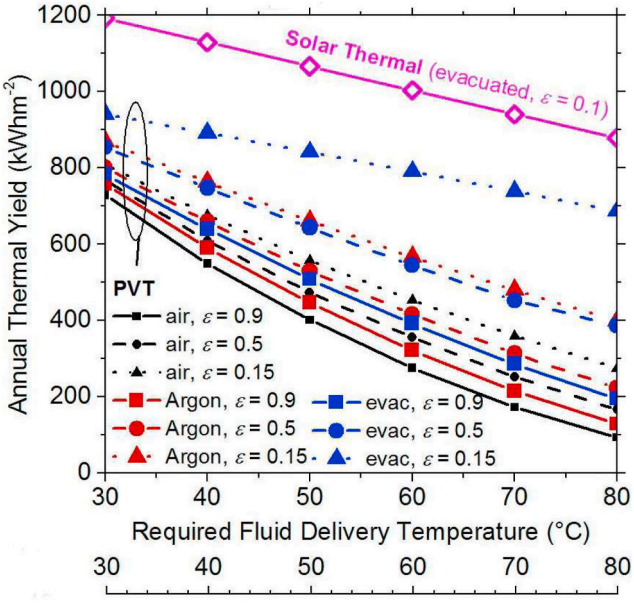


Fig. 28. Projected thermal yield per unit of collector area, as a function of the fluid delivery temperature, from a PV-T collector located in the Mediterranean (Athens) with different emissivity and collector filling: air, Argon or vacuum. Reprinted from Mellor et al. [22] under the Creative Commons Attribution 4.0 International (CC-BY 4.0) license.

without optical concentration. A spectral splitting system makes this strategy viable since the thermal receiver and PV receiver(s) are typically physically separated so they can be considered as 'thermally decoupled'. That is, since they are uncoupled, operating the thermal receiver at elevated temperatures does not necessarily have a detrimental impact on PV cell performance in a beam-splitting system.

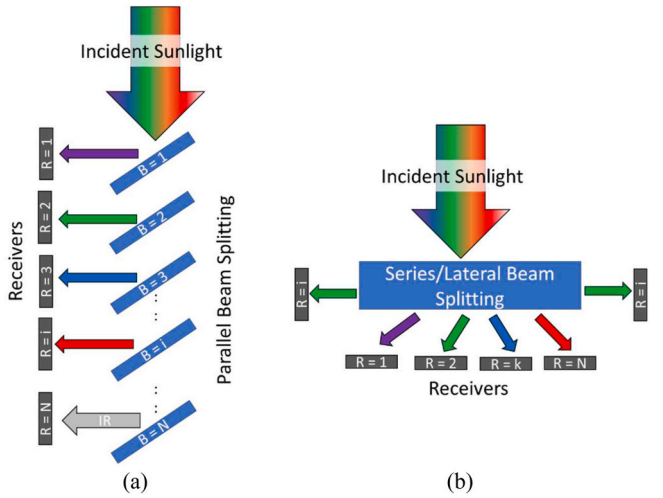


Fig. 29. Generalized spectral splitting configurations with N receivers: (a) parallel; and (b) series/lateral. Note that several combinations of these general configurations have been used in the literature.

Harvesting the solar spectrum at its highest potential is motivating and challenging, so numerous approaches have been devised in the past few decades. These approaches can be broken down into a few major categories, which include liquid filters, dichroic mirrors/filters, holographic filters, refraction/prisms, luminescent/fluorescent materials, and the utilization of intrinsic PV material transmission/reflection.

3.4.1. Solid spectral splitters

As one of the oldest optical elements, a prism can split up the solar spectrum. Since a prism splits light laterally, much like Fig. 29, a simple design can be envisioned in which PV cells and/or thermal receivers would simply be placed at the appropriate location to collect their portion of the dispersed light. While this seems relatively straightforward, it requires rotational tracking and some optimization to avoid overlap of the spectral band with the PV band-gap energies [411,412]. A limitation of this approach is that spatial separation for each part of the spectrum is limited. However, this can be mitigated by collecting light over a larger area by using a saw tooth design rotational tracking [413]. PV-only panel studies have been conducted for linear focus systems (with concentration ratios of $>100\times$), which achieved electrical conversion efficiencies of up to 60% [414]. As an example, some authors used an optimized plastic prismatic structure (a curved sawtooth) to split the solar spectrum into three parts, for cells with short, medium, and long band-gaps [415]. They found that with this design it is possible to send 91% of the 400–730 nm band to a gallium arsenide cell, 76% of the 730–1000 to a silicon cell, and 71% of the 1000–1350 nm band to the germanium cell [415]. This type of system is relatively easily converted to a PV-T design by replacing the lowest efficiency or highest cost (e.g., any non-silicon) PV cells with a thermal receiver.

Another solid material for spectral splitting is selectively absorbing glass. A simple configuration for silicon-based PV cells is to place a coloured glass (which absorbs short wavelengths) before the cells. If the coloured glass has a pure fluid like water flowing over it, such as in Mojiri et al. [416], this design represents a robust and cost-effective PV-T system that can be employed with or without concentrating optics to pre-filter out all the unused portions of the solar spectrum before they hit the PV cell.

3.4.2. Liquid spectral splitters

All inorganic (e.g., water and ionic liquids) and organic (e.g., natural oils and synthetic heat transfer fluids) liquids exhibit some amount of spectral selectivity since their optical properties are not constant over the whole electromagnetic spectrum. However, the ideal spectral splitting liquid would provide both good thermophysical properties and optical properties which match with a PV cell. Intriguingly, pure water is quite close to the ideal. As shown in Fig. 30, water provides a good match with silicon solar cells (i.e., it absorbs IR and a bit of UV, but it is transparent to the visible spectrum). The long-wavelength absorption of water is due to the stretching and bending modes of hydrogen bonds between the water atoms [417]. Fig. 30 shows that the key non-ideality of this approach is that it is nearly impossible to achieve a sharp spectral splitting curve. That is, the sharp, square-shaped ideal Si PV filter curve shown in Fig. 30 is impossible to achieve with a real fluid. In terms of performance, this means that neither the PV cells nor the thermal receiver will receive the full, ideal spectrum. Imprecise spectral splitting is not a major loss for the thermal receiver since it should be able to absorb well outside of the ideal range but can significantly hurt the performance of the PV cells.

Water is intriguing because of its relatively low cost (<1 USD/L), higher stability, and good thermal properties for heat extraction. In contrast, while oils and heat transfer fluids can provide slightly better selective optical properties for a PV-T system (see Fig. 30), they are more expensive (e.g., >1 USD/L) and much less stable when exposed directly to ultraviolet radiation [418]. This is because they include organic bonds such as carbon–carbon bonds and carbon-oxygen (i.e., single bonds) which are weaker than the oxygen-hydrogen bonds of pure water, ~350 kJ/mol compared to 460 kJ/mol [417]. The relative stability of these fluids when exposed to sunlight is apparent when comparing these bond energies are compared to the Plank–Einstein relation for the energy carried by incoming light (converting to a kJ/mol basis) [417]:

$$E=\frac{hc}{\lambda}=\frac{6.63\times10^{-37}\ (\mathrm{kJ\ s})\ 3.0\times10^{17}\ \left(\frac{\mathrm{nm}}{\mathrm{s}}\right)\ 6.02\times10^{23}\ \left(\mathrm{mol}^{-1}\right)}{\lambda} \tag{3.8}$$

Rearranging to solve for the cut-off wavelength which has enough energy to break bonds gives:

$$\lambda=\frac{1.2\times10^{5}\ (\mathrm{kJ\ nm/mol})}{E\ (\mathrm{kJ/mol})} \tag{3.9}$$

Thus, by substituting $E=350$ kJ/mol and 460 kJ/mol into (Eq. (3.9), it can be realized that UV light of 340 nm and shorter has enough energy to break organic bonds, while it takes 260 nm UV light to break the stronger hydrogen-oxygen bonds of water. For reference, 3.7% of the energy in the extra-terrestrial spectrum and 0.8% of the energy in the AM1.5 spectrum is ≤ 340 nm and shorter. In contrast, only 0.27% of the extra-terrestrial spectrum and a negligible amount of the AM1.5 spectrum is ≤ 260 nm. Thus, aside from the challenges of selecting fluids with good optical properties and good thermal stability, organic fluids also need some form of protection from direct UV exposure to maintain

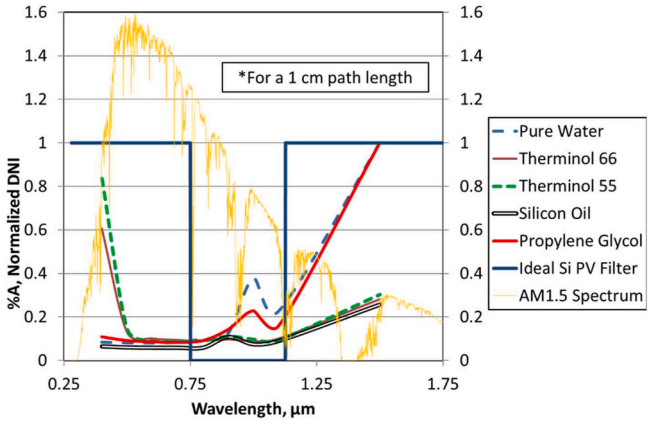


Fig. 30. Absorbance of selected pure fluids compared to the spectrum of AM1.5 direct normal irradiance and to an 'ideal' silicon PV-T filter.

their stability in a PV-T system.

3.4.3. Dichroic mirrors/filters

Dichroic mirrors use a stack of alternating layers of high and low refractive index materials (e.g., SiN_x/SiO_2 [419]) to achieve selective reflection/transmission. As optical elements, these are essentially thin-film interferometers, wherein the incident beam is superimposed with itself to achieve destructive interference to suppress the propagation of desired spectral bands. As such, these devices are essentially just extensions from Fabry and Perot's original interferometer [420] which used a pair of partially reflecting mirrors to create interference fringes that can be used to analyse (or control) the spectral properties of light propagating through a system. Modern chemical vapour deposition and sputtering methods now allow nanometre-level control over each layer of the resulting thin film structure to ensure a sharp transition from high transmission to high reflection at the design 'cut-off' wavelength(s). (Note: A similar approach is used in a distributed Bragg reflector when such layers are embedded inside a waveguide material). A dichroic mirror was employed in 2015 by Green et al. [421] to exceed 40.4 ± 2.8% efficiency with a design that split incoming concentrated light between a multi-junction cell and a silicon cell.

The underlying physics of these types of thin film is that interference occurs when light partially reflects off layers which are roughly 1/4th of the thickness of the target incident wavelength. By stacking combinations of these quarter wavelength designs together, the resulting dichroic mirror can be designed to create a simple edge-pass/edge-stop filter or a band-stop/band-pass optical element (such as the one used in Green et al. [421]). Several companies offer stock and custom designs of these materials [422–424], but they are typically orders of magnitude too expensive (e.g., 1×10^5 to 1×10^6 USD/m^2) for PV-T collectors [425]. Ignoring their cost, nearly ideal optical properties can be achieved through careful design. Thin-film software packages, such as OpenFilters or OptiLayer, use the needle optimization technique to specify the number of layers and the thickness of each layer for a given pair of dielectric materials [419,426,427]. Dichroic filters are often custom designed for many optical applications, such as metrology equipment and laser applications. Thus, while they have also been applied to PV-T systems before (as shown in Fig. 31(a), from Crisostomo et al. [419]), they have not been mass-produced for this application so their main drawback is cost. It is unclear if they can meet the cost requirements of solar collectors in the long term since they require very pure materials and (typically) hundreds of layers to be deposited with precise deposition techniques [295]. Thus, to date, these dichroic mirrors have not yet proven viable for PV-T systems at commercial scales.

On the other hand, dichroic mirrors are mass-produced for the architectural glazing market (a 40 Billion USD/year market by 2024 [428]). With these so-called 'low-emissivity' windows, modern buildings can reduce their solar heat gain (and indoor heat loss) without reducing the amount of natural daylight they receive. This feature is enabled by spectral splitting dichroic coatings deposited on the inner pane of a double or triple-glazed frame (which reflects all solar wavelengths except the visible light) [425]. Given their ubiquitous use in high-efficiency buildings, dichroic-coated glass might also be mass-produced for PV-T products in the future. This would require two fundamental changes from today's architectural glazing manufacturing processes: (a) broadening of the transmitted spectrum (perhaps requiring different materials and layer thicknesses) to shift the transmission window from about 450 to 750 nm to, say, 700–1100 nm band for Silicon cells [425]; and (b) use of low-iron or 'solar glass' substrates (rather than typical window glass), which is less absorbing of these longer wavelengths.

In terms of how dichroic mirrors can be employed in a PV-T collector, they can be used equally well as a "heat mirror" to reflect the longer wavelengths away from the PV cells (similar to a low-emissivity glass) or they can be designed to reflect the shorter wavelengths of sunlight towards PV cells. In either case, the primary cut-off is determined by the band-gap of the PV cell. If a bandpass/stop filter is used, a secondary cut-off can be employed on the short wavelength side (e.g., ~700 nm for silicon cells). A characteristic design of how dichroic mirrors could be configured in a CPV-T system is shown in Fig. 31(b).

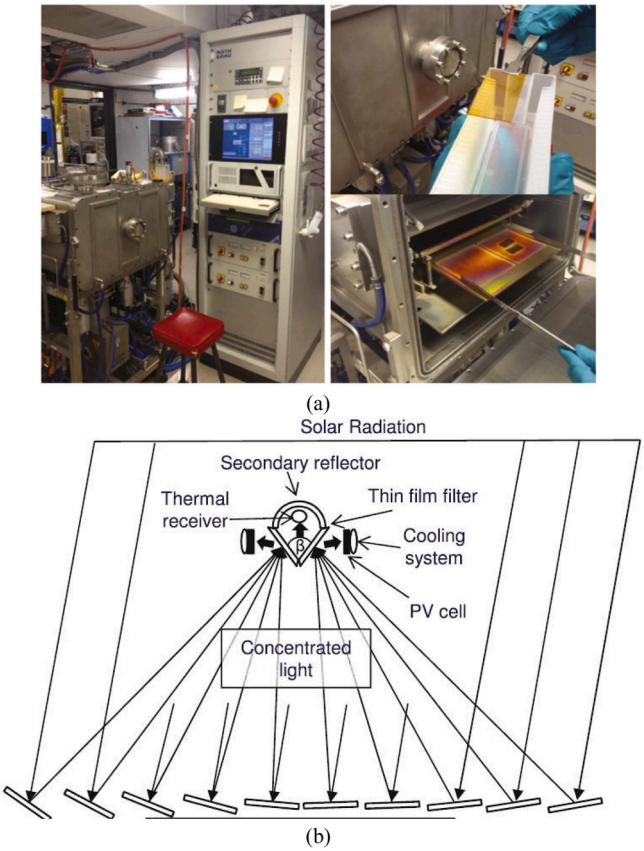


Fig. 31. Example dichroic mirror-based PV-T system: (a) plasma-enhanced chemical vapour deposition of SiN_x/SiO_2 layers on a quartz substrate (using a Roth&Rau AK400 instrument); and (b) PV-T configuration where (concentrated) short wavelengths are reflected out of the optical path towards PV cells. Images reprinted from Crisostomo et al. [419], with permission from Elsevier.

3.4.4. Holographics

Using slightly different principles, holographics can achieve the same splitting function as dichroic mirrors or filters. In a volume phase hologram, a permanent pattern is recorded by modifying the refractive index of a photosensitive material through (e.g., using a nickel-ion-doped photopolymer [429]). This enables a thin slab of material that selectively diffracts light with little absorption of light as it travels through the medium. Since most photosensitive materials only interact with a small spectral band, an edge-pass or band-pass filter requires several holograms to be layered together in a foil to achieve controlled transmission over a wider range. Holographic techniques were first applied to solar technologies through "passive tracking" devices in which multiple curved surfaces were utilized to "switch" among concentrator shapes designed for different angles of incidence. In one of the first examples of this, Bloss et al. [430] demonstrated the use of high-efficiency volume phase transmission holograms in which several holograms were produced at various recording angles in photosensitive (i.e., dichromate gelatine) plates. These were then encapsulated and the diffraction efficiency was found to be as high as 97%. Later studies have found even higher diffraction efficiencies, with scattering and optical losses, remarkably, under 0.2% [431]. Concerning using holographics in PV-T applications, like dichroics, the real challenge is cost-effectively creating a device that has broadband reflectivity (e.g., for 700–1,100

nm for reflecting light towards Silicon PV cells). Both thin-film dichroics and holographics suffer from the high cost of ensuring manufacturing tolerances are tight enough to ensure sharp transitions in their transmission/reflections curves [432–434]. On the other hand, holographics have a few (potentially) major advantages over dichroics. Holographic foils are usually quite flexible, so they can be arbitrarily shaped and—once encapsulated—are also reportedly very stable to both thermal exposure (up to ~120 °C) and UV-exposure [431].

In one interesting design [435], Cassegrainian concentrating optics (e.g., a mixture of refractive/reflective elements in a compact design like a telescope) were employed to redirect radiation off a primary hyperboloidal-shaped mirror onto a solar cell placed at the lower focal line. The longer wavelengths were then transmitted to an evacuated tube (thermal) absorber positioned at the upper focal line. Although this type of system requires high tracking accuracy, it is interesting because it has a low profile. A low-profile is desirable because it may lower the cost and it reduces wind loading requirements for the structural design of the system [436,437]. Ultimately, if the cost of the holographics can be equal to or lower than either the PV cell or the thermal receivers (in USD per m^2) it is possible to achieve a system-level cost reduction, since concentrated receivers typically produce higher conversion efficiencies. Another example of a solar holographic system was reported by Vorndran et al. [438]. For their design (shown in Fig. 32(a)), a holographic lens transmits the long wavelengths (without diffraction) to a parabolic mirror, which concentrates these wavelengths back onto an evacuated tube attached at the middle of the holographic foil. For the PV receiver, the holographic lens concentrates the short wavelengths (e.g., which have a peak of ~700 nm, as shown in Fig. 32(b)). The authors estimated that about 60% of the output power comes from the PV receiver and the balance comes from the thermal receiver. This resulted in overall hybrid conversion efficiency of ~18%.

Researchers have also shown that spectral splitting holograms can be beneficial in non-concentrated configurations. Although not always referred to as PV-T designs, holograms have been proposed to serve as both space heating/daylighting and PV power generators [439,440]. These work by transmitting light low-angle winter sun while blocking high incidence angle summer sun (e.g., applicable mainly in latitudes above 25°) [435]. Experimental systems of this type have found that holographics can reduce building heating costs, remarkably, by up to 50% [441]. As one example, Rosenberg patented a dual-film holographic device where the first hologram redirects the 400–700 nm band and the second hologram redirects near-infrared energy (i.e., 700–1,100 nm) [442]. When integrated into a waveguide plate, this design was found to work a wide range of incidence angles, enabling operation across most of the daylight hours (up to 11 h). The peak diffraction efficiency was reported as 65% and the PV receiver had an electrical conversion efficiency of just over 6% [442]. Despite the research inroads mentioned above, holographics have a TRL in the range of 5–7 because they have not been scaled up or deployed as commercialized PV-T systems. Future work in this area will include scaled-up demonstrations to prove stability, reliability, and performance along with some viable mechanisms for manufacturing cost reductions.

3.4.5. *Luminescent splitters/concentrators*

A 'luminescent' flat plate splitter/concentrator is created when quantum dots or organic dyes are embedded in a solar slab/substrate. As such, a luminescent optical element relies upon the scattering and/or absorption/re-emission of small particles/molecules to selectively interact with the desired portion of the solar spectrum. If the transparent medium has a high refractive index (i.e., >1.5), most of the scattered/emitted light will propagate at angles less than the critical angle for total internal reflection. Assuming multiple scattering absorption/re-emission events can be avoided, much of the desired spectrum will be efficiently guided to the sidewalls for harvesting by the solar receiver. Thus, a typical luminescent system places PV cells around the edges of a luminescent slab—nominally in a square or circular configuration—with the PV cells chosen to match the band that is predominantly scattered or emitted by the embedded particles [443]. Depending on the aspect ratio and the losses in the system (e.g., ideally <25%), the spectral irradiance at the sides walls will be higher than the incident, by a factor of 1–15 [443]. This essentially reduces the solar receiver area needed to harvest the same power output and, more subtly yields concentration without the need for tracking systems, both of which may enable cost reductions. An attractive feature of some luminescent concentrators is that they also down-convert (e.g., 'split' high-energy photons into two or lower energy photons) or up-convert (e.g., 'combine' low-energy photons via sequential excitation of electrons into an excited state) portions of the incident spectrum to make more of the solar spectrum match the PV cell [444,445]. In a recent prototype [446], lanthanide-doped surface-functionalized ionosilicas were embedded in poly(methyl methacrylate) (PMMA). This, in turn, was placed on the surface of a commercial Si-based PV panel for testing (as in Fig. 33) [446].

Luminescent concentrators for solar cell applications were first proposed in the mid-1970s, and have had numerous advances in the decades since then [447,448]. In selecting the dyes/scattering particles, one must make a considered trade-off between increasing the concentration of the embedded scatterers/emitters (i.e., higher utilization of the incident light) and the probability of subsequent re-absorption/scattering as the desired spectrum propagates towards the

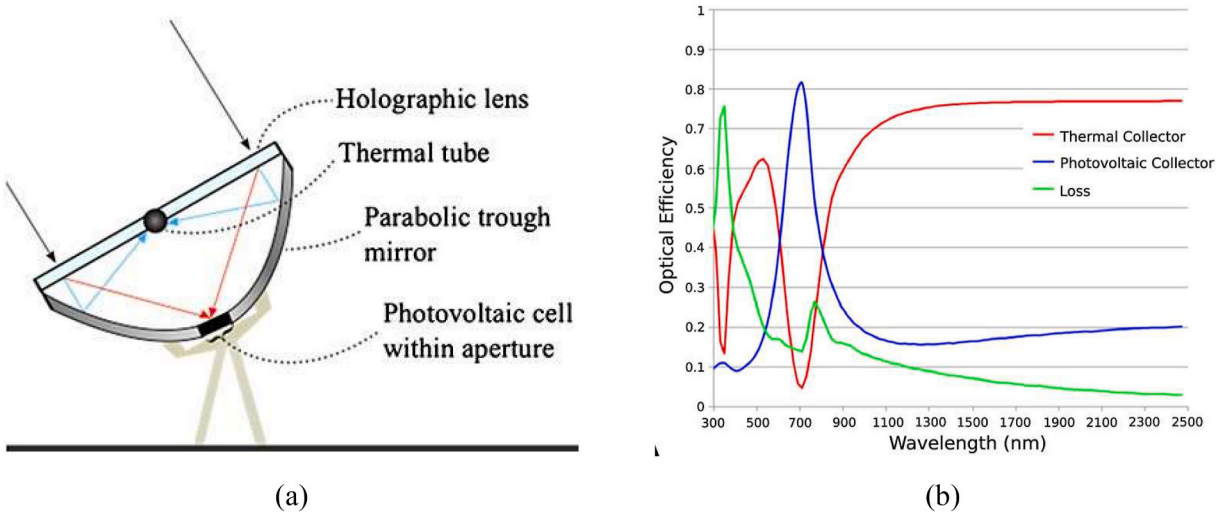


Fig. 32. (a) CPV-T collector design; and (b) calculated optical efficiency curves. Reused from Vorndran et al. [438], with permission from Wiley and Sons.

edges of the slab. Re-absorption can significantly impact the performance of the system, particularly as the aspect ratio between the aperture area and the PV edge area becomes large. Another design choice comes from the fact that different scatterers/emitters can be combined inside the material to achieve broader spectral control, as was demonstrated by Goetzberger and Greube [449]. In another example [450], this concept was utilized to good effect for a PMMA slab containing two dyes (i.e., 0.01 wt.% Lumogen F Red305 and 0.003 wt.%. Fluorescence Yellow (CRS040) from Radiant Colour) [450]. This design achieved an experimental efficiency of just over 7% when GaAs cells were attached to it [450]. Although the research in luminescent concentrators has slowed down in recent years (according to a 2020 Google Scholar search by year), this type of optical element could still have the potential for further development in PV-T systems. Considering Fig. 33, if standard commercial Si modules are used below the luminescent slab, the concentrated light could be guided to thermal receivers (operating at elevated temperatures) at the sides or vice versa.

3.4.6. PV cell-based splitting

Most PV cells (if made thin enough and assembled without an opaque metal backing) can serve as spectral splitting filters. That is, they will transmit the parts of the solar spectrum that they do not use for generating electricity [451]. Transmissive PV cells are interesting for BIPV systems because they allow light (and heat) to transmit through them to the building occupants [230]. For example, CdTe thin-film cells are semi-transparent to the IR spectral region which can result in considerable energy saving for an office building with a relatively large window-to-wall ratio (i.e., ≥45%) [452]. In recent years, transmissive PV cells have also been applied to spectral-splitting PV-T collectors. In this configuration, the transmissive PV cells act as not only the electricity generator, but also the spectral-splitting filter in the spectral-splitting PV-T collector. As an example, a transmissive triple-junction solar cell (AlGaInP/InAlGaAs/GaAs) was developed by Xu et al. [453], which can absorb light with a wavelength of less than 880 nm and is highly transparent (~80%) to the rest of light with a wavelength longer than 880 nm. This transmissive triple-junction solar cell was then applied to a spectral-splitting PV-T collector by the same research group [454]. The UV and visible light were absorbed by the triple-junction solar cell for electricity generation, while IR light passed through the PV cell and was absorbed by a thermal absorber to generate high-temperature thermal energy. The solar cells were cooled to below 110 °C by additional active and passive cooling structures. Their numerical analysis showed that the triple-junction solar cell had a high efficiency of close to 44% for in-band light (300–873 nm). The efficiency and temperature of the thermal absorber were not stated by the authors.

A recent prototype was built and tested in San Diego in 2019 [455], which is shown in Fig. 34. In this design, a spectral-splitting transmissive GaAs-substrate III-V triple-junction PV panel with cooling channels was installed in the focal position of a parabolic concentrator dish with a concentration ratio of 130. Their experimental results show that 53% of the solar energy incident on the PV-T collector was transmitted through the PV cells, 18% was dissipated as waste heat in the PV cells, 4% was converted to electricity by the PV cells, and 23% was lost to reflection. Although the electrical efficiency was not high, this experiment work has shown the feasibility and potential of transmissive solar cells to be used in spectral-splitting PV-T collectors.

Another approach is to use the PV cells as a reflector, wherein any unused portions of the spectrum are bounced off a reflector behind the cell and redirected to a thermal receiver. This approach is also interesting since it may be possible to deposit PV materials onto curved surfaces, opening up a path toward concentrating PV reflectors. This approach was used in a recent study [456], in which it was reported that a concentration ratio of 60 was achieved in a non-imaging optical system. Abdelhamid et al. [456] reported a thermal efficiency of 37% at a high temperature, of 365 °C, and a relatively low overall cost of 285 USD/m^2.

In either approach—reflective or transmissive PV assemblies—the key non-ideality comes from undesired spectral absorption/scattering in the PV cells and other components in the optical path. Within the PV cell itself, this can be mitigated to some extent through high-purity and/or thin materials. However, electricity is typically more valuable than thermal energy, placing the PV first will naturally prioritize the PV output, which can be considered an advantage over the other spectral splitting approaches.

3.5. Nanofluids

One pathway for improving PV-T collector performance is to improve the thermal efficiency of the system. Since the thermal

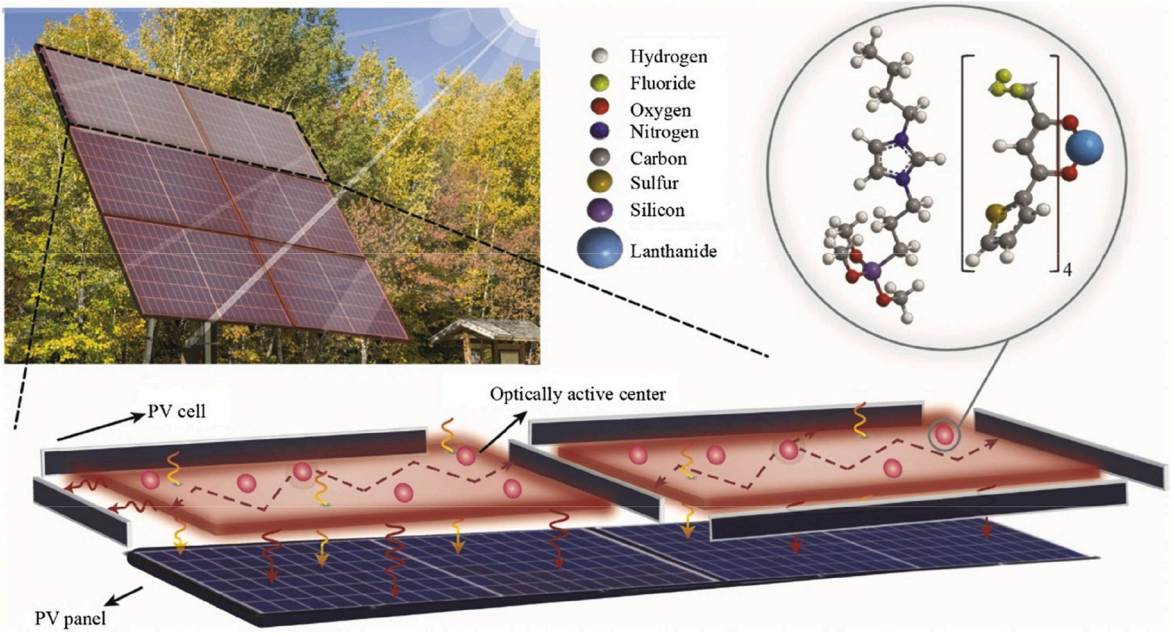


Fig. 33. A 2020 prototype of a down-shifting luminescent solar concentrator which transmits to a commercial Si module and also emits to PV cells on the sides. Reused from Cardoso et al. [446], with permission from Elsevier.

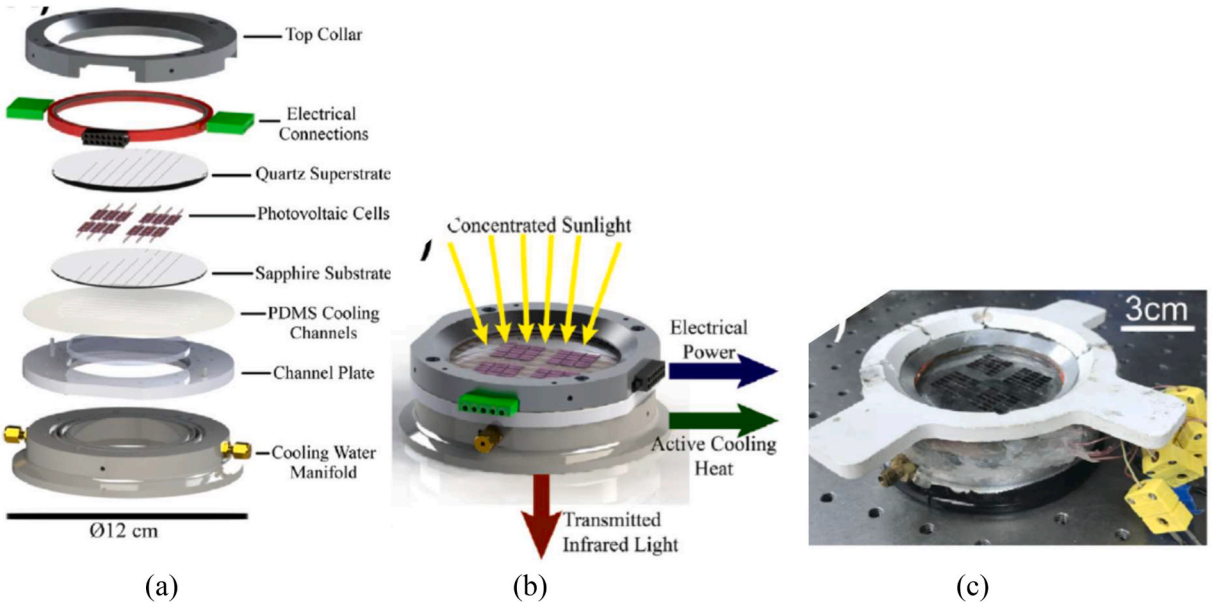


Fig. 34. Experimental testing of a spectrum-splitting transmissive concentrator PV panel: (a) exploded view of the design; (b) assembled view; and (c) mounted design with sensors. Reused from Keblinski et al. [455], with permission from Elsevier.

efficiency is higher when the useful heat gained by the working fluid is maximized relative to the input solar energy, increasing heat transfer to the working fluid will result in efficiency increases. As noted above, design modifications can result in improvements, while this section focusses purely on improving thermal performance through the modifications of fluids. Nanofluids, or nm-sized particle suspensions in liquids, have long been of interest as a means to increase the thermal conductivity of a base fluid [457,458]. While nanofluids result in increases in thermal conductivity, they also drastically alter the optical properties of the base fluid at low-volume fractions, making them a potential option for spectral filtration [459] and broadband absorption [418]. Thus, for beam splitting, changes in the thermal properties (from the base fluid) can be neglected. In addition, metals (with a strong plasmonic response) and other optically selective materials (e.g.,

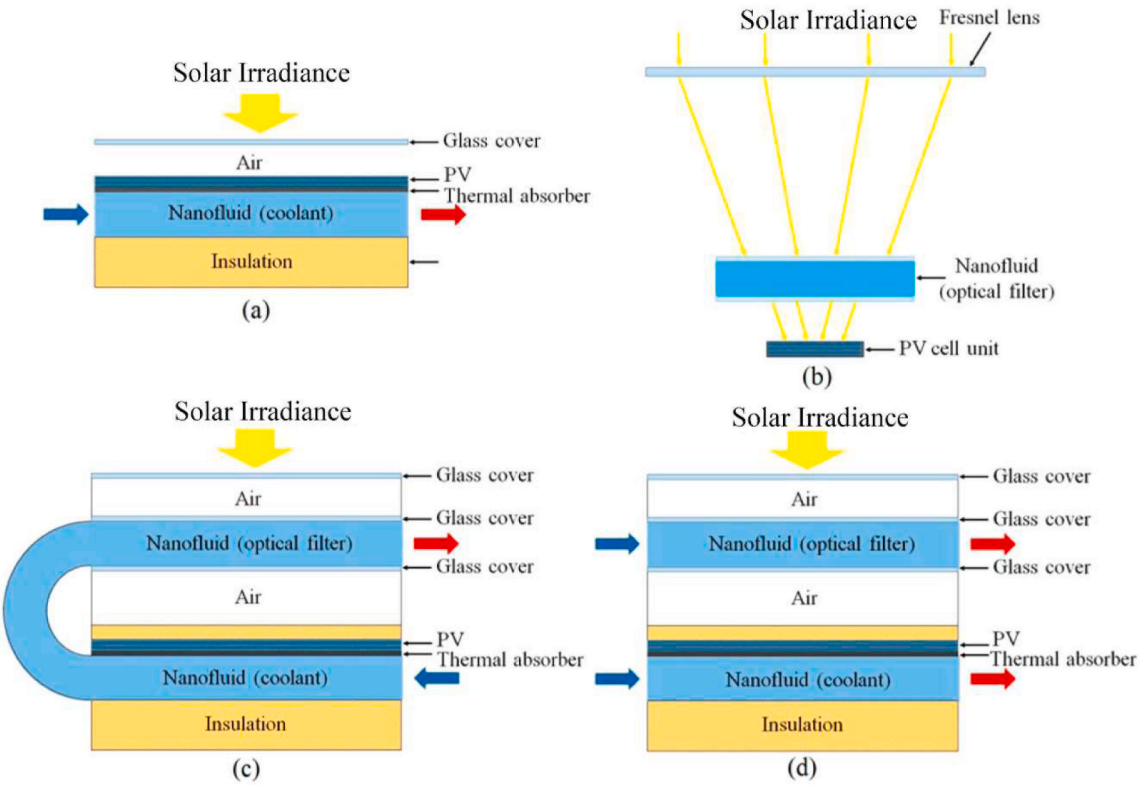


Fig. 35. Different design arrangements used for nanofluid-based PV-T collectors: (a) single-pass coolant beneath PV cells; (b) optical filter in front of PV cells; (c) optical filter in front of PV cells with nanofluid as the coolant; and (d) decoupled nanofluid optical filter and nanofluid coolant. Images reprinted from Yazdanifard et al. [461], with permission from Elsevier.

quantum dots) represent the most useful nanomaterials for spectral splitting. For the interested reader, the approach and key equations for calculating the optical properties of spectral splitting nanofluids can be found in, e.g., Ref. [460].

Fig. 35 summarizes the major design configurations that can be used in PV-T collectors utilizing nanofluids [461]. Fig. 35(a) represents the simplest configuration where the nanofluid acts as the coolant for the PV cell and flows beneath the PV cell, hence it is not directly exposed to solar irradiance. Fig. 35(b) uses the nanofluid as an optical filter by placing the nanofluid before the PV cell and directly heating the fluid by absorbing incoming solar flux. Fig. 35(c) and (d) represent arrangements where the nanofluid acts both as an optical filter and as a coolant, with Fig. 35(d) decoupling the coolant and optical filter fluid streams. These configurations represent different approaches to improve the performance of a hybrid PV-T collector, solely through improving the thermal performance and will be discussed in more detail below, with an emphasis on flat-plate PV-T collectors, while other recent reviews cover low and high concentration systems [301,462].

As with natural liquid splitting—although there is a beneficial extra degree of freedom for optimization—the main non-ideality of this approach is that it is nearly impossible to achieve a sharp spectral splitting curve. This imprecise spectral splitting will not create a major loss in performance for the thermal receiver since broad-based absorption is easily achieved, but it can derate the output of the PV cells. Some electrical loss is unavoidable since even the best nanofluids will not transmit all of the light incident on the collector aperture that falls within their spectral response curve to the PV cells.

3.5.1. Heat transfer enhancement

Improving the thermal conductivity of base fluids through the addition of nanoparticles garnered significant interest following the original publication of Choi and Eastman [463]. While these results spawned a whole flurry of research into measuring the thermal transport properties of nanofluids [464], the application of nanofluids in ST collectors for enhanced thermal transport did not appear until 2012. The first experimental demonstration of nanofluids for conventional flat plate solar thermal collectors was undertaken by Yousefi et al. [465,466] in a variety of publications investigating the role of nanoparticles on the collector efficiency for multi-wall carbon nanotubes, and Al_2O_3 nanoparticles [467], both suspended in water. These studies indicated that the use of nanoparticles for enhancing the thermal conductivity of the base fluid could be used to enhance the efficiency of flat-plate ST collectors. One of the first investigations of nanofluids as coolants in PV-T collectors was Sardarabadi et al. [468], where SiO_2/water nanofluids were used in a 40 W monocrystalline silicon PV-T collector. As shown in Fig. 36(a) the overall efficiency of the device improves by up to 8%, driven both by a combination of thermal efficiency and electrical efficiency (see Fig. 36(b)).

Some authors investigated the improvement in electrical efficiency of PV cells cooled by rectangular microchannels containing a Boehmite (AlOOH)-water nanofluid [469]. The results indicated the highest increase in electrical efficiency of 27% at 0.01 wt.% over the case of pure water, no measurement in thermal efficiency was measured as the primary interest was the PV cell cooling. Meanwhile, other authors presented an experimental measurement of a copper oxide-water nanofluid where a decrease in electrical efficiency and an increase in thermal efficiency was observed relative to pure water [470], this was attributed to a poor heat exchanger that resulted in increased inlet temperatures. A novel experiment investigated the role of ferrofluids, Fe_3O_4 nanoparticle-water nanofluids, under conditions with and without external magnetic fields (both constant and alternating) [471]. Using their experimental setup (see Fig. 37), an improvement in the overall efficiency of the system of 45% when ferrofluids were used relative to that of pure water, this improvement increased to 50% when a 50 Hz alternating magnetic field was applied.

In the study of Rejeb et al. [472], a numerical model of uncovered nanofluid-based PV-T collectors was developed and validated against experimental data for Al_2O_3 and CuO nanoparticles, with results showing increases in both electrical and thermal energy yields in different locations. Another modelling effort focussed on the exergy payback time and reduction of CO_2 equivalent emissions of multiple configurations of PV-T collectors in comparison to pure PV systems [473]. This work focussed on two primary system types, nanofluid as pure coolant (see Fig. 35(a)) and nanofluid as optical filter and coolant (see Fig. 35(d)). The cases where the nanofluid acted as filter and coolant outperformed the others in terms of exergy output with an exergy payback time of 2 years. Additionally, the same configuration may prevent emissions on the order of 448 $kgCO_{2eq}/(m^2$ year). Sardarabadi and Passandideh-Fard followed up their initial work by investigating several different metallic oxide nanoparticles (TiO_2, ZnO, and

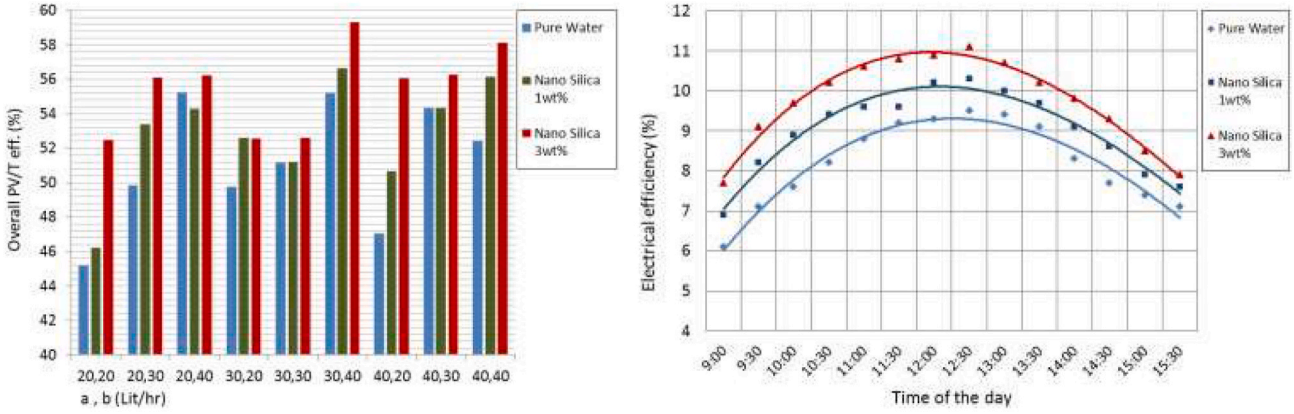


Fig. 36. (a) Overall PV-T collector efficiency as a function of flow rate with different weight fractions of SiO_2; and (b) the resulting increase in PV cell efficiency. Reprinted from Sardarabadi et al. [468], with permission from Elsevier.

[2] The Hoffmann voltameter is an early electrolyser with an operating principle similar to the contemporary alkaline electrolyser described above.

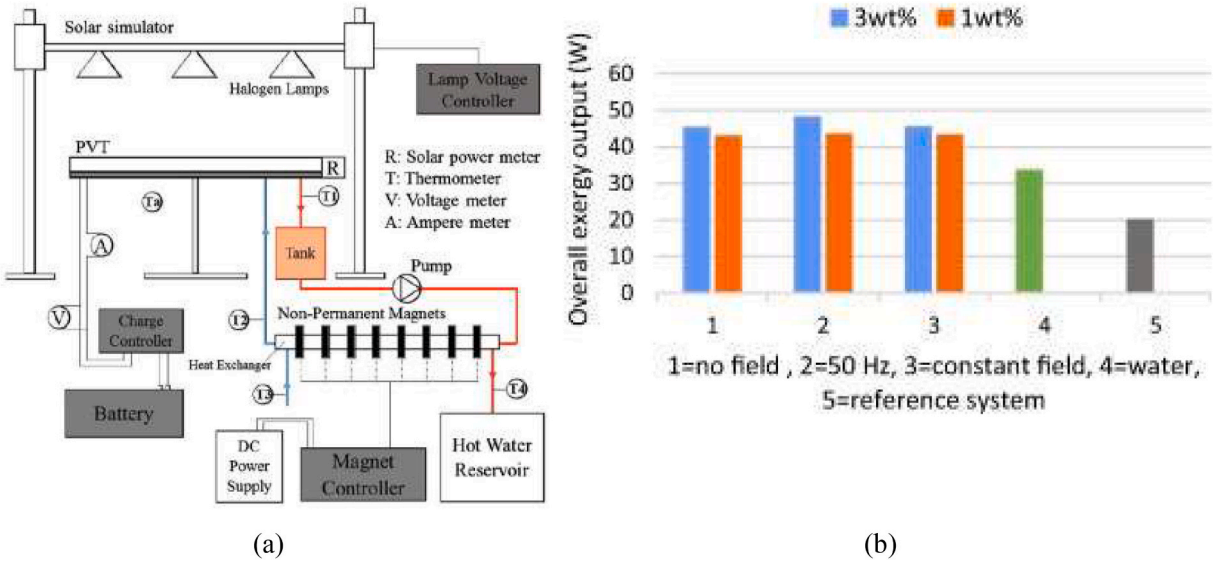


Fig. 37. PV-T collector employing ferrofluids: (a) experimental setup; and (b) overall exergy output for different applied fields and pure water. Reprinted from Ghadiri et al. [471], with permission from Elsevier.

Al_2O_3) as the coolant in PV-T collectors [474], both experimentally and numerically. All nanoparticle types resulted in an increased, although small, PV cell efficiency through cooling and an increased collector temperature difference, with the ZnO performing best. As shown in Fig. 38(a), increasing the mass fraction greatly increases the collected thermal energy (collector temperature difference), but only has a mild impact on the overall cell efficiency.

More recent studies have focussed on the use of carbon-based nanoparticles, including graphene, to improve the performance, with an increase of 19% in the total efficiency over pure water achieved with graphene [475]. In a similar effort, a total increase in exergetic efficiency was observed of roughly 20% for a PV-T collector using graphene nanoplatelets in water over a pure-water PV-T collector [476]. An expanded area of interest has been the coupling of nanofluid-based PV-T collectors with thermal energy storage, particularly with PCMs to achieve increased thermal energy collection in the solar collector and increased heat transfer in the PCM. In one instance, a neural network approach was used to model the performance of this style of collector with the results providing a similar linear prediction with low error [477] and experimental results showing almost a doubling of the system's electrical efficiency, which increased from 7% to close to 14% [373].

3.5.2. *Optical absorption*

While nanofluids have often been the study of investigations thanks to the improvement in the base fluid thermal conductivity that they offer, they can also be used to radically alter the base fluid optical properties [478] either for direct absorption or spectral splitting [459]. Nanofluids were first proposed to serve as both the absorber and the heat transfer fluid in a numerical work [479], and later demonstrated experimentally [480]. In principle, nanofluids for use in direct absorption solar collectors (DASCs) can be designed for either broadband absorption or spectral filtration [459]. In practice, a broadband DASC PV-T collector is less than desirable as the fluid flowing in front of the PV cell, as shown in Fig. 35(b–d), will result in decreased solar energy to the PV cells resulting in a substantial decrease in the PV cell efficiency, as demonstrated experimentally recently for MXene-based nanofluid [481]. It should be noted that broadband DASCs using nanofluids could be advantageous relative to existing surface-based approaches [482] for PV-T collectors using the spectral splitting arrangements outlined in Section 3.4, where the thermal collector is spatially removed from the PV cell. The focus here is on spectral filtering applications of nanofluids [301] in PV-T collectors. Importantly, several materials have sharp absorption peaks when properly sized or doped creating the ability of spectral filtering above what is offered in the base fluid, which is typically poor at short path lengths [483], also shown in Fig. 39. In a PV-T collector where the fluid acts as the spectral absorber and filter, the goal is to absorb the maximum amount of solar energy outside of wavelengths just above the cell band-gap and just above a lower cut-off [460]. This approach is similar for both low and high temperatures (corresponding to concentration) but the lower cut-off wavelength can be selected and optimized based on temperature [484] and the split between thermal and electrical energy, often termed a merit factor [485].

While the vast majority of spectral filtering articles focus on systems using concentration where higher temperatures are desired from the thermal system, there are a few experimental demonstrations. Arguably, the first proposed use of this approach was by Taylor et al. [460], where several nanofluids were modelled for different PV applications. One of the earliest studies of spectral filtration investigated the stagnation temperature observed in a nanofluid composed of gold and silver nanoparticles in water placed in front of a PV cell [486]. Higher stagnation temperatures were observed in the nanofluids, but no PV cell efficiency was recorded. In a similar effort, the authors tested Ag@TiO_2 core–shell nanoparticles in water without fluid flow or concentration under a lamp (see Fig. 40) [487]. Other authors tested silver nanoparticles in water and $CoSO_4$ with a solar simulator, but no flow was used and the performance was only measured as a filter nor as a collector of useful energy [488]. Similarly, another work tested Ag@TiO_2 nanofluids as a spectral filter without flow and demonstrated increasing temperatures and lower PV production when the nanoparticle concentration increased [489]. From these results, it can be seen that more work is needed for these low-temperature and concentration collectors to demonstrate the potential when there is actual flow in the fluid filter generating useful energy.

In general, it is estimated that PV-T collectors that include nanofluids for heat transfer enhancement or for optical absorption are at TRL 6 where prototypes have been done. To the best knowledge of the authors, no large-scale demonstrations have been completed. Finally, it is noted that nanofluids have faced some controversy, arising from limitations related to their use in practice that arise from technical issues, such as agglomeration, sedimentation or otherwise decrease in concentration leading to a drop in efficacy over time. For proposed solutions to stand a chance of implementation in real applications of interest, these need to be addressed and these challenges overcame to demonstrate safety as well as the full lifecycle implications of their use [490].

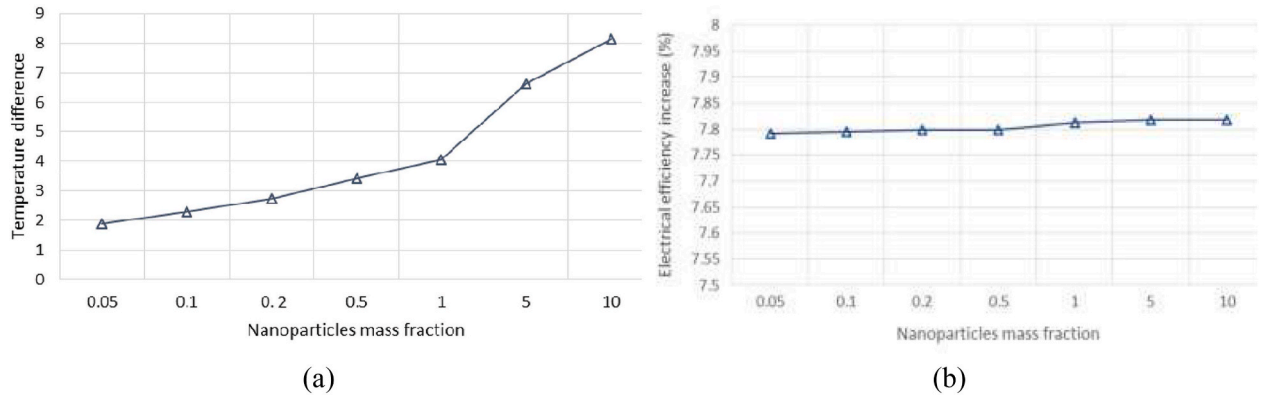


Fig. 38. Role of ZnO nanoparticle mass fraction on: (a) collector temperature difference; and (b) increase in electrical efficiency relative to pure water. Reprinted from Sardarabadi et al. [474], with permission from Elsevier.

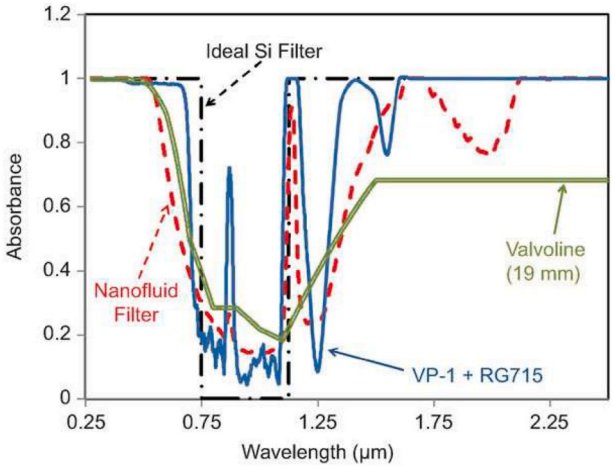


Fig. 39. Fluid filter spectra for a silicon solar cell. Curves demonstrate the ideal filter, as well as a potential filter using various pure fluids and a nanofluid. Reprinted from Taylor et al. [460] with permission under the Creative Commons Attribution 3.0 Unported (CC-BY) license.

3.6. Optimization methods of PV-T collectors

The geometric parameters and operating conditions have a direct effect on the overall performance of PV-T collectors. Recent studies on the optimization of PV-T collectors are summarized in Table 8.

The Taguchi method is a statistical method developed by Genichi Taguchi that aims at improving the quality of manufactured products, and has been widely applied to different engineering fields [497]. Liu et al. [491] used the Taguchi method to optimize performance-related parameters, and specifically to maximize the equivalent overall energy output of a PV-T-PCM collector. Their optimization results showed that the mass flow rate has a strong effect, whereas the thickness of the PCM has a limited impact on collector performance (Table 8 shows the optimal values). A hybrid Taguchi and analytic hierarchy process (AHP) method was developed by Kuo et al. [492] to optimize the selection of collector materials, the number of pipes and tank volume, among others. The electrical and thermal efficiencies of the optimized water-based PV-T collector were 14% and 45%, respectively, which are 13% and 34% higher compared to the conventional PV-T collector.

Artificial neural networks (ANNs) are another common algorithm that has been used to predict and optimize the performance of PV-T collectors. Ammar et al. [493] developed an ANN to optimize the flow rate for the maximum overall (thermal + electrical) energy output of a water-based PV-T collector under different ambient temperatures and solar irradiance levels (Table 8 shows the optimal values). A hybrid ANN

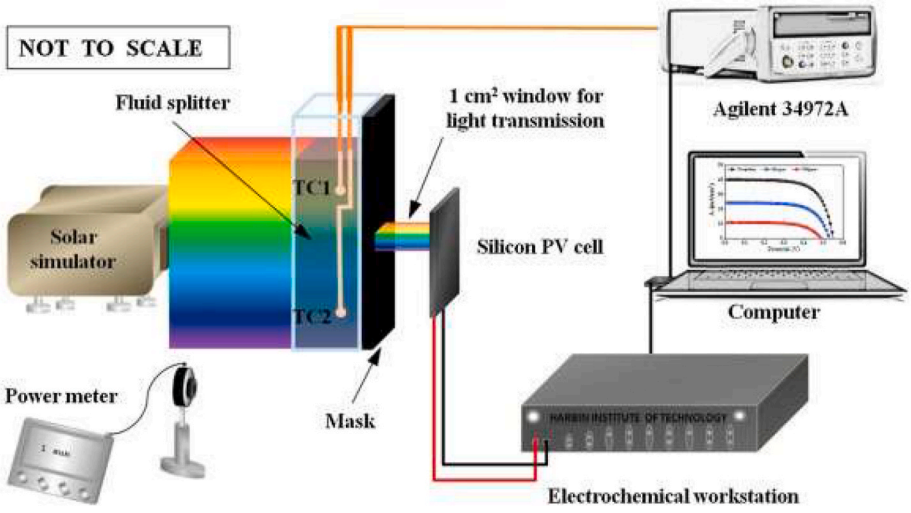


Fig. 40. Experimental test arrangement of nanofluid-based spectral filtering for PV-T collector. Images reprinted from Saroha et al. [487], with permission from Elsevier.

Table 8
Optimization methods of PV-T collectors.

PV-T type	Optimization algorithm	Control parameters	Optimization objectives	Key results	Ref.
PCM-based PV-T collectors	Taguchi method	PCM thickness, water pipe diameter, mass flow rate and water inlet temperature	Equivalent overall output energy	Optimal thickness of PCM is 20 mm, optimal diameter of water pipe is 6 mm, and optimal flow rate is ~1 kg/s	[491]
Water-based PV-T collectors	Taguchi method combined with AHP	Collector material, angle, azimuth, number of tubes, mass flow rate and storage tank volume/area (V/A) ratio	Electrical and thermal efficiencies	Optimal values: material is copper, number of tubes is 12, the flow rate is 0.01 kg/s/m^2, V/A ratio is 123	[492]
Water-based PV-T collectors	ANN	Mass flow rate (for different solar radiation, ambient temperature)	Electrical and thermal outputs	The optimal flow rate is ~0.012 kg/s (for an ambient temperature of 30 °C and solar irradiance of 1000 W/m^2)	[493]
Air-based PV-T collectors	ANN and hybrid particle swarm optimization models	Length, width, and depth of the air channel, air mass flow rate	Total (thermal + electrical) outputs	The optimal number of neurons in the hidden layer of ANN is 8	[494]
Water-based PV-T collectors	Genetic algorithm	Tube diameter, tube number, mass flow rate, tube spacing.	Electrical and thermal efficiencies	The optimization method is able to achieve 9% and 12% extra electrical power and thermal energy	[495]
Water-based PV-T collectors	NSGA-II and TOPSIS	Mass flow rate, inlet temperature, and inclination angle	Electrical and thermal efficiencies	Optimal values: flow rate is 0.02 kg/s, the inlet temperature is 32 °C and the inclination angle is 39°	[496]

and particle swarm optimization model was developed by Alnaqi et al. [494] to optimize the performance of an air-based PV-T collector for space heating applications. This work introduced details on developing such a hybrid optimization model.

A genetic algorithm is a widely-used method for single- or multi-objective optimization. Khani et al. [495] developed a single-objective (electrical efficiency) and a multi-objective (electrical and thermal efficiencies) genetic algorithm to optimize a water-based PV-T collector. The optimized design (tube diameter: 0.02 m, tube number: 14, tube spacing: 0.065 m, and flow rate: 0.004 kg/s) achieved 9% and 12% extra electrical power and thermal energy compared to a conventional design. A two-step procedure, combining a hybrid non-dominated sorting genetic algorithm (NSGA-II) and a technique for order preference by similarity to ideal solution (TOPSIS), was developed by Podder et al. [496] to optimize the electrical and thermal efficiencies of a water-based PV-T collector. The thermal and electrical efficiencies of the water-based PV-T collector reached 83% and 10%, respectively, with an optimal flow rate of 0.02 kg/s, an inlet temperature of 32 °C and an inclination angle of 39°.

4. PV-T polygeneration systems and their applications

Typical applications of PV-T systems include both domestic and commercial buildings and industries. These applications have high energy demands for both heat and electricity. Due to the additional thermal output of the PV-T collectors, they are more efficient in terms of area utilization and cost-effective than separate PV and ST units of the same area. The various types of PV-T collectors are best suited to different applications as shown in Fig. 41, which summarizes the state-of-the-art of the main applications.

Table 9 summarizes research on PV-T polygeneration systems, specifying whether the studies are theoretical (simulation-based), lab-scale (test-rig experiments) or site-scale (real condition experiments), the type of PV-T collector used, and the energy performance, where available. It is observed that the majority of the studies are theoretical (simulation-based), although there are also some lab-scale (test apparatus) or site-scale (under real conditions) studies that analyse different systems that provide water heating, electricity and/or cooling. More details of these studies can be found in the following sections.

The market survey undertaken under Task 60 [25], shows that the majority of the PV-T systems installed by the end of 2018 were for the application of solar air (pre)heating/cooling for buildings, with 20,121 installations reported, with a total accumulated area of around 440,000 m^2. The survey reported 2,169 systems of uncovered water-based PV-T collectors in operation, corresponding to total a gross area of approximately 610,000 m^2, out of which 75% were used for DHW provision in buildings, around 21% for electricity, space heating and DHW provision in households, and the remaining 4% for other applications such as industrial processes, district heating, and swimming pool heating. The covered water-based PV-T system installations reported were mainly used for electricity, space heating and DHW provision in buildings [92].

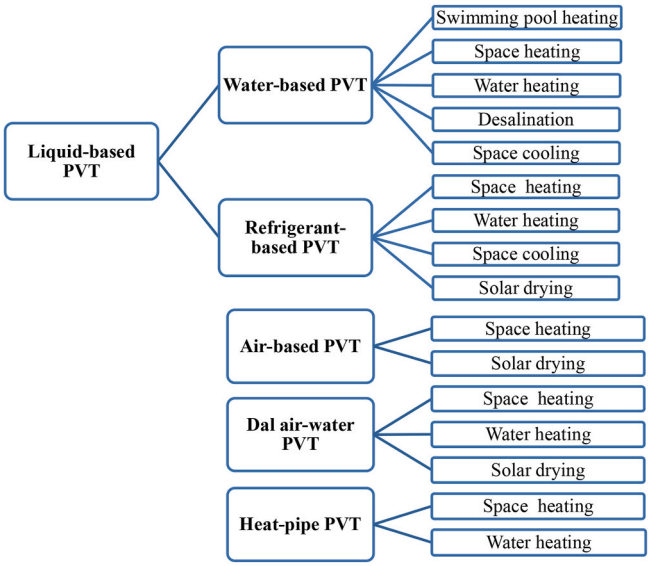


Fig. 41. The main applications of the different types of PV-T collectors addressed in this work.

4.1. Solar combined heat and power systems

Air-based PV-T collectors produce electricity and hot air, which is typically used for space heating or solar drying (see Section 4.5). These collectors normally have an HP as a backup system [28,393,506].

Alternatively, liquid-based PV-T collectors are widely used for heat and power provision. There are different applications depending on the PV-T collector type and liquid outlet temperature [507]:

- Low-temperature applications, up to 50 °C: include swimming pool heating or spas (~27–35 °C) using normally uncovered PV-T collectors with water as circulating fluid. Meanwhile, operating temperatures up to 50 °C are required for space heating via radiant underfloor heating (UFH), for which both uncovered and covered

Table 9
Summary of research on solar PV-T polygeneration systems.

System description	Location	Nature of work			PV-T collector design	COP[d](HP)	Thermal efficiency	Electrical efficiency	Ref.
		Theoretical	Lab-scale	Site-scale					
BIPV-T water heating system	Hong Kong	X			Water-based	–	38%	9%	[272]
PV-T water heating, thermosiphon (open-loop) system	China	X	X		Water-based	–	38–45%	10–12%	[343]
PV-T water heating, thermosiphon (open-loop) vs. Active (closed-loop) system	Nicosia (Cyprus), Athens (Greece), Madison (US)	X	X		Water-based	–	–	–	[74]
PV-T water heating active (closed-loop) system	The Netherlands	X			Water-based	–	33%	7%	[128]
PV-T water heating active (closed-loop) system	UK	X			Water-based	–	–	–	[27]
PV-T water heating active (closed-loop) system	France	X			Water-based	–	–	–	[318]
PV-T water heating active (closed-loop) system	Athens (Greece), Munich (Germany), Dundee (UK)	X			Water-based	–	7% (Dundee)–18% (Athens)	10% (Dundee) −10% (Athens)	[322]
PV-T water heating active (closed-loop) system	UK	X			Water-based	–	–	–	[498]
PV-T DX-SAHP for heating	UK	X			Refrigerant-based	–	55%	19%	[147]
PV-T DX-SAHP for heating			X		Refrigerant-based	10.4 (max), 5.4 (av.)	–	13%	[148]
PV-T DX-SAHP for heating	Tibet	X			Refrigerant-based	6.0	48%	14%	[150]
BIPV-T DX-SAHP for heating		X	X		Refrigerant-based	–	–	–	[153]
ventilated PV-T façade system DX-SAHP	Dalian			X	Refrigerant-based	3.1 (max)	–	9% (av.)	[154]
PV-T dual source SAHP water heater system		X			Refrigerant-based	2.0 (av.)	–	–	[145]
PV-T DX-SAHP for heating	Lvliang City (China)			X	Refrigerant-based	4.7 (av.)	57%	15%	[155]
PV-T DX-SAHP for heating	Northern China			X	Refrigerant-based	6.2	–	12%	[157]
PV-T DX-SAHP for heating	Nottingham (UK)		X		Refrigerant-based (evacuated)	2.9–4.6	–	4–5%	[158]
low CPV-T DX-SAHP	Nanjing (China)			X	Refrigerant-based (CPV-T)	4.8 (av.)	–	18%	[159]
PV-T DX-SAHP for heating	–	X			Refrigerant-based	4.6–4.2	32–49%	16-15%.	[161]
PV-T DX-SAHP for heating	Hong Kong (China)	X			Refrigerant-based	5.9[c]	–	12%	[163]
PV-T DX-SAHP for heating	Shanghai (China)	X	X		Heat-pipe	–	40%	10%	[165]
PV-T SAHP water heating system	Hong Kong, Shanghai, London	X			Heat-pipe	–	52%, 39%, 27%[a]	9%[a]	[499]
PV-T IDX-SAHP for heating	Northern China			X	Water-based	4.9	32%	14%	[342]
PV-T IDX-SAHP for heating	China			X	Water-based	3.2 and 2.5[b]	38%	14%	[330]
PV-T double pass façade for space heating	New Delhi (India)	X			Air-based		–	8–11%	[500]
Air-based PV-T + HP water heating system	Busan (South Korea)			X	Air-based	3.4 (av.)	30% (av.)	17% (av.)	[501]
PV-T active (closed-loop) system for water heating	Mâcon (France)	X			Water-based	–	–	–	[123]
S–CCHP system (PV-T + absorption chiller)	Naples (Italy)	X			Water-based	–	29%	10%	[502]
S–CCHP system (PV-T + absorption chiller)	Guangzhou (China)	X			Water-based	–	–	9%	[503]
S–CCHP system (PV-T + air–water rev-HP)	Zaragoza (Spain)			X	Water-based	4.5	10%	16%	[504]
PV-T DX-SAHP on refrigeration mode	Dalian (China)			X	Refrigerant-based	2.8 (av.)	–	–	[505]

[a] In Hong Kong, Shanghai, and London, respectively.
[b] For PV-T + WSHP and PV-T + W&ASHP systems, respectively.
[c] Yearly averaged COP.
[d] av = average; max = maximum.

water-based PV-T collectors are used. Alternatively, UFH can also be satisfied with PV-T collectors integrated with low-temperature HPs.

- Medium-temperature applications, up to 80 °C: include space heating via conventional water radiators or DHW provision, for which a temperature of 60 °C is usually required to prevent Legionellosis [508], although downstream, the delivery temperature can be lower depending on the end-user needs (typically 45–50 °C). In both cases, covered water-based PV-T collectors are normally used.

- High-temperature applications, over 80 °C: for cooling purposes via refrigeration cycles, usually temperatures above 80 °C are required to drive thermally-driven cooling cycles such as absorption chillers. Similarly, high temperatures are required for certain industrial processes. Here, covered water-based PV-T collectors and CPV-T collectors are required, along with an auxiliary heater to increase the temperature when required.

4.1.1. Swimming pool heating

Swimming pools consume a significant amount of energy for water heating, but also space heating, ventilation and the operation of pumps. The annual energy consumption of a swimming pool facility varies from hundreds to thousands of kWh/m^2, depending on the volume and area of the pool, operation schedule, location, weather and types [509,510]. Typical temperatures for swimming pools for athletic activities range from 26 °C to 28 °C. This implies that low-temperature solar heating technologies are a good option for energy saving in such applications. Various studies have been devoted to ST collector heating systems [511,512], or SAHP heating systems with conventional ST collectors [513,514]. Water-based PV-T collectors, as an emerging solar technology, have recently been examined for meeting the heating and power demands of swimming pools. A few thermo-economic analyses have been undertaken via transient simulations and sensitivity analyses performed in TRNSYS [24,515,516]. The results from an analysis undertaken in Naples (Italy) [515] showed that the considered system was not yet profitable without public funding policies and became viable only after introducing thermal feed-in tariffs due to the high PV-T collector costs. Meanwhile, the analysis of the PV-T system for heat and power provision in Bari (Italy), concluded that the economic savings of the PV-T system were between those of the conventional PV and ETC systems; the system had a payback time of 13.7 years and a levelized cost of energy of 0.109 €/kWh. One of the main advantages of PV-T systems is the larger CO_2 emission reduction potential, 40–75% larger than those of conventional (PV and ST) solar systems [24].

PV-T collectors can also be integrated with heat-to-power conversion systems, which act to generate secondary power from the thermal output of the PV-T collectors thus delivering an even higher electrical output. Such systems have been considered, e.g., for the provision of heating and power to swimming pool facilities (see Fig. 42) [516]. In this study, an extra 4% of electricity was obtained with an ORC engine in the PV-T-ORC S–CHP system proposed by the authors [516]. Although the economic viability of this type of system is generally low at present, similar to and for the same reasons as the PV-TEG-microchannel heat-pipe collector discussed in Section 2.3, there may be a role for such systems in space-constrained applications where the electricity demand is high and that for heat is lower. Another study [24] of a hybrid solar-biomass renewable cogeneration system based on a biomass boiler, PV-T collectors and an ORC engine showed a more promising route of renewable heating for swimming pools. If designed properly, the PV-T-ORC system can provide all the renewable energy supply to the sports facilities with a payback time of 11.5 years.

4.1.2. Space heating

Space heating (SH) demand is characterized by seasonal variation due to variable weather conditions. In most climates, the majority of the SH demand occurs in winter, with less demand in the spring and autumn, and little to no demand in the summer. The demand also varies during the day, usually experiencing peaks early in the morning and in the evening, with reduced demand during the main sun hours of the day [517].

Several authors studied air-based PV-T collectors for SH [246,393,500,506]. For instance, a semi-transparent PV-T double-pass façade was proposed in previous work [500] to preheat air that could heat the room air temperature by 5–6 °C above the ambient. Air-based PV-T collectors can also be integrated with HPs to provide space heating in buildings [28,76]. Some authors analysed an air-based BIPV-T collector coupled with an air-source HP, where the HP uses the warm air generated in the BIPV-T collector for SH provision in residential households. The modelling results showed that the proposed system was a highly efficient heating system in winter conditions [246]. Air-based PV-T collectors have a simpler structure and are normally easier to integrate with space heating than water-based PV-T collectors (e.g., direct hot air space heating), resulting in lower capital costs. However, the low density and small heat capacity of air limit improvements in the air-based PV-T collector performance, although this type of collector is attractive in applications where water is limited [501].

Water-based PV-T collectors can also provide SH [28,320,502,517,518]. The delivery temperature depends on the heat delivery component of the SH in the building, with conventional water radiators requiring temperatures between 70 °C and 80 °C, while UFH and fan-coil systems require lower temperatures (35–45 °C) [123,517,519]. Therefore, the latter heat delivery components are more appropriate for integration with water-based PV-T collectors, as those temperatures allow the collector to operate at high electrical efficiencies, while minimizing the requirements of the auxiliary heater if the system is correctly sized [123,519]. For this application, the solar system is usually a closed-loop circuit with oxygen-free and non-corrosive water or a mixture of glycol-water to avoid freezing in temperate and cold climates [517]. The hot water generated by the PV-T collectors is usually collected in a hot water storage tank. This tank is connected through a heat exchanger to

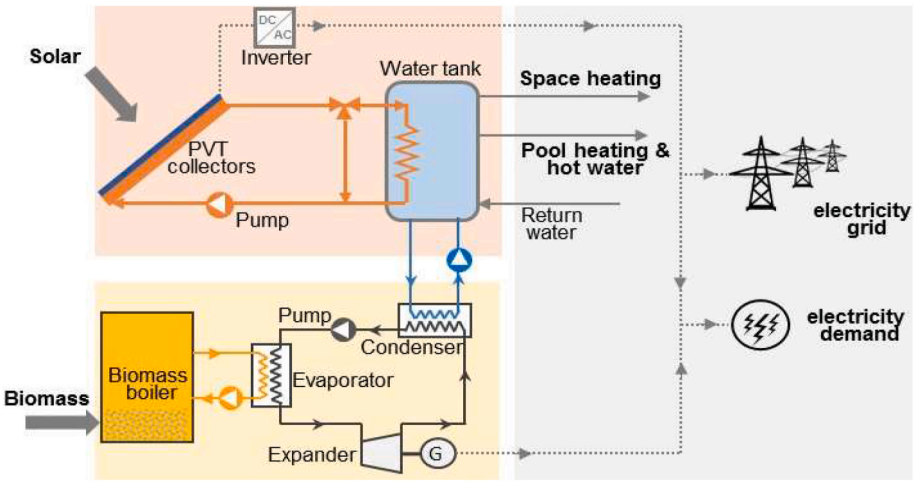


Fig. 42. Simplified schematic of a PV-T-ORC system for sport centre application [24].

the heat delivery units of the building, for instance, fan coils [502], UFH [517,520] or conventional water radiators [518]. Techno-economic analyses show discounted payback times of 11.6 and 15.6 years in Mediterranean countries (Spain and Greece, respectively), while in low solar irradiance and lower ambient temperature countries such as the UK, Germany, etc., the estimated payback time is longer (22.7 years) and closer to the system's lifetime [518]. This configuration is usually more complex and expensive than air-based PV-T collectors, but typically has higher efficiencies, exhibits better versatility, and is more compact. However, unless additives are used, water-based PV-T collectors face the problem of freezing in regions where the temperature drops, especially in winter nights.

Another alternative is to integrate refrigerant-based PV-T collectors with HPs, which can maximize solar energy utilization and at the same time enhance the COP of the HP [45,65]. Here, the heat produced by the PV-T collectors is used as the source for an HP [521] to provide SH or water heating. These systems can find a broad range of applications in the domestic sector, as well as in-service buildings (e.g., offices, schools or universities), and in various industrial processes where low-grade heat is required, such as in food and beverages industries, textile, machinery or pharmaceuticals [68].

These systems are characterized by the integration of PV-T collectors and HPs in direct-expansion solar-assisted (DX-SAHP) or indirect-expansion solar-assisted heat pump (IDX-SAHP) systems [68,79] (see Fig. 43). In DX-SAHP systems, the PV-T collector acts as the HP evaporator, leading to an energy output increase from the condenser and thus an increase in the HP COP. In this case, the cooling fluid circulating through the PV-T collector is usually refrigerant. Previous studies proposed a multi-port flat extruded aluminium tube as the absorber of a refrigerant-based PV-T collector, working as the evaporator of an HP, and a storage tank as the condenser. The results throughout a year in 2 different climates in China showed COPs from 3.4 to 5.2, with larger COPs in Hong Kong because of the larger solar radiation and higher outdoor air temperature throughout the year [142]. Recently, some authors proposed the integration of a roll-bond PV-T collector as the evaporator of a single-stage compression HP for the provision of heat and power in northern China during summer [157]. The experimental results showed that the system operates in a long-term stable condition during the daytime with a good cogeneration performance, reaching heating COP of around 6, and that the thermal performance depends both on the weather conditions and on the condensation temperature. Apart from the challenges of refrigerant-based PV-T systems mentioned in Section 2.2.2, previous authors concluded that refrigerant distribution and PV cell temperature control become more complicated as the system size increases [68].

Alternatively, in IDX-SAHP systems there is an intermediate heat exchanger between the PV-T collector and the HP, which can be used as heat storage (see Fig. 43). The heat transfer medium is typically an antifreeze solution (or a mixture of antifreeze and water), water or air. These systems are more expensive and thus usually have a longer payback times than DX-SAHP systems, so they are recommended in larger applications such as commercial or industrial applications [68]. There are three IDX-SAHP system types: series, parallel and dual system (see Fig. 44) [65,79].

Previous studies have considered a combination of ST and water-based PV-T collectors, e.g., with mini-channel aluminium channels (28 × 5 mm) integrated with a water-to-water HP for SH in a typical house in China. Experimental results on clear days showed an average solar efficiency of 45% and a whole system average COP of 4.9 [342]. More recently, other authors also proposed a water-based PV-T collector integrated with a water-to-water HP for the provision of SH and electricity to households. The mathematical model developed was used to analyse the influence of solar irradiance, the water storage tank size and the water flow rate through the PV-T collectors on the performance of the system. The results showed that increasing the flowrate enhances the total PV-T collector efficiency (from 61% to 65% when the flow rate increases from 3 L/min (for which the flow is laminar) to 17 L/min (for which the flow is turbulent) and that increasing the size of the storage tank also increases the total efficiency of the collector. A minimum COP of 4.2 was obtained [161].

Other studies analysed and compared four alternative SAHP heating systems, using FPC, PV-T and FPC collectors with PV panels coupled with a water-source HP (WSHP), and also PV panels coupled with an air-source HP (ASHP). The results showed that the most suitable alternative is strongly dependent on the electricity price, with the PV panels coupled with an ASHP being the most sustainable option for electricity prices up to 0.23 €/kWh, while for higher electricity prices PV-T collectors integrated with a WSHP seems the best alternative [522].

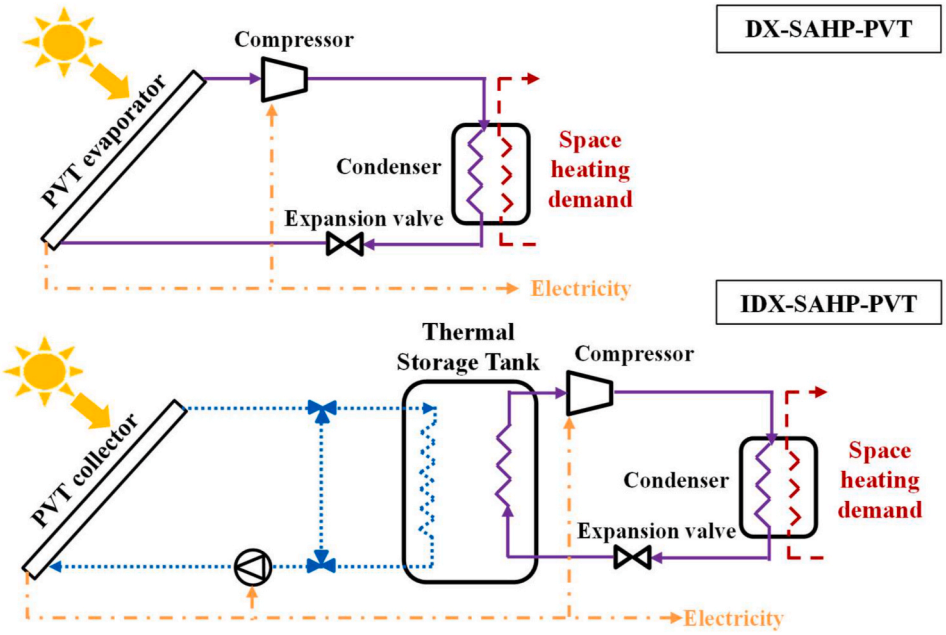


Fig. 43. Schematic diagram of a direct-expansion solar-assisted heat pump (DX-SAHP) system and an indirect-expansion solar-assisted heat pump (IDX-SAHP) system. Figure based on Vaishak and Bhale [68].

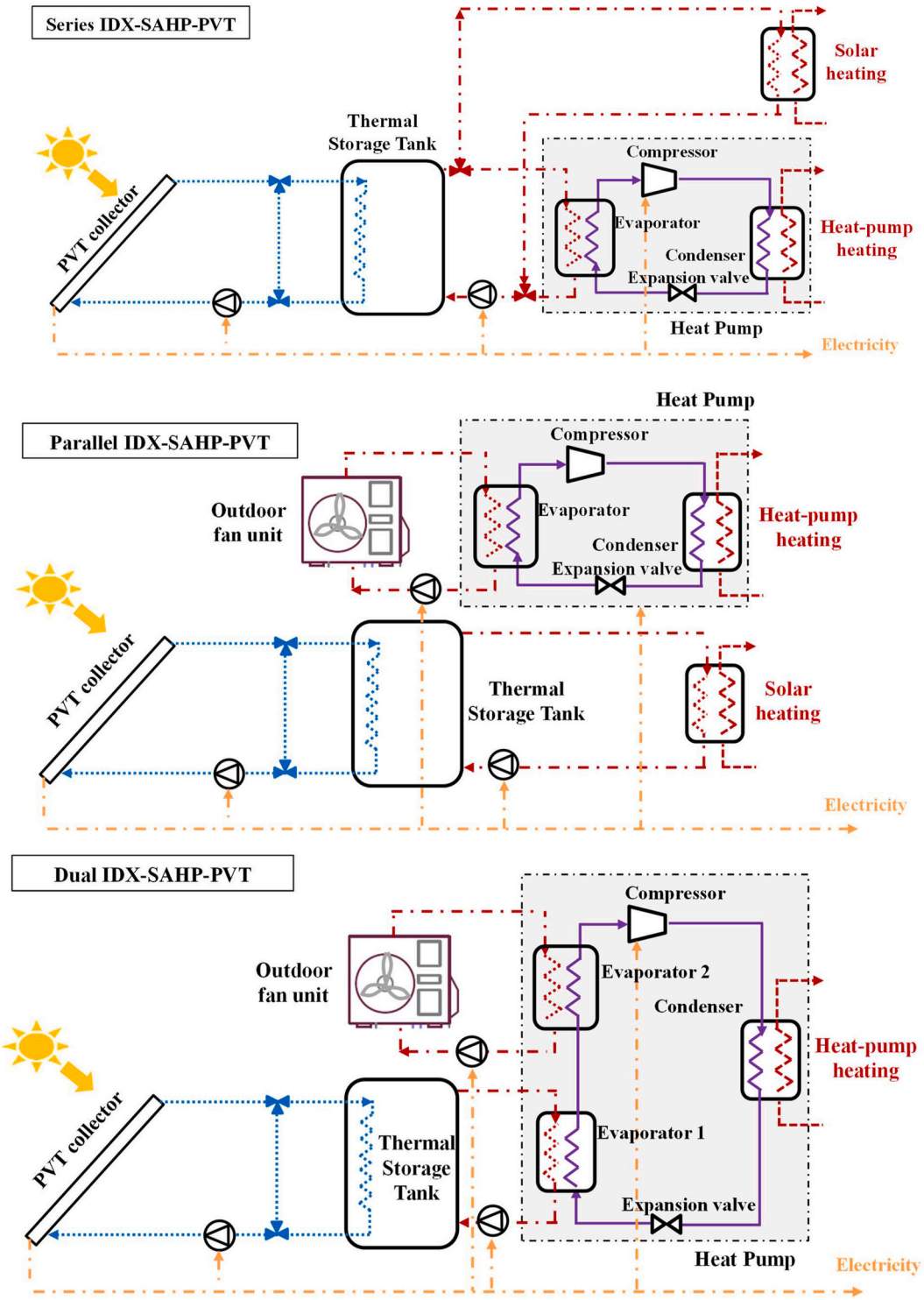


Fig. 44. Schematic diagrams of series, parallel and dual IDX-SAHP systems [65,79].

Alternatively, other investigators developed a dynamic model to analyse the performance of a dual IDX-SAHP system, with the PV-T collector acting as the evaporator and connected in parallel with an air-source HP, operating simultaneously. The thermal absorber of the PV-T collector was a serpentine copper coil. The influence of solar irradiance, ambient temperature and packing factor were analysed, and the results showed that the PV-T evaporator can compensate for the performance degradation of the air-source evaporator caused by the increasing condensing temperature, while the air-source evaporator can recover heat under low radiation levels as the evaporating capacity of the PV-T evaporator is low under these circumstances. The proposed system achieved an average COP above 2 under low temperature and irradiance levels (10 °C and 100 W/m^2) [145]. The most appropriate and efficient IDX-SAHP configuration depends on the specific application as well as on the boundary conditions (e.g., weather conditions, utility prices, and user demand characteristics).

Water-based PV-T collectors with microchannels as the thermal absorber have also been proposed in the literature [523], with the

collectors integrated with different types of HP to operate in alternative operating modes: (a) for heating and power a PV-T collector and a WSHP, or PV-T collector and water & air-source HP (W&ASHP) system; and (b) for water heating and power a PV-T collector and ASHP or simply water-based PV-T collectors. The results showed that, under experimental conditions, the COPs of PV-T-WSHP and PV-T-W&ASHP systems for heating were 3.2 and 2.5, values higher than the COP of 2.2 of an ASHP (without PV-T collectors). This was attributed to the additional solar energy that could improve the evaporating temperature of the HP [330].

Finally, it should be mentioned that heat-pipe PV-T collectors can also be integrated with the evaporator of an HP system [165,499], eliminating any mechanical component for working fluid circulation, while avoiding freezing in cold regions [68,524]. However, some authors concluded that the thermal performance of this type of PV-T collector is not satisfactory in low-irradiance conditions on cloudy days [173,525].

4.1.3. Water heating

Most studies in literature focus on the supply of DHW demand in buildings [65,83,113,269,314,316,321,332,479–483]. Generally, solar systems designed for DHW provision are smaller than those designed for DHW and SH provision, as the energy required for DHW generation usually represents 10–40% of the energy required for SH [531], except in hot and tropical climates where the SH demand is small or null. Moreover, SH and DHW have different demand profiles and temperature requirements, so the design of the solar system should be done accordingly depending on the specific needs [507]. DHW demand occurs all year long with small seasonal variation and with a daily profile with usually short peaks early in the morning and later in the evening.

A solar DHW system usually comprises an open-loop circuit with water entering the storage tank from the mains at a low temperature, normally around 4–20 °C depending on the season and on the location, and the water leaves the tank at 60 °C due to regulations in many countries to prevent Legionellosis [508,532]. The final delivery temperature might be lower depending on the end-user needs (45–60 °C), for which a mixing device is typically used. These solar systems can be configured as direct (open-loop) systems, such as thermosiphon systems (Fig. 45(b)), in which potable water is heated directly in the PV-T collectors [272,337,528,529]; or indirect (closed-loop) systems, where potable water is heated through a heat exchanger usually immersed in a water storage tank, inside which the hot water in the solar closed-loop circuit circulates (see Fig. 45(a)) [27,91,344,526,530].

Thermosiphon systems have been widely studied, as the elimination of the circulation pump saves both investment costs and electricity. Some studies [72,337] concluded that thermosiphon systems are a good option in locations with subtropical and temperature climate conditions, showing better thermal performance than with a circulation pump in warm climate applications [272]. Kalogirou and Tripanagnostopoulos [74] studied thermosiphon (open-loop) systems in different cities (Nicosia (35°), Athens (38°) and Madison (43°)), and compared them with closed-loop systems. They concluded that at lower latitude locations, thermosiphon systems can cover all thermal energy required in a single-family house for DHW consumption during summer, while in the higher latitude locations, it is possible to cover a considerable amount of the DHW needs, but some extra thermal auxiliary system is required. However, at higher latitudes, the outdoor temperatures can remain below the freezing point of water, typically for more than a third of the year, in which case the addition of antifreeze liquid into the fluid circuit reduces their thermal performance by about 15% [74,526], and makes them a less appropriate solution. In these cases, closed-loop systems might be more appropriate.

There are numerous examples of indirect (closed-loop) systems. Early field studies tested different types of water-based PV-T collectors for DHW provision in the Netherlands and concluded that covered sheet-and-tube collectors are the most promising PV-T concept for water heating, achieving annual average solar efficiencies of 34–39% [120,128]. Several authors [504,534,535] have proposed a double heat exchanger in the thermal storage tank, one in the lower part for the PV-T collector loop, and another in the upper part for the auxiliary heater, to facilitate stratification and avoid heating the water that flows through the PV-T collectors.

Other studies focussed on energy and economic assessments of commercially available water-based PV-T collectors (which usually use a water-glycol mixture to avoid freezing) for electricity and DHW production, analysing the influence of different systems [27,536] and economic parameters [91], in different countries and climates to assess the influence of climatic [318,517] and economic conditions [322,520]. The results of dynamic simulations showed that the system thermal output highly depends on the control parameters (e.g., pump operation, differential thermostat controller, flow rate setting) in response to the varying weather conditions [498]. Previous research concluded that water-based PV-T closed-loop systems can cover up to about 50% of the total electricity demand, and 35–50% of the DHW demand of a typical household in London (UK) [27,498], with discounted payback times of 11 years [91], while fully covering the electrical demand and around 70% of the DHW demand of a household in Larnaca (Cyprus) [537]. These systems are more expensive and thus usually have a longer payback time than thermosiphon systems, but normally have higher efficiencies and more versatility. The operating conditions (water flow rate, temperature set-points) of the indirect (closed-loop) systems can be also controlled and optimized with more flexibility than direct systems.

Some investigators have also proposed IDX-SAHP systems based on water-based PV-T collectors for water heating in sports centres [335]. Annual simulation results have shown that the proposed systems achieve 66–76% energy savings depending on the location, with collector thermal efficiencies of 43–49% and electrical efficiencies around 10% [335].

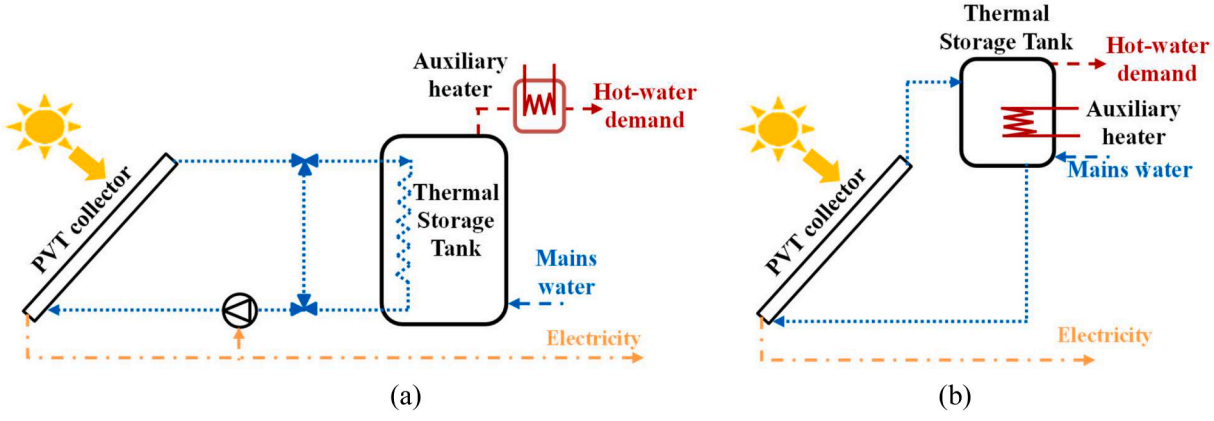


Fig. 45. Schematic diagram of: (a) a typical indirect water heating system [27,79]; and (b) a thermosiphon water heating system [533].

More recently, other authors analysed the dynamic performance of the thermal part of a SAHP system based on water-based PV-T collectors coupled with a brine-to-water HP. To this end, they designed a demonstration system, which was installed and tested in Denmark under real weather conditions and with automated draw-offs to replicate a realistic DHW demand. The results showed that the uninsulated PV-T collectors operated as PV-T collectors during sunny periods and as energy absorbers with the ambient during periods with very low or no solar irradiance [538]. One of the main advantages of IDX-SAHP systems is the lower operating temperature of the PV-T collector, which allows the collector to operate at higher efficiencies. However, the integration of PV-T collectors with HPs is usually more complex than with a conventional auxiliary heater.

Water-based PV-T collectors can also be used for water heating in the industry [539,540], showing promising results as reported by Berardi [540], who analysed the techno-economic potential of this type of collectors to provide warm water in a paper mill in four different locations in Romania.

Alternatively, refrigerant-based PV-T collectors can be integrated with HP systems for water heating, using the PV-T collector as the evaporator of the HP [151]. The results showed that the mean electrical efficiency can improve by up to 24% in comparison with that of a conventional PV panel, and the water temperature in the water tank can rise from 20 °C to 42 °C. Heat-pipe PV-T collectors have also been analysed for electricity and DHW production in cold regions, to avoid freezing [541]. One of the main advantages of these systems is that they do not require an auxiliary heater and/or another fuel apart from electricity to meet the hot water demand, because the HP acts as the auxiliary heater. However, these systems are more complex than water-based PV-T collectors and an auxiliary heater.

Regarding the type of water storage tank, some studies consider a fully-mixed water storage tank [27,74,272,355] while others consider a stratified storage tank [127,344,517,520,526,530] as they claim that the thermal performance of PV-T collectors has enhanced thanks to thermal stratification [527]. The reason attributed to this is the lower temperature of the water exiting the water storage tank and entering the PV-T collectors as usually, this water comes from the bottom of the tank, which is colder than the top, such that the hot water exiting the PV-T collectors enters the tank to heat the water inside.

4.2. Solar cooling systems

Solar cooling systems represent an interesting target for the development of PV-T collectors since several technologies might beneficially use their outputs to achieve cooling, as shown in Fig. 46. Importantly, it should be noted that even if one of the thermally-driven cycles of Fig. 46 is used, electricity is still required to distribute a chilled fluid to the application. In fact, the electrical requirements for a thermally-driven cooling cycle can be quite large since the air handling unit in a commercial building consumes a significant portion of the HVAC systems' energy budget. Thus, PV-T collectors represent a solution to provide both the primary driving heat and also the electricity to drive the fans which distribute cold air (through ducts) to the building. A previous review concluded that PV-T collectors combined with single-effect absorption chillers seem a competitive alternative both technically and economically [57]. In this line, the thermal outputs of water-based PV-T and CPV-T collectors have been integrated with solar thermal-driven cooling units, such as absorption, adsorption or desiccant, for cooling provision [64,542].

The obvious benefit of making this switch to solar for cooling applications is that it can be a more sustainable option than burning fossil fuels. Since buildings account for more than 30% of total global final energy use, and air conditioning systems represent the fastest-growing share of the building energy consumption share around the world [543], PV-T systems could play a big role in reducing future carbon impacts of maintaining comfortable interior spaces. The not-so-obvious

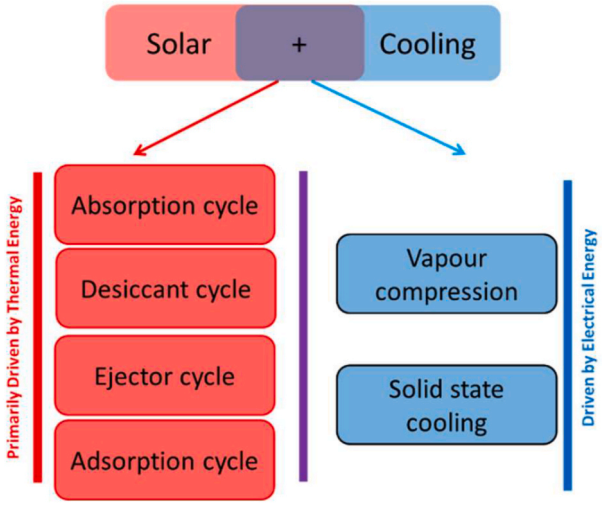


Fig. 46. Breakdown of solar-powered cooling systems.

benefit is while hot days (which require the most cooling) have more solar resources available, there are a few hours of lag time between the solar supply and the cooling demand. Since thermal energy is much easier to store, PV-T systems can potentially provide a better link between the solar supply (that hits the building's rooftop) and the required cooling demand compared to PV-only systems. Although there are no large-scale PV-T solar cooling installations to date, several large-scale, thermally-driven systems have been installed in recent years, as shown in Fig. 47. Interest in solar air-conditioning has grown steadily over the last 10 years. If small-scale systems are included, the total number of thermally-driven solar cooling installations is above 1,200 systems [544]. More than 75% of the installations worldwide are located in Europe, led by Spain, Italy and Germany. The vast majority of the installed solar air-conditioning systems are coupled with either flat-plate ST collectors or ETCs [59]. Limited examples of the use of concentrated collectors (Fresnel or PTCs) can be found in installations in India, Turkey and Australia [11]. To date, there is still a small number of companies that offer packaged solar air-conditioning systems. The majority of the systems currently available include independent components that have been installed on-site together to meet the specific needs of different projects [69]. In order for solar air-conditioning solutions to become broadly available, there is need for growing expertise in installing, commissioning and operation of such systems [545].

It should be noted that the jury is still out on whether thermally-driven or electrically-driven systems represent the best way forward for cooling, or even for heating [546,547]. Among several

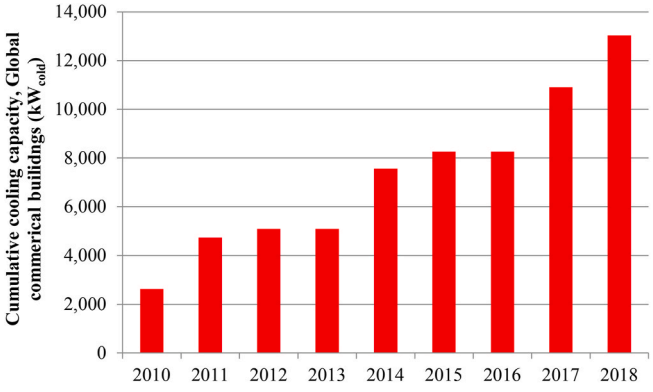


Fig. 47. Estimation of the recently installed capacity of thermal-driven solar cooling systems in large-scale, commercial buildings, raw data from Weiss et al. [6].

techno-economic issues, the overall efficiency may be worse than electrically-driven systems since high COP rev-HP (i.e., with COP ≈ 4–6) driven by modern silicon PV panels are hard to beat [51]. Currently, the average conversion efficiency of most commercial PV panels is relatively low (10–15%) [548], but when combined with a high COP HP system, the overall sun-to-cooling efficiency of PV-driven systems can range from 40% to 90% (e.g., 10–15% × 4–6 = 40–90%). In comparison, thermally-driven cooling systems have a lower COP (0.6–1.8) but higher collector efficiency (35–70%), so the overall sun-to-cooling efficiency of thermally-driven systems realistically ranges from 35% to 80%, since the chiller's COP and the collector efficiency are inversely related, and both depend on the operation temperature. Additionally, from a broader techno-economic perspective, several other factors have been debated in the literature [544,549–552], which include the facts that PV panels have no moving parts and their installed cost has dramatically decreased in recent years. That said, the aspirational aim of a carbon-neutral (or even carbon-positive) building may tilt the equation towards thermally-driven cooling systems since the high cost of battery storage limits PV-only-driven systems. Another tangible advantage of thermal-driven systems is the removal of the vibration and noise associated with the compressor. For these reasons, PV-T or ST cooling systems are much more likely to be taken up at larger scales (i.e., >50 kW), and in regions/buildings which require year-round cooling, for these benefits to offset the relatively higher overhead costs of installation, operation, and maintenance [548,552].

As shown in Fig. 46, the most common thermally-driven cooling options in solar applications are based on absorption, desiccant, ejector, and (the emerging) adsorption cycles. In all of these options, the basic idea is to remove the need for an energy-intensive gas compression step which requires an electrical input to a mechanical compressor. A comparative study in a subtropical city of different solar cooling systems including solar electric compression, solar mechanical compression, solar absorption and solar solid desiccant concluded that solar absorption and solar electric compression lead to the largest energy savings [553].

The absorption cycle uses a secondary fluid—an absorbent—in addition to the working refrigerant. The absorbent is used to absorb the refrigerant vapour, allowing it to be compressed as a liquid (rather than as a gas), which significantly reduced the need for a mechanical work input. The main components of the absorption cycle are an evaporator, an absorber, a solution pump, a generator, a condenser and expansion valves, which are shown in Fig. 48. With these components, the cycle follows an analogous process to a vapour compression cycle, with the absorption cycle operating between two pressure levels. The low-pressure level corresponds to the evaporator and absorber, while the condenser and generator operate at the high-pressure level. Typically, the high-pressure level is 10 × the low-pressure level, allowing the heat rejection from the refrigerant to occur at commonly useable temperatures. More advanced systems have also been proposed to use double and triple effects, which require higher driving temperatures, ~120 °C and ~180 °C, respectively [554]. From the perspective of a PV-T collector, achieving these temperatures with the thermal receiver would require solar concentration and solar tracking.

The most common absorption cycles are based on lithium bromide-water (LiBr–H_2O) [555] or ammonia-water (NH_3–H_2O) [51] as the working-fluid pair. Most previous research in this space has considered the use of ST collectors (FPC, ETC, PTC, CPC) to drive these units [69]. However, some studies focussed on combining CPV-T collectors with LiBr–H_2O absorption units [556–558], or flat-plate PV-T collectors with LiBr–H_2O absorption units [518,559]. Recent studies have shown that COPs of up to 0.8 can be achieved by solar-driven single-effect LiBr–H_2O absorption chillers [51,560,561]. NH_3–H_2O absorption chillers require higher heat supply temperatures than LiBr–H_2O units, but can generate a cooling effect below 0 °C [51,562].

A desiccant cooling cycle has a very different operating principle. Rather than trying to reproduce the vapour compression cycle, it simply controls the humidity levels to make clever moves around the psychrometric chart to produce a net evaporative cooling effect for the supply air. Although it can get relatively complicated in a multi-stage system, the basic desiccant cycle employs a liquid or a solid desiccant material to absorb water from an incoming air stream. Water is then sprayed into the resulting dehumidified air stream, thereby lowering its temperature and providing evaporative cooling. The outgoing air can be heated with a solar collector to regenerate the desiccant, which is typically contained in a rotating wheel. Advanced systems have been proposed to build upon this basic operation to recycle as much of the latent and sensible energy as possible by using multiple desiccant and heat regenerator components [563].

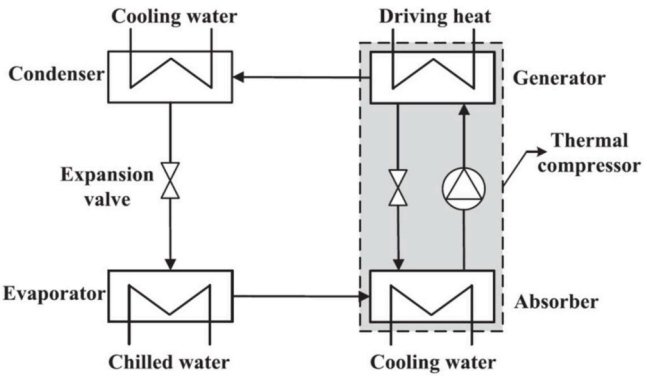


Fig. 48. Absorption cooling cycle. Reprinted from Shirazi et al. [544], with permission from Elsevier.

Investigators have analysed the energy and economic performance of desiccant cooling systems (DEC) that used either single-glazed standard air ST collectors or air-based PV-T collectors. They concluded that DEC equipped based on PV-T collectors have better performance in terms of primary energy savings than conventional systems based on vapour compression chillers and PV panels [564]. More recently, two alternative DEC systems were proposed based on PV-T collectors in a humid climate, Abu Dhabi (UAE), obtaining COPs of 0.25–0.27 and solar shares of 32–37% [565]. Guo et al. [63] reviewed the utilization of recovered heat from flat plate PV-T collectors for desiccant cooling and dehumidification that requires a temperature in the range 50–60 °C. The review revealed that the outlet fluid temperature from existing PV-T demonstrations could almost match the temperatures required by dehumidification and cooling applications with reasonable electrical and thermal efficiencies.

An ejector cooling cycle goes back to the concept of making a thermal compressor to replace the mechanical compressor. While it is an emerging technology, the physics of the cycle are relatively well-known. The ejector part of the cycle simply requires a supersonic nozzle, a mixing chamber, and a diffuser to compress a refrigerant. The ejector operates by utilizing thermal heat (e.g., potentially from a PV-T collector since it is under 100 °C) as the motive force from a generator to pressurize the refrigerant [563]. One major advantage of an ejector cycle is that the compressor now has no moving parts since a nozzle is a passive device.

Another emerging cycle that can use the output of a PV-T collector is the adsorption cooling cycle [566]. Such a cycle relies on the phenomenon of physical adsorption between the refrigerant vapour and a solid adsorbent to achieve a cooling effect. Silica gel, zeolite and carbon-based materials are commonly used as the adsorbents in this cycle, with water, methanol and ethanol as typical candidates for the refrigerants.

A basic adsorption cycle diagram is shown in Fig. 49, from a detailed review of these systems by Goyal et al. [567]. As shown in the figure, there are four basic processes in an adsorption cycle. When heated by a solar input, the solid absorber releases its vapour and pressurizes the vessel in which it is contained. Although the pressure is relatively low, this can be considered a thermal compressor. In the next step, the vessel continues to heat while the vapour is desorbed. Following this, the

low-pressure vapour enters the adsorber by passing from the evaporator. This reduces the temperature and pressure in an isosteric cooling phase. To get back to the starting point of the cycle, the vessel undergoes an isobaric adsorption process which significantly reduces the temperature. This is where the cooling effect is generated. Several studies have been conducted on how solar energy can be used as the driver for these systems, covered in detail in the review by Goyal et al. [567]. A notable difference in solar integration is that the operation is fundamentally intermittent. That is, rather than simply continuously applying the heat from the PV-T collector to a generator (as is done in the absorption cycle in Fig. 49), it is a batch process where once the vessel is heated and pressurized, no more solar heat is needed for a time. There are two ways around this: 1) size the vessel/PV-T heating so that only one batch occurs per day (which is unlikely); and 2) use two or more adsorber vessels to control and redirect thermal energy to different vessels as needed (using some PV-derived electrical energy for the control system). A recent patent was also published by Alelyani et al. [568] on how to incorporate the adsorbent bed directly inside of the evacuated tubes of an evacuated tube array solar collector.

As mentioned above, one of the key enablers of these thermally-driven systems is their ability to economically store thermal energy, acting as a buffer to overcome the intermittent nature of solar energy and the variation in load demand of buildings. It also provides residence time buffering, preventing it from frequent turning on and off. There are two basic approaches to integrating a thermal storage unit into a thermally-driven solar cooling system. The first is to store the solar-derived heat in a thermal storage tank, which can be later used to drive the chiller. The second option is to store the cold energy produced by the chiller in a cold storage unit. The potential benefit of incorporating a cold storage unit is that it could reduce the chiller capacity and, depending on the overall efficiency, the total storage size. However, since condensation on the tank could represent a major energy loss and cold storage is more valuable, a cold thermal storage system requires better insulation, which could make it more expensive than a hot storage tank. Another key choice is whether the thermal storage medium will be a sensible solid or liquid medium or a latent heat medium, which uses the high latent heat of a PCM. To date, most solar cooling installations have used sensible storage mediums due to their relatively low cost, but future systems may go for solid/liquid PCM candidates since they could reduce the size of the storage tank (regardless of whether it is cold storage or hot storage).

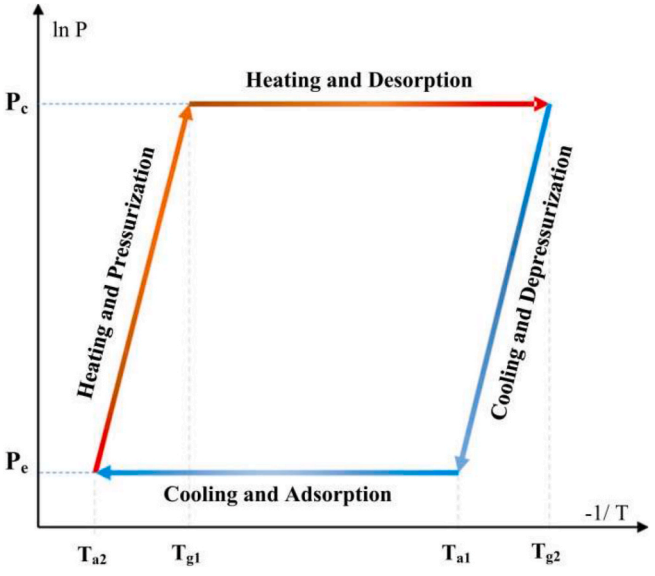


Fig. 49. Adsorption cycle diagram, reprinted from Ref. [567], with permission from Elsevier.

Alternatively, PV-T collectors can be used at night-time to cool water through radiative cooling [156,181,505,569]. Previous work measured cooling power levels between 60 and 65 W/m^2 when the PV-T collector was used to cool a warm storage tank and 40–45 W/m^2 when the energy was directly used to cool a ceiling. The results revealed a promising ratio of cooling energy to electrical energy required for pumping water through the PV-T collector, with values between 17 and 30 [570]. More recently, experimental work in northern China assessed the refrigeration mode of a DX-SAHP unit that used the PV-T collector as the condenser during summer. The results showed an average COP of 3.0 under clear conditions, and 2.7 under overcast conditions, concluding that the proposed system performed with long-term stable operation [505].

In the general field of solar cooling, there is a major international effort to increase the TRL of these technologies. This effort is mainly led by the IEA, which has organized several dedicated tasks as part of the SHC program. These began with Task 25 in 1999, which aimed to improve conditions for the market entry of solar-assisted cooling systems. Task 38 began in 2006, with an emphasis on accelerating the market introduction of small and medium-sized solar thermal air-conditioning and refrigeration systems. Task 45 ran from 2011 to 2014, intending to develop a sustainable market for large-scale SHC systems by focussing on cost-effectiveness and performance reliability. Task 48 focussed on quality assurance and support measures for solar cooling. Task 53 ran from 2014 to 2018 and focussed on smaller SHC systems, ranging from 1 kW to a few tens of kW (i.e., residential applications). The latest Task, Task 55, which started in 2016, was dedicated to looking into how solar inputs can fit into district heating and cooling networks. While most of the reports produced to date in Task 55 have focussed on the heating aspects, PV with HPs and ST collectors-only systems are included as part of the scope of work.

Based upon the overview given above, it is clear that although there is significant research taking place on solar cooling, much less effort is in being placed specifically on PV-T collectors as a potential driver for solar-cooling systems, so this is an area that continues to require attention. If scalable and cost-effective PV-T systems can be developed, solar cooling is a low-hanging fruit where they could be beneficially employed.

4.3. Solar combined cooling, heat and power systems

Heating and cooling correspond to approximately 50% of the total final energy use in the EU [571]. SHC systems can use solar radiation to provide heating and/or cooling. PV-T collectors can also be integrated with SHC technologies to generate electricity, heating and/or cooling. Some studies integrate CPV-T [556–558,572], air-based PV-T [246] and water-based PV-T collectors [502,518,562,573] with cooling technologies. Previous research concluded that S–CCHP systems based on PV-T collectors can cover more than 60% of the combined heating demand of SH and DHW, along with more than 50% of the cooling needs of households with reasonable installation areas [574,575].

Parabolic dish CPV-T collectors readily reach higher water temperatures so they can be integrated with double-effect LiBr–H_2O absorption chillers, which have a higher COP than single-effect LiBr–H_2O absorption chillers, to provide electricity, SH, cooling and DHW to buildings [556,557], albeit at a higher upfront cost and complexity than single-effect chillers. Numerical results have shown electrical efficiencies of 19–25% (using triple-junction PV panels), and thermal efficiencies of ~60% over a wide range of operating conditions [556].

Several authors [502,503,518,573,575] integrated water-based PV-T collectors with absorption chillers and concluded that this combination has an important energy-saving potential thanks to the provision of SH/DHW, cooling and electricity. Both uncovered and covered PV-T collectors have been integrated with half-effect or single-effect LiBr–H_2O absorption chillers. The results show that covered PV-T collectors coupled with a half-effect absorption chiller achieve the highest solar COP (of 0.07) and solar utilization factor (of 0.24), while the shortest payback time is achieved with uncovered PV-T collectors

coupled with a half-effect absorption chiller [503]. These systems need an auxiliary system (usually an auxiliary boiler, or an HP) to ensure a safe operation and also to provide the energy demands when there is not enough solar irradiance [502,503,518,562]. Recent work showed that a 1.68-MW_p S–CCHP system composed of water-based PV-T collectors and LiBr–H_2O absorption chillers (see Fig. 50) has the potential to cover 21%, 55% and 16% of the SH, cooling and electrical demands of a University Campus in Bari (Italy), respectively, with a payback time of 16.7 years, and roof-space availability being a major limiting factor [518]. The economic analyses showed that the cost-competitiveness of these systems is highly dependent on the utility prices of the specific application [518, 562] and that in most cases public funding or economic incentives are required to make these systems competitive with conventional alternatives (e.g., systems based on ST or PV panels) [502,503].

Another study of interest here compared the techno-economic performance of different types of water-based PV-T collectors integrated with either absorption or adsorption chillers for the provision of combined SH, space cooling, electricity and DHW to a small cluster of four buildings located in different European cities [69]. The results from this work showed that the most suitable thermally-driven technology depends most strongly on the solar irradiance availability and, also, on the selected solar collector technology. Single-effect absorption chillers or high-temperature adsorption chillers are recommended with CPV-T or low-emissivity PV-T collectors, in locations with medium or high solar irradiance. Meanwhile, the performance of low-temperature adsorption chillers does not depend as much on the PV-T collector technology and solar irradiance levels [69].

Reversible HPs (rev-HP) can also be integrated with the thermal output of water-based PV-T collectors, increasing the COP in the heating mode in winter [559,575], while in summer the electrical output generated by PV-T collectors can be used to run the HP to provide cooling [575]. The integration of ST or PV-T collectors with rev-HPs appeared to take advantage of the higher source temperature of the collectors to enhance the HP performance. In S–CCHP systems, the electrical output of PV-T collectors can feed air-to-air HPs or water-to-water HPs for cooling provision, or air-source rev-HPs for heating and cooling provision [575]. For instance, recently some authors [504] proposed an S–CCHP system, with water-based PV-T collectors heating a thermal storage tank and connected in parallel with an air-to-water HP, operating simultaneously. The results showed that the electrical output of the PV-T collectors can meet the HP electricity needs. Meanwhile, the thermal output can be used to preheat the water in the tank, decreasing the HP electricity consumption in winter, while in summer can satisfy all the DHW demand. A detailed LCA [576] showed that this system can reduce the environmental impacts of buildings in a wide diversity of solar irradiance levels and electricity mix scenarios, even in climates with low irradiance levels or in countries with a highly decarbonized electricity supply.

Water-based PV-T collectors can also be integrated with water-to-water HP systems [575,577] and/or adsorption chillers [578]. A polygeneration system proposed by some authors [579] used the thermal energy generated by the PV-T collectors as the HP evaporator in winter to provide SH, while in summer the thermal energy was used to run an adsorption chiller to provide space cooling. The proposed system also provided electricity and DHW for residential buildings [579], or fitness centres and offices [559]. The main limitation of the proposed system is the high complexity and size, as it is composed of a large number of different units, which also increases the system costs. Alternatively, other authors proposed water-based PV-T collectors coupled with water-to-water rev-HPs, using the PV-T electrical output to run the rev-HP unit for heating/cooling respectively, while the PV-T thermal output was used to maintain the temperature of the HP source at around 15 °C all year round, maximizing the rev-HP COP and thus reducing the electricity consumption [575]. A similar S–CCHP system was proposed in a more recent work, where electricity, cold water (below 17 °C) and hot water (80–90 °C) were generated by a PV-T-cascade HP system in tropical weather (see Fig. 51), obtaining a payback time of 7.9 years [577].

Recently, some authors have proposed a DXSAHP with a new roll-bond PV-T collector acting as the HP evaporator in heating mode and as the condenser in refrigeration mode [156,505]. This system operates in refrigeration mode at night-time during summer in two steps, chilled water process and ice process. The experimental results showed COPs from 2.4 to 3.5 with an average value of 2.8 during the chilled water process, and COPs from 1.9 to 2.9 with an average value of 2.3 during the ice process [505]. The modelling and experimental results show that the proposed system has the potential to provide space cooling, hot water, and electricity for buildings with high efficiency and long-term stable working condition [156]. In this line, other authors proposed a trifunctional photovoltaic-photothermic-radiative cooling system, which generated electricity and/or heating during the daytime and cooling at night through radiative cooling [181].

Alternatively, other authors investigated the performance of uncovered water-based PV-T collectors for direct provision of electricity, DHW and cooling, using longwave radiative cooling [569]. Three residential case studies were analysed, located in three different European climates, showing that the performance of the proposed system strongly depends on the energy demand profile, the climatic conditions and the utility prices. The best results are obtained for locations with high irradiance levels and electricity prices [569].

An IDX-SAHP system based on uncovered PV-T collectors integrated via thermal storage tanks with an air-to-water reversible HP (rev-HP) was recently proposed. The system covered the heating, cooling and electricity demands of an industrial building. The PV-T collector circuit worked at night to cool the water in the tank and satisfy part of the cooling demand through radiative cooling. The results show that the proposed system can cover between 19% and 47% of the cooling demand through radiative cooling, along with more than 60% of the heating demand, between 32% and 49% of the electricity demand of the analysed building [534].

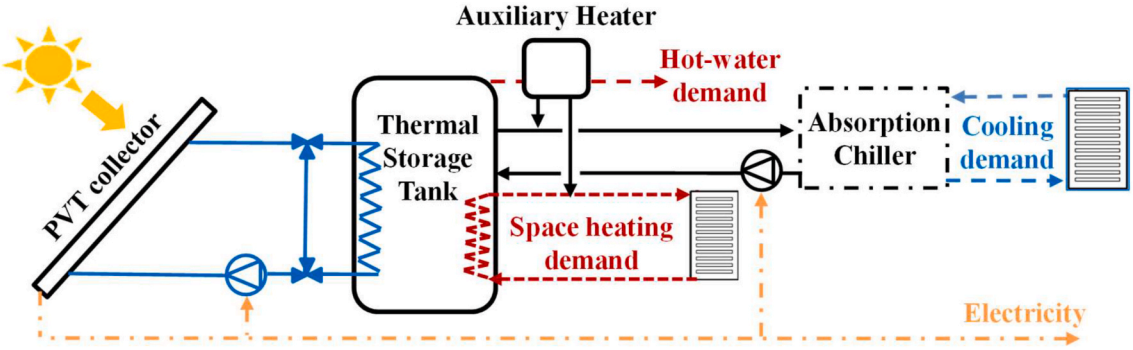


Fig. 50. Schematic of the S–CCHP system based on water-based PV-T collectors integrated with an absorption chiller through a thermal store for SH, cooling, hot water and electricity provision [518,562].

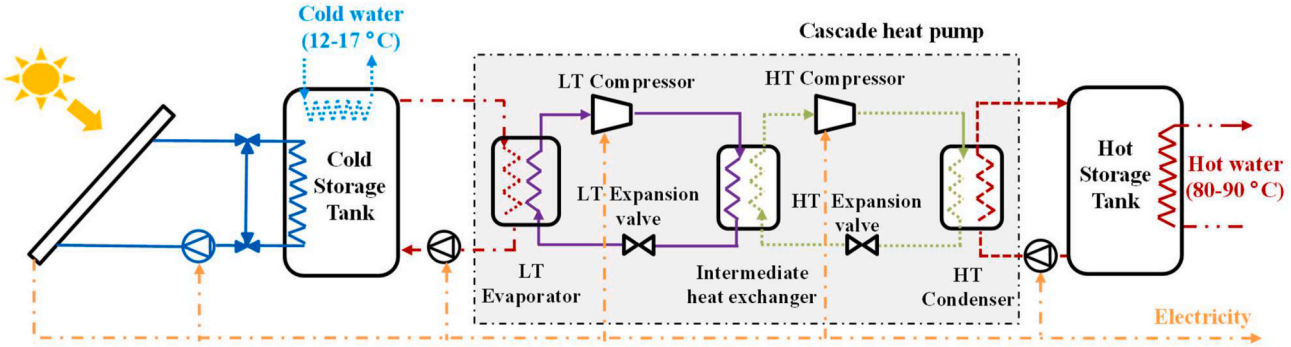


Fig. 51. Schematic of the S–CCHP system based on water-based PV-T collectors integrated with a water-to-water cascade HP for cold water, hot water and electricity provision. Figure based on Kong et al. [577].

4.4. Solar desalination

Another application area for a PV-T collector is within a desalination system. Similar to solar energy, where there are two conversion pathways for the incoming sunlight (direct to electrical or to thermal), desalination can be broken into two primary techniques: thermally-driven, and electrically-driven. Because of this nature, desalination coupled with PV-T collector has some natural synergy. Thermally-based desalination is primarily composed of four main approaches: multi-effect distillation (MED), humidification-dehumidification (HDH), solar stills, and membrane distillation (MD). Reverse osmosis (RO) is the primary method for electrically-driven (via high-pressure pump) desalination. Notably, in all of the thermal approaches electrical energy is needed for pumping power and thermal energy can be used in RO to pre-heat the incoming feed [80].

Giwa et al. [580] investigated theoretically the use of thermal energy from an air-based PV-T collector for its use in powering a HDH cycle. In the proposed system, air was used as the cooling media for the PV-T collector. Results indicated that the proposed system could produce a daily average of 2.3 L of freshwater for every square meter of PV-T collector. This was shown to decrease the environmental impacts by 83% when compared to a PV-driven RO system, primarily driven by the chemical needed for antiscalant and anti-foulant in the RO.

Elsafi [581] considered a double-pass low-concentration PV-T collector in the context of providing air heating to an HDH cycle, see Fig. 52, in an exergetic-cost model to study its performance. The design in this work considered 3 PV panels in parallel per collector with 4 collectors in total, with a total aperture area of 9 m^2. Modelling results predicted annual freshwater production of 12 m^3 and electrical production of 900 kWh, for 10.5 USD/m^3 and 0.29 USD/kWh. Otanicar and Qu [81] modelled a higher concentration PV-T system coupled with HDH using thermovapour compression, resulting in high levels of produced electricity and water enabled by the higher temperature steam injected into the cycle.

Recently, a parametric analysis was completed comparing a variety of design parameters and operating conditions to determine the optimal operating conditions of a PV-T-HDH system [582]. In particular, the authors compared a PV-T-HDH system with a purely thermal system and a side-by-side thermal plus PV-HDH system. The authors noted that at low electricity prices the pure thermal system results in the lowest water costs, but that as the electricity price increases, the PV-T-based system results in the lowest water cost due to the excess electricity from the system, which is of particular interest in select global regions.

Ong et al. [583] investigated a high-concentration PV-T system where the waste heat recovery at 75–80 °C is both stored and then used in a multi-effect MD system. As shown in Fig. 53, fluid is used to cool a multi-junction PV cell, which can then be used to drive the heating process needed in a multi-stage vacuum MD system. A 13.5 m^3 thermal storage tank is used to allow for continuous desalination to generate 3 m^3/day of freshwater from 124 m^2 of collector area. Experiments were conducted on a

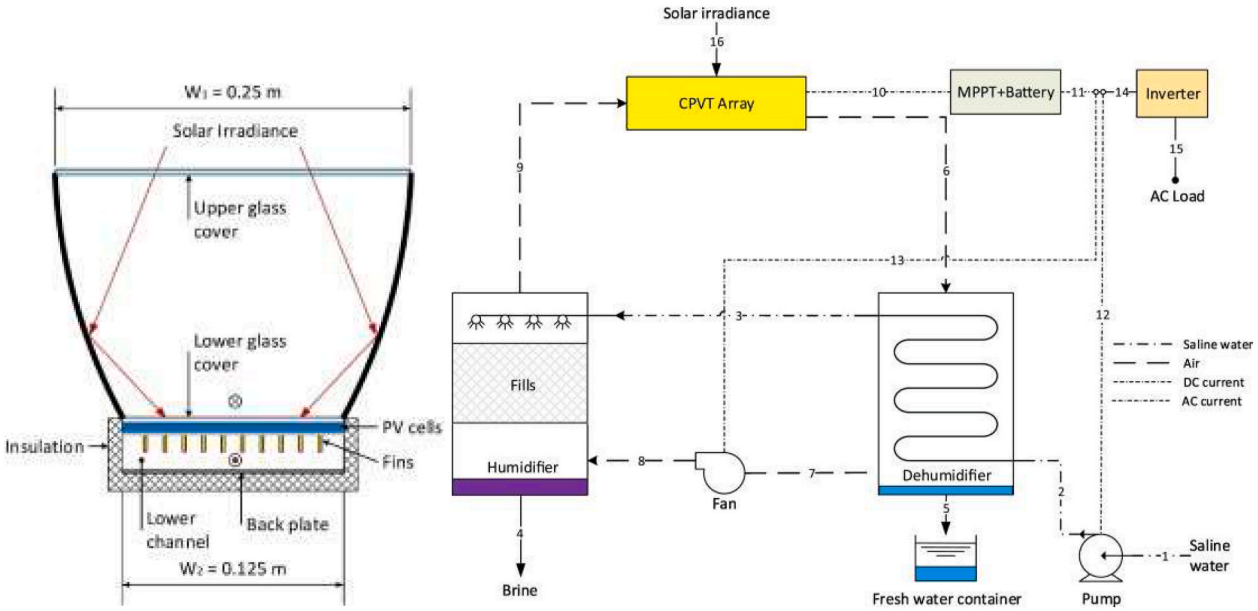


Fig. 52. Proposed low-concentration double-pass PV-T collector and corresponding HDH cycle. Images reprinted from Elsafi [581], with permission from Elsevier.

laboratory vacuum MD multi-effect system that revealed the modelling was within ±15% accuracy. That model showed that 85% of the solar irradiation was converted into useful energy. In a similar work, a concentrating PV system coupled to direct contact membrane distillation (DCMD) was proposed for desalination [584]. The experimental focus was on the water production across a PTFE membrane in a DCMD setup, but the system was not coupled to a working PV-T collector. Hughes et al. [585] investigated a CPV-T system coupled to an MD system through separate testing of a CPV-T collector and MD unit. Notably, in the studies referenced above, while demonstrating the potential for coupling PV-T systems with MD systems, the experimental work in all 3 cases never physically coupled the two.

Another desalination concept is the solar still, where water is evaporated from a free surface and then condensed on a sloped cover. Kumar and Tiwari [586] proposed an active solar still (where the water is directly heated from incoming solar flux) coupled to a PV-T collector. The PV-T collector is partially covered with PV cells (in the low-temperature region) to provide electrical output, as shown in Fig. 54. However, conventional single basin passive solar stills are not widely used due to their low yield and low thermal efficiency (maximum around 30%), which is very dependent on solar irradiation [45]. Results indicated an increase in the exergetic efficiency from 0.4% to 2.2% when the active solar still is used relative to a passive solar still. Flat-plate PV-T collectors can be integrated with solar stills in a hybrid PV-T active solar still [587–589]. The cost of distilled water produced from a PV-T active solar still is higher than for a passive solar still, and the payback period is also higher, but the use of PV-T solar still can be advantageous when electricity is unavailable [590]. Using the same experimental setup, Dev and Tiwari [589] expanded their prior work on active solar stills with flat-plate solar collectors and hybrid PV-T systems to develop characteristic equations for predicting the instantaneous thermal efficiency of these types of collectors. In a further extension of this experimental setup, two partially covered PV-T flat-plate collectors were connected to an active solar still for experimental and theoretical comparison [591]. More promising results were found for an active PV-T solar still system in New Delhi climatic conditions, with a payback time of 4.2 years [592]. Other research concluded that the productivity can be increased by coupling the PV-T collectors with a storage tank [593].

A more recent study investigated the interaction of a stepped solar still with that of a PV-T collector [594]. The authors determined the optimal flow rate of saline water in the collector that maximizes the energy efficiency and reported that the PV-T system could produce ~1 kW of power over the needed pumping power.

CPV-T systems were again investigated in a detailed simulation for coupling to MED plants [595]. In particular, the model focussed on when a PV-T system with desalination was competitive against solar-driven RO, especially in markets where the cost of electricity was high as the excess electricity in the PV-T system adds significant value. This also required low installation costs to be competitive with commercial RO systems on water costs. Other authors investigated a solar trigeneration system where a PV-T collector generates electricity and thermal energy, which subsequently drives a MED system and an absorption cooling unit [596]. The complex simulation focussed on a dynamic yearly assessment of the proposed system which indicated high performance in summer as the full thermal output could be used, but poor performance in the winter when auxiliary heaters are required to drive the MED system. Alternatively, some authors [597,598] investigated CPV-T collectors based on nanofluid spectral splitting techniques to enhance solar distillation. In the proposed system, gold nanoparticles are added to the water to absorb solar radiation as well as to act as a spectral splitting filter to enhance the distillation of water.

While most of the research on desalination has focussed on using the thermal-energy output from PV-T collectors to drive the desalination process, it is possible to use the electrical output as well to drive a RO unit. Ammous and Chaabene [599] investigated a multi-criteria sizing approach for a RO plant supplied by hybrid PV-T collectors. As shown in Fig. 55, the thermal energy output from the collector preheats the feed water while the electrical output provides power to the high-pressure pumps in the RO unit. The study focussed on the optimal sizing of the full plant considering the size of the storage tank and the size of the solar field. Wiesenfarth et al. [600] proposed a CPV-T system combined with both MD and RO to handle high-salinity feed streams. In this approach, an RO unit is driven with the electrical output to desalinate a low salinity feed stream at low specific energy levels, followed by treatment of the higher salinity stream in the MD system driven by thermal energy from the PV-T collector. In the design calculation, a total of 4,310 L of freshwater is produced and 370 L of wastewater is produced for a

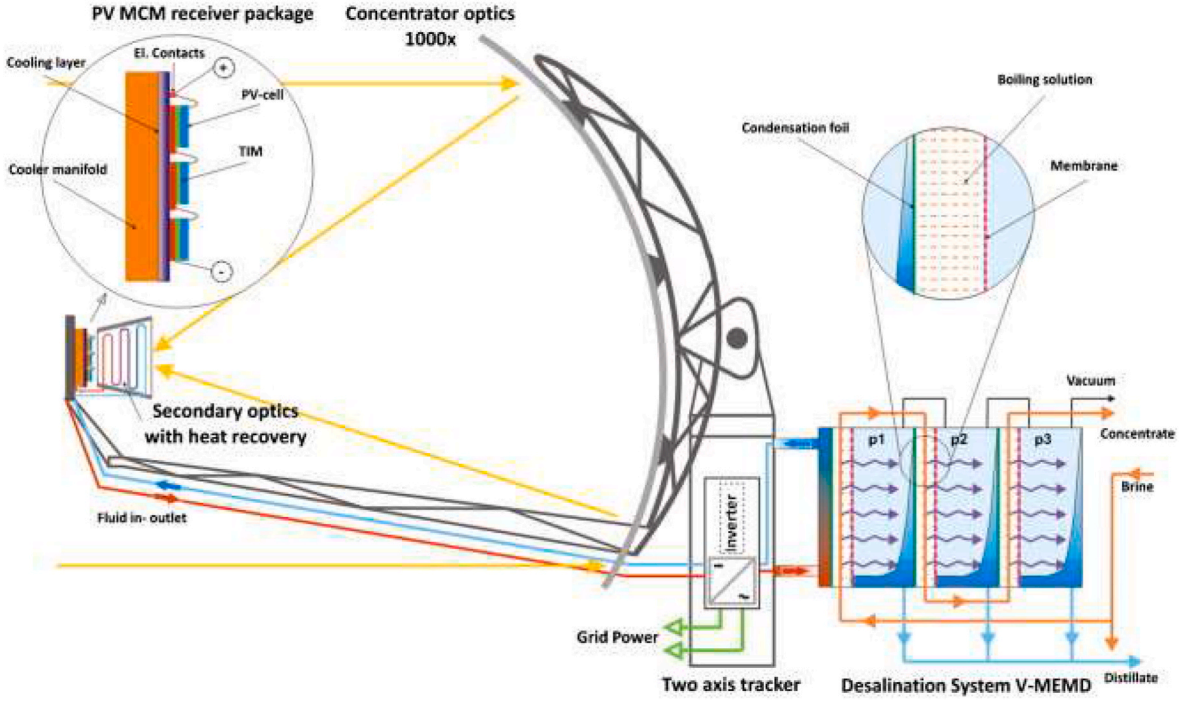


Fig. 53. High-concentration PV-T collector coupled to a multiple-effect MD unit. Image reprinted from Ong et al. [583], with permission from Elsevier.

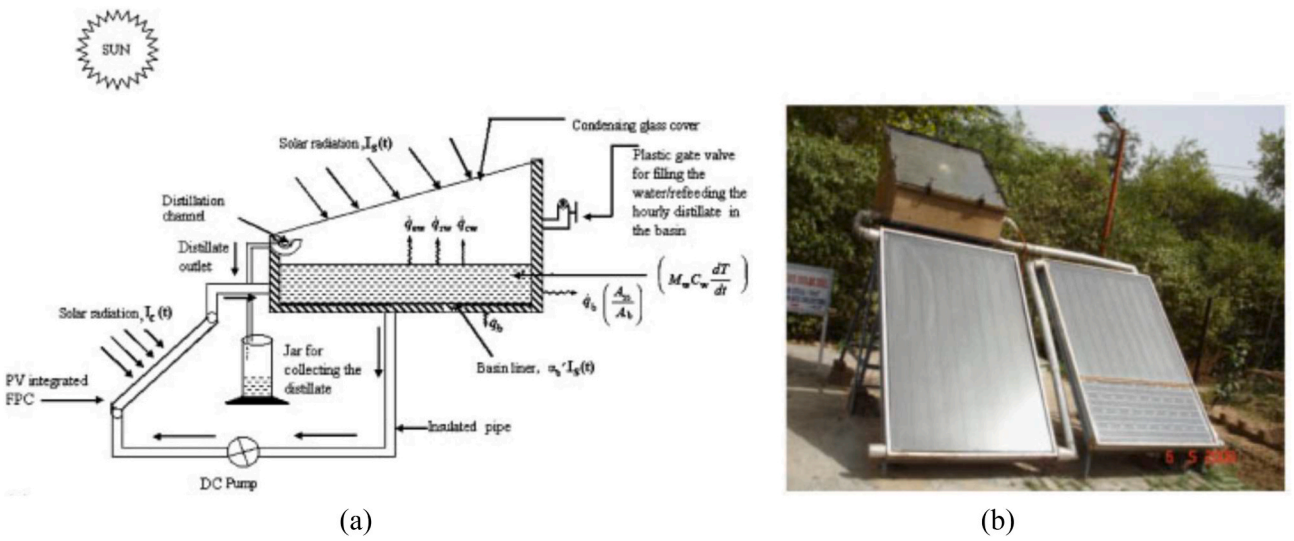


Fig. 54. (a) Schematic; and (b) photograph of an active solar still coupled to a hybrid PV-T collector. Images reprinted from Kumar and Tiwari [586], with permission from Wiley.

recovery ratio of 92% with a thermal energy demand of 112 kWh and electrical demand of 12.3 kWh.

As can be seen from the above discussion, PV-T systems can be used in various ways to drive multiple types of desalination systems, while also simultaneously providing additional thermal and/or electrical energy (depending on the type of desalination route chosen). A typical method for assessing a system's performance is the levelized cost of water. However, the evaluation of this indicator can be more difficult for the PV-T-driven systems reviewed here as including the value of excess energy can drastically alter the calculation and becomes highly dependent on the costing scenario selected. Furthermore, the overall system performance in terms of water production and/or a specific energy standpoint is driven primarily by the desalination system selected. The overall PV-T system configuration has less influence on the desalination performance but only on the energy split and any potential excess energy from the system. A major advantage of using PV-T collectors within a wider system with desalination arises from this excess energy, particularly in the case where a thermal-based desalination technology is employed (e.g., existing equipment, high salinity feed waters, or a high value of electricity) and excess electricity is of high value.

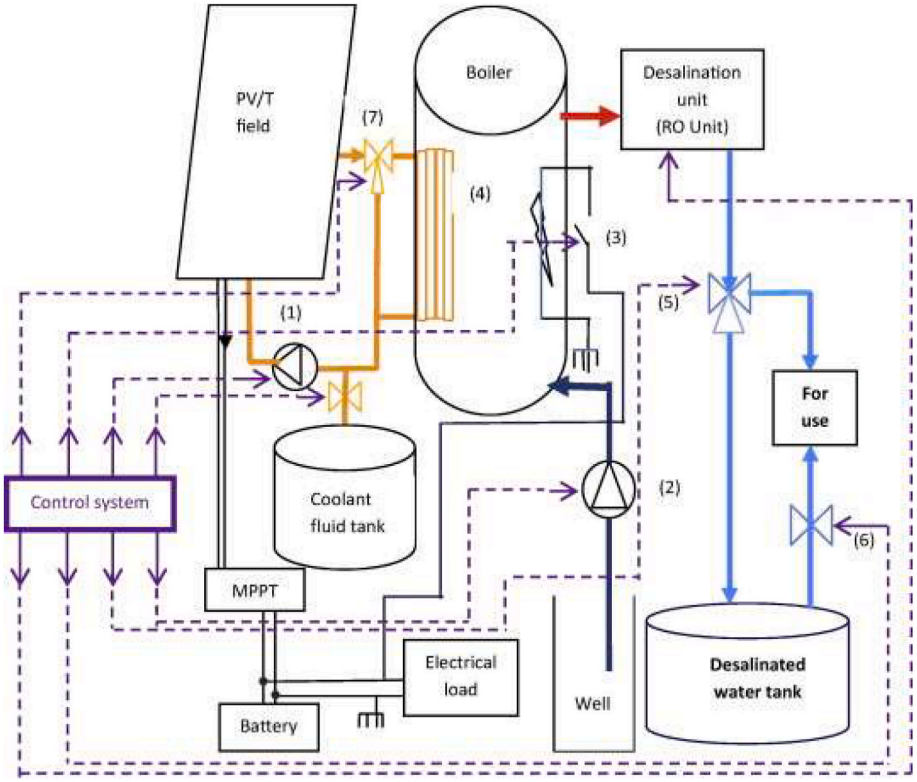


Fig. 55. Overview of plant design for utilizing PV-T collectors for driving an RO desalination unit. Image reprinted from Ammous and Chaabene [599], with permission from Elsevier.

4.5. Solar drying

Solar drying is one of the oldest applications of solar energy for food preservation, and there are several types of solar dryers, which can be classified as: open sun, direct, indirect and mixed [601,602]. From these, mixed solar drying performs better than direct solar drying, as crops are heated both through direct radiation and solar collectors [603]. Hot air generated by air-based PV-T collectors can be directly used for drying foods such as fruits, meat fish and cereals [604]. These collectors can also be integrated with greenhouses, both in clear weather conditions such as in New Delhi [82,605], and in more variable weather conditions such as in The Netherlands [606,607]. Electricity generated by the PV-T collector can be used to drive electric devices in the dryer, such as fans, sensors and controllers. Thus, PV-T solar dryers are particularly suitable for off-grid applications, which are considered a sustainable and promising way to dry crops in remote rural areas. A spectral selective coating can be added on the covering to reflect the near-infrared radiation, which contains about 50% of the solar heat load which is not required for crop production [607].

There are two common PV-T solar-dryer designs, as shown in Fig. 56. In the first design, the hot air generated by a PV-T collector is sent to a separate cabinet dryer, as shown in Fig. 56(a). Some authors [608] designed and fabricated an air-based CPV-T collector, which was connected to a cabinet dryer. An outdoor test in Malaysia showed that the system had a combined efficiency of 20–40%. The PV-T solar dryer was able to improve the colour, flavour and taste of the drying food. The authors also highlighted that the PV-T solar dryer was suitable for remote rural areas where no power supply from the grid was available. A PV-T cabinet solar dryer with forced convection has also been designed and used to dry tomato slices [609]. The moisture content of the tomato in the PV-T solar dryer dropped from 92% to 22% after 44h outdoor test in Tunisia in September, while the moisture content of the tomato with the naturally open sun drying only dropped to 30%. The PV-T cabinet drying with forced convection proved to be more efficient than the naturally open sun drying. The thermal efficiency varied from 26% to 65%, while the electrical efficiency varied from 8% to 12% when the PV cell temperature varied from 30 °C to 65 °C.

Another common design integrates PV-T collectors with a greenhouse solar dryer, as shown in Fig. 56(b). In a PV-T greenhouse dryer with a 100 kg drying capacity [610], two PV-T collectors were mounted on the south roof of the greenhouse to produce both electricity and hot air. A 20-W PV panel was enough for driving the fan which was used to drive the airflow inside the greenhouse. A 7-h outdoor test conducted in New Delhi in April showed that the PV-T greenhouse dryer was able to effectively dry the grape samples although the colour of the dried grape was not satisfactory. This research was extended [611] and the PV-T greenhouse dryer was improved by using a PV-T collector to cover the entire roof of the greenhouse, to prevent direct solar radiation on the grapes. The colour of the dried grapes was significantly improved, which showed a more bright colour compared to their previous results without the PV-T collector. The thermal and electrical efficiencies were around 25% and 14% at 1 pm with the PV cell temperature of 60 °C on a typical day of May in New Delhi. The payback time of a 1.32-m^2 PV-T greenhouse dryer was about 1.2 years based on an exergoeconomic analysis [612]. In this line, other authors [613] proposed a hybrid PV-T collector with ultraviolet (UV) stabilized polyethylene greenhouse to dry mint leaves, while Mortezapour et al. [83] proposed hybrid PV-T collectors integrated with an HP saffron drying.

A BIPV-T solar drying system was built and tested to dry fodders in Savoy, France [614]. The results showed that the air was pre-heated by 7.8 °C, the system's daily thermal and electrical efficiencies were up to 28% and 13% respectively, which indicated that the system was suitable for fodder drying applications. Daghigh et al. [615] tested and compared the performance of solar dryers using a flat plate PV-T collector and ETCs in Sanandaj, Iran. The ETC solar dryer was more effective than the flat-plate PV-T solar dryer due to the nearly twice higher thermal efficiency of the ETC compared to the PV-T collector. The payback time of the ETC solar dryer was 2.6 years, which is slightly longer than that of the PV-T solar dryer (2.3 years).

The PV-T solar drying systems introduced in this section do not use any external source of fuel or electricity and can be considered zero-emission systems. These systems are particularly suitable for off-grid applications in remote rural areas and have also been proven capable of improving the quality (colour, flavour, taste) of drying foods. However, the current system designs considered in the literature are still at early readiness levels and have not been optimized, leading to limited drying efficiencies. The performance of these systems can be improved, for instance, by recovering waste heat from the dryer and optimizing the heat/mass transfer inside this component.

4.6. Solar hydrogen production

The electrolysis of water produces hydrogen using excess solar electricity, which presents one means to achieve long-term energy storage in the global energy system [616]. A typical electrolyser is composed of an anode and cathode separated by a diaphragm and is discussed in detail elsewhere [617]. Briefly, as current flows through the electrolyser, hydroxide ions (anions) travel to the anode to surrender electrons where oxygen gas O_2 is evolved, hydrogen ions (protons) travel to the cathode to receive electrons where hydrogen gas H_2 is evolved. In the case of alkaline electrolysers, potassium or sodium hydroxide are added to increase the conductivity of the electrolyte [618], in the case of a proton exchange membrane (PEM) electrolyser a semi-permeable polymer membrane is used to only allow hydrogen ions to reach the cathode [619].

The half-reactions for electrolysis can be written as:

$$\text{Cathode}: \quad 2H^+ + 2e^- \rightarrow H_2 \tag{4.1}$$

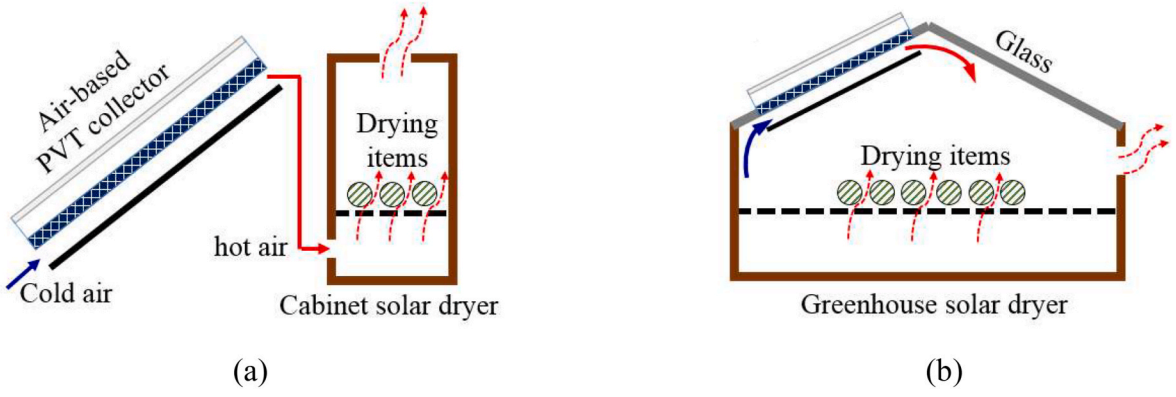


Fig. 56. Schematics of PV-T-integrated solar dryers: (a) cabinet [608]; and (b) greenhouse solar dryer [610].

$$\text{Anode}: \quad 2OH^- \rightarrow \frac{1}{2}O_2 + H_2O + 2e^- \tag{4.2}$$

For cell voltages above 1.48 V, the reaction is exothermic, but for cell voltages below 1.48 V, the reaction may still proceed and becomes endothermic. At increasing temperature, the enthalpy and hence thermo-neutral voltage drops slowly at a rate of -0.176 mV/K but the Gibbs free energy drops much faster at a rate of -0.79 mV/K [620] illustrated in Fig. 57(b). In practice, electrically driven alkaline electrolysers operate at cell voltages of 1.8–2.2 V and at temperatures between 343 and 363 K [621], the over-potential being required to overcome a series of barriers for hydrogen and oxygen reactions, bubble formation and finite electrolyte conductivity [617]. However, when driving the reaction using PV cell electricity, there is an evident benefit in supplying solar heat in addition to electrical power from a PV-T collector.

Several studies have examined the theoretical benefit of using solar heat to augment electrolyser performance. Most of the previous studies are theoretical, where either the electricity or the thermal output of the CPV-T collectors are used for hydrogen production [622,623], while there are fewer studies on low-temperature PV-T collectors where both outputs are used in a PEM electrolyser [85,624]. A 2.5-fold increase in the solar-to-hydrogen production was estimated for a PV-T collector over a conventional PV panel and electrolyser running at ambient temperature in Phoenix, USA [84]. Wang et al. [624] calculated the equilibrium temperature for a PV-T system for a range of different cell technologies and PV-T panel emissivity, suggesting that a 17% solar-to-hydrogen efficiency is possible. One of the few practical demonstrations of PV-T hydrogen production was performed using both air-based PV-T and water-based PV-T systems together with a conventional PV panel driving a Hoffman voltameter[2] [85]. The results of this comparison are shown in Fig. 58. They reported an increase in the respective hydrogen production rate of 1.7 × and 2.1 × that of a conventional PV system.

5. Storage, performance enhancement and opportunities for system innovation

Potential pathways to enhance the performance of solar systems include, among others: (a) the use of more compact and optimized thermal storage; (b) implementation of control strategies; (c) improvements of the electrical storage; and (d) improved monitoring and control to minimize O&M costs.

5.1. Thermal energy storage options

Thermal energy storage (TES) refers to a method that store excessive energy in thermal forms (heat or cold) and use the stored thermal energy either directly or indirectly through energy conversion processes when needed. TES technologies are usually classified, according mainly to the materials used for storing the thermal energy, into three categories (see Fig. 59): sensible heat storage (SHS, based on the temperature change of the TES materials), latent heat storage (LHS, based on phase change of the TES materials) and thermochemical storage (TCS, based on sorption and/or reversible chemical reactions) [625,626]. SHS is a relatively mature and already widely used technology; LHS has recently started industrial applications (e.g., Jinhe Energy), whereas TCS is still at an early stage. TES technologies currently account for approximately 55% of the global non-pumped hydro installations.

Due to the fluctuating nature of solar irradiation, most solar-thermal systems including, but not limited to PV-T systems, inherently benefit from integration with some form of TES to balance energy generation and demand. Depending on the operating temperature of the PV-T collector, there are various thermal energy options with different levels of technology maturity, some of which have been already implemented in previous studies and in existing applications. For low-temperature heating purposes (<100 °C), such as water heating or space heating, the most widely adopted TES option for PV-T systems is water-based SHS.

Higher-temperature SHS (100–400 °C or higher) can be used in high-temperature PV-T systems, although relevant studies are still scarce. As

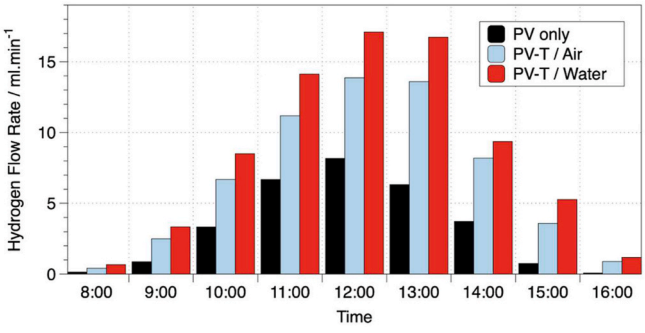


Fig. 58. Hydrogen flow rate from three combinations of PV panel and electrolyser: conventional PV panel, air-based PV-T collector and water-based PV-T collector at a mass flow rate of 0.011 kg/s. Data derived from Ref. [85].

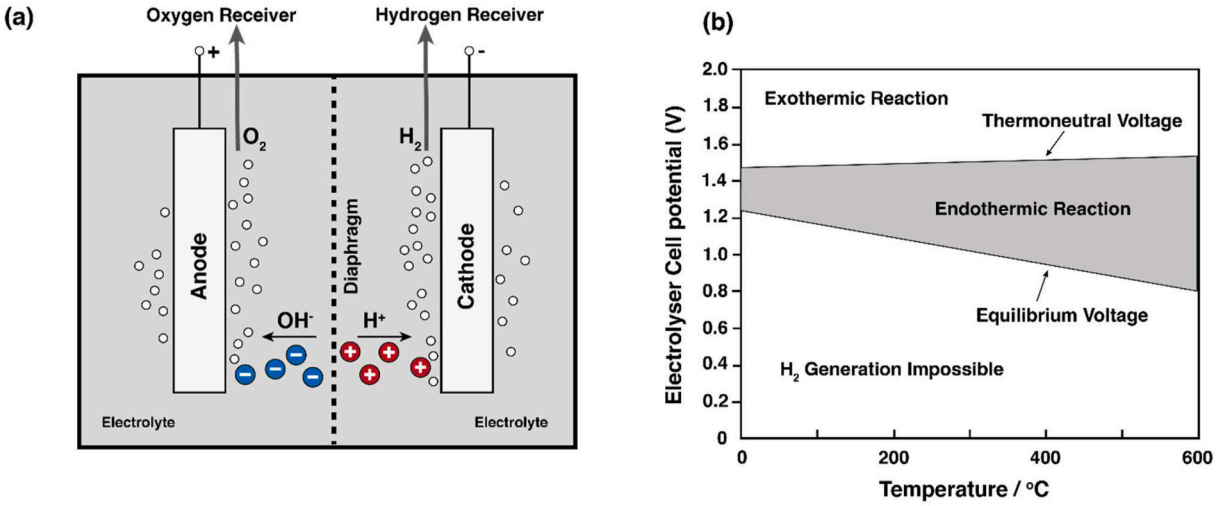


Fig. 57. (a) Schematic diagram of electrolyser; and (b) electrolyser reaction regimes plotted as a function of cell potential and temperature. Figure reproduced from Zeng and Zhang [617].

the temperature is much higher than the typical tolerant range of PV cells in such systems, the collectors are mostly based on spectral-splitting CPV-T designs, where the PV cells and heat collection elements are disconnected, and the thermal energy collection and storage are similar to those of CSP systems. In this sense, the available TES options for CSP systems can be used for such spectral-splitting CPV-T systems, if needed, following appropriate collector and system designs. For instance, Wang et al. [627] proposed a spectral-splitting parabolic trough CPV-T system for CHP provision, in which Syltherm-800 thermal oil (typically employed in CSP systems) was used for high-temperature storage, along with a hot water tank for low-temperature storage.

LHS, typically implemented with the use of PCMs, has been widely studied for PV-T applications, as discussed in Section 3.1.4. Most of the existing studies on PV-T-PCM collectors focus on low-temperature applications, thus low melting point PCMs, such as paraffin waxes, are commonly used. Nevertheless, as shown in Section 2, there is a wide variety of PV-T collector designs aiming at different temperature levels, which opens possibilities for using different PCMs. Similarly, TCS may also find a role in future PV-T applications [628,629], as there are overlaps between the operating temperature of PV-T collectors and TCS depending on the specific needs and system design. As many TES technologies are still under development, existing studies on the combination of PV-T collectors and TES are restricted to those more mature and low-cost TES options, but a considerable potential is foreseen for using those emerging TES technologies for PV-T applications.

Three main aspects should be considered in the design of a TES: thermal properties, cost-effectiveness and environmental impact. First of all, a high thermal storage capacity is key to reduce the system volume and to increase efficiency, and a good heat transfer rate should be maintained to ensure an adequate speed of thermal energy release/absorption. Furthermore, good stability of the storage material should be ensured to avoid mechanical and chemical degradation with time. Other criteria should be considered apart from the above, such as the operation strategy, and the integration within the overall solar system [630].

5.1.1. *Sensible heat storage*

SHS works by raising or reducing the temperature of a TES material. The amount of stored thermal energy is proportional to the mass and specific heat capacity of the TES material, and the temperature change during the charging and discharging processes [631]. It is therefore related to the internal energy change of the TES material during the charging and discharging process. One can achieve a high energy storage capacity of an SHS system by selecting TES materials with a high density and a high specific heat capacity, or increasing the working temperature range and the storage volume. Due to the limited temperature range and available space in real applications, the use of high energy density materials is often preferred.

According to the working temperature range, SHS technologies can be divided into low temperature (less than ~100 °C), medium temperature (between ~100 °C and 250 °C) and high temperature (higher than ~250 °C). The classification can also be done according to the chemical nature of the SHS materials, leading to organic and inorganic-based SHS technologies. In many cases, SHS technologies are simply classified, according to the physical state of the SHS materials, into solid, liquid and solid–liquid mixture-based technologies. In the following, more details are given to the liquid and solid TES materials.

5.1.1.1. Liquid-based SHS materials. Liquid-based SHS TES materials are materials that are used in a liquid state during the charging and

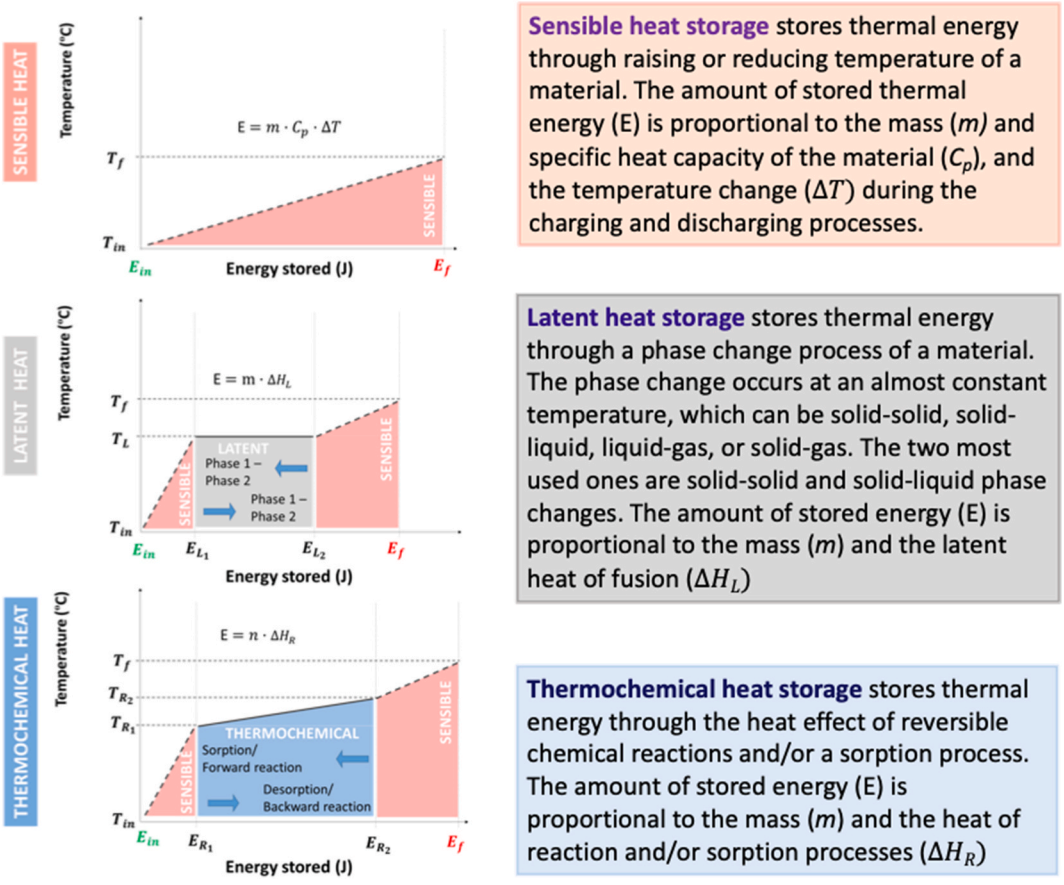


Fig. 59. Thermal energy storage methods, mechanisms and calculations.

discharging processes. Such materials are often used both as storage and heat transport mediums. Commonly used liquid-based SHS materials are water, heat transfer oils, organic liquids, molten salts, ionic liquids, and liquid metals. Table 10 shows a list of common liquid-based SHS materials, working temperatures and properties. Significant efforts have been made to increase their thermal properties. For example, ceramic, metallic and carbon-based nanoparticles have been proposed and studied as additives to enhance the thermophysical properties [632,633].

Table 10 shows that water has the highest energy density due to its high specific heat capacity, compared to other liquid-based SHS materials. Because of this, together with other advantages such as low cost, harmless nature, abundance, and easiness in transportation and storage, water has been the most popular and commercially used SHS material for low-temperature (~0–100 °C) storage applications [634]. A considerable amount of work has also been done on enhancing the thermophysical properties of water through the use of nanoparticles [635]. There has also been recent research in enhancing the specific heat capacity of SHS materials through the introduction of nanoparticles [463,636,637].

For elevated temperature applications, organic-based thermal oils have been used due to their lower vapour pressure than water at elevated temperatures, which allows operation at lower pressures. For example, Dowtherm A oil [638] has a vapour pressure of 7.6 bar at 374 °C at which water has a vapour pressure well over 200 bar. The disadvantages of thermal oils are their low specific heat capacity, low thermal conductivity, and high costs. Safety is also a concern for the transportation, storage and use of these oils.

For applications at temperatures over ~400 °C, molten salts are a preferred option due to their high thermal stability and low vapour pressures. As a result, molten salts have been used in large-scale applications in concentrated solar thermal power (CSP) plants [639]. They are also considered as heat transfer and heat carrier fluids for future Generation III nuclear reactors [640]. Disadvantages of molten salts include their low thermal conductivities, low heat capacities and high corrosivity. Nano-additives have been studied recently for enhancing the properties of molten salts [641]. Some authors [642,643] studied experimentally the mechanical dispersion of CuO and TiO_2 nanoparticles in molten salts and their effects on the specific heat capacity of binary nitrate salt mixtures. Their results suggested a noticeable enhancement in the specific heat capacity for both nanoparticles at 440 °C. Other authors [644] investigated the effect of silica nanoparticles on the specific heat capacity of a low melting point salt and reported an enhancement of up to 17–21%. Hu et al. [645] studied the specific heat capacity of a binary salt containing 2 wt.% Al_2O_3 nanoparticles and observed an enhancement of up to 8%. An extensive experimental and numerical investigation using silica nanoparticles-based nitrate salt suspensions as a model system suggested a mechanistic interpretation of specific heat capacity enhancement [646,647].

Liquid metals have unique characteristics such as a large temperature gap between boiling point and melting point, and low vapour pressure at elevated temperatures [648] and hence a good potential for applications across a wide temperature range. Liquid metals have also been considered for use as a heat transfer fluid for CSP plants and nuclear reactors. There have been discussions on the use of the so-called nano-liquid metals as heat carriers and transport fluids [649]. The drawbacks of such SHS materials are their high cost, corrosiveness, and prone to oxidation. In addition, liquid metals such as sodium also have a risk of pyrophoricity.

Ionic liquids are mainly made of organic cations or organic anions [650–654] with some favourable thermophysical properties for thermal energy storage, including low vapour pressure, good thermal stability, good operating temperature range, and a high specific heat capacity [655,656]. The main disadvantage of such fluids is their low thermal conductivity and high costs.

Table 10
List of some common liquid-based SHS materials and their properties.

Material	Density (kg/m^3)	Specific heat capacity (kJ/(kg·K))	Energy density ($MJ/(m^3·K)$)	Working temperature range (°C)
Water	1,000	4.2	4.2	0–100
Mineral oil	850	2.0	1.7	−20–300
Calorie HT43	870	2.2	1.9	12–260
Dowtherm A	900	1.6	1.5	12–400
Sytherm XLT	660	2.2	1.4	−111–260
Therminol VP-1	900	2.1	1.9	12–400
Helisol®5A	920	1.7	1.6	−5–430
Solar salt	1,840	1.5	2.7	220–584
Hitec	1,790	1.6	2.8	142–535
Hitec XL	1,990	1.5	2.9	130–500
LMPS II	1,910	1.5	2.9	83–625
Isopentanol	830	2.2	1.8	<148
Octane	700	2.4	1.7	<126
Liquid Na	1,040	1.3	1.4	98–883
Liquid NaK	780	0.89	0.69	−13–785
Liquid LBE	10,300	0.14	0.14	125–1,530

5.1.1.2. Solid-based SHS materials. Solid-based SHS materials such as rocks, pebbles, bricks, concrete, ceramics, sand, gravel and metals have been used widely for medium and high-temperature applications [657]. Compared to liquid-based SHS materials discussed above, solid SHS materials have inherent advantages of high density, low cost, almost zero vapour pressure even at elevated temperatures, and a much great operating temperature range with no leakage risks. The main drawback, however, is their low specific heat capacity, leading to a low volumetric energy density.

Table 11 gives a list of some common SHS materials and their properties, which illustrates that naturally available materials such as clay, rocks, sands, gravels, and wood can be used for sensible heat storage [658]. These materials are cheap, non-toxic and easily available, and can be packed into thermal storage tanks in the form of a packed bed [659]. Industrial waste ceramic materials have also been studied for potential TES applications [660], motivated by the so-called circular economy. Different concrete formulations have also been studied as TES materials. The advantages of this type of material include low cost, ease to shape, non-toxic, little fire risks, and fairly mechanically strong. Concrete-based TES materials, however, have a low thermal conductivity, a low specific heat capacity, and a limited working temperature range compared to ceramics and rocks. As a result, research efforts have been made to improve concrete thermal properties [661]. Metals such as cast iron and cast steel have a high volumetric energy density due to their high density and can be used at elevated temperatures [662]. However, their cost is fairly high [663] though scrap iron and steel could offer a more affordable option.

5.1.2. Latent heat storage

LHS solutions rely on the storage of thermal energy while employing a phase change process, which occurs almost at a fixed temperature. LHS is also more popularly called PCM-based TES. The phase change can be solid–solid, solid–liquid, liquid–gas and solid–gas; with solid–solid and solid–liquid phase change mostly used [664–674]. Very often the total stored thermal energy in a PCM system includes both the latent heat and the sensible heat below and above the phase change temperatures [664,669].

Attractive features of PCM-based TES technologies include high energy density (compared to SHS-based TES) and a nearly isothermal process during the phase change. PCMs are often classified according to their chemical nature, namely, organic, inorganic and eutectic. Examples of organic PCMs include paraffin wax and fatty acids, which are mostly for applications at temperatures below ~180 °C. Hydrates are typical/common examples of inorganic PCMs, which are mainly for

Table 11
List of common solid SHS materials and their properties.

Material	Density (kg/m^3)	Specific heat capacity (kJ/(kg K))	Thermal conductivity (W/m K) at 25 °C	Volumetric energy density (MJ/(m^3 K))	Working temperature (°C)
Clay	1460	1.98	0.15 (dry)	2.88	<1200
Silica fire brick	1800	1.15	0.50–0.70	2.07	700
Magnesia fire brick	3000	1.15	12–18	3.45	1200
Rock	2560	1.00	1.6–4.2	2.56	<2000
Sand and gravel	2200	0.71	0.15–0.70	1.56	300
Concrete	2000	0.88	0.29	1.76	400
Cofalit®	3120	1.03	2.7	3.21	<1500
Castable ceramics	3500	0.86	0.14	3.01	<1500
Aluminium	2710	0.89	240	2.42	<660
Cast iron	7900	0.56	52	4.42	<400
Cast steel	7800	0.60	45	4.68	<700

applications at temperatures below ~120 °C. Other popular inorganic PCMs are salts and metallic materials and are mainly for applications over ~200 °C. These materials have different characteristics and hence present various challenges [670]: metallic materials have a high thermal conductivity but can be corrosive and expensive; inorganic hydrates often suffer from super-cooling and phase segregation; organic PCMs have low thermal conductivity and are often flammable; and salts can be highly corrosive and have a low thermal conductivity. A significant amount of work has been done on addressing these challenges. For example, various forms of composite PCMs have been developed including micro- and nano-encapsulation of PCMs, the inclusion of PCMs in a structured material, and the dispersion of highly thermally conductive particles in PCMs. Due to the length limitation, this will not be discussed further. The following sub-sections provide a summary of different PCMs.

5.1.2.1. Organic PCMs. Organic PCMs can be further divided into paraffin and non-paraffin based. Paraffin consists of a mixture of mostly straight-chain n-alkanes, CH_3–(CH_2)–CH_3. The crystallization of the (CH_3)-chain releases a large amount of latent heat. Both the melting point and latent heat of fusion increase with the chain length. The use of paraffin as LHS materials benefits from the availability in a large temperature range. Due to cost considerations, however, only technical grade paraffin can be practically used in latent heat storage systems. Paraffins are safe, reliable, predictable, less expensive and non-corrosive. They have a low vapour pressure in liquid form, a relatively small volume change during phase change and long thermal cycle life. They are chemically inert and stable below the decomposition temperature. However, paraffins are relatively expensive and have a low thermal conductivity. They are moderately flammable and may not be all chemically compatible with plastic materials. These undesirable features could be mitigated using various methods; see for example Sharma et al. [668]. Non-paraffin based PCMs include esters, fatty acids, alcohols, and glycols. These organic PCMs can be further divided into two subgroups of fatty acids and other non-paraffin organic materials. The general formula for all fatty acids takes the form of $CH_3(CH_2)_{2n}COOH$. Fatty acids have a high heat of fusion comparable to paraffins and, similar to paraffins, a long thermal cycle lifespan with no subcooling [671,672]. The main drawbacks of fatty acids lie in their moderate corrosion, as well as costs (~2–2.5 × higher than that of technical grade paraffins) [668].

5.1.2.2. Inorganic PCMs. Inorganic PCMs can be further classified into salts, salt hydrates and metallic based. They often have a higher volumetric energy density than organic PCMs due to higher mass density. However, some inorganic PCMs are highly corrosive, leading to challenges in containing them in practical applications. Inorganic salts and their mixtures can be used for TES over a wide temperature range from below ~100 °C to above ~1000 °C. A recent study has shown the composition dependence of the latent heat of salt mixtures. A deviation from eutectic concentration lowers the activation energy of diffusion, leading to a higher phase change resistance during solidification with a higher activation energy and a larger latent heat during the phase change [673].

Salt hydrates can be generally written as $A_xB_y.n(H_2O)$ with n the number of water molecules and A_xB_y representing salts such as metal carbonates, sulphites, phosphates, nitrites, acetates and chlorides. In these compounds, water molecules are bonded to inorganic molecules in an ion-dipole form, which contains an ion (cation or anion) and a polar molecule (H_2O). The force between the ion and the dipole result from the electrostatic attraction between the ion and the neutral molecule (water) that has a dipole. This means that the water molecules are attached to the anion (normally) or the cation. As a result, the phase change enthalpy of a salt hydrate depends on the bond strength between the water molecules and the salt. Note that the difference between the salt hydrates as PCMs and salt hydrates as thermochemical storage materials (Section 5.1.3) lies in that the former have a liquid–solid phase transition. The main technical challenges in the use of salt hydrates-based PCMs include subcooling during crystallization, incongruent melting, and corrosion in contact with some commonly used metals such as copper, aluminium, and stainless steel. Several studies have been performed to address these challenges [668].

Metal-based PCMs have not yet been investigated in depth as PCMs for thermal energy storage due to low heat of fusion per unit mass and low specific heat [668]. Having said so, metallic PCMs have the advantages of high heat of fusion per unit volume, high thermal conductivity and relatively low vapour pressure [668].

5.1.2.3. Eutectic PCMs. Eutectic PCMs are made of two or more components and can be subdivided into organic–organic, inorganic–inorganic, and inorganic-organic eutectics. Each component in a eutectic PCM melts and freezes congruently forming a mixture of the component crystals during crystallization. A eutectic almost always melts and freezes without phase segregation because it freezes to give an intimate mixture of crystals, leaving little opportunity for the components to separate. On melting all components liquefy simultaneously, again with little separation [668].

5.1.3. Thermochemical storage

TCS solutions store thermal energy through the heat effect of reversible chemical reactions and/or sorption processes. The key advantages of such an approach lie in their high energy density and long storage duration [675]. The principle of TCS can be simply illustrated by the following scheme:

$$\text{Charging}: C + \text{heat} \rightarrow A + B \quad (5.1)$$

Storing: A and B stored separately (no or little heat losses) (5.2)

$$\text{Discharging}: A + B \rightarrow C + \text{heat} \quad (5.3)$$

where A, B and C are reactants or products depending on the charge or discharge processes. Examples of A include hydroxide, hydrate, carbonate and ammoniate; and examples of B include water, CO, ammonia, and hydrogen. C can be in solid or a liquid form and A and B can be any phase.

The amount of heat stored in a TCS system is proportional to the amount of TCS material, the heat of reaction and/or sorption and the extent of the reaction/sorption. TCS materials have been widely reported to have the highest thermal energy storage density media, typically over 0.5–3 GJ/m^3 with a process involving almost little loss during the storage period [676]. Despite the considerable efforts that have been made over the past few decades, TCS technologies are still faced with high costs, high complexity, and short lifespan challenges, and remain in the early stages of research and development with a very low TRL.

Table 12 gives a list of some TCS materials and their properties, which fall broadly into two main groups of reversible sorption and chemical reactions based on the latter often include the former process [677,678].

5.1.3.1. Sorption-based TCS. Sorption-based TCS stores heat by breaking the binding forces such as van der Waals forces or covalent forces, between a sorbent and a sorbate [678]. The heat required to break the binding forces can be higher than that associated with the evaporation heat of a pure sorbate (e.g., water). As a result, the energy density of sorption-based TCS materials can be significantly higher than that of PCMs. The sorption-based TCS can be further subdivided into liquid-sorption and solid-sorption TCS. Examples of liquid sorption-based TCS materials include LiBr–H_2O, LiCl–H_2O and $CaCl_2$–H_2O pairs; whereas silica gel-H_2O and zeolite-H_2O pairs are examples of solid sorption-based TCS material pairs [679]. Apart from pure TCS materials, composite TCS materials have also been studied for overcoming performance degradation and short lifespan particularly due to structural changes of the TCS materials. For example, $MgSO_4$ and $MgCl_2$ have been impregnated into porous matrices such as silica gel or zeolites (which also produce heat effect and hence also termed as active supporting matrices), graphite, vermiculite and magnesium oxide (which provides a large capacity for the TCS materials) [680]. Microencapsulation of TCS materials with a polymeric shell [681,682] or a nanocoating [683] has also been studied for enhancing the lifespan and reducing structural degradation of TCS materials.

5.1.3.2. Reversible-chemical-reaction-based TCS. Reversible-chemical-reaction-based TCS relies on endothermic (heat storage) and exothermic (heat release) processes of the reaction. The major benefits of the TCS materials lie in their high energy density, ~5 × higher than the LHS materials and ~10 × higher than SHS materials, unlimited storage period due to the limited thermal loss during storage, and storage at ambient temperature [684].

Table 12
List of selected TCS materials and their properties [677,678].

Material	Energy density	Working temperature range (°C)	Classification
$MgSO_4$·7H_2O	2.8 GJ/m^3	~30–150	Sorption
$MgCl_2$·6H_2O	3.1 GJ/m^3	~35–120	Sorption
$CaCl_2$·6H_2O	2.8 GJ/m^3	~35–95	Sorption
$SbBr_2$·6H_2O	2.0 GJ/m^3	~35–80	Sorption
Zeolite	300–500 kJ/kg	~65–350	Sorption
Silica gel	180–160 kJ/kg	~50–120	Sorption
LiBr/H_2O	2020 kJ/kg	~20–60	Sorption
$CaCO_3$/CaO	3.2 GJ/m^3	~770–810	Chemical reaction
CuO/Cu_2O	810 kJ/kg	~1010–1020	Chemical reaction
Co_3O_4/CoO	820 kJ/kg	~875–890	Chemical reaction

5.2. Control and demand-side management

Several investigators [685–688] have proposed the integration of optimized control strategies to govern the pump operation to improve the solar-thermal system performance. A recent study [686] compared four empirical strategies to adjust the mass flow rate as a function of the instantaneous ambient conditions and collector temperatures. Two controllers were considered: an optimized on-off controller and a proportional controller which maximized a target function at each time instant during the system operation. The former strategy operated the system at an optimized fixed flow rate based on the forecasted weather and demand profile and maximized the daily solar energy conversion at the collector [685]. The results showed that the system operates stably at high flow rates during cloudy and overcast days, whereas during sunny days the pump was shut-off frequently. This behaviour was associated with the lower collector efficiency at high temperatures reached during the sunny day, leading to a reduced energy conversion rate for a continuous operation of the pump. Similar results were found in previous research [688]. In the latter method, the flow rate was either adjusted linearly with the solar irradiance, or varied depending on the temperature difference between the collector and the fully-mixed storage tank. A recent study [687] proposed an optimal controller for ST system with two storage tanks and two circulation pumps. The results showed an 8% increase in thermal energy collected while the thermal losses through the connecting pipes were reduced between 5% and 7%. A proportional-integral-derivative (PID) controller was developed [689] to regulate and limit the collector temperature. The transfer function of a solar collector was generated to this intend based on a dynamic model that takes into account the variation of the efficiency with the collector flow rate. A more recent study of 2020 [690], employed a machine learning method to identify the optimal operating schedules for a solar hot water system. A tabular Q-learning algorithm was used to control a heat-recovery chiller and a water pump to maximize energy efficiency and user satisfaction. The simulation results showed that this intelligent control system was able to effectively improve the system performance by 21% comparing to nominal operation schedule in July.

To facilitate the interaction of the users with the technology, and give them the possibility of adapting their behaviour to real-time variable energy prices, real-time monitoring of the system performance is required [691]. In this line, to guarantee the expected long-term performance and reduce O&M costs, automatic and advanced control and monitoring of solar energy systems should be implemented. Advanced monitoring also allows integrating the aforementioned control strategies. Furthermore, automatic monitoring and control, in conjunction with forecasted weather and user behaviour, can increase the system's reliability as well as energy and cost savings by ensuring optimized performance [692].

One of the strategies to achieve the challenging targets established by the energy policy against climate change is to place consumers at the core of the energy policy, encouraging them to take the lead in the energy transition through the integration of new technologies in their households to benefit from reductions in the energy bills, also participating actively in the market. Therefore, the aim is to switch from passive consumers to prosumers, i.e., producers and consumers of renewable energy, through the process of self-consumption [4]. As shown in Fig. 60, there are two main options to increase self-consumption for solar system installations in buildings: energy storage and demand-side management (DSM), which can be used either separately or combined [4,87]. DSM usually refers to load shifting, that is, to shift power demands of building electrical devices (for example, washing machines, dishwashers or dryers) from time periods of high demand but low electricity generation (i.e., at night) to periods of surplus generation and low demand (i.e., midday). Thanks to DSM measures, the periods with higher distribution grid interaction (either

importing or exporting) can be reduced. Load shifting can be done manually or automatically, which requires smart metering and smart appliances, and can be also combined with battery storage to further increase self-consumption [87]. It is estimated that shifting these loads from peak times to other periods can reduce peak generation needs in the EU by about 10% [693].

On the other hand, energy storage helps store the surplus onsite renewable generation in a period of low demand for its use when energy demand is high and renewable production is low. The size of the electrical battery storage should be carefully selected as both the degree of self-consumption achieved and the total investment cost are significantly affected by the total battery capacity [87], and small sizes increase the system stress, reducing the battery lifetime [694]. In general, a larger battery capacity will increase the self-consumption but also the associated battery costs. It should be considered that the profit of batteries (which only store, do not produce, energy) comes from the difference in selling and buying the electricity, so a balance is required between consumption, generation and storage capacity [87]. Another important factor to consider when selecting the battery's size is the specific application requirements, that is, if it is only necessary to "absorb" some of the daily peaks of generation/demand, or longer storage periods are required (i.e., in more isolated cases).

For residential solar systems, hydrogen, solid-state battery storage, or a combination of both, are being proposed by most investigators as the most suitable options for electricity storage [695–697]. Power-to-heat systems such as hot water boilers or HPs, which convert excess electricity into thermal energy, could also be used but it does not seem an interesting alternative for electricity conversion and storage due to the low efficiency defined by the Carnot cycle. Batteries have high conversion efficiencies but they also self-discharge, at a higher or lower extent depending on the battery technology, so they are more appropriate for balancing daily fluctuations [698]. One of the main drawbacks of battery storage is cost, which ranges from less than one hundred to several hundred USD per kWh of storage capacity [699,700]. The most suitable technologies for residential applications are: lead-acid, lithium-ion (Li-ion), sodium-sulphur (NaS), nickel-cadmium (NiCd) and nickel metal hydride (NiMH) [701]. Conversely, hydrogen conversion has much lower round-trip efficiency (around 45% [695]). They are more suitable for seasonal energy storage using high-pressure tanks and reconverted to electricity with a fuel cell. The rate of self-discharge is close to zero in this case [698].

Furthermore, in recent years, battery costs have decreased significantly, thanks to technological development and economies of scale. The cost of Li-ion batteries, for example, decreased by 73% between 2010 and 2016, and an additional reduction of ~60% is projected by 2030 [700]. If instead of using individual decentralized energy storage systems at a household level, distributed systems are adopted on a neighbourhood or community basis, the cost per kWh is expected to decrease, while allowing the integration of higher volumes of distributed renewable energy [4]. It is estimated that with DSM and/or decentralized energy storage, the self-consumption rate of an average Central European household with a PV system can be around 65–75% [4]. However, without these flexibility measures, the self-consumption rate is reduced to about 30% (see Fig. 60), and the excess of electricity injected into the grid might create new challenges for the grid operation [4]. Therefore, flexibility measures appear essential to achieve a successful integration of RES in the energy system.

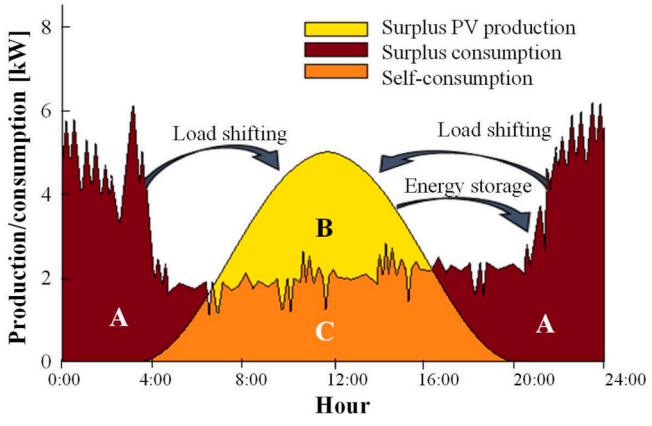


Fig. 60. Schematic outline of daily electricity demand (A + C), PV/PV-T electrical generation (B + C) and absolute self-consumption (C) in a building with an on-site PV/PV-T collector. It also indicates the function of the two main options (load shifting and energy storage) for increasing self-consumption [87].

6. System-level assessments and carbon mitigation potential

The previous sections of this review introduced numerous innovative PV-T technologies which can displace conventional primary energy use (i.e., burning fossil fuels) for meeting the modern demand for both electrical and thermal energy. PV-T technologies, therefore, have a clear potential to represent part of the solution in achieving the Paris agreement aim of holding the global average temperature to 2 °C above pre-industrial levels. The Paris agreement sets no specific technological pathway to achieve this goal, just broad carbon dioxide equivalent emissions targets based on pre-industrial levels [702].

Although 2020–2021 saw a temporary reduction in global carbon emissions resulting from the reduced economic activity due to COVID-19, it is expected that global emissions will rebound to exceed 2019 levels [702]. Thus, reducing total annual global greenhouse gas emissions to 32 $GtCO_2$/year by 2030 (to achieve the temperature limit of <2 °C above pre-industrial levels by 2100) continues to represent a difficult challenge [703,704]. Renewable technologies—including perhaps PV-T technologies—are expected to be at the core of this transition, but significant step-changes in technology, policy and adoption rates are still needed to accelerate clean energy growth [705]. Investment policies in renewable technologies for non-residential sectors (i.e., transport, industrial) should be prioritized [706]. Importantly, about 65% of total global emissions are related directly or indirectly to household consumption [707], and thus policies are needed to encourage investment and adoption of solar technologies (including emerging technologies, such as PV-T collectors).

Although the authors recognize that PV-T technologies account for only a small part of the energy share today, this section aims to estimate how much of a role PV-T technologies *could* play in this grand challenge. The motivation for this is that PV-T technologies can be utilized in both residential and non-residential sectors and have the potential, along with more traditional PV and ST technologies, to harness the enormous solar resource to make continuous improvements in embodied emissions [708]. The large projected growth of solar technologies is due to massive cost reductions that have been achieved over the past decades in PV technologies. In many places around the world, PV technologies are now more cost-effective than conventional electricity generators, particularly if any cost is associated with carbon emissions, since solar technologies have a much lower carbon intensity per kWh of energy generated [709]. As an example of the potential impact of solar energy technologies, the IEA Energy Technologies Perspectives report for 2020 included both a "sustainable development scenario" and a "faster innovation case", both of which rapidly ramp up the use of solar technologies to achieve (or exceed) the Paris agreement target. This report analyses over 800 technology options to see which has the biggest impact on emissions mitigation [702]. Some key relevant comments in this report are that "*spreading the use of electricity into more parts of the economy is the single largest contributor to reaching net-zero emissions*" and, as part of that, "*renewable technologies need to supply the energy needed for heating, cooking and other appliances in buildings*". In addition, the IEA report's "faster innovation case" essentially requires new technologies to be deployed (e.g., PV-T technologies) by rapidly progressing new

technologies up the TRL scale [702].

Historically, solar technologies have focussed on performance and cost improvements [710], while carbon emission mitigation potential may eventually become one of the main driving goals in future renewable energy developments [704]. Using carbon emission mitigation potential as a more holistic objective would force solar technologies to consider their whole life cycle, including: manufacturing, transportation, use phase, and end-of-life recycling. Although much more complex, this perspective would provide a bigger picture view of their overall benefit to society [546]. As an example, Fig. 61 shows the carbon intensity of the displaced energy supply mix as a function of solar irradiation for characteristic Chinese-made crystalline PV panels. PV-T collectors are expected to have a higher mitigation potential than standalone PV panels [518,575], which could result in even more CO_2 emission savings compared to traditional PV panels. These modules consume 870 gCO_2/kWh during their manufacture (e.g., embodied emissions) and, as shown in Fig. 61, their overall greenhouse gas emission mitigation potential is higher in high irradiation locations (e.g., higher in Australia compared to the UK) [711]. It can be observed that countries with relatively low-carbon intensity energy systems and relatively low solar resources (e.g., Norway and France), may only see a marginal carbon emissions mitigation potential from installing PV systems. However, for locations with relatively high-carbon intensity and high solar resources (e.g., Australia, and India), PV installations can have a large impact. In either case, PV-T technologies can potentially 'boost' the carbon mitigation potential (depending on their lifecycle emissions) since they can harvest more useful energy per unit than PV panels alone.

When considering the carbon mitigation potential of solar PV and ST technologies independently, recent global studies [710,712,713] have found that performance depends on climate factors such as the direct normal incident irradiance (DNI), global horizontal irradiance (GHI), and ambient temperature. Fig. 62 shows a global map wherein the 'optimal solar mix' was reported between ST collectors and PV panels for the same application [710]. For this study, it was assumed that a given rooftop has a fixed amount of space and that this space could be filled with a mixture of ST and PV collectors (PV-T technologies were not considered). It was found that ST collectors outperform PV panels in high solar irradiance, high-temperature locations (i.e., the 'red' locations on the map), while PV panels should be used to fill the rooftop in low solar irradiance locations (i.e., the 'yellow' locations on the map). The study noted that it is still unclear which technology should be selected in 'medium' solar irradiance locations, or when PV-T technologies should play a role. What is clear is that many variables lead to the whole lifecycle emission mitigation potential of solar technologies, with the local solar resource and the existing energy mix being two of the most important factors.

6.1. Carbon emissions and PV-T technology

To achieve the global warming temperature limit of 2 °C above pre-industrial levels, many countries have set targets, pathways and action plans complemented by a wide variety of commitments and regulations [714]. Based upon these plans, countries have been grouped based on their nationally determined contribution (NDC) ambitions and climate-resilient pathways. These groupings have enabled forecasters to produce scenario estimates which vary from low to very high changes in the trajectory towards carbon mitigations [715]. Since these scenarios do not include PV-T technologies, they can be used as reference cases. One reference case that can be used in the business-as-usual perspective case, which includes the government's current policies, plans, and NDC's commitments, in which global emissions will peak at 35 $GtCO_2$/year in 2050 [716]. However, in this work, we will build upon a more optimistic scenario. This scenario is the renewable energy roadmap (REmap) proposed by IRENA, with a 66% probability to achieve 9.7 $GtCO_2$/year in 2050 to limit the temperature to 2 °C above pre-industrial levels by 2100. This reference case was selected as a baseline and compared to the total emission mitigation estimations (data from IRENA [716]).

6.2. PV-T technology carbon mitigation estimates

In an effort to appreciate how PV-T technologies could fit into this scenario, estimates are needed for the potential emissions savings associated with these technologies. Such estimates were made by polling the section authors to obtain quantitative estimates for the potential of the technologies they reviewed herein. Table 13 shows the estimated lifetime and annual carbon potential savings of these technologies. It is noted that these potential emission savings were estimated according to the total available area for solar installations.

For the estimates listed in Table 13, it is important to note that the annual emission savings of PV-T collectors are not fixed, but depend strongly on the solar irradiance, the energy demands of the building, the operating temperature, and the CO_2 emission factors of conventional energy systems (which are country dependent, as noted in the previous section above). Therefore, the emission savings of an air-based PV-T collector installed in India is significantly higher than that of a liquid-based PV-T collector in the UK, as shown in Table 13. Similarly, the emission savings of a liquid-PV-T collector installed in Athens is more

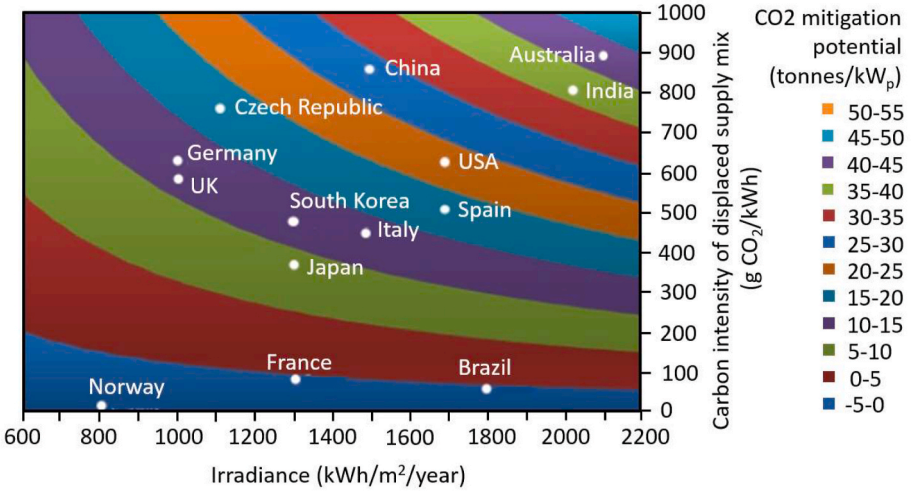


Fig. 61. Emission mitigation potential in various countries using c-Si PV panels. Figure reproduced from Briner [711].

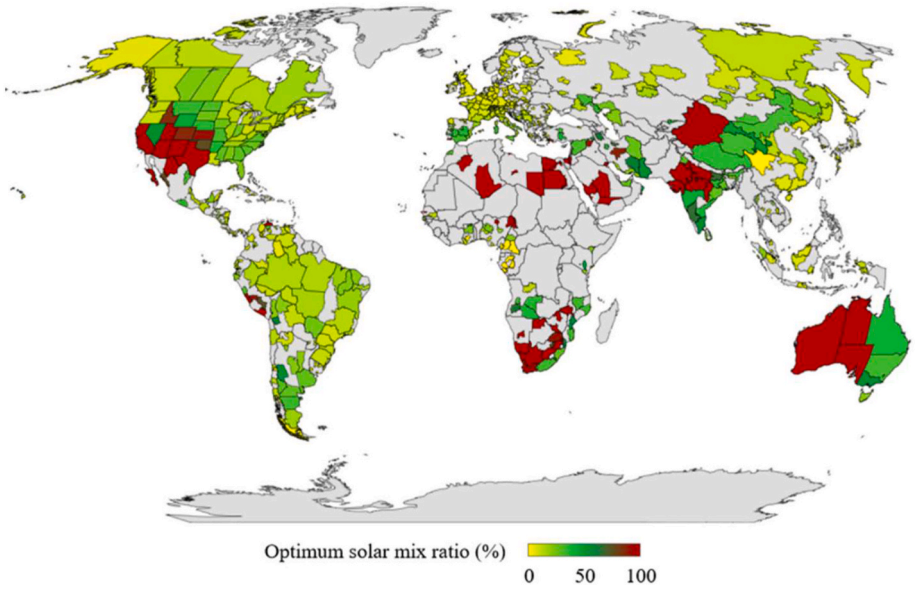


Fig. 62. Comparison of the 'optimum mix' between ST collectors and PV panels in various locations globally (red = ST collectors alone; yellow = PV panel alone). Reprinted from Mousa and Taylor [710] with permission under the Creative Commons Attribution 3.0 Unported (CC-BY) license.

than twice what it would be if installed in London and Zaragoza, owing to the high irradiance levels and high CO_2 emission factor of the electricity grid in Greece [517].

In addition, it was assumed that BIPV-T technology is covered by water or air-based PV-T collectors, and only one type of spectral splitting technology (i.e., a solid-based technology) was estimated. The contribution of PV-T technology for hydrogen production was considered negligible, while storage systems were assumed to be included in other technologies which have storage included.

Based upon Table 13, solar drying has the second highest estimated potential for emission mitigation due to the enormous land size that could be used (>35 million km^2), and solar desalination has the largest potential for carbon emission savings. However, for solar desalination, there is extremely high uncertainty in the estimate (from 0.9 to 410 $MtCO_2$/year, based on adoption rates). Moreover, hybrid PV-T technologies and PCM-based PV-T collectors were assumed to be competitive in terms of carbon emission mitigation (with 11–19 $MtCO_2$/year). Other PV-T technologies, such as spectral splitting, were estimated to have a lower impact due to low adoption rates, but high carbon-saving potential. It should also be noted that the low potential estimated for solar cooling systems compared to other ones can be attributed to net savings over existing high-efficiency systems in the type of building considered (large commercial buildings) and the relatively low number of systems that were estimated to be installed going forward, compared to other PV-T technology variants.

6.3. PV-T results comparison

Fig. 63 shows the IRENA REmap baseline case of a 22.2-Gt CO_2 reduction in emissions by 2050 (blue curve) compared to 2020 relative to the emissions shift if PV-T technologies were installed. The red curve of "*Solar technologies emissions mitigation*" is the sum of the values provided above in Table 13 for the "*Estimated maximum potential saving per year*", with a total installation increasing linearly (e.g., assuming a linear 10% PV-T system capacity increase each year). Fig. 63 shows that, relative to the optimistic baseline emissions curve, PV-T technologies could over 10 years produce a further drop in global emissions of ~600 Mt CO_2 (~3%) by 2030 if the systems mentioned in this study are installed as estimated. Overall, this is a significant saving, one which could continue to accrue compounding savings beyond 2030 if cost reductions can follow a similar learning curve to PV technologies, potentially increasing to an emission mitigation potential of ~1700 Mt CO_2 (~18%) by 2050.

7. Conclusions and future outlook

7.1. Overview

Based on this review, the following conclusions are drawn:

- Dual air–water PV-T collectors combine the advantages of water- and air-based PV-T collectors, but they are slightly more complex and expensive than typical water-based PV-T collectors. The best design seems to have water channels in thermal contact with the PV cell rear surface and the air heat exchangers below it, also acting as thermal insulation.
- It is believed that heat-pipe PV-T collectors may have the potential to overcome some of the problems faced by refrigerant-based PV-T collectors. However, this type of collector is typically harder to manufacture and integrate into larger power systems, and the operation of these systems strongly depends on the working fluid, design and performance parameters. Some investigators have concluded that the thermal performance of this type of PV-T collector is not satisfactory in cloudy, low-irradiance conditions.
- BIPV-T collectors can be based on all types of PV-T collectors reviewed in this work: air, water, dual air–water, heat-pipe, PCMs. BIPV-T systems can offer savings in materials and electricity costs, thus reducing the use of fossil fuels, by simultaneously serving as a building envelope material and a power generator. However, the larger complexity and risks of BIPV-T collectors compared to standalone PV-T collectors have acted to hinder their potential and uptake, so more research is required in the detailed modelling, analysis of any impacts on the building structure, integration methods for installation as well as more experimental assessments and long-term performance analyses.
- An ambitious strategy for boosting the potential and market uptake of this technology would involve optimizing PV-T collectors to deliver thermal energy at higher temperatures with simple, affordable designs, whilst mitigating thermal and electrical losses, and ensuring collector reliability and longevity.
- The selection of an appropriate PCM is key and depends on many factors, including the desired temperature of thermal output,

Table 13
Total carbon emission mitigation estimated for selected solar PV-T technologies.

Technology	Estimated maximum potential saving per year (CO_2 million tonnes/year)	Rated lifetime (years)	References/assumptions
Liquid-based PV-T collector	12	20–30	• Emission saving of 53 $kgCO_2/(m^2$ year) in the UK [27] • Assumed 8 million houses • Average 140 m^2 of which 20% of the roof area is useable
Dual air–water PV-T collector	13	20–30	• 10% more utilization than the water-based PV-T collector • Similar average efficiency ratio as the water-based PV-T collector in the UK [182]
Air-based PV-T collector	61	20–30	• Emission saving of 273 $kgCO_2/(m^2$ year) in India [103,104] • Operating temperature is around 40 °C
Heat-pipe PV-T collector	12	20–30	• Similar average efficiency ratio as the water-based PV-T collector in the UK
PCM enhancements	14	25	• 15% extra carbon savings compared to the water-based PV-T collector [473]
Solid-based spectral splitting	0.2	10	• 50 kW systems • 4 h of daily operation • 100 days operation per year • Emission saving of 0.82 $kgCO_2$/kWh • Utilization of 1,000 systems each year [544]
Polygeneration systems	19	20–30	• Emission saving of 83 $kgCO_2/(m^2$ year) [518] • Assumed 8 million houses • Average 140 m^2 of which 20% of the roof area is useable
Solar cooling systems	0.2	10	• Utilization of 1,000 systems each year for large commercial buildings [544] • 50 kW systems • 4 h of daily operation • 100 days operation per year • Emission saving of 0.8 $kgCO_2$/kWh
S–CHP systems	17	20–30	• Emission saving of 77 $kgCO_2/(m^2$ year) [517]
Solar desalination	MED/MSF (3.5–410) RO (0.9–50)	25	• Commercial scale desalination is 25% of total desalination market • Total worldwide capacity is ~80 × 10^6 m^3/day • RO storage is 60% of the global capacity • MED emissions/volume is 0.3–27 $kgCO_2/m^3$ • MSF emissions/volume is 0.3–35 $kgCO_2/m^3$ • RO emissions/volume is 0.1–4.3 $kgCO_2/m^3$
Solar drying	29	20–30	• Emission saving of 720 $kgCO_2/(m^2$ year) [613] • 35,000,000 km^2 agricultural land in the world • 1/100,000 km^2 assumed to for PV-T solar drying

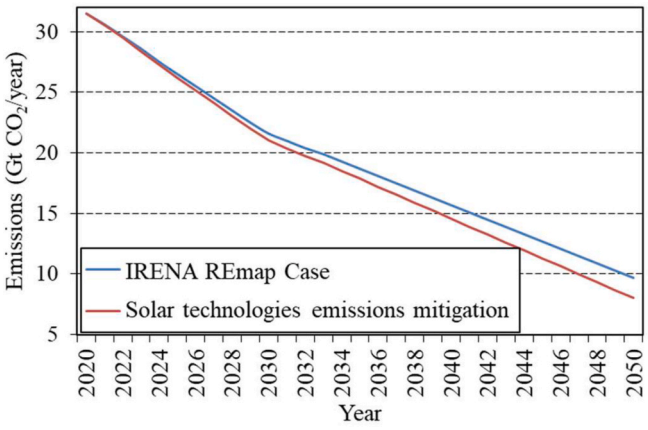


Fig. 63. Solar technologies emission mitigation potential compared to the REmap baseline case of reaching emissions of 22 Gt CO_2/year in 2030 and 9.7 Gt CO_2/year in 2050. (A linear 10% installation rate of PV-T systems was assumed each year).

weather conditions, or weighting between electrical and thermal efficiencies. Trade-offs are always needed between the thermal and electrical outputs.

- From the perspective of achieving the smallest temperature coefficient of the PV panel, it is desirable to use a high-band-gap semiconductor, since it will leave many photons unabsorbed, which could be used for thermal generation. CdTe and GaAs cells have low-temperature coefficients.
- Spectral selectivity is an attractive way to decouple thermally the thermal absorber from the PV cells, although the overall performance of each design should be relatively weighted by the values of electricity and thermal energy to the end-user, which can vary across climates and countries.
- Nanofluids have demonstrated good potential for both improving the thermal conductivity of the working fluids in solar collectors, as well as the potential to make direct solar absorption working fluids. However, challenges remain to their use in practical systems where sustained efforts are still required.
- Space heating can be satisfied by all the PV-T collector designs analysed in this work. The most suitable PV-T collector type depends on the specific location (solar irradiance, ambient temperature) and the space heating system, if available, among others.
- Thermally-driven cooling options including absorption, desiccant, ejector and adsorption cycles are available where cooling is required and the value of heat is low. At least one relevant comparative study concluded that absorption and electric compression lead to the largest energy savings, but further studies are required to gain a

complete understanding of the relevant benefits in different applications.

- All PV-T collectors presented in this work can be integrated with SHC technologies to generate electricity, heating and/or cooling. The most suitable PV-T collector and SHC technology depend on the specific location (solar irradiance, ambient temperatures) and specific application, among others.
- Solar PV-T technology has been demonstrated in both flat-plate and concentrated solar collector designs, where the waste heat from the PV systems is used for driving thermal distillation techniques, and where the electrical energy is used for auxiliary loads and re-injection for the grid. The high energy demands of thermal distillation can make an ST collector limited for clean water production.
- Several studies have examined the theoretical benefits of using solar heat to augment electrolyser performance, with an up to 2.5-fold increase in the solar-to-hydrogen production for a PV-T collector over a conventional PV panel and electrolyser running at ambient temperature.
- Three main aspects should be considered in the design of a TES system for employment within PV-T systems: thermal properties, cost-effectiveness, and environmental impact.
- Water has a high energy density compared to other liquid-based sensible heat storage materials. Because of this, together with other advantages such as low cost, harmless nature, abundance, and ease of handling, transportation and storage, water has been the most popular and commercially used SHS material for low-temperature (~0–100 °C) storage applications. A considerable amount of research has also been done on enhancing the thermophysical and optical properties of water through the use of nanoparticle additives.
- Organic-based thermal oils have been used in elevated-temperature applications, thanks to their lower vapour pressure than water at these temperatures, while for applications at temperatures over ~400 °C, molten salts are the preferred option due to their high thermal stability and very low vapour pressure.
- LHS, more popularly called PCM-based TES, stores thermal energy through a phase change, which occurs at a near-fixed temperature. Attractive features of PCM-based TES technologies include high energy density (compared to SHS-based TES) and a nearly isothermal process during the phase change.

7.2. Challenges for adoption

Some challenges need to be overcome for the widespread of PV-T technology, including:

- Further research on the integration of PV-T-based systems in the distribution grid, life cycle assessment, detailed economic analysis including key performance indicators (KPIs) such as payback time and life-cycle savings (LCS), and environmental analysis comprising KPIs such as CO_2 emission saving potential ($kgCO_2$/year) and the impact on global warming (using well-known methodologies such as the ReCiPe 2016 endpoint (H/A) and the carbon footprint IPCC 2013,100 years).
- Field research on long-term reliability: Due to the limited maturity of this technology, there is a lack of studies on the long-term operation of PV-T systems to assess the long-term reliability of PV-T collectors, through KPIs such as system lifetime, or degradation performance rate.
- Cost: The cost of PV-T collectors is still considerably larger than the cost of separate PV panels and ST collectors. Some alternatives to decrease the cost is the replacement of c-Si PV cells with a-Si or some non-crystalline PV materials. Furthermore, the PV-T collector cost is expected to decrease with the wider installation of PV-T systems thanks to the economies of scale.
- Lack of awareness: separate PV panel and ST collectors are mature and well-known technologies, while people are still not aware of the existence of hybrid PV-T collectors, their overall efficiency and high performance. This is expected to improve with the outcomes of Task 60 "Application of PV-T Collectors and New Solutions in HVAC Systems" of the IEA.
- Lack of certification rules for PV-T collectors: Currently a specific norm for testing PV-T collectors as such is not available, and it is needed to compare the different PV-T technologies available in the market. Currently, the thermal performance of PV-T collectors can be tested according to standard ISO 9806:2017, but this has several limitations, as it is aimed at ST collectors and does not consider the electrical output.
- The main technical challenges for the use of salt-hydrate-based PCMs in TES include subcooling during crystallization, incongruent melting, and corrosion in contact with some commonly used metals such as copper, aluminium, and stainless steel. TCS technology still faces the challenges of high costs, high complexity and short lifespans, and remains in the early stages of research and development.

7.3. Recommendations and future outlook

Potential pathways for improvement of PV-T collectors include collector design modifications, the addition of PCMs, selective coatings, or the use of spectral splitting techniques or nanofluids. The following recommendations and future work are proposed:

- Enhancement of PV-T collector performance through the modification of the thermal absorber to increase the heat-transfer area (for instance through extended surfaces, ribs, and corrugations), and/or the use of selective coatings by developing a cost-effective method to integrate the coating in the absorber surface.
- Further research on integrating PCMs with PV-T collectors, including work in the addition of nanoparticles into PCMs (PV-T-NePCM collectors) to improve thermal and electrical efficiencies, as well as more research to improve the cost-competitiveness of PV-T-PCM collectors to make them practically more attractive.
- More research is also required in the use of nanofluids in PV-T collectors, regarding the life cycle, stability and environmental impact of the nanomaterials used, as usually, nanoparticles lose their thermal properties over time due to degradation.
- Future work in holographic filters including scaled-up demonstrations to prove stability, reliability, and performance along with some viable mechanisms for manufacturing cost reductions.
- Although the research in luminescent concentrators has slowed down in recent years, this type of optical element could still have the potential for further development in PV-T systems.
- More work is needed in optical absorption nanofluids for low temperature and concentration collectors to demonstrate the potential when there is actual flow in the fluid filter generating useful energy.
- Proposed future work regarding thermal energy storage includes further investigations on the use of salt-hydrate-based PCMs to overcome the challenges mentioned in the previous section, as well as further research on TCS technology to face the challenges of high costs, high complexity and short lifespans.

From the different applications reviewed here, the following recommendations and future work are proposed:

- At locations with low irradiance levels and low ambient temperatures, where significant space heating is required almost all year long, air-based PV-T collectors can be a cost-effective alternative, usually integrated with an HP as a backup system.
- At locations with high solar irradiance and ambient temperatures, water-based PV-T collectors appear as a good alternative to pre-heat water for DHW and space heating. These collectors are usually integrated with the current heating system (e.g., a boiler) as a backup and auxiliary system.

- While there is a lot of ongoing research in solar cooling, little of it has considered PV-T collectors as a potential driver in solar-cooling systems. If scalable and cost-effective PV-T systems can be developed, solar cooling is clearly an area of low-hanging fruit where they could be beneficially employed.
- Combining PV-T collectors with desalination would be particularly attractive for rural areas with desalination needs to provide both clean water and useable electricity. Understanding the scope of the system in terms of water output and electrical output is further needed to fully evaluate its effectiveness.
- Most of the previous work found in the literature involves theoretical studies where either the electricity or the thermal output of the CPV-T collectors are used for hydrogen production, while there are fewer practical studies on low-temperature PV-T collectors where both outputs are used in a PEM electrolyser. So convincing practical demonstrations of the potential of PV-T collectors for hydrogen production are missing.

CRediT author statement

María Herrando: Conceptualization, Methodology, Formal analysis, Visualization, Writing - Original draft preparation, Writing - Reviewing and Editing, **Kai Wang:** Formal analysis, Writing - Original draft preparation, Writing - Reviewing and Editing, **Gan Huang:** Formal analysis, Visualization, Writing - Original draft preparation, Writing - Reviewing and Editing, **Todd Otanicar:** Formal analysis, Visualization, Writing - Original draft preparation, Writing - Reviewing and Editing, **Osama Bany Mousa:** Formal analysis, Writing - Original draft preparation, Writing - Reviewing and Editing, **Rafaela A. Agathokleous:** Formal analysis, Visualization, Writing - Original draft preparation, Writing - Reviewing and Editing, **Yulong Ding:** Writing - Original draft preparation, Writing - Reviewing and Editing, Funding acquisition, **Soteris Kalogirou:** Writing - Reviewing and Editing, Writing - Reviewing and Editing, **Ned Ekins-Daukes:** Formal analysis, Visualization, Writing - Original draft preparation, Writing - Reviewing and Editing, **Robert A Taylor:** Formal analysis, Writing - Original draft preparation, Writing - Reviewing and Editing, **Christos N. Markides:** Conceptualization, Methodology, Writing - Reviewing and Editing, Supervision, Project administration, Funding acquisition.

Declaration of competing interest

The authors declare that they have no known competing financial interests or personal relationships that could have appeared to influence the work reported in this paper.

Data availability

Data will be made available on request.

Acknowledgements

This work was supported by the UK Engineering and Physical Sciences Research Council (EPSRC) [grant numbers EP/M025012/1, EP/R045518/1, and EP/S032622/1] and an Imperial College London EPSRC Impact Acceleration Account [grant number EP/R511547/1]. The work was also supported by the Royal Society under an International Collaboration Award 2020 [grant number ICA\R1\201302]. The authors would like to thank UK company Solar Flow Ltd. (www.solar-flow.co.uk). Data supporting this publication can be obtained on request from cep-lab@imperial.ac.uk. For the purpose of Open Access, the authors have applied a CC BY public copyright licence to any Author Accepted Manuscript version arising from this submission.

References

[1] The United Nations. Rio declaration on enviornment and development. 1992. http://www.unesco.org/education/pdf/RIO_E.PDF. [Accessed 25 June 2017].
[2] UNEP Climate Action. COP 21 Paris France sustainable innovation forum. 2015. http://www.cop21paris.org. [Accessed 25 June 2017].
[3] EG Science. Background on impacts, emission pathways, mitigation options and costs. The 2°C target. Information Reference Document; 2008.
[4] European Commission. Best practices on renewable energy self-consumption. 2015. Brussels.
[5] REN21. Renewables 2020 global status report. Renewable Energy Policy Network for the 21st Century; 2020.
[6] Weiss W, Spokr-dur M. Solar heat worldwide. 2020.
[7] IEA, Key renewables trends. Excerpt from: renewables information. 2016.
[8] IRENA. Renewable energy and jobs – Annual review, 2020; 2020.
[9] Graabak I, Korpås M. Variability characteristics of European wind and solar power resources—a review. Energies 2016;9:449. https://doi.org/10.3390/en9060449.
[10] IEA. Photovoltaic power systems technology collaboration Programme. PVPS annual report. 2016.
[11] Mauthner F, Weiss W, Spörk-Dür M. Solar heat worldwide. Market and contribution to the energy supply 2014. In: Solar heating and cooling Programme. SHC); 2016.
[12] Jordan DC, Kurtz SR. Photovoltaic degradation rates - an analytical review. 2012.
[13] International Energy Agency. Review of failures of photovoltaic modules. 2014.
[14] statista. Cumulative installed solar PV capacity worldwide from 2000 to 2018 (in megawatts). 2019. https://www.statista.com/statistics. [Accessed 23 December 2020].
[15] Green MA. Commercial progress and challenges for photovoltaics. Nat Energy 2016;1:15015. https://doi.org/10.1038/nenergy.2015.15.
[16] Solar PV module prices. Our World Data; 2019. https://ourworldindata.org/grapher/solar-pv-prices. [Accessed 23 December 2020].
[17] International Energy Agency. World energy outlook 2020. 2020. https://www.iea.org/events/world-energy-outlook-2020.
[18] IEA SHC. Germany country report. https://www.iea-shc.org/countries/germany/report; 2020.
[19] Bhattarai S, Oh J, Euh S, Krishna G, Hyun D. Simulation and model validation of sheet and tube type photovoltaic thermal solar system and conventional solar collecting system in transient states. Sol Energy Mater Sol Cells 2012;103:184–93. https://doi.org/10.1016/j.solmat.2012.04.017.
[20] Yang C. Reconsidering solar grid parity. Energy Pol 2010;38:3270–3. https://doi.org/10.1016/j.enpol.2010.03.013.
[21] Ekins-Daukes NJ. Solar energy for heat and electricity: the potential for mitigating climate change. Grantham Inst. Clim. Chang. 2009;1:1–12.
[22] Mellor A, Alonso Alvarez D, Guarracino I, Ramos A, Riverola Lacasta A, Ferre Llin L, et al. Roadmap for the next-generation of hybrid photovoltaic-thermal solar energy collectors. Sol Energy 2018;174:386–98. https://doi.org/10.1016/j.solener.2018.09.004.
[23] Makki A, Omer S, Sabir H. Advancements in hybrid photovoltaic systems for enhanced solar cells performance. Renew Sustain Energy Rev 2015;41:658–84. https://doi.org/10.1016/j.rser.2014.08.069.
[24] Wang K, Herrando M, Pantaleo AM, Markides CN. Technoeconomic assessments of hybrid photovoltaic-thermal vs. conventional solar-energy systems: case studies in heat and power provision to sports centres. Appl Energy 2019;254:113657. https://doi.org/10.1016/J.APENERGY.2019.113657.
[25] International Energy Agency. Task 60: PVT systems: application of PVT collectors and new solutions in HVAC systems. 2018. http://task60.iea-shc.org. [Accessed 3 March 2021].
[26] Ramos A, Guarracino I, Mellor A, Alonso-álvarez D, Childs P, Ekins-daukes NJ, et al. Solar-thermal and hybrid photovoltaic-thermal systems for renewable heating. Grantham Institute, Brief. Pap. No 22. Imperial College London; 2017.
[27] Herrando M, Markides CN, Hellgardt K. A UK-based assessment of hybrid PV and solar-thermal systems for domestic heating and power: system performance. Appl Energy 2014;122:288–309. https://doi.org/10.1016/j.apenergy.2014.01.061.
[28] Michael JJ, Iniyan S, Goic R. Flat plate solar photovoltaic-thermal (PV/T) systems: a reference guide. Renew Sustain Energy Rev 2015;51:62–88. https://doi.org/10.1016/j.rser.2015.06.022.
[29] Riverola A, Mellor A, Alonso Alvarez D, Ferre Llin L, Guarracino I, Markides CN, et al. Mid-infrared emissivity of crystalline silicon solar cells. Sol Energy Mater Sol Cells 2018;174:607–15. https://doi.org/10.1016/j.solmat.2017.10.002.
[30] Alonso-Álvarez D, Augusto A, Pearce P, Llin LF, Mellor A, Bowden S, et al. Thermal emissivity of silicon heterojunction solar cells. Sol Energy Mater Sol Cells 2019;201:110051. https://doi.org/10.1016/j.solmat.2019.110051.
[31] Hirst LC, Ekins-Daukes NJ. Fundamental losses in solar cells. Prog Photovoltaics Res Appl 2011;19:289–93. https://doi.org/10.1002/pip1024.
[32] Wilson GM, Al-Jassim M, Metzger WK, Glunz SW, Verlinden P, Xiong G, et al. The 2020 photovoltaic technologies roadmap. J Phys D Appl Phys 2020;53. https://doi.org/10.1088/1361-6463/ab9c6a.
[33] Dupré O, Vaillon R, Green MA. Physics of the temperature coefficients of solar cells. Sol Energy Mater Sol Cells 2015;140:92–100. https://doi.org/10.1016/j.solmat.2015.03.025.
[34] Zondag HA. Flat-plate PV-Thermal collectors and systems: a review. Renew Sustain Energy Rev 2008;12:891–959. https://doi.org/10.1016/j.rser.2005.12.012.
[35] Chow TT. A review on photovoltaic/thermal hybrid solar technology. Appl Energy 2010;87:365–79. https://doi.org/10.1016/j.apenergy.2009.06.037.

[36] Aste N, del Pero C, Leonforte F. Water flat plate PV-thermal collectors: a review. Sol Energy 2014;102:98–115. https://doi.org/10.1016/j.solener.2014.01.025.
[37] Jia Y, Alva G, Fang G. Development and applications of photovoltaic–thermal systems: a review. Renew Sustain Energy Rev 2019;102:249–65. https://doi.org/10.1016/j.rser.2018.12.030.
[38] Sathe TM, Dhoble AS. A review on recent advancements in photovoltaic thermal techniques. Renew Sustain Energy Rev 2017;76:645–72. https://doi.org/10.1016/j.rser.2017.03.075.
[39] Al-Waeli AHA, Sopian K, Kazem HA, Chaichan MT. Photovoltaic/Thermal (PV/T) systems: status and future prospects. Renew Sustain Energy Rev 2017;77:109–30. https://doi.org/10.1016/j.rser.2017.03.126.
[40] Das D, Kalita P, Roy O. Flat plate hybrid photovoltaic- thermal (PV/T) system: a review on design and development. Renew Sustain Energy Rev 2018;84:111–30. https://doi.org/10.1016/j.rser.2018.01.002.
[41] Zhang X, Zhao X, Smith S, Xu J, Yu X. Review of R&D progress and practical application of the solar photovoltaic/thermal (PV/T) technologies. Renew Sustain Energy Rev 2012;16:599–617. https://doi.org/10.1016/j.rser.2011.08.026.
[42] Pang W, Cui Y, Zhang Q, Wilson GJ, Yan H. A comparative analysis on performances of flat plate photovoltaic/thermal collectors in view of operating media, structural designs, and climate conditions. Renew Sustain Energy Rev 2020;119:109599. https://doi.org/10.1016/j.rser.2019.109599.
[43] Sultan SM, Ervina Efzan MN. Review on recent Photovoltaic/Thermal (PV/T) technology advances and applications. Sol Energy 2018;173:939–54. https://doi.org/10.1016/j.solener.2018.08.032.
[44] Wu J, Zhang X, Shen J, Wu Y, Connelly K, Yang T, et al. A review of thermal absorbers and their integration methods for the combined solar photovoltaic/thermal (PV/T) modules. Renew Sustain Energy Rev 2017;75:839–54. https://doi.org/10.1016/j.rser.2016.11.063.
[45] Brahim T, Jemni A. Economical assessment and applications of photovoltaic/thermal hybrid solar technology: a review. Sol Energy 2017;153:540–61. https://doi.org/10.1016/j.solener.2017.05.081.
[46] Abdelrazik AS, Al-Sulaiman FA, Saidur R, Ben-Mansour R. A review on recent development for the design and packaging of hybrid photovoltaic/thermal (PV/T) solar systems. Renew Sustain Energy Rev 2018;95:110–29. https://doi.org/10.1016/j.rser.2018.07.013.
[47] Lamnatou C, Chemisana D. Photovoltaic/thermal (PVT) systems: a review with emphasis on environmental issues. Renew Energy 2017;105:270–87. https://doi.org/10.1016/j.renene.2016.12.009.
[48] Daghigh R, Ruslan MH, Sopian K. Advances in liquid based photovoltaic/thermal (PV/T) collectors. Renew Sustain Energy Rev 2011;15:4156–70. https://doi.org/10.1016/j.rser.2011.07.028.
[49] Ullah KR, Saidur R, Ping HW, Akikur RK, Shuvo N. A review of solar thermal refrigeration and cooling methods. Renew Sustain Energy Rev 2013;51:1428–45. https://doi.org/10.1016/j.rser.2015.07.011.
[50] Bataineh K, Taamneh Y. Review and recent improvements of solar sorption cooling systems. Energy Build 2016;128:22–37. https://doi.org/10.1016/j.enbuild.2016.06.075.
[51] Lazzarin RM, Noro M. Past, present, future of solar cooling: technical and economical considerations. Sol Energy 2018;172:2–13. https://doi.org/10.1016/J.SOLENER.2017.12.055.
[52] Nkwetta DN, Sandercock J. A state-of-the-art review of solar air-conditioning systems. Renew Sustain Energy Rev 2016;60:1351–66. https://doi.org/10.1016/j.rser.2016.03.010.
[53] Sarbu I, Sebarchievici C. Review of solar refrigeration and cooling systems. Energy Build 2013;67:286–97. https://doi.org/10.1016/j.enbuild.2013.08.022.
[54] Al-Alili A, Hwang Y, Radermacher R. Review of solar thermal air conditioning technologies. Int J Refrig 2014;39:4–22. https://doi.org/10.1016/j.ijrefrig.2013.11.028.
[55] Ghafoor A, Munir A. Worldwide overview of solar thermal cooling technologies. Renew Sustain Energy Rev 2015;43:763–74. https://doi.org/10.1016/j.rser.2014.11.073.
[56] Infante Ferreira C, Kim DS. Techno-economic review of solar cooling technologies based on location-specific data. Int J Refrig 2014;39:23–37. https://doi.org/10.1016/j.ijrefrig.2013.09.033.
[57] Leonzio G. Solar systems integrated with absorption heat pumps and thermal energy storages: state of art. Renew Sustain Energy Rev 2017;70:492–505. https://doi.org/10.1016/J.RSER.2016.11.117.
[58] Montagnino FM. Solar cooling technologies. Design, application and performance of existing projects. Sol Energy 2017;154:144–57. https://doi.org/10.1016/J.SOLENER.2017.01.033.
[59] Allouhi A, Kousksou T, Jamil A, Bruel P, Mourad Y, Zeraouli Y. Solar driven cooling systems: an updated review. Renew Sustain Energy Rev 2015;44:159–81. https://doi.org/10.1016/j.rser.2014.12.014.
[60] Zeyghami M, Goswami DY, Stefanakos E. A review of solar thermo-mechanical refrigeration and cooling methods. Renew Sustain Energy Rev 2015;51:1428–45. https://doi.org/10.1016/j.rser.2015.07.011.
[61] Ge TS, Wang RZ, Xu ZY, Pan QW, Du S, Chen XM, et al. Solar heating and cooling: present and future development. Renew Energy 2018;126:1126–40. https://doi.org/10.1016/J.RENENE.2017.06.081.
[62] Settino J, Sant T, Micallef C, Farrugia M, Spiteri Staines C, Licari J, et al. Overview of solar technologies for electricity, heating and cooling production. Renew Sustain Energy Rev 2018;90:892–909. https://doi.org/10.1016/j.rser.2018.03.112.
[63] Alobaid M, Hughes B, Kaiser J, Connor DO, Heyes A. A review of solar driven absorption cooling with photovoltaic thermal systems. Renew Sustain Energy Rev 2017;76:728–42. https://doi.org/10.1016/j.rser.2017.03.081.
[64] Guo J, Lin S, Bilbao JI, White SD, Sproul AB. A review of photovoltaic thermal (PV/T) heat utilisation with low temperature desiccant cooling and dehumidification. Renew Sustain Energy Rev 2017;67:1–14. https://doi.org/10.1016/J.RSER.2016.08.056.
[65] Kamel RS, Fung AS, Dash PRH. Solar systems and their integration with heat pumps: a review. Energy Build 2015;87:395–412. https://doi.org/10.1016/j.enbuild.2014.11.030.
[66] Buonomano A, Calise F, Palombo A. Solar heating and cooling systems by absorption and adsorption chillers driven by stationary and concentrating photovoltaic/thermal solar collectors: modelling and simulation. Renew Sustain Energy Rev 2018;82:1874–908. https://doi.org/10.1016/j.rser.2017.10.059.
[67] Wang X, Xia L, Bales C, Zhang X, Copertaro B, Pan S, et al. A systematic review of recent air source heat pump (ASHP) systems assisted by solar thermal, photovoltaic and photovoltaic/thermal sources. Renew Energy 2020;146:2472–87. https://doi.org/10.1016/j.renene.2019.08.096.
[68] Mohanraj M, Belyayev Y, Jayaraj S, Kaltayev A. Research and developments on solar assisted compression heat pump systems – a comprehensive review (Part A: modeling and modifications). Renew Sustain Energy Rev 2018;83:90–123. https://doi.org/10.1016/J.RSER.2017.08.022.
[69] Vaishak S, Bhale PV. Photovoltaic/thermal-solar assisted heat pump system: current status and future prospects. Sol Energy 2019;189:268–84. https://doi.org/10.1016/j.solener.2019.07.051.
[70] Herrando M, Ramos A. Photovoltaic-thermal (PV-T) systems for combined cooling, heating and power in buildings: a review. Energies 2022;15. https://doi.org/10.3390/en15093021.
[71] Tripanagnostopoulos Y, Nousia TH, Souliotis M, Yianoulis P. Hybrid photovoltaic/thermal solar systems. Sol Energy 2002;72:217–34.
[72] He W, Chow T, Ji J, Lu J, Pei G. Hybrid photovoltaic and thermal solar-collector designed for natural circulation of water. Appl Energy 2006;83:199–210. https://doi.org/10.1016/j.apenergy.2005.02.007.
[73] Tripanagnostopoulos Y. Aspects and improvements of hybrid photovoltaic/thermal solar energy systems. Sol Energy 2007;81:1117–31. https://doi.org/10.1016/j.solener.2007.04.002.
[74] Kalogirou SA, Tripanagnostopoulos Y. Hybrid PV/T solar systems for domestic hot water and electricity production. Energy Convers Manag 2006;47:3368–82. https://doi.org/10.1016/j.enconman.2006.01.012.
[75] Erdil E, Ilkan M, Egelioglu F. An experimental study on energy generation with a photovoltaic (PV)– solar thermal hybrid system. Energy 2008;33:1241–5. https://doi.org/10.1016/j.energy.2008.03.005.
[76] Affolter P, Eisenmann W, Fechner H, Rommel M, Schaap A, Sorensen H, et al. PVT roadmap: a European guide for the development and market introduction of PV-Thermal technology, Present. 20th Eur Photovolt Sol Energy Conf Exhib 2005;6:10. http://www.ecn.nl/publications/default.aspx?nr=rx05170.
[77] Collins M, Zondag HA. Recommended standard for the characterization and monitoring of PV/Thermal systems. 2009.
[78] IEA. Trends. In: Photovoltaic applications. Survey report of selected IEA countries between 1992 and 2014; 2015.
[79] Chu J, Cruickshank CA. Solar-assisted heat pump systems: a review of existing studies and their applicability to the Canadian residential sector. J Sol Energy Eng 2014;136. https://doi.org/10.1115/1.4027735.
[80] Giwa A, Yusuf A, Dindi A, Balogun HA. Polygeneration in desalination by photovoltaic thermal systems: a comprehensive review. Renew Sustain Energy Rev 2020;130:109946. https://doi.org/10.1016/j.rser.2020.109946.
[81] Otanicar T, Qu W. Thermodynamic analysis of hybrid humidification-dehumidification (HDH) - reverse osmosis (RO) desalination system powered by concentrating photovoltaic/thermal solar collector. 2018. https://doi.org/10.1063/1.5067164.
[82] Nayak S, Kumar A, Singh AK, Tiwari GN. Energy matrices analysis of hybrid PVT greenhouse dryer by considering various silicon and non-silicon PV modules. Int J Sustain Energy 2014;33:336–48. https://doi.org/10.1080/14786451.2012.751914.
[83] Mortezapour H, Ghobadian B, Minaei S, Khoshtaghaza MH. Saffron drying with a heat pump–assisted hybrid photovoltaic–thermal solar dryer. Dry Technol 2012;30:560–6. https://doi.org/10.1080/07373937.2011.645261.
[84] Oruc ME, Desai AV, Kenis PJA, Nuzzo RG. Comprehensive energy analysis of a photovoltaic thermal water electrolyzer. Appl Energy 2016;164:294–302. https://doi.org/10.1016/j.apenergy.2015.11.078.
[85] Senthilraja S, Gangadevi R, Marimuthu R, Baskaran M. Performance evaluation of water and air based PVT solar collector for hydrogen production application. Int J Hydrogen Energy 2020;45:7498–507. https://doi.org/10.1016/j.ijhydene.2019.02.223.
[86] Pillai GG, Putrus GA, Georgitsioti T, Pearsall NM. Near-term economic benefits from grid-connected residential PV (photovoltaic) systems. Energy 2014;68:832–43. https://doi.org/10.1016/j.energy.2014.02.085.
[87] Luthander R, Widen J, Nilsson D, Palm J. Photovoltaic self-consumption in buildings: a review. Appl Energy 2015;142:80–94. https://doi.org/10.1016/j.apenergy.2014.12.028.
[88] Thygesen R, Karlsson B. Simulation and analysis of a solar assisted heat pump system with two different storage types for high levels of PV electricity self-consumption. Sol Energy 2014;103:19–27. https://doi.org/10.1016/j.solener.2014.02.013.
[89] Vanhoudt D, Geysen D, Claessens B, Leemans F, Jespers L, Van Bael J. An actively controlled residential heat pump: potential on peak shaving and maximization of self-consumption of renewable energy. Renew Energy 2014;63:531–43. https://doi.org/10.1016/j.renene.2013.10.021.

[90] Lopes RA, ~ Ao Martins J, Aelenei D, Lima CP. A cooperative net zero energy community to improve load matching. Renew Energy 2016;93:1–13. https://doi.org/10.1016/j.renene.2016.02.044.

[91] Herrando M, Markides CN. Hybrid PV and solar-thermal systems for domestic heat and power provision in the UK: techno-economic considerations. Appl Energy 2016;161:512–32. https://doi.org/10.1016/j.apenergy.2015.09.025.

[92] Baggenstos A, Mellor A, Gagliano A, Corino C, Zenhäusern D, Cabral D, et al. Existing PVT systems and solutions. IEA SHC Task60, PVT Systems; 2020. p. 130. https://doi.org/10.18777/ieashc-task60-2020-0001. Report A1.

[93] Kramer K, Amrizal N, Beyssac JB, Brottier L, Gagliano A, Fischer S, et al. Status quo of PVT characterization. SHC task 60 - report B1. 2020. https://doi.org/10.18777/ieashc-task60-2020-0004.

[94] Tyagi VV, Kaushik SC, Tyagi SK. Advancement in solar photovoltaic/thermal (PV/T) hybrid collector technology. Renew Sustain Energy Rev 2012;16:1383–98. https://doi.org/10.1016/j.rser.2011.12.013.

[95] Tyagi VV, Panwar NL, Rahim NA, Kothari R. Review on solar air heating system with and without thermal energy storage system. Renew Sustain Energy Rev 2012;16:2289–303. https://doi.org/10.1016/j.rser.2011.12.005.

[96] Joshi SS, Dhoble AS. Photovoltaic -Thermal systems (PVT): technology review and future trends. Renew Sustain Energy Rev 2018;92:848–82. https://doi.org/10.1016/j.rser.2018.04.067.

[97] Sahota L, Tiwari GN. Review on series connected photovoltaic thermal (PVT) systems: analytical and experimental studies. Sol Energy 2017;150:96–127. https://doi.org/10.1016/j.solener.2017.04.023.

[98] Farshchimonfared M, Bilbao JI, Sproul AB. Channel depth, air mass flow rate and air distribution duct diameter optimization of photovoltaic thermal (PV/T) air collectors linked to residential buildings. Renew Energy 2015;76:27–35. https://doi.org/10.1016/j.renene.2014.10.044.

[99] Tonui JK, Tripanagnostopoulos Y. Performance improvement of PV/T solar collectors with natural air flow operation. Sol Energy 2008;82:1–12. https://doi.org/10.1016/j.solener.2007.06.004.

[100] Bambrook SM, Sproul AB. A solvable thermal circuit for modelling PVT air collectors. Sol Energy 2016;138:77–87. https://doi.org/10.1016/j.solener.2016.09.007.

[101] Özakin AN, Kaya F. Effect on the exergy of the PVT system of fins added to an air-cooled channel: a study on temperature and air velocity with ANSYS Fluent. Sol Energy 2019;184:561–9. https://doi.org/10.1016/j.solener.2019.03.100.

[102] Fudholi A, Zohri M, Rukman NSB, Nazri NS, Mustapha M, Yen CH, et al. Exergy and sustainability index of photovoltaic thermal (PVT) air collector: a theoretical and experimental study. Renew Sustain Energy Rev 2019;100:44–51. https://doi.org/10.1016/j.rser.2018.10.019.

[103] Agrawal S, Tiwari GN. Performance analysis in terms of carbon credit earned on annualized uniform cost of glazed hybrid photovoltaic thermal air collector. Sol Energy 2015;115:329–40. https://doi.org/10.1016/j.solener.2015.02.030.

[104] Agrawal S, Tiwari GN. Enviroeconomic analysis and energy matrices of glazed hybrid photovoltaic thermal module air collector. Sol Energy 2013;92:139–46. https://doi.org/10.1016/j.solener.2013.02.019.

[105] Slimani MEA, Amirat M, Kurucz I, Bahria S, Hamidat A, Chaouch WB. A detailed thermal-electrical model of three photovoltaic/thermal (PV/T) hybrid air collectors and photovoltaic (PV) module: comparative study under Algiers climatic conditions. Energy Convers Manag 2017;133:458–76. https://doi.org/10.1016/j.enconman.2016.10.066.

[106] Hussain F, Othman MYH, Sopian K, Yatim B, Ruslan H, Othman H. Design development and performance evaluation of photovoltaic/thermal (PV/T) air base solar collector. Renew Sustain Energy Rev 2013;25:431–41. https://doi.org/10.1016/j.rser.2013.04.014.

[107] del Amo A, Martínez-Gracia A, Bayod-Rújula AA, Antoñanzas J. An innovative urban energy system constituted by a photovoltaic/thermal hybrid solar installation: design, simulation and monitoring. Appl Energy 2017;186:140–51. https://doi.org/10.1016/j.apenergy.2016.07.011.

[108] Shahsavar A, Ameri M. Experimental investigation and modeling of a direct-coupled PV/T air collector. Sol Energy 2010;84:1938. https://doi.org/10.1016/j.solener.2010.07.010. –1958.

[109] Gholampour M, Ameri M. Energy and exergy analyses of Photovoltaic/Thermal flat transpired collectors: experimental and theoretical study. Appl Energy 2016;164:837–56. https://doi.org/10.1016/j.apenergy.2015.12.042.

[110] Bambrook SM, Sproul AB. Maximising the energy output of a PVT air system. Sol Energy 2012;86:1857–71. https://doi.org/10.1016/j.solener.2012.02.038.

[111] Kim JH, Park SH, Kim JT. Experimental performance of a photovoltaic-thermal air collector. Energy Proc 2014;48:888–94. https://doi.org/10.1016/j.egypro.2014.02.102.

[112] Singh S, Agarwal S, Tiwari GN, Chauhan D. Application of genetic algorithm with multi-objective function to improve the efficiency of glazed photovoltaic thermal system for New Delhi (India) climatic condition. Sol Energy 2015;117:153–66. https://doi.org/10.1016/J.SOLENER.2015.04.025.

[113] Fan W, Kokogiannakis G, Ma Z, Cooper P. Development of a dynamic model for a hybrid photovoltaic thermal collector – solar air heater w ith fins. Renew Energy 2017;101:816–34. https://doi.org/10.1016/j.renene.2016.09.039.

[114] Tonui JK, Tripanagnostopoulos Y. Air-cooled PV/T solar collectors with low cost performance improvements. Sol Energy 2007;81:498–511. https://doi.org/10.1016/J.SOLENER.2006.08.002.

[115] Hussain MI, Kim JT. Performance evaluation of photovoltaic/thermal (Pv/t) system using different design configurations. Sustain Times 2020;12:1–17. https://doi.org/10.3390/su12229520.

[116] Diwania S, Siddiqui AS, Agrawal S, Kumar R. Performance assessment of PVT-air collector with V-groove absorber: a theoretical and experimental analysis. Heat Mass Transf. Und Stoffuebertragung. 2021;57:665–79. https://doi.org/10.1007/s00231-020-02980-0.

[117] Adeli MM, Sobhnamayan F, Farahat S, Alavi MA, Sarhaddi F. Experimental performance evaluation of a photovoltaic thermal (PV/T) air collector and its optimization. Stroj. Vestnik/Journal Mech. Eng. 2012;58:309–18. https://doi.org/10.5545/sv-jme.2010.007.

[118] Tripanagnostopoulos Y, Souliotis M. Application aspects of hybrid PV/T solar systems. 2002.

[119] Ibrahim A, Othman MY, Ruslan MH, Alghoul MA, Yahya M, Zaharim A, et al. Performance of photovoltaic thermal collector (PVT) with different absorbers design. WSEAS Trans Environ Dev 2009;5:321–30.

[120] Zondag HA, de Vries DW, van Helden WGJ, van Zolingen RJC, van Steenhoven AA. The yield of different combined PV-thermal collector designs. Sol Energy 2003;74:253–69. https://doi.org/10.1016/S0038-092X(03)00121-X.

[121] Guarracino I, Freeman J, Ramos A, Kalogirou SA, Ekins-Daukes NJ, Markides CN. Systematic testing of hybrid PV-thermal (PVT) solar collectors in steady-state and dynamic outdoor conditions. Appl Energy 2019;240:1014–30. https://doi.org/10.1016/j.apenergy.2018.12.049.

[122] Herrando M, Ramos A, Zabalza I, Markides CN. A comprehensive assessment of alternative absorber-exchanger designs for hybrid PVT-water collectors. Appl Energy 2019;235:1583–602. https://doi.org/10.1016/J.APENERGY.2018.11.024.

[123] Fraisse G, Ménézo C, Johannes K. Energy performance of water hybrid PV/T collectors applied to combisystems of Direct Solar Floor type. Sol Energy 2007;81:1426–38. https://doi.org/10.1016/j.solener.2006.11.017.

[124] Moreno D, Fernandez M, Esquivias PM. A comparison of closed-form and finite-element solutions for heat transfer in a nearly horizontal, unglazed flat plate PVT water collector: performance assessment. Sol Energy 2017;141:11–24. https://doi.org/10.1016/j.solener.2016.11.015.

[125] Chow TT. Performance analysis of photovoltaic-thermal collector by explicit dynamic model. Sol Energy 2003;75:143–52. https://doi.org/10.1016/j.solener.2003.07.001.

[126] Chen JF, Zhang L, Dai YJ. Performance analysis and multi-objective optimization of a hybrid photovoltaic/thermal collector for domestic hot water application. Energy 2018;143:500–16. https://doi.org/10.1016/j.energy.2017.10.143.

[127] Santbergen R, Rindt CCM, Zondag HA, van Zolingen RJC. Detailed analysis of the energy yield of systems with covered sheet-and-tube PVT collectors. Sol Energy 2010;84:867–78. https://doi.org/10.1016/j.solener.2010.02.014.

[128] Zondag HA, De Vries DW, Van Helden WGJ, Van Zolingen RJC, van Steenhoven AA. The thermal and electrical yield of a PV-thermal collector. Sol Energy 2002;72:113–28. https://doi.org/10.1016/S0038-092X(01)00094-9.

[129] Fudholi A, Sopian K, Yazdi MH, Ruslan MH, Ibrahim A, Kazem HA. Performance analysis of photovoltaic thermal (PVT) water collectors. Energy Convers Manag 2014;78:641–51. https://doi.org/10.1016/j.enconman.2013.11.017.

[130] Bakker M, Zondag HA, van Helden WGJ. Design of a dual flow photovoltaic/thermal combi panel. IST World; 2002.

[131] Rosa-Clot M, Rosa-Clot P, Tina GM. TESPI: thermal electric solar panel integration. Sol Energy 2011;85:2433–42. https://doi.org/10.1016/j.solener.2011.07.003.

[132] Chow TT, Ji J, He W. Photovoltaic-thermal collector system for domestic application. J Sol Energy Eng 2007;129:205. https://doi.org/10.1115/1.2711474.

[133] Kalogirou SA. Use of TRNSYS for modelling and simulation of a hybrid pv–thermal solar system for Cyprus. Renew Energy 2001;23:247–60. https://doi.org/10.1016/S0960-1481(00)00176-2.

[134] Tripanagnostopoulos Y, Souliotis M, Battisti R, Corrado A. Energy, cost and LCA results and hybrid PV/T solar systems. Prog Photovoltaics Res Appl 2005;13:235–50. https://doi.org/10.1002/pip.590.

[135] Energies-sol. Soluciones de Energias Solares y Eolicas. http://www.energies-sol.com/index_612.htm. [Accessed 4 August 2017].

[136] EndeF. Endef solar solutions. http://endef.com. [Accessed 15 November 2021].

[137] Newform Energy. Welcome to Newform Energy Ireland a forward thinking renewable energy company. http://products.newformenergy.ie/hybrid-solar-solution.php. [Accessed 4 August 2017].

[138] Millennium Electric. Millennium electric T.O.U Ltd. http://www.millenniumsolar.com. [Accessed 4 August 2017].

[139] Dupeyrat P, Ménézo C, Rommel M, Henning HM. Efficient single glazed flat plate photovoltaic-thermal hybrid collector for domestic hot water system. Sol Energy 2011;85:1457–68. https://doi.org/10.1016/j.solener.2011.04.002.

[140] Abora Solar. The most cost-effective solar panel in the world. https://abora-solar.com/en/. [Accessed 17 October 2022].

[141] Kern J, E C, Russell MC. Combined photovoltaic and thermal hybrid collector systems. In: IEEE photovolt. Spec. Conf. Washington, DC, USA, United States; 1978. p. 1153–7. https://www.osti.gov/biblio/6352146.

[142] Xu G, Deng S, Zhang X, Yang L, Zhang Y. Simulation of a photovoltaic/thermal heat pump system having a modified collector/evaporator. Sol Energy 2009;83:1967–76. https://doi.org/10.1016/j.solener.2009.07.008.

[143] Ji J, Keliang L, Chow TT, Pei G, Wei H, Hanfeng H. Performance analysis of a photovoltaic heat pump. Appl Energy 2008;85:680–93. https://doi.org/10.1016/j.apenergy.2008.01.003.

[144] Ji J, Pei G, Chow TT, Keliang L, Hanfeng H, Jianping L, et al. Experimental study of photovoltaic solar assisted heat pump system. Sol Energy 2008;82:43–52. https://doi.org/10.1016/j.solener.2007.04.006.

[145] Bakker M, Zondag HA, Elswijk MJ, Strootman KJ, Jong MJM. Performance and costs of a roof-sized PV/thermal array combined with a ground coupled heat

pump. Sol Energy 2005;78:331–9. https://doi.org/10.1016/j.solener.2004.09.019.
[146] Zhao X, Zhang X, Riffat SB, Su Y. Theoretical study of the performance of a novel PV/e roof module for heat pump operation. Energy Convers Manag 2011;52:603–14. https://doi.org/10.1016/j.enconman.2010.07.036.
[147] Ji J, Hanfeng H, Chow T, Pei G, He W, Liu K. Distributed dynamic modeling and experimental study of PV evaporator in a PV/T solar-assisted heat pump. Int J Heat Mass Tran 2009;52:1365–73. https://doi.org/10.1016/j.ijheatmasstransfer.2008.08.017.
[148] Vaishak S, Bhale PV. Performance analysis of a heat pump-based photovoltaic/thermal (PV/T) system, Clean Technol. Environ Pol 2020. https://doi.org/10.1007/s10098-020-01839-6.
[149] Keliang L, Ji J, Tin-tai C, Pei G, Hanfeng H, Aiguo J, et al. Performance study of a photovoltaic solar assisted heat pump with variable-frequency compressor – a case study in Tibet. Renew Energy 2009;34:2680–7. https://doi.org/10.1016/j.renene.2009.04.031.
[150] Fang G, Hu H, Liu X. Experimental investigation on the photovoltaic-thermal solar heat pump air-conditioning system on water-heating mode. Exp Therm Fluid Sci 2010;34:736–43. https://doi.org/10.1016/j.expthermflusci.2010.01.002.
[151] Mohanraj M, Gunasekar N, Velmurugan V. Comparison of energy performance of heat pumps using a photovoltaic–thermal evaporator with circular and triangular tube configurations. Build Simulat 2016;9:27–41. https://doi.org/10.1007/s12273-015-0256-1.
[152] Tsai H-L. Modeling and validation of refrigerant-based PVT-assisted heat pump water heating (PVTA–HPWH) system. Sol Energy 2015;122:36–47. https://doi.org/10.1016/J.SOLENER.2015.08.024.
[153] Liang R, Pan Q, Wang P, Zhang J. Experiment research of solar PV/T cogeneration system on the building façade driven by a refrigerant pump. Energy 2018;161:744–52. https://doi.org/10.1016/j.energy.2018.07.189.
[154] Cai J, Ji J, Wang Y, Zhou F, Yu B. A novel PV/T-air dual source heat pump water heater system: dynamic simulation and performance characterization. Energy Convers Manag 2017;148:635–45. https://doi.org/10.1016/J.ENCONMAN.2017.06.036.
[155] Zhou J, Zhao X, Ma X, Qiu Z, Ji J, Du Z, et al. Experimental investigation of a solar driven direct-expansion heat pump system employing the novel PV/micro-channels-evaporator modules. Appl Energy 2016;178:484–95. https://doi.org/10.1016/j.apenergy.2016.06.063.
[156] Zhou C, Liang R, Riaz A, Zhang J, Chen J. Experimental investigation on the tri-generation performance of roll-bond photovoltaic thermal heat pump system during summer. Energy Convers Manag 2019;184:91–106. https://doi.org/10.1016/j.enconman.2018.12.028.
[157] Zhou C, Liang R, Zhang J, Riaz A. Experimental study on the cogeneration performance of roll-bond-PVT heat pump system with single stage compression during summer. Appl Therm Eng 2019;149:249–61. https://doi.org/10.1016/j.applthermaleng.2018.11.120.
[158] Chen H, Riffat SB, Fu Y. Experimental study on a hybrid photovoltaic/heat pump system. Appl Therm Eng 2011;31:4132–8. https://doi.org/10.1016/j.applthermaleng.2011.08.027.
[159] Xu G, Zhang X, Deng S. Experimental study on the operating characteristics of a novel low-concentrating solar photovoltaic/thermal integrated heat pump water heating system. Appl Therm Eng 2011;31:3689–95. https://doi.org/10.1016/j.applthermaleng.2011.01.030.
[160] Li YW, Wang RZ, Wu JY, Xu YX. Experimental performance analysis on a direct-expansion solar-assisted heat pump water heater. Appl Therm Eng 2007;27:2858–68. https://doi.org/10.1016/j.applthermaleng.2006.08.007.
[161] Obalanlege MA, Mahmoudi Y, Douglas R, Ebrahimnia-Bajestan E, Davidson J, Bailie D. Performance assessment of a hybrid photovoltaic-thermal and heat pump system for solar heating and electricity. Renew Energy 2020;148:558–72. https://doi.org/10.1016/j.renene.2019.10.061.
[162] Chata FBG, Chaturvedi SK, Almogbel A. Analysis of a direct expansion solar assisted heat pump using different refrigerants. Energy Convers Manag 2005;46:2614–24. https://doi.org/10.1016/j.enconman.2004.12.001.
[163] Chow TT, Fong KF, Pei G, Ji J, He M. Potential use of photovoltaic-integrated solar heat pump system in Hong Kong. Appl Therm Eng 2010;30:1066–72. https://doi.org/10.1016/j.applthermaleng.2010.01.013.
[164] Pei G, Ji J, Liu KL, He HF, Jiang AG. Numerical study of PV/T-SAHP system. J Zhejiang Univ - Sci A 2008;9:970–80. https://doi.org/10.1631/jzus.A0720143.
[165] Zhang X, Zhao X, Xu J, Yu X. Characterization of a solar photovoltaic/loop-heat-pipe heat pump water heating system. Appl Energy 2013;102:1229–45. https://doi.org/10.1016/j.apenergy.2012.06.039.
[166] Chaturvedi SK, Abazeri M. Transient simulation of a capacity-modulated, direct-expansion, solar-assisted heat pump. Sol Energy 1987;39:421–8. https://doi.org/10.1016/S0038-092X(87)80060-9.
[167] Faghri A. Review and advances in heat pipe science and technology. J Heat Tran 2012;134:123001. https://doi.org/10.1115/1.4007407.
[168] Chen H, Zhang H, Li M, Liu H, Huang J. Experimental investigation of a novel LCPV/T system with micro-channel heat pipe array. Renew Energy 2018;115:773–82. https://doi.org/10.1016/j.renene.2017.08.087.
[169] Hou L, Quan Z, Zhao Y, Wang L, Wang G. An experimental and simulative study on a novel photovoltaic-thermal collector with micro heat pipe array (MHPA-PV/T). Energy Build 2016;124:60–9. https://doi.org/10.1016/j.enbuild.2016.03.056.
[170] Zhang T, Yan ZW, Xiao L, Fu HD, Pei G, Ji J. Experimental, study and design sensitivity analysis of a heat pipe photovoltaic/thermal system. Appl Therm Eng 2019;162:114318. https://doi.org/10.1016/j.applthermaleng.2019.114318.
[171] Long H, Chow T-T, Ji J. Building-integrated heat pipe photovoltaic/thermal system for use in Hong Kong. Sol Energy 2017;155:1084–91. https://doi.org/10.1016/j.solener.2017.07.055.
[172] Pei G, Huide F, Huijuan Z, Ji J. Performance study and parametric analysis of a novel heat pipe PV/T system. Energy 2012;37:384–95. https://doi.org/10.1016/j.energy.2011.11.017.
[173] Pei G, Huide F, Tao Z, Ji J. A numerical and experimental study on a heat pipe PV/T system. Sol Energy 2011;85:911–21. https://doi.org/10.1016/j.solener.2011.02.006.
[174] Wu S-Y, Zhang Q-L, Xiao L, Guo F-H. A heat pipe photovoltaic/thermal (PV/T) hybrid system and its performance evaluation. Energy Build 2011;43:3558–67. https://doi.org/10.1016/j.enbuild.2011.09.017.
[175] Wang Z, Zhang J, Wang Z, Yang W, Zhao X. Experimental investigation of the performance of the novel HP-BIPV/T system for use in residential buildings. Energy Build 2016;130:295–308. https://doi.org/10.1016/j.enbuild.2016.08.060.
[176] Farahat MA. Improvement the thermal electric performance of a photovoltaic cells by cooling and concentration techniques. 39th Int. Univ. Power Eng. Conf. IEEE. 2004;2:623–8.
[177] Makki A, Omer S, Su Y, Sabir H. Numerical investigation of heat pipe-based photovoltaic–thermoelectric generator (HP-PV/TEG) hybrid system. Energy Convers Manag 2016;112:274. https://doi.org/10.1016/j.enconman.2015.12.069. 287.
[178] Shittu S, Li G, Zhao X, Zhou J, Ma X, Akhlaghi YG. Experimental study and exergy analysis of photovoltaic-thermoelectric with flat plate micro-channel heat pipe. Energy Convers Manag 2020;207:112515. https://doi.org/10.1016/j.enconman.2020.112515.
[179] Markides CN. Low-concentration solar-power systems based on organic Rankine cycles for distributed-scale applications: overview and further developments. Front Energy Reseach 2015;3:473389. https://doi.org/10.3389/fenrg.2015.00047. 47.
[180] El Manssouri O, Hajji B, Tina GM, Gagliano A, Aneli S. Electrical and thermal performances of Bi-fluid PV/thermal collectors. Energies 2021;14. https://doi.org/10.3390/en14061633.
[181] Hu M, Zhao B, Ao X, Ren X, Cao J, Wang Q, et al. Performance assessment of a trifunctional system integrating solar PV, solar thermal, and radiative sky cooling. Appl Energy 2020;260:114167. https://doi.org/10.1016/j.apenergy.2019.114167.
[182] Ji J, Guo C, Sun W, He W, Wang Y, Li G. Experimental investigation of tri-functional photovoltaic/thermal solar collector. Energy Convers Manag 2014;88:650–6. https://doi.org/10.1016/j.enconman.2014.09.030.
[183] Ma J, Sun W, Ji J, Zhang Y, Zhang A, Fan W. Experimental and theoretical study of the efficiency of a dual-function solar collector. Appl Therm Eng 2011;31:1751–6. https://doi.org/10.1016/j.applthermaleng.2011.02.019.
[184] Benemann J, Chehab O, Schaar-Gabriel E. Building-integrated PV modules. Sol Energy Mater Sol Cells 2001;67:345–54. https://doi.org/10.1016/S0927-0248(00)00302-0.
[185] Zhang X, Lau S-K, Lau SSY, Zhao Y. Photovoltaic integrated shading devices (PVSDs): a review. Sol Energy 2018;170:947–68. https://doi.org/10.1016/J.SOLENER.2018.05.067.
[186] Heinstein P, Ballif C, Perret-Aebi L-E. Building integrated photovoltaics (BIPV): review, potentials, barriers and myths. Green 2013;3. https://doi.org/10.1515/green-2013-0020.
[187] Assoa YB, Mongibello L, Carr A, Kubicek B, Machado M, Merten J, et al. Thermal analysis of a BIPV system by various modelling approaches. Sol Energy 2017;155:1289–99. https://doi.org/10.1016/J.SOLENER.2017.07.066.
[188] Eder G, Peharz G, Trattnig R, Bonomo P, Saretta E, Frontini F, et al. Coloured BIPV - market. Research and Development; 2019.
[189] G.I.A. Inc., BIPV Market analysis, trends and forecasts.
[190] Yang T, Athienitis AK. A study of design options for a building integrated photovoltaic/thermal (BIPV/T) system with glazed air collector and multiple inlets. Sol Energy 2014;104:82–92. https://doi.org/10.1016/j.solener.2014.01.049.
[191] Bertram E, Glembin J, Rockendorf G. Unglazed PVT collectors as additional heat source in heat pump systems with borehole heat exchanger. Energy Proc 2012;30:414–23. https://doi.org/10.1016/j.egypro.2012.11.049.
[192] Fossa M, Ménézo C, Leonardi E. Experimental natural convection on vertical surfaces for building integrated photovoltaic (BIPV) applications. Exp Therm Fluid Sci 2008;32:980–90. https://doi.org/10.1016/j.expthermflusci.2007.11.004.
[193] Agathokleous RA, Kalogirou SA, Karellas S. Exergy analysis of a naturally ventilated Building Integrated Photovoltaic/Thermal (BIPV/T) system. Renew Energy 2018;128:541–52. https://doi.org/10.1016/j.renene.2017.06.085.
[194] Agathokleous RA, Kalogirou SA. Part II: thermal analysis of naturally ventilated BIPV system: modeling and Simulation. Sol Energy 2018;169:682–91. https://doi.org/10.1016/J.SOLENER.2018.02.057.
[195] Saadon S, Gaillard L, Giroux-Julien S, Ménézo C. Simulation study of a naturally-ventilated building integrated photovoltaic/thermal (BIPV/T) envelope. Renew Energy 2016;87:517–31. https://doi.org/10.1016/J.RENENE.2015.10.016.
[196] Agathokleous RA, Kalogirou SA. Double skin facades (DSF) and building integrated photovoltaics (BIPV): a review of configurations and heat transfer characteristics. Renew Energy 2016;89:743–56. https://doi.org/10.1016/j.renene.2015.12.043.
[197] Griffih B. A model for naturally ventilated cavities on the exteriors of opaque building thermal envelopes 1 Brent Griffith. Simbuild 2006 Conference 2006:153–9.

[198] Lau S-K, Zhao Y, Shabunko V, Chao Y, Lau SS-Y, Tablada A, et al. Optimization and evaluation of naturally ventilated BIPV façade design. Energy Proc 2018;150:87–93. https://doi.org/10.1016/J.EGYPRO.2018.09.003.
[199] Brinkworth BJ, Marshall RH, Ibarahim Z. A validated model of naturally ventilated PV cladding. Sol Energy 2000;69:67–81. https://doi.org/10.1016/S0038-092X(99)00076-6.
[200] Li Y, Zhuang Z, Tan H, Su W. Simulation study of a naturally-ventilated photovoltaic (PV) façade for high-rise buildings. Procedia Eng 2017;205:1381–8. https://doi.org/10.1016/J.PROENG.2017.10.291.
[201] Saadon S, Gaillard L, Giroux S, Ménézo C. Simulation study of a naturally ventilated building integrated photovoltaic (BIPV) envelope. Energy Proc 2015;78:2004–9. https://doi.org/10.1016/J.EGYPRO.2015.11.394.
[202] Hailu G, Athienitis AK, Yang T, Fung AS. Computational fluid dynamics (CFD) analysis of building integrated photovoltaic thermal (BIPV/T) systems. In: Web portal ASME. American Society of Mechanical Engineers); 2014. https://doi.org/10.1115/ES2014-6394.
[203] Getu A, Yang H, Athienitis T, Fung AK. Computational fluid dynamics (CFD) analysis of building integrated photovoltaic thermal. BIPV_T) Systems; 2016. p. 1–6.
[204] Ceylan I, Gurel AE. Exergetic Analysis of a new design photovoltaic and thermal (PV/T) System. Environ Prog Sustain Energy 2015;34:1249–53. https://doi.org/10.1002/ep.12108.
[205] Candanedo LM, Athienitis A, Park K-W. Convective heat transfer coefficients in a building-integrated photovoltaic/thermal system. J Sol Energy Eng 2011;133:021002. https://doi.org/10.1115/1.4003145.
[206] Friling N, Jiménez MJ, Bloem H, Madsen H. Modelling the heat dynamics of building integrated and ventilated photovoltaic modules. Energy Build 2009;41:1051–7. https://doi.org/10.1016/J.ENBUILD.2009.05.018.
[207] Kaiser AS, Zamora B, Mazón R, García JR, Vera F. Experimental study of cooling BIPV modules by forced convection in the air channel. Appl Energy 2014;135:88–97. https://doi.org/10.1016/J.APENERGY.2014.08.079.
[208] Infield D, Eicker U, Fux V, Mei L, Schumacher J. A simplified approach to thermal performance calculation for building integrated mechanically ventilated PV facades. Build Environ 2006;41:893–901. https://doi.org/10.1016/j.buildenv.2005.04.010.
[209] Sanjuan C, Sánchez MN, Enríquez R, Del Rosario Heras Celemín M. Experimental PIV techniques applied to the analysis of natural convection in open joint ventilated facades. Energy Proc 2012;30:1216–25. https://doi.org/10.1016/j.egypro.2012.11.134.
[210] Sanjuan C, Suárez MJ, González M, Pistono J, Blanco E. Energy performance of an open-joint ventilated façade compared with a conventional sealed cavity façade. Sol Energy 2011;85:1851–63. https://doi.org/10.1016/j.solener.2011.04.028.
[211] Mei L, Infield D, Eicker U, Fux V. Thermal modelling of a building with an integrated ventilated PV facade. Energy Build 2003;35:605–17. https://doi.org/10.1016/S0378-7788(02)00168-8.
[212] Brinkworth B, Cross B, Marshall R, Yang H. Thermal regulation of photovoltaic cladding. Sol Energy 1997;61:169–78. https://doi.org/10.1016/S0038-092X(97)00044-3.
[213] Gan G. Effect of air gap on the performance of building-integrated photovoltaics. Energy 2009;34:913–21. https://doi.org/10.1016/j.energy.2009.04.003.
[214] Brinkworth BJ, Sandberg M. Design procedure for cooling ducts to minimise efficiency loss due to temperature rise in PV arrays. Sol Energy 2006;80:89–103. https://doi.org/10.1016/j.solener.2005.05.020.
[215] Li S, Karava P. Evaluation of turbulence models for airflow and heat transfer prediction in BIPV/T systems optimization. Energy Proc 2012;30:1025–34. https://doi.org/10.1016/j.egypro.2012.11.115.
[216] Zogou O, Stapountzis H. Flow and heat transfer inside a PV/T collector for building application. Appl Energy 2012;91:103–15. https://doi.org/10.1016/j.apenergy.2011.09.019.
[217] Wang Z, Zhang H, Dou B, Zhang G, Wu W. Influence of inlet structure on thermal stratification in a heat storage tank with PCMs: CFD and experimental study. Appl Therm Eng 2019;162:114151. https://doi.org/10.1016/j.applthermaleng.2019.114151.
[218] Brinkworth B. Estimation of flow and heat transfer for the design of PV cooling ducts. Sol Energy 2000;69:413–20. https://doi.org/10.1016/S0038-092X(00)00082-7.
[219] Sanjuan C, Sánchez MN, Heras MDR, Blanco E. Experimental analysis of natural convection in open joint ventilated façades with 2D PIV. Build Environ 2011;46:2314–25. https://doi.org/10.1016/j.buildenv.2011.05.014.
[220] Zogou O, Stapountzis H. Experimental validation of an improved concept of building integrated photovoltaic panels. Renew Energy 2011;36:3488–98. https://doi.org/10.1016/j.renene.2011.05.034.
[221] Shukla AK, Sudhakar K, Baredar P. Recent advancement in BIPV product technologies: a review. Energy Build 2017;140:188–95. https://doi.org/10.1016/J.ENBUILD.2017.02.015.
[222] Debbarma M, Sudhakar K, Baredar P. Comparison of BIPV and BIPVT: a review. Resour Technol 2017;3:263–71. https://doi.org/10.1016/J.REFFIT.2016.11.013.
[223] Yang T, Athienitis AK. A review of research and developments of building-integrated photovoltaic/thermal (BIPV/T) systems. Renew Sustain Energy Rev 2016;66:886–912. https://doi.org/10.1016/J.RSER.2016.07.011.
[224] Osseweijer FJW, van den Hurk LBP, Teunissen EJHM, van Sark WGJHM. A comparative review of building integrated photovoltaics ecosystems in selected European countries. Renew Sustain Energy Rev 2018;90:1027–40. https://doi.org/10.1016/J.RSER.2018.03.001.
[225] Martellotta F, Cannavale A, Ayr U. Comparing energy performance of different semi-transparent, building-integrated photovoltaic cells applied to “reference” buildings. Energy Proc 2017;126:219–26. https://doi.org/10.1016/J.EGYPRO.2017.08.143.
[226] Hassanien RHE, Li M, Yin F. The integration of semi-transparent photovoltaics on greenhouse roof for energy and plant production. Renew Energy 2018;121:377–88. https://doi.org/10.1016/J.RENENE.2018.01.044.
[227] Yoon J-H, Song J, Lee S-J. Practical application of building integrated photovoltaic (BIPV) system using transparent amorphous silicon thin-film PV module. Sol Energy 2011;85:723–33. https://doi.org/10.1016/J.SOLENER.2010.12.026.
[228] Ng PK, Mithraratne N, Kua HW. Energy analysis of semi-transparent BIPV in Singapore buildings. Energy Build 2013;66:274–81. https://doi.org/10.1016/J.ENBUILD.2013.07.029.
[229] James PAB, Jentsch MF, Bahaj AS. Quantifying the added value of BiPV as a shading solution in atria. Sol Energy 2009;83:220–31. https://doi.org/10.1016/J.SOLENER.2008.07.016.
[230] Tae Y, Kim J, Park H, Shin B. Building energy performance evaluation of building integrated photovoltaic (BIPV) window with semi-transparent solar cells. Appl Energy 2014;129:217–27. https://doi.org/10.1016/j.apenergy.2014.04.106.
[231] Agathokleous RA, Kalogirou SA. Status, barriers and perspectives of building integrated photovoltaic systems. Energy 2020;191:116471. https://doi.org/10.1016/j.energy.2019.116471.
[232] Ekoe A Akata AM, Njomo D, Agrawal B. Assessment of Building Integrated Photovoltaic (BIPV) for sustainable energy performance in tropical regions of Cameroon. Renew Sustain Energy Rev 2017;80:1138–52. https://doi.org/10.1016/J.RSER.2017.05.155.
[233] Lee E, Selkowitz S, Bazjanac V, Inkarojrit V, Kohler C. High-performance commercial building façades. 2002.
[234] D’Orazio M, Di Perna C, Di Giuseppe E. Experimental operating cell temperature assessment of BIPV with different installation configurations on roofs under Mediterranean climate. Renew Energy 2014;68:378–96. https://doi.org/10.1016/J.RENENE.2014.02.009.
[235] Aelenei L, Pereira R, Ferreira A, Gonçalves H, Joyce A. Building integrated photovoltaic system with integral thermal storage: a case study. Energy Proc 2014;58:172–8. https://doi.org/10.1016/J.EGYPRO.2014.10.425.
[236] Probst MC, Roecker C. Solar energy systems in architecture. integration criteria and guidelines; 2012.
[237] Zhang R, Mirzaei PA, Carmeliet J. Prediction of the surface temperature of building-integrated photovoltaics: development of a high accuracy correlation using computational fluid dynamics. Sol Energy 2017;147:151–63. https://doi.org/10.1016/j.solener.2017.03.023.
[238] Hu Z, He W, Ji J, Hu D, Lv S, Chen H, et al. Comparative study on the annual performance of three types of building integrated photovoltaic (BIPV) Trombe wall system. Appl Energy 2017;194:81–93. https://doi.org/10.1016/J.APENERGY.2017.02.018.
[239] Hasan A, McCormack SJ, Huang MJ, Norton B. Evaluation of phase change materials for thermal regulation enhancement of building integrated photovoltaics. Sol Energy 2010;84:1601–12. https://doi.org/10.1016/j.solener.2010.06.010.
[240] Jun Huang M. The effect of using two PCMs on the thermal regulation performance of BIPV systems. Sol Energy Mater Sol Cells 2011;95:957–63. https://doi.org/10.1016/J.SOLMAT.2010.11.032.
[241] Bazilian MD, Kamalanathan H, Prasad DK. Thermographic analysis of a building integrated photovoltaic system. Renew Energy 2002;26:449–61. https://doi.org/10.1016/S0960-1481(01)00142-2.
[242] Gaillard L, Giroux-Julien S, Ménézo C, Pabiou H. Experimental evaluation of a naturally ventilated PV double-skin building envelope in real operating conditions. Sol Energy 2014;103:223–41. https://doi.org/10.1016/j.solener.2014.02.018.
[243] Chatzipanagi A, Frontini F, Virtuani A. BIPV-Temp: a demonstrative building integrated photovoltaic installation. Appl Energy 2016;173:1–12. https://doi.org/10.1016/J.APENERGY.2016.03.097.
[244] Yang T, Athienitis AK. Experimental investigation of a two-inlet air-based building integrated photovoltaic/thermal (BIPV/T) system. Appl Energy 2015;159:70–9. https://doi.org/10.1016/J.APENERGY.2015.08.048.
[245] Wang W, Liu Y, Wu X, Xu Y, Yu W, Zhao C, et al. Environmental assessments and economic performance of BAPV and BIPV systems in Shanghai. Energy Build 2016;130:98–106. https://doi.org/10.1016/J.ENBUILD.2016.07.066.
[246] Kamel RS, Fung AS. Modeling, simulation and feasibility analysis of residential BIPV/T+ASHP system in cold climate—Canada. Energy Build 2014;82:758–70. https://doi.org/10.1016/j.enbuild.2014.07.081.
[247] Crawford RH, Treloar GJ, Fuller RJ, Bazilian M. Life-cycle energy analysis of building integrated photovoltaic systems (BiPVs) with heat recovery unit. Renew Sustain Energy Rev 2006;10:559–75. https://doi.org/10.1016/J.RSER.2004.11.005.
[248] Cheng CL, Chan CY, Chen CL. Empirical approach to BIPV evaluation of solar irradiation for building applications. Renew Energy 2005;30:1055–74. https://doi.org/10.1016/J.RENENE.2004.06.006.
[249] Ordenes M, Marinoski DL, Braun P, Rüther R. The impact of building-integrated photovoltaics on the energy demand of multi-family dwellings in Brazil. Energy Build 2007;39:629–42. https://doi.org/10.1016/J.ENBUILD.2006.10.006.
[250] Lu L, Yang HX. Environmental payback time analysis of a roof-mounted building-integrated photovoltaic (BIPV) system in Hong Kong. Appl Energy 2010;87:3625–31. https://doi.org/10.1016/J.APENERGY.2010.06.011.
[251] Chen Y, Athienitis AK, Galal K. Modeling, design and thermal performance of a BIPV/T system thermally coupled with a ventilated concrete slab in a low energy

solar house: Part 1, BIPV/T system and house energy concept. Sol Energy 2010; 84:1892–907. https://doi.org/10.1016/J.SOLENER.2010.06.013.
[252] Wittkopf S, Valliappan S, Liu L, Ang KS, Cheng SCJ. Analytical performance monitoring of a 142.5 kWp grid-connected rooftop BIPV system in Singapore. Renew Energy 2012;47:9–20. https://doi.org/10.1016/J.RENENE.2012.03.034.
[253] Salem T, Kinab E. Analysis of building-integrated photovoltaic systems: a case study of commercial buildings under Mediterranean climate. Procedia Eng 2015; 118:538–45. https://doi.org/10.1016/J.PROENG.2015.08.473.
[254] Jayathissa P, Jansen M, Heeren N, Nagy Z, Schlueter A. Life cycle assessment of dynamic building integrated photovoltaics. Sol Energy Mater Sol Cells 2016;156: 75–82. https://doi.org/10.1016/J.SOLMAT.2016.04.017.
[255] Wang H, Wang A, Yang H, Huang J. Study on the thermal stress distribution of crystalline silicon solar cells in BIPV. Energy Proc 2016;88:429–35. https://doi.org/10.1016/J.EGYPRO.2016.06.019.
[256] Assoa YB, Gaillard L, Ménézo C, Negri N, Sauzedde F. Dynamic prediction of a building integrated photovoltaic system thermal behaviour. Appl Energy 2018; 214:73–82. https://doi.org/10.1016/J.APENERGY.2018.01.078.
[257] Roeleveld D, Hailu G, Fung AS, Naylor D, Yang T, Athienitis AK. Validation of computational fluid dynamics (CFD) model of a building integrated photovoltaic/thermal (BIPV/T) system. Energy Proc 2015;78:1901–6. https://doi.org/10.1016/j.egypro.2015.11.359.
[258] Agathokleous RA, Kalogirou SA. Part I: thermal analysis of naturally ventilated BIPV system: experimental investigation and convective heat transfer coefficients estimation. Sol Energy 2018;169:673–81. https://doi.org/10.1016/J.SOLENER.2018.02.048.
[259] Kim J-H, Kim J-T. A simulation study of air-type building-integrated photovoltaic-thermal system. Energy Proc 2012;30:1016–24. https://doi.org/10.1016/J.EGYPRO.2012.11.114.
[260] Bigaila E, Rounis E, Luk P, Athienitis A. A study of a BIPV/T collector prototype for building façade applications. Energy Proc 2015;78:1931–6. https://doi.org/10.1016/J.EGYPRO.2015.11.374.
[261] [. 260] Photovoltaic/Thermal system modelling under varying wind and temperature conditions. Sol Energy 2016;139:157–70. https://doi.org/10.1016/J.SOLENER.2016.09.023.
[262] Rounis ED, Bigaila E, Luk P, Athienitis A, Stathopoulos T. Multiple-inlet BIPV/T modeling: wind effects and fan induced suction. Energy Proc 2015;78:1950–5. https://doi.org/10.1016/j.egypro.2015.11.379.
[263] Norton B, Eames PC, Mallick TK, Huang MJ, McCormack SJ, Mondol JD, et al. Enhancing the performance of building integrated photovoltaics. Sol Energy 2011;85:1629–64. https://doi.org/10.1016/J.SOLENER.2009.10.004.
[264] Bellazzi A, Belussi L, Meroni I. Estimation of the performance of a BIPV façade in working conditions through real monitoring and simulation. Energy Proc 2018; 148:479–86. https://doi.org/10.1016/J.EGYPRO.2018.08.123.
[265] Tardif JM, Tamasauskas J, Delisle V, Kegel M. Performance of air based BIPV/T heat management strategies in a Canadian home. Procedia Environ Sci 2017;38: 140–7. https://doi.org/10.1016/J.PROENV.2017.03.095.
[266] Zomer CD, Costa MR, Nobre A, Rüther R. Performance compromises of building-integrated and building-applied photovoltaics (BIPV and BAPV) in Brazilian airports. Energy Build 2013;66:607–15. https://doi.org/10.1016/J.ENBUILD.2013.07.076.
[267] Karthick A, Murugavel KK, Ramanan P. Performance enhancement of a building-integrated photovoltaic module using phase change material. Energy 2018;142: 803–12. https://doi.org/10.1016/J.ENERGY.2017.10.090.
[268] Jie J, Hua Y, Wei H, Gang P, Jianping L, Bin J. Modeling of a novel Trombe wall with PV cells, Build. Environ Times 2007;42:1544–52. https://doi.org/10.1016/J.BUILDENV.2006.01.005.
[269] Rounis ED, Athienitis AK, Stathopoulos T. BIPV/T curtain wall systems: design, development and testing. J Build Eng 2021;42:103019. https://doi.org/10.1016/J.JOBE.2021.103019.
[270] Ge M, Zhao Y, Xuan Z, Zhao Y, Wang S. Experimental research on the performance of BIPV/T system with water-cooled wall. Energy Rep 2022;8: 454–9. https://doi.org/10.1016/J.EGYR.2022.05.179.
[271] Tripathy M, Yadav S, Panda SK, Sadhu PK. Performance of building integrated photovoltaic thermal systems for the panels installed at optimum tilt angle. Renew Energy 2017;113:1056–69. https://doi.org/10.1016/J.RENENE.2017.06.052.
[272] Chow TT, Chan ALS, Fong KF, Lin Z, He W, Ji J. Annual performance of building-integrated photovoltaic/water-heating system for warm climate application. Appl Energy 2009;86:689–96. https://doi.org/10.1016/j.apenergy.2008.09.014.
[273] Kim JH, Park SH, Kang JG, Kim JT. Experimental performance of heating system with building-integrated PVT (BIPVT) collector. Energy Proc 2014;48:1374–84. https://doi.org/10.1016/J.EGYPRO.2014.02.155.
[274] Yoo S-H. Simulation for an optimal application of BIPV through parameter variation. Sol Energy 2011;85:1291–301. https://doi.org/10.1016/j.solener.2011.03.004.
[275] Lee H, Lee R, Kim D, Yoon J, Kim H, Lee G. Performance evaluation of sputter-coating based color BIPV modules under the outdoor operational condition: a comparative analysis with a non-color BIPV module. Energy Rep 2022;8: 5580–90. https://doi.org/10.1016/J.EGYR.2022.04.034.
[276] Ghani F, Duke M, Carson JK. Estimation of photovoltaic conversion efficiency of a building integrated photovoltaic/thermal (BIPV/T) collector array using an artificial neural network. Sol Energy 2012;86:3378–87. https://doi.org/10.1016/J.SOLENER.2012.09.001.
[277] Kim H-R, Boafo FE, Kim J-H, Kim J-T. Investigating the effect of roof configurations on the performance of BIPV system. Energy Proc 2015;78:1974–9. https://doi.org/10.1016/J.EGYPRO.2015.11.387.
[278] Maturi L, Lollini R, Moser D, Sparber W. Experimental investigation of a low cost passive strategy to improve the performance of Building Integrated Photovoltaic systems. Sol Energy 2015;111:288–96. https://doi.org/10.1016/J.SOLENER.2014.11.001.
[279] Yang T, Athienitis AK. Performance evaluation of air-based building integrated photovolta-ic/thermal (BIPV/T) system with multiple inlets in a cold climate. Procedia Eng 2015;121:2060–7. https://doi.org/10.1016/J.PROENG.2015.09.207.
[280] Kuo H-J, Hsieh S-H, Guo R-C, Chan C-C. A verification study for energy analysis of BIPV buildings with BIM. Energy Build 2016;130:676–91. https://doi.org/10.1016/J.ENBUILD.2016.08.048.
[281] Yadav S, Panda SK, Tripathy M. Performance of building integrated photovoltaic thermal system with PV module installed at optimum tilt angle and influenced by shadow. Renew Energy 2018;127:11–23. https://doi.org/10.1016/J.RENENE.2018.04.030.
[282] Wang Y, Tian W, Ren J, Zhu L, Wang Q. Influence of a building's integrated-photovoltaics on heating and cooling loads. Appl Energy 2006;83:989–1003. https://doi.org/10.1016/J.APENERGY.2005.10.002.
[283] Aste N, Del Pero C, Leonforte F. The first Italian BIPV project: case study and long-term performance analysis. Sol Energy 2016;134:340–52. https://doi.org/10.1016/J.SOLENER.2016.05.010.
[284] Pereira R, Aelenei L. Optimization assessment of the energy performance of a BIPV/T-PCM system using Genetic Algorithms. Renew Energy 2018. https://doi.org/10.1016/J.RENENE.2018.06.118.
[285] Azadian F, Radzi MAM. A general approach toward building integrated photovoltaic systems and its implementation barriers: a review. Renew Sustain Energy Rev 2013;22:527–38. https://doi.org/10.1016/J.RSER.2013.01.056.
[286] Goh KC, Yap ABK, Goh HH, Seow TW, Toh TC. Awareness and initiatives of building integrated photovoltaic (BIPV) implementation in Malaysian housing industry. Procedia Eng 2015;118:1052–9. https://doi.org/10.1016/J.PROENG.2015.08.548.
[287] Anderson TN, Duke M, Morrison GL, Carson JK. Performance of a building integrated Photovoltaic/Thermal (BIPVT) solar collector. Sol Energy 2009;83: 445–55. https://doi.org/10.1016/j.solener.2008.08.013.
[288] Ghani F, Duke M, Carson JK. Effect of flow distribution on the photovoltaic performance of a building integrated photovoltaic/thermal (BIPV/T) collector. Sol Energy 2012;86:1518–30. https://doi.org/10.1016/J.SOLENER.2012.02.013.
[289] Chen F, Yin H. Fabrication and laboratory-based performance testing of a building-integrated photovoltaic-thermal roofing panel. Appl Energy 2016;177: 271–84. https://doi.org/10.1016/j.apenergy.2016.05.112.
[290] Gagliano A, Tina GM, Aneli S, Chemisana D. Analysis of the performances of a building-integrated PV/Thermal system. J Clean Prod 2021;320:128876. https://doi.org/10.1016/j.jclepro.2021.128876.
[291] Buonomano A, Calise F, Palombo A, Vicidomini M. BIPVT systems for residential applications: an energy and economic analysis for European climates. Appl Energy 2016;184:1411–31. https://doi.org/10.1016/j.apenergy.2016.02.145.
[292] Ji J, Luo C, Chow TT, Sun W, He W. Thermal characteristics of a building-integrated dual-function solar collector in water heating mode with natural circulation. Energy 2011;36:566–74. https://doi.org/10.1016/j.energy.2010.10.004.
[293] Hafez AZ, Yousef AM, Harag NM. Solar tracking systems: technologies and trackers drive types – a review. Renew Sustain Energy Rev 2018;91:754–82. https://doi.org/10.1016/j.rser.2018.03.094.
[294] Vossier A, Zeitouny J, Katz EA, Dollet A, Flamant G, Gordon JM. Performance bounds and perspective for hybrid solar photovoltaic/thermal electricity-generation strategies. Sustain Energy Fuels 2018;2:2060–7. https://doi.org/10.1039/C8SE00046H.
[295] Crisostomo F, Taylor RA, Surjadi D, Mojiri A, Rosengarten G, Hawkes ER. Spectral splitting strategy and optical model for the development of a concentrating hybrid PV/T collector. Appl Energy 2015;141. https://doi.org/10.1016/j.apenergy.2014.12.044.
[296] Zeitouny J, Lalau N, Gordon JM, Katz EA, Flamant G, Dollet A, et al. Assessing high-temperature photovoltaic performance for solar hybrid power plants. Sol Energy Mater Sol Cells 2018;182:61–7. https://doi.org/10.1016/j.solmat.2018.03.004.
[297] Everett V, Harvey J, Surve S, Thomsen E, Walter D, Vivar M, et al. Evaluation of electrical and thermal performance of a rooftop-friendly hybrid linear CPV-T micro-concentrator system. In: 40th ASES Natl. Sol. Conf. 2011, Sol. 2011, 1; 2011. p. 342–7. http://www.scopus.com/inward/record.url?eid=2-s2.0-84867016382&partnerID=tZOtx3y1.
[298] Vivar M, Thomsen E, Harvey J, Ratcliff T, Walter D, Everett V, et al. Reliability assessment of a linear Pv-thermal microconcentrator receiver based on the Iec 62108. ASES, Nth Carolina; 2011.
[299] Chatterjee A, Bernal E, Seshadri S, Mayer O, Greaves M. Linear Fresnel reflector based solar radiation concentrator for combined heating and power. AIP Conf Proc 2011;1407:257–61. https://doi.org/10.1063/1.3658339.
[300] Ju X, Xu C, Han X, Du X, Wei G, Yang Y. A review of the concentrated photovoltaic/thermal (CPVT) hybrid solar systems based on the spectral beam splitting technology. Appl Energy 2017;187:534–63. https://doi.org/10.1016/j.apenergy.2016.11.087.
[301] Goel N, Taylor RA, Otanicar T. A review of nanofluid-based direct absorption solar collectors: design considerations and experiments with hybrid PV/Thermal and direct steam generation collectors. Renew Energy 2020;145:903–13. https://doi.org/10.1016/j.renene.2019.06.097.

[302] Yao Y, Liu H, Wu W. Spectrum splitting using multi-layer dielectric meta-surfaces for efficient solar energy harvesting. Appl Phys A 2014;115:713–9. https://doi.org/10.1007/s00339-014-8419-y.

[303] Kandilli C. Performance analysis of a novel concentrating photovoltaic combined system. Energy Convers Manag 2013;67:186–96. https://doi.org/10.1016/j.enconman.2012.11.020.

[304] Yu ZJ, Fisher KC, Wheelwright BM, Angel RP, Holman ZC. PVMirror: a new concept for tandem solar cells and hybrid solar converters. IEEE J Photovoltaics 2015:1–9. https://doi.org/10.1109/JPHOTOV.2015.2458571.

[305] Raush J, Chambers T. Initial field testing of concentrating solar photovoltaic (CSPV) thermal hybrid solar energy generator utilizing large aperture parabolic trough and spectrum selective mirrors. Int J Sustain Green Energy 2014;3:123–31. https://doi.org/10.11648/j.ijrse.20140306.12.

[306] Widyolar B, Jiang L, Winston R. Spectral beam splitting in hybrid PV/T parabolic trough systems for power generation. Appl Energy 2018;209:236–50. https://doi.org/10.1016/j.apenergy.2017.10.078.

[307] Wingert R, O'Hern H, Orosz M, Harikumar P, Roberts K, Otanicar T. Spectral beam splitting retrofit for hybrid PV/T using existing parabolic trough power plants for enhanced power output. Sol Energy 2020;202:1–9. https://doi.org/10.1016/j.solener.2020.03.066.

[308] Stanley C, Mojiri A, Rahat M, Blakers A, Rosengarten G. Performance testing of a spectral beam splitting hybrid PVT solar receiver for linear concentrators. Appl Energy 2016;168:303–13. https://doi.org/10.1016/j.apenergy.2016.01.112.

[309] Crisostomo F, Hjerrild N, Mesgari S, Li Q, Taylor RA. A hybrid PV/T collector using spectrally selective absorbing nanofluids. Appl Energy 2017;193:1–14. https://doi.org/10.1016/j.apenergy.2017.02.028.

[310] An W, Wu J, Zhu T, Zhu Q. Experimental investigation of a concentrating PV/T collector with Cu9S5nanofluid spectral splitting filter. Appl Energy 2016;184:197–206. https://doi.org/10.1016/j.apenergy.2016.10.004.

[311] An W, Li J, Ni J, Taylor RA, Zhu T. Analysis of a temperature dependent optical window for nanofluid-based spectral splitting in PV/T power generation applications. Energy Convers Manag 2017;151:23–31. https://doi.org/10.1016/j.enconman.2017.08.080.

[312] Otanicar T, Dale J, Orosz M, Brekke N, DeJarnette D, Tunkara E, et al. Experimental evaluation of a prototype hybrid CPV/T system utilizing a nanoparticle fluid absorber at elevated temperatures. Appl Energy 2018;228:1531–9. https://doi.org/10.1016/j.apenergy.2018.07.055.

[313] Huang BJ, Lin TH, Hung WC, Sun FS. Performance evaluation of solar photovoltaic/thermal systems. Sol Energy 2001;70:443–8.

[314] Suman S, Khan MK, Pathak M. Performance enhancement of solar collectors - a review. Renew Sustain Energy Rev 2015;49:192–210. https://doi.org/10.1016/j.rser.2015.04.087.

[315] Giovannetti F, Föste S, Ehrmann N, Rockendorf G. High transmittance, low emissivity glass covers for flat plate collectors: applications and performance. Sol Energy 2014;104:52–9. https://doi.org/10.1016/j.solener.2013.10.006.

[316] Antonanzas J, del Amo A, Martinez-Gracia A, Bayod-Rujula AA, Antonanzas-Torres F. Towards the optimization of convective losses in photovoltaic–thermal panels. Sol Energy 2015;116:323–36. https://doi.org/10.1016/j.solener.2015.04.013.

[317] Hadorn J, Lämmle M, Kramer K, Munz G, Ryan G, Herrando M, et al. Design guidelines for PVT collectors. In: International energy agency (IEA). Task 60 appl. PVT collect. New solut. HVAC syst.. SHC programme; 2020. https://doi.org/10.18777/ieashc-task60-2020-0003.

[318] Dupeyrat P, Ménézo C, Fortuin S. Study of the thermal and electrical performances of PVT solar hot water system. Energy Build 2014;68:751–5. https://doi.org/10.1016/j.enbuild.2012.09.032.

[319] Fujisawa T, Tani T. Annual exergy evaluation on photovoltaic-thermal hybrid collector. Sol Energy Mater Sol Cells 1997;47:135–48.

[320] Vokas G, Christandonis N, Skittides F. Hybrid photovoltaic – thermal systems for domestic heating and cooling — a theoretical approach. Sol Energy 2006;80:607–15. https://doi.org/10.1016/j.solener.2005.03.011.

[321] EndeF engineering, technical datasheet ECOMESH panel. 2017. www.endef.com. [Accessed 23 August 2016].

[322] Axaopoulos PJ, Fylladitakis ED. Performance and economic evaluation of a hybrid photovoltaic/thermal solar system for residential applications. Energy Build 2013;65:488–96. https://doi.org/10.1016/j.enbuild.2013.06.027.

[323] Dubey S, Tiwari GN. Thermal modeling of a combined system of photovoltaic thermal (PV/T) solar water heater. Sol Energy 2008;82:602–12. https://doi.org/10.1016/j.solener.2008.02.005.

[324] Aste N, Del Pero C, Adhikari RS, Marenzi G. Effectiveness and weaknesses of supporting policies for solar thermal systems—a case-study. Sustain Cities Soc 2015;14:146–53. https://doi.org/10.1016/j.scs.2014.09.003.

[325] Ji J, Lu JP, Chow TT, He W, Pei G. A sensitivity study of a hybrid photovoltaic/thermal water-heating system with natural circulation. Appl Energy 2007;84:222–37. https://doi.org/10.1016/j.apenergy.2006.04.009.

[326] Mittag M. Reliability of TPedge PV modules successfully tested. Freiburg; 2017. https://www.ise.fraunhofer.de/en/press-media/press-releases/2017/reliability-of-tpedge-pv-modules-successfully-tested.html.

[327] Lämmle M, Hermann M, Kramer K, Panzer C, Piekarczyk A, Thoma C, et al. Development of highly efficient, glazed PVT collectors with overheating protection to increase reliability and enhance energy yields. Sol Energy 2018;176:87–97. https://doi.org/10.1016/j.solener.2018.09.082.

[328] Zakharchenko R, Licea-Jimeenez L, Pérez-García SA, Vorobiev P, Dehesa-Carrasco U, Pérez-Robles JF, et al. Photovoltaic solar panel for a hybrid PV/thermal system. Sol Energy Mater Sol Cells 2004;82:253–61. https://doi.org/10.1016/j.solmat.2004.01.022.

[329] Liang R, Zhang J, Ma L, Li Y. Performance evaluation of new type hybrid photovoltaic/thermal solar collector by experimental study. Appl Therm Eng 2015;75:487–92. https://doi.org/10.1016/j.applthermaleng.2014.09.075.

[330] Wang G, Zhao Y, Quan Z, Tong J. Application of a multi-function solar-heat pump system in residential buildings. Appl Therm Eng 2018;130:922–37. https://doi.org/10.1016/j.applthermaleng.2017.10.046.

[331] Ji J, Han J, Chow TT, Yi H, Lu J, He W, et al. Effect of fluid flow and packing factor on energy performance of a wall-mounted hybrid photovoltaic/water-heating collector system. Energy Build 2006;38:1380–7. https://doi.org/10.1016/j.enbuild.2006.02.010.

[332] Bergene T, Lovvik OM. Model calculations on a flat-plate solar heat collector with integrated solar cells. Sol Energy 1995;55:453–62. https://doi.org/10.1016/0140-6701(96)88784-4.

[333] Aste N, Leonforte F, Del Pero C. Design, modeling and performance monitoring of a photovoltaic-thermal (PVT) water collector. Sol Energy 2015;112:85–99. https://doi.org/10.1016/j.solener.2014.11.025.

[334] Pierrick H, Christophe M, Leon G, Patrick D. Dynamic numerical model of a high efficiency PV-T collector integrated into a domestic hot water system. Sol Energy 2015;111:68–81. https://doi.org/10.1016/j.solener.2014.10.031.

[335] Bai Y, Chow TT, Ménézo C, Dupeyrat P. Analysis of a hybrid PV/thermal solar-assisted heat pump system for sports center water heating application. Int J Photoenergy 2012;2012. https://doi.org/10.1155/2012/265838.

[336] Dupeyrat P, Ménézo C, Wirth H, Rommel M. Improvement of PV module optical properties for PV-thermal hybrid collector application. Sol Energy Mater Sol Cells 2011;95:2028–36. https://doi.org/10.1016/j.solmat.2011.04.036.

[337] Chow TT, He W, Ji J. Hybrid photovoltaic-thermosyphon water heating system for residential application. Sol Energy 2006;80:298–306. https://doi.org/10.1016/j.solener.2005.02.003.

[338] Cristofari C, Canaletti J, Notton G, Darras C. Innovative patented PV/TH Solar Collector: optimization and performance evaluation. Energy Proc 2012;14:235–40.

[339] Cristofari C, Notton G, Poggi P, Louche A. Modelling and performance of a copolymer solar water heating collector. Sol Energy 2002;72:99–112. https://doi.org/10.1016/S0038-092X(01)00092-5.

[340] Shan F, Cao L, Fang G. Dynamic performances modeling of a photovoltaic-thermal collector with water heating in buildings. Energy Build 2013;66:485–94. https://doi.org/10.1016/j.enbuild.2013.07.067.

[341] Sandnes B, Rekstad J. A photovoltaic/thermal (PV/T) collector with a polymer absorber plate. Experimental study and analytical model. Sol Energy 2002;72:63–73. https://doi.org/10.1016/S0038-092X(01)00091-3.

[342] Zhou J, Zhao X, Ma X, Du Z, Fan Y, Cheng Y, et al. Clear-days operational performance of a hybrid experimental space heating system employing the novel mini-channel solar thermal & PV/T panels and a heat pump. Sol Energy 2017;155:464–77. https://doi.org/10.1016/j.solener.2017.06.056.

[343] Chow TT, He W, Ji J. Hybrid photovoltaic-thermosyphon water heating system for residential application. Sol Energy 2006;80:298–306. https://doi.org/10.1016/j.solener.2005.02.003.

[344] Cristofari C, Notton G, Canaletti JL. Thermal behavior of a copolymer PV/Th solar system in low flow rate conditions. Sol Energy 2009;83:1123–38. https://doi.org/10.1016/j.solener.2009.01.008.

[345] Ji J, Han J, Chow TT, Han C, Lu J, Wei H. Effect of flow channel dimensions on the performance of a box-frame photovoltaic/thermal collector. Proc Inst Mech Eng Part A-Journal Power Energy 2006;220:681–8. https://doi.org/10.1234/09576509jpe316.

[346] Kroiß A, Pröbst A, Hamberger S, Spinnler M, Tripanagnostopoulos Y, Sattelmayer T. Development of a seawater-proof hybrid photovoltaic/thermal (PV/T) solar collector. Energy Proc 2014;52:93–103. https://doi.org/10.1016/j.egypro.2014.07.058.

[347] Chow TT, Tiwari GN, Menezo C. Hybrid solar: a review on photovoltaic and thermal power integration. Int J Photoenergy 2012;2012. https://doi.org/10.1155/2012/307287.

[348] Digital engineering, new solar collector materials modeled with COMSOL multiphysics - digital engineering. 2017. http://www.digitaleng.news/de/new-solar-collector-materials-modeled-with-comsol-multiphysics/. [Accessed 20 December 2016].

[349] Carlsson B, Persson H, Meir M, Rekstad J. A total cost perspective on use of polymeric materials in solar collectors - importance of environmental performance on suitability. Appl Energy 2014;125:10–20. https://doi.org/10.1016/j.apenergy.2014.03.027.

[350] Ghaffari Mosanenzadeh S, Liu MW, Osia A, Naguib HE. Thermal composites of biobased polyamide with boron nitride micro networks. J Polym Environ 2015;23:566–79. https://doi.org/10.1007/s10924-015-0733-8.

[351] Yoon Y, Oh M, Kim A, Kim N. The Development of Thermal Conductive Polymer Composites for Heat Sink. 6. 2012. p. 515–9.

[352] Xu P, Zhang X, Shen J, Zhao X, He W, Li D. Parallel experimental study of a novel super-thin thermal absorber based photovoltaic/thermal (PV/T) system against conventional photovoltaic (PV) system. Energy Rep 2015;1:30–5. https://doi.org/10.1016/j.egyr.2014.11.002.

[353] Said Z, Arora S, Bellos E. A review on performance and environmental effects of conventional and nanofluid-based thermal photovoltaics. Renew Sustain Energy Rev 2018;94:302–16. https://doi.org/10.1016/j.rser.2018.06.010.

[354] Michael JJ, Selvarasan I. Experimental investigation of a copper sheet-laminated solar photovoltaic thermal water collector. Energy Effic 2017;10:117–28. https://doi.org/10.1007/s12053-016-9443-x.

[355] Dubey S, Tiwari GN. Analysis of PV/T flat plate water collectors connected in series. Sol Energy 2009;83:1485–98. https://doi.org/10.1016/j.solener.2009.04.002.
[356] Huang MJ, Eames PC, Norton B. Phase change materials for limiting temperature rise in building integrated photovoltaics. Sol Energy 2006;80:1121–30. https://doi.org/10.1016/j.solener.2005.10.006.
[357] Wang K, Qin Z, Tong W, Ji C. Thermal energy storage for solar energy utilization: fundamentals and applications. In: Renew. Energy - Resour. Challenges Appl. IntechOpen; 2020. https://doi.org/10.5772/intechopen.91804.
[358] Islam MM, Pandey AK, Hasanuzzaman M, Rahim NA. Recent progresses and achievements in photovoltaic-phase change material technology: a review with special treatment on photovoltaic thermal-phase change material systems. Energy Convers Manag 2016;126:177–204. https://doi.org/10.1016/j.enconman.2016.07.075.
[359] Huang MJ, Eames PC, Norton B. Comparison of predictions made using a new 3D phase change material thermal control model with experimental measurements and predictions made using a validated 2D model. Heat Tran Eng 2007;28:31–7. https://doi.org/10.1080/01457630600985634.
[360] Huang MJ, Eames PC, Norton B. Thermal regulation of building-integrated photovoltaics using phase change materials. Int J Heat Mass Tran 2004;47:2715–33. https://doi.org/10.1016/j.ijheatmasstransfer.2003.11.015.
[361] Biwole PH, Eclache P, Kuznik F. Phase-change materials to improve solar panel's performance. Energy Build 2013;62:59–67. https://doi.org/10.1016/j.enbuild.2013.02.059.
[362] Ho CJ, Chou WL, Lai CM. Thermal and electrical performance of a water-surface floating PV integrated with a water-saturated MEPCM layer. Energy Convers Manag 2015;89:862–72. https://doi.org/10.1016/j.enconman.2014.10.039.
[363] Hasan A, McCormack SJ, Huang MJ, Norton B. Energy and cost saving of a photovoltaic-phase change materials (PV-PCM) System through temperature regulation and performance enhancement of photovoltaics. Energies 2014;7:1318–31. https://doi.org/10.3390/en7031318.
[364] Hendricks JH, van Sark WGJHM. Annual performance enhancement of building integrated photovoltaic modules by applying phase change materials. Prog Photovoltaics Res Appl 2013;21:620–30. https://doi.org/10.1002/pip.1240.
[365] Park J, Kim T, Leigh SB. Application of a phase-change material to improve the electrical performance of vertical-building-added photovoltaics considering the annual weather conditions. Sol Energy 2014;105:561–74. https://doi.org/10.1016/j.solener.2014.04.020.
[366] Chandel SS, Agarwal T. Review of cooling techniques using phase change materials for enhancing efficiency of photovoltaic power systems. Renew Sustain Energy Rev 2017;73:1342–51. https://doi.org/10.1016/j.rser.2017.02.001.
[367] Ho CJ, Jou BT, Lai CM, Huang CY. Performance assessment of a BIPV integrated with a layer of water-saturated MEPCM. Energy Build 2013;67:322–33. https://doi.org/10.1016/j.enbuild.2013.08.035.
[368] Malvi CS, Dixon-Hardy DW, Crook R. Energy balance model of combined photovoltaic solar-thermal system incorporating phase change material. Sol Energy 2011;85:1440–6. https://doi.org/10.1016/j.solener.2011.03.027.
[369] Kazemian A, Taheri A, Sardarabadi A, Ma T, Passandideh-Fard M, Peng J. Energy, exergy and environmental analysis of glazed and unglazed PVT system integrated with phase change material: an experimental approach. Sol Energy 2020;201:178–89. https://doi.org/10.1016/j.solener.2020.02.096.
[370] Fayaz H, Rahim NA, Hasanuzzaman M, Rivai A, Nasrin R. Numerical and outdoor real time experimental investigation of performance of PCM based PVT system. Sol Energy 2019;179:135–50. https://doi.org/10.1016/j.solener.2018.12.057.
[371] Browne MC, Lawlor K, Kelly A, Norton B, Cormack SJM. Indoor characterisation of a photovoltaic/thermal phase change material system. Energy Proc 2015;70:163–71. https://doi.org/10.1016/j.egypro.2015.02.112.
[372] Lin W, Ma Z, Sohel MI, Cooper P. Development and evaluation of a ceiling ventilation system enhanced by solar photovoltaic thermal collectors and phase change materials. Energy Convers Manag 2014;88:218–30. https://doi.org/10.1016/j.enconman.2014.08.019.
[373] Al-Waeli AHA, Sopian K, Chaichan MT, Kazem HA, Ibrahim A, Mat S, et al. Evaluation of the nanofluid and nano-PCM based photovoltaic thermal (PVT) system: an experimental study. Energy Convers Manag 2017;151:693–708. https://doi.org/10.1016/j.enconman.2017.09.032.
[374] Al-waeli AHA, Sopian K, Kazem HA, Yousif JH, Chaichan MT, Ibrahim A, et al. Comparison of prediction methods of PV/T nano fl uid and nano-PCM system using a measured dataset and artificial neural network. Sol Energy 2018;162:378–96. https://doi.org/10.1016/j.solener.2018.01.026.
[375] Abdelrazik AS, Al-sulaiman FA, Saidur R. Numerical investigation of the effects of the nano-enhanced phase change materials on the thermal and electrical performance of hybrid PV/thermal systems. Energy Convers Manag 2020;205:112449. https://doi.org/10.1016/j.enconman.2019.112449.
[376] Khodadadi M, Ali S, Ebrahimpour Z, Sheikholeslami M. Thermal performance of nanofluid with employing of NEPCM in a PVT-LFR system. Sustain Energy Technol Assessments 2021;47:101340. https://doi.org/10.1016/j.seta.2021.101340.
[377] Khodadadi M, Sheikholeslami M. Numerical simulation on the efficiency of PVT system integrated with PCM under the influence of using fins. Sol Energy Mater Sol Cells 2021;233:111402. https://doi.org/10.1016/j.solmat.2021.111402.
[378] Islam MM, Hasanuzzaman M, Rahim NA, Pandey AK, Rawa M, Kumar L. Real time experimental performance investigation of a NePCM based photovoltaic thermal system : an energetic and exergetic approach. Renew Energy 2021;172:71–87. https://doi.org/10.1016/j.renene.2021.02.169.
[379] Selimefendigil F, Ceylin S. Energy and exergy analysis of a hybrid photovoltaic/thermal-air collector modified with nano-enhanced latent heat thermal energy storage unit. 2022. p. 45. https://doi.org/10.1016/j.est.2021.103467.
[380] Jensen KI, Schultz JM, Kristiansen FH. Development of windows based on highly insulating aerogel glazings. J Non-Cryst Solids 2004;350:351–7. https://doi.org/10.1016/j.jnoncrysol.2004.06.047.
[381] Mcenaney K, Weinstein L, Kraemer D, Ghasemi H, Chen G. Nano Energy Aerogel-based solar thermal receivers. Nano Energy 2017;40:180–6. https://doi.org/10.1016/j.nanoen.2017.08.006.
[382] Fesmire JE. Aerogel insulation systems for space launch applications. Cryogenics (Guildf) 2006;46:111–7. https://doi.org/10.1016/j.cryogenics.2005.11.007.
[383] Weinstein LA, Strobach E, Ren Z, Wang EN, Weinstein LA, Mcenaney K, et al. A hybrid electric and thermal solar receiver A hybrid electric and thermal solar receiver. Joule 2018;2:962–75. https://doi.org/10.1016/j.joule.2018.02.009.
[384] Reim M, Beck A, Korner W, Petricevic R, Glora M, Weth M, et al. Highly insulating aerogel glazing for solar energy usage. Sol Energy 2002;72:21–9.
[385] Wu L, Zhao B, Ao X, Yang H, Ren X, Yu Q, et al. Performance analysis of the aerogel-based PV/T collector: a numerical study. Sol Energy 2021;228:339–48. https://doi.org/10.1016/j.solener.2021.09.077.
[386] Du M, Tang GH, Wang TM. Exergy analysis of a hybrid PV/T system based on plasmonic nano fluids and silica aerogel glazing. Sol Energy 2019;183:501–11. https://doi.org/10.1016/j.solener.2019.03.057.
[387] Wen X, Ji J, Song Z. Performance comparison of two micro-channel heat pipe LFPV/T systems plus thermoelectric generators with and without aerogel glazing. Energy 2021;229:120704. https://doi.org/10.1016/j.energy.2021.120704.
[388] Fraunhofer Institute for solar energy systems. Photovoltaics Report; 2012.
[389] Siefer G, Abbott P, Baur C, Schegl T, Bett AW. Determination of the temperature coefficients of various III-V solar cells. In: Proc. From 20th Eur. Photovolt. Sol. Energy conf.; 2005.
[390] Friesen G, Pavanello D, Virtuani A. Overview of temperature coefficients of different thin film photovoltaic technologies. In: 25th Eur. Photovolt. Sol. Energy conf. Exhib./5th world conf. Photovolt. Energy conversion, 6-10 Sept. 2010, val. Spain; 2010. p. 4248–52. https://doi.org/10.4229/25thEUPVSEC2010-4AV.3.83.
[391] Bätzner DL, Andrault Y, Andreetta L, Büchel A, Frammelsberger W, Guerin C, et al. Properties of high efficiency silicon heterojunction cells. Energy Proc 2011;8:153–9. https://doi.org/10.1016/j.egypro.2011.06.117.
[392] Green MA, Emery K, Blakers A. Silicon solar cells with reduced temperature sensitivity, 18; 1982. p. 97–8.
[393] Tiwari GN, Mishra RK, Solanki SC. Photovoltaic modules and their applications: a review on thermal modelling. Appl Energy 2011;88:2287–304. https://doi.org/10.1016/j.apenergy.2011.01.005.
[394] Parida B, Iniyan S, Goic R. A review of solar photovoltaic technologies. Renew Sustain Energy Rev 2011;15:1625–36. https://doi.org/10.1016/j.rser.2010.11.032.
[395] Makrides G, Zinsser B, Norton M, Georghiou GE, Schubert M, Werner JH. Potential of photovoltaic systems in countries with high solar irradiation. Renew Sustain Energy Rev 2010;14:754–62. https://doi.org/10.1016/j.rser.2009.07.021.
[396] Pusch A, Pearce P, Ekins-Daukes NJ. Analytical expressions for the efficiency limits of radiatively coupled tandem solar cells. IEEE J Photovoltaics 2019;9:679–87. https://doi.org/10.1109/JPHOTOV.2019.2903180.
[397] Granqvist CG. Spectrally selective surfaces for heating and cooling applications. SPIE Press; 1989. https://doi.org/10.1117/3.2512522.
[398] Jelle BP, Kalnæs SE, Gao T. Low-emissivity materials for building applications: a state-of-the-art review and future research perspectives. Energy Build 2015;96:329–56. https://doi.org/10.1016/j.enbuild.2015.03.024.
[399] Alonso-Álvarez D, Ferre Llin L, Ekins-Daukes NJ, Paul DJ. ITO and AZO films for low emissivity coatings in hybrid photovoltaic-thermal applications. Sol Energy 2017;155:82–92. https://doi.org/10.1016/j.solener.2017.06.033.
[400] Alonso-Álvarez D, Ferre Llin L, Mellor A, Paul DJ, Ekins-Daukes NJ. Comparative study of annealed and high temperature grown ITO and AZO films for solar energy applications. MRS Adv 2017;2:3117–22. https://doi.org/10.1557/adv.2017.448.
[401] Ehrmann N, Reineke-Koch R, Föste S, Giovannetti F. The influence of process parameters and coating properties of double glazing coated with transparent conducting oxides on the efficiency of solar-thermal flat-plate collectors. Thin Solid Films 2013;532:132–40. https://doi.org/10.1016/j.tsf.2012.11.145.
[402] Lämmle M, Kroyer T, Fortuin S, Wiese M, Hermann M. Development and modelling of highly-efficient PVT collectors with low-emissivity coatings. Sol Energy 2016;130:161–73. https://doi.org/10.1016/j.solener.2016.02.007.
[403] Mellor A, Guarracino I, Llin LF, Alonso-Alvarez D, Riverola A, Thoms S, et al. Specially designed solar cells for hybrid photovoltaic-thermal generators. In: Conf. Rec. IEEE photovolt. Spec. Conf. 2016-Novem; 2016. p. 2960–3. https://doi.org/10.1109/PVSC.2016.7750203.
[404] Halme J, Mäkinen P. Theoretical efficiency limits of ideal coloured opaque photovoltaics. Energy Environ Sci 2019;12:1274–85. https://doi.org/10.1039/c8ee03161d.
[405] Maghrabie HM, Elsaid K, Sayed ET, Abdelkareem MA, Wilberforce T, Olabi AG. Building-integrated photovoltaic/thermal (BIPVT) systems: applications and challenges. Sustain Energy Technol Assessments 2021;45:101151. https://doi.org/10.1016/j.seta.2021.101151.
[406] Stanley C, Mojiri A, Rosengarten G. Spectral light management for solar energy conversion systems. Nanophotonics 2016;5:161–79. https://doi.org/10.1515/nanoph-2016-0035.

[407] Liang H, Wang F, Yang L, Cheng Z, Shuai Y, Tan H. Progress in full spectrum solar energy utilization by spectral beam splitting hybrid PV/T system. Renew Sustain Energy Rev 2021;141:110785. https://doi.org/10.1016/j.rser.2021.110785.
[408] Korun M, Navruz TS. Comparison of Ge, InGaAs p-n junction solar cell. J Phys Conf Ser 2016;707. https://doi.org/10.1088/1742-6596/707/1/012035. 0–6.
[409] An W, Zhang J, Zhu T, Gao N. Investigation on a spectral splitting photovoltaic/thermal hybrid system based on polypyrrole nanofluid: preliminary test. Renew Energy 2016;86:633–42. https://doi.org/10.1016/j.renene.2015.08.080.
[410] Ni J, Li J, An W, Zhu T. Performance analysis of nanofluid-based spectral splitting PV/T system in combined heating and power application. Appl Therm Eng 2018;129:1160–70. https://doi.org/10.1016/j.applthermaleng.2017.10.119.
[411] Dettling JR. High Efficiency Converter of Solar Energy to Electricity. 4. 1975. p. 267. 021.
[412] Spring KH. Direct generation of electricity. New York, United States: Academic Press; 1965.
[413] Kaplan Converse A. Refractive spectrum splitting optics for use with photovoltaic cells. Conf Rec IEEE Photovolt Spec Conf 1996;373:1299–302. https://doi.org/10.1109/pvsc.1996.564371.
[414] Penn JP. High concentration spectrum splitting solar collector, 6; 2002. p. 241. 469.
[415] Stefancich M, Zayan A, Chiesa M, Rampino S, Kimerling L, Michel J. Single element spectral splitting solar concentrator for multiple cells CPV system. Opt Express 2012;20:9004–18.
[416] Mojiri A, Taylor R, Thomsen E, Rosengarten G. Spectral beam splitting for efficient conversion of solar energy - a review. Renew Sustain Energy Rev 2013;28. https://doi.org/10.1016/j.rser.2013.08.026.
[417] Atkins P, DePaula J, Keeler. Atkins' physical chemistry. 11th ed. Oxford University Press UK; 2018.
[418] Taylor RA, Phelan PE, Otanicar TP, Adrian R, Prasher R. Nanofluid optical property characterization: towards efficient direct absorption solar collectors. Nanoscale Res Lett 2011;6:225. https://doi.org/10.1186/1556-276X-6-225.
[419] Crisostomo F, Taylor RA, Zhang T, Perez-Wurfl I, Rosengarten G, Everett V, et al. Experimental testing of SiNx/SiO2 thin film filters for a concentrating solar hybrid PV/T collector. Renew Energy 2014;72:79–87. https://doi.org/10.1016/j.renene.2014.06.033.
[420] Fabry C, Perot A. On a new form of interferometer. Astrophys J 1901;13:265. https://doi.org/10.1086/140817.
[421] Green MA, Keevers MJ, Thomas I, Lasich JB, Emery K, King RR. 40% efficient sunlight to electricity conversion. Prog Photovoltaics Res Appl 2015;23:685–91. https://doi.org/10.1002/pip.
[422] Semrock. BrightLine short-pass filter. 2016.
[423] Edmund Optics, High performance hot mirrors.
[424] Thorlabs. Hot and cold mirrors. 2016.
[425] Taylor RA, Hewakuruppu Y, Dejarnette D, Otanicar TP. Comparison of selective transmitters for solar thermal applications. Appl Opt 2016;55. https://doi.org/10.1364/AO.55.003829.
[426] FCSEL. Open filters. 2016.
[427] Motamedi M, Crisostomo F, Yao Y, Mofarah SS, Chen WF, Koshy P, et al. Single-layer, anti-reflective thin films of porous MgF2 for solar thermal applications. J Phys D Appl Phys 2019;52. https://doi.org/10.1088/1361-6463/ab1f5e.
[428] BusinessWire. Global low-E glass market report (2019 to 2024). 2020.
[429] Aswathy G, Rajesh CS, Sreejith MS, Vijayakumar KP, Sudha Kartha C. Designing photovoltaic concentrators using holographic lens recorded in nickel ion doped photopolymer material. Sol Energy 2018;163:70–7. https://doi.org/10.1016/j.solener.2018.01.017.
[430] Bloss WH, Griesinger M, Reinhardt ER. Dispersive concentrating systems based on transmission phase holograms for solar applications. Appl Opics 1982;21:3739–42.
[431] Jannson T, Jannson J. Bragg holograms and concentrator optics. Appl Hologr 1985:219. https://doi.org/10.1117/12.946286. 0523.
[432] Stojanoff CG, Kubitzek R, Tropartz S. Optimization procedure for A holographic lens solar concentrator. Opt Mater Technol Energy Effic Sol Energy Convers VII. 1989;1016:226. https://doi.org/10.1117/12.949935.
[433] Bainier C, Hernandez C, Courjon D. Solar concentrating systems using holographic lenses. Sol Wind Technol 1988;5:395–404. https://doi.org/10.1016/0741-983X(88)90006-9.
[434] Ludman JE, Riccobono J, Semenova IV, Reinhand NO, Tai W, Li X, et al. The optimization of a holographic system for solar power generation. Sol Energy 1997;60:1–9. https://doi.org/10.1016/S0038-092X(96)00148-X.
[435] Stojanoff CG, Schulat J, Eich M. Bandwidth- and angle-selective holographic films for solar energy applications. In: Proc. SPIE 3789. Sol. Opt. Mater. XVI; 1999. p. 38–49. https://doi.org/10.1117/12.367569.
[436] Zheng C, Li Q, Rosengarten G, Hawkes E, Taylor RA. Compact, semi-passive beam steering prism array for solar concentrators. Appl Opt 2017;56. https://doi.org/10.1364/AO.56.004158.
[437] Li Q, Zheng C, Shirazi A, Bany Mousa O, Moscia F, Scott JA, et al. Design and analysis of a medium-temperature, concentrated solar thermal collector for air-conditioning applications. Appl Energy 2017;190. https://doi.org/10.1016/j.apenergy.2017.01.040.
[438] Vorndran S, Russo JM, Wu Y, Gordon M, Kostuk R. Holographic diffraction-through-aperture spectrum splitting for increased hybrid solar energy conversion efficienc. Int J Energy Res 2015;39:326–35. https://doi.org/10.1002/er.3245.
[439] Müller HFO. Application of holographic optical elements in buildings for various purposes like daylighting, solar shading and photovoltaic power generation. Renew Energy 1994;5:935–41. https://doi.org/10.1016/0960-1481(94)90114-7.
[440] Hui SCM, Müller HFO. Holography: art and science of light in architecture. Architect Sci Rev 2001;44:221–6. https://doi.org/10.1080/00038628.2001.9697476.
[441] Bradbury R, Ludman JE, White JW. Holographic lighting for energy efficient greenhouses. Pract Hologr 1986:104. https://doi.org/10.1117/12.961028. 0615.
[442] Rosenberg GA. Device for concentrating optical radia 1997;5(877):874.
[443] van Sark WGJHM, Barnham KWJ, Slooff LH, Chatten AJ, Büchtemann A, Meyer A, et al. Luminescent Solar Concentrators - a review of recent results. Opt Express 2008;16:21773. https://doi.org/10.1364/oe.16.021773.
[444] Trupke T, Green Ma, Würfel P. Improving solar cell efficiencies by down-conversion of high-energy photons. J Appl Phys 2002;92:4117. https://doi.org/10.1063/1.1505677.
[445] Trupke T, Green Ma, Würfel P. Improving solar cell efficiencies by up-conversion of sub-band-gap light. J Appl Phys 2002;92:4117. https://doi.org/10.1063/1.1505677.
[446] Cardoso MA, Correia SFH, Frias AR, Gonçalves HMR, Pereira RFP, Nunes SC, et al. Solar spectral conversion based on plastic films of lanthanide-doped ionosilicas for photovoltaics: down-shifting layers and luminescent solar concentrators. J Rare Earths 2020;38:531–8. https://doi.org/10.1016/j.jre.2020.01.007.
[447] Meinardi F, Bruni F, Brovelli S. Luminescent solar concentrators for building-integrated photovoltaics. Nat Rev Mater 2017;2:1–9. https://doi.org/10.1038/natrevmats.2017.72.
[448] Zastrow A. Physics and applications of fluorescent concentrators: a review, Proc. SPIE 2255. Opt Mater Technol Energy Effic Sol Energy Convers XIII. 1994;2255:534–47. https://doi.org/10.1117/12.185397.
[449] Goetzberger A, Greube W. Solar energy conversion with fluorescent collectors. Appl Phys 1977;14:123–39. https://doi.org/10.1007/BF00883080.
[450] Slooff LH, Bende EE, Burgers AR, Budel T, Pravettoni M, Kenny RP, et al. A Luminescent Solar Concentrator with 7.1% power conversion efficiency. Phys Status Solidi Rapid Res Lett 2008;2:257–9. https://doi.org/10.1002/pssr.200802186.
[451] Ji Y, Xu Q, Riggs B, Islam K, Ollanik A, Ermer JH, et al. Optical design and validation of an infrared transmissive spectrum splitting concentrator photovoltaic module. IEEE J Photovoltaics 2017;7:1469–78.
[452] Sun Y, Shanks K, Baig H, Zhang W, Hao X, Li Y, et al. Integrated semi-transparent cadmium telluride photovoltaic glazing into windows : energy and daylight performance for different architecture designs. Appl Energy 2018;231:972–84. https://doi.org/10.1016/j.apenergy.2018.09.133.
[453] Xu Q, Ji Y, Krut DD, Ermer JH, Escarra MD. Transmissive concentrator multijunction solar cells with over 47 % in-band power conversion efficiency. Appl Phys Lett 2016;109:1–5. https://doi.org/10.1063/1.4967376.
[454] Xu Q, Ji Y, Riggs B, Ollanik A, Farrar-foley N, Ermer JH, et al. A transmissive , spectrum-splitting concentrating photovoltaic module for hybrid photovoltaic-solar thermal energy conversion. Sol Energy 2016;137:585–93. https://doi.org/10.1016/j.solener.2016.08.057.
[455] Robertson J, Riggs B, Islam K, Vera Y, Spitler CM, Gupta N, et al. Field testing of a spectrum-splitting transmissive concentrator photovoltaic module. Renew Energy 2019;139:806–14. https://doi.org/10.1016/j.renene.2019.02.117.
[456] Abdelhamid M, Widyolar BK, Jiang L, Winston R, Yablonovitch E, Scranton G, et al. Novel double-stage high-concentrated solar hybrid photovoltaic/thermal (PV/T) collector with nonimaging optics and GaAs solar cells reflector. Appl Energy 2016;182:68–79. https://doi.org/10.1016/j.apenergy.2016.07.127.
[457] Keblinski P, Eastman J, Cahill D. Nanofluids for thermal transport. Mater Today 2005;8:36–44. https://doi.org/10.1016/S1369-7021(05)70936-6.
[458] Prasher R, Bhattacharya P, Phelan P. Thermal conductivity of nanoscale colloidal solutions (nanofluids). Phys Rev Lett 2005;94. https://doi.org/10.1103/PhysRevLett.94.025901.
[459] Otanicar TP, DeJarnette D, Hewakuruppu Y, Taylor RA. Filtering light with nanoparticles: a review of optically selective particles and applications. Adv Opt Photon 2016;8:541. https://doi.org/10.1364/AOP.8.000541.
[460] Taylor RA, Otanicar TP, Rosengarten G. Nanofluid-based optical filter optimization for PV/T systems. Nat Light Sci Appl 2012;1.
[461] Yazdanifard F, Ameri M, Ebrahimnia-Bajestan E. Performance of nanofluid-based photovoltaic/thermal systems: a review. Renew Sustain Energy Rev 2017;76:323–52. https://doi.org/10.1016/j.rser.2017.03.025.
[462] Hemmat Esfe M, Kamyab MH, Valadkhani M. Application of nanofluids and fluids in photovoltaic thermal system: an updated review. Sol Energy 2020;199:796–818. https://doi.org/10.1016/j.solener.2020.01.015.
[463] Choi SUS, Eastman JA. Enhancing thermal conductivity of fluids with nanoparticles. In: ASME int. Mech. Eng. San Francisco: . Congr. Expo.; 1995.
[464] Murshed SMS, Leong KC, Yang C. Thermophysical and electrokinetic properties of nanofluids – a critical review. Appl Therm Eng 2008;28:2109–25. https://doi.org/10.1016/j.applthermaleng.2008.01.005.
[465] Yousefi T, Shojaeizadeh E, Veysi F, Zinadini S. An experimental investigation on the effect of pH variation of MWCNT–H2O nanofluid on the efficiency of a flat-plate solar collector. Sol Energy 2012;86:771–9. https://doi.org/10.1016/j.solener.2011.12.003.
[466] Yousefi T, Veisy F, Shojaeizadeh E, Zinadini S. An experimental investigation on the effect of MWCNT-H2O nanofluid on the efficiency of flat-plate solar collectors. Exp Therm Fluid Sci 2012;39:207–12. https://doi.org/10.1016/j.expthermflusci.2012.01.025.
[467] Yousefi T, Veysi F, Shojaeizadeh E, Zinadini S. An experimental investigation on the effect of Al2O3–H2O nanofluid on the efficiency of flat-plate solar collectors. Renew Energy 2012;39:293–8. https://doi.org/10.1016/j.renene.2011.08.056.

[468] Sardarabadi M, Passandideh-Fard M, Zeinali Heris S. Experimental investigation of the effects of silica/water nanofluid on PV/T (photovoltaic thermal units). Energy 2014;66:264–72. https://doi.org/10.1016/j.energy.2014.01.102.

[469] Karami N, Rahimi M. Heat transfer enhancement in a hybrid microchannel-photovoltaic cell using Boehmite nanofluid. Int Commun Heat Mass Tran 2014; 55:45–52. https://doi.org/10.1016/j.icheatmasstransfer.2014.04.009.

[470] Michael JJ, Iniyan S. Performance analysis of a copper sheet laminated photovoltaic thermal collector using copper oxide – water nanofluid. Sol Energy 2015;119:439–51. https://doi.org/10.1016/j.solener.2015.06.028.

[471] Ghadiri M, Sardarabadi M, Pasandideh-fard M, Moghadam AJ. Experimental investigation of a PVT system performance using nano ferrofluids. Energy Convers Manag 2015;103:468–76. https://doi.org/10.1016/j.enconman.2015.06.077.

[472] Rejeb O, Sardarabadi M, Ménézo C, Passandideh-Fard M, Dhaou MH, Jemni A. Numerical and model validation of uncovered nanofluid sheet and tube type photovoltaic thermal solar system. Energy Convers Manag 2016;110:367–77. https://doi.org/10.1016/j.enconman.2015.11.063.

[473] Hassani S, Saidur R, Mekhilef S, Taylor RA. Environmental and exergy benefit of nanofluid-based hybrid PV/T systems. Energy Convers Manag 2016;123:431–44. https://doi.org/10.1016/j.enconman.2016.06.061.

[474] Sardarabadi M, Passandideh-Fard M. Experimental and numerical study of metal-oxides/water nanofluids as coolant in photovoltaic thermal systems (PVT). Sol Energy Mater Sol Cells 2016;157:533–42. https://doi.org/10.1016/j.solmat.2016.07.008.

[475] Alwan Sywan Alshaheen A, Kianifar A, Baradaran Rahimi A. Experimental study of using nano-(GNP, MWCNT, and SWCNT)/water to investigate the performance of a PVT module. J Therm Anal Calorim 2020;139:3549–61. https://doi.org/10.1007/s10973-019-08724-5.

[476] Alous S, Kayfeci M, Uysal A. Experimental investigations of using MWCNTs and graphene nanoplatelets water-based nanofluids as coolants in PVT systems. Appl Therm Eng 2019;162:114265. https://doi.org/10.1016/j.applthermaleng.2019.114265.

[477] Al-Waeli AHA, Kazem HA, Yousif JH, Chaichan MT, Sopian K. Mathematical and neural network modeling for predicting and analyzing of nanofluid-nano PCM photovoltaic thermal systems performance. Renew Energy 2020;145:963–80. https://doi.org/10.1016/j.renene.2019.06.099.

[478] Phelan PE, Taylor R, Adrian RJ, Prasher RS, Otanicar TP. Light induced energy conversion in liquid nanoparticle suspensions. In: Mikowycz WJ, Sparrow EM, Abraham JP, editors. Nanoparticle heat transf. Fluid flow. CRC Press; 2012.

[479] Tyagi H, Phelan P, Prasher R. Predicted efficiency of a low-temperature nanofluid-based direct absorption solar collector. J Sol Energy Eng 2009;131: 041004. https://doi.org/10.1115/1.3197562.

[480] Otanicar TP, Phelan PE, Prasher RS, Rosengarten G, Taylor Ra. Nanofluid-based direct absorption solar collector. J Renew Sustain Energy 2010;2:033102. https://doi.org/10.1063/1.3429737.

[481] Abdelrazik AS, Tan KH, Aslfattahi N, Arifutzzaman A, Saidur R, Al-Sulaiman FA. Optical, stability and energy performance of water-based MXene nanofluids in hybrid PV/thermal solar systems. Sol Energy 2020;204:32–47. https://doi.org/10.1016/j.solener.2020.04.063.

[482] Hewakuruppu YL, Taylor Ra, Tyagi H, Khullar V, Otanicar T, Coulombe S, et al. Limits of selectivity of direct volumetric solar absorption. Sol Energy 2015;114: 206–16. https://doi.org/10.1016/j.solener.2015.01.043.

[483] Looser R, Vivar M, Everett V. Spectral characterisation and long-term performance analysis of various commercial Heat Transfer Fluids (HTF) as Direct-Absorption Filters for CPV-T beam-splitting applications. Appl Energy 2014;113: 1496–511. https://doi.org/10.1016/j.apenergy.2013.09.001.

[484] Bierman DM, Lenert A, Wang EN. Spectral splitting optimization for high-efficiency solar photovoltaic and thermal power generation. Appl Phys Lett 2016; 109:243904. https://doi.org/10.1063/1.4971309.

[485] Hjerrild NE, Mesgari S, Crisostomo F, Scott JA, Amal R, Taylor RA. Hybrid PV/T enhancement using selectively absorbing Ag–SiO2/carbon nanofluids. Sol Energy Mater Sol Cells 2016;147:281–7. https://doi.org/10.1016/j.solmat.2015.12.010.

[486] Saroha S, Mittal T, Modi PJ, Bhalla V, Khullar V, Tyagi H, et al. Theoretical analysis and testing of nanofluids-based solar photovoltaic/thermal hybrid collector. J Heat Tran 2015;137:091015. https://doi.org/10.1115/1.4030228.

[487] Li H, He Y, Wang C, Wang X, Hu Y. Tunable thermal and electricity generation enabled by spectrally selective absorption nanoparticles for photovoltaic/thermal applications. Appl Energy 2019;236:117–26. https://doi.org/10.1016/j.apenergy.2018.11.085.

[488] Han X, Chen X, Wang Q, Alelyani SM, Qu J. Investigation of CoSO4-based Ag nanofluids as spectral beam splitters for hybrid PV/T applications. Sol Energy 2019;177:387–94. https://doi.org/10.1016/j.solener.2018.11.037.

[489] He Y, Hu Y, Li H. An Ag@TiO2/ethylene glycol/water solution as a nanofluid-based beam splitter for photovoltaic/thermal applications in cold regions. Energy Convers Manag 2019;198:111838. https://doi.org/10.1016/j.enconman.2019.111838.

[490] Mahian O, Bellos E, Markides CN, Taylor RA, Alagumalai A, Yang L, et al. Recent advances in using nanofluids in renewable energy systems and the environmental implications of their uptake. Nano Energy 2021;86:106069. https://doi.org/10.1016/j.nanoen.2021.106069.

[491] Method T, Liu X, Zhou Y, Li C, Lin Y, Yang W. Optimization of a new phase change material integrated photovoltaic/thermal panel with the active cooling technique using. 2019. p. 1–22. https://doi.org/10.3390/en12061022.

[492] Kuo CJ, Liu J, Lazuardi M, Lan W. The photovoltaic-thermal system parameter optimization design and practical verification. Energy Convers Manag 2019;180: 358–71. https://doi.org/10.1016/j.enconman.2018.10.080.

[493] Ben Ammar M, Chaabene M, Chtourou Z. Artificial Neural Network based control for PV/T panel to track optimum thermal and electrical power. Energy Convers Manag 2013;65:372–80. https://doi.org/10.1016/j.enconman.2012.08.003.

[494] Alnaqi AA, Moayedi H, Shahsavar A, Nguyen TK. Prediction of energetic performance of a building integrated photovoltaic/thermal system thorough artificial neural network and hybrid particle swarm optimization models. Energy Convers Manag 2019;183:137–48. https://doi.org/10.1016/j.enconman.2019.01.005.

[495] Khani MS, Baneshi M, Eslami M. Bi-objective optimization of photovoltaic-thermal (PV/T) solar collectors according to various weather conditions using genetic algorithm : a numerical modeling. Energy 2019;189:116223. https://doi.org/10.1016/j.energy.2019.116223.

[496] Podder B, Biswas A, Saha S. Multi-objective optimization of a small sized solar PV-T water collector using controlled elitist NSGA-II coupled with TOPSIS. Sol Energy 2021;230:688–702. https://doi.org/10.1016/j.solener.2021.10.078.

[497] Roy RK. A primer on the Taguchi method. Society of Manufacturing Engineers; 2010.

[498] Guarracino I, Mellor A, Ekins-Daukes NJ, Markides CN. Dynamic coupled thermal-and-electrical modelling of sheet-and-tube hybrid photovoltaic/thermal (PVT) collectors. Appl Therm Eng 2016;101:778–95. https://doi.org/10.1016/j.applthermaleng.2016.02.056.

[499] Zhang X, Shen J, Xu P, Zhao X, Xu Y. Socio-economic performance of a novel solar photovoltaic/loop-heat-pipe heat pump water heating system in three different climatic regions. Appl Energy 2014;135:20–34. https://doi.org/10.1016/j.apenergy.2014.08.074.

[500] Kamthania D, Nayak S, Tiwari GN. Performance evaluation of a hybrid photovoltaic thermal double pass facade for space heating. Energy Build 2011;43: 2274–81. https://doi.org/10.1016/j.enbuild.2011.05.007.

[501] Choi H-U, Kim Y-B, Son C-H, Yoon J-I, Choi K-H. Experimental study on the performance of heat pump water heating system coupled with air type PV/T collector. Appl Therm Eng 2020;178:115427. https://doi.org/10.1016/j.applthermaleng.2020.115427.

[502] Calise F, Dentice D'Accadia M, Vanoli L. Design and dynamic simulation of a novel solar trigeneration system based on hybrid photovoltaic/thermal collectors (PVT). Energy Convers Manag 2012;60:214–25. https://doi.org/10.1016/j.enconman.2012.01.025.

[503] Chen H, Li Z, Xu Y. Evaluation and comparison of solar trigeneration systems based on photovoltaic thermal collectors for subtropical climates. Energy Convers Manag 2019;199:111959. https://doi.org/10.1016/j.enconman.2019.111959.

[504] Herrando M, Coca-ortegón A, Guedea I, Fueyo N. Experimental study of a solar system based on hybrid PVT collectors for the provision of heating, cooling and electricity in non-residential buildings. In: 16th conf. Sustain. Dev. Energy, water environ. Syst. SDEWES2021.0062, dubrovnik; 2021. p. 1–14.

[505] Liang R, Zhou C, Zhang J, Chen J, Riaz A. Characteristics analysis of the photovoltaic thermal heat pump system on refrigeration mode: an experimental investigation. Renew Energy 2020;146:2450–61. https://doi.org/10.1016/j.renene.2019.08.045.

[506] Kumar R, Rosen MA. A critical review of photovoltaic–thermal solar collectors for air heating. Appl Energy 2011;88:3603–14. https://doi.org/10.1016/j.apenergy.2011.04.044.

[507] Kalogirou SA. Solar energy engineering: processes and systems. 2nd ed. Academic Press; 2014. https://doi.org/10.1016/B978-0-12-374501-9.00014-5.

[508] Hansen J, Sorensen H. IEA SHC task 35 PV/thermal solar systems. IEA; 2006.

[509] Trianti-Stourna E, Spyropoulou K, Theofylaktos C, Droutsa K, Balaras CA, Santamouris M, et al. Energy conservation strategies for sports centers: Part A. Sports halls. Energy Build 1998;27:109–22. https://doi.org/10.1016/s0378-7788(97)00040-6.

[510] Li Y, Nord N, Huang G, Li X. Swimming pool heating technology: a state-of-the-art review. Build Simulat 2020;2. https://doi.org/10.1007/s12273-020-0669-3.

[511] Singh M, Tiwari GN, Yadav YP. Solar energy utilization for heating of indoor swimming pool. Energy Convers Manag 1989;29:239–44. https://doi.org/10.1016/0196-8904(89)90027-7.

[512] Ruiz E, Martínez PJ. Analysis of an open-air swimming pool solar heating system by using an experimentally validated TRNSYS model. Sol Energy 2010;84: 116–23. https://doi.org/10.1016/J.SOLENER.2009.10.015.

[513] Tagliafico LA, Scarpa F, Tagliafico G, Valsuani F. An approach to energy saving assessment of solar assisted heat pumps for swimming pool water heating. Energy Build 2012;55:833–40. https://doi.org/10.1016/J.ENBUILD.2012.10.009.

[514] Chow TT, Bai Y, Fong KF, Lin Z. Analysis of a solar assisted heat pump system for indoor swimming pool water and space heating. Appl Energy 2012;100:309–17. https://doi.org/10.1016/J.APENERGY.2012.05.058.

[515] Buonomano A, De Luca G, Figaj RD, Vanoli L. Dynamic simulation and thermo-economic analysis of a PhotoVoltaic/Thermal collector heating system for an indoor–outdoor swimming pool. Energy Convers Manag 2015;99:176–92. https://doi.org/10.1016/J.ENCONMAN.2015.04.022.

[516] Wang K, Herrando M, Pantaleo AM, Markides CN. Thermodynamic and economic assessments of a PVT- ORC combined heating and power system for swimming pools. In: HEAT POWERED CYCLES 2018 conf. Bayreuth: Proc.; 2018. p. 531–8.

[517] Herrando M, Ramos A, Freeman J, Zabalza I, Markides CN. Technoeconomic modelling and optimisation of solar combined heat and power systems based on flat-box PVT collectors for domestic applications. Energy Convers Manag 2018; 175:67–85. https://doi.org/10.1016/j.enconman.2018.07.045.

[518] Herrando M, Pantaleo AM, Wang K, Markides CN. Solar combined cooling, heating and power systems based on hybrid PVT, PV or solar-thermal collectors for building applications. Renew Energy 2019;143:637–47. https://doi.org/10.1016/j.renene.2019.05.004.

[519] Sedigas. Guia sobre aplicaciones de la energía solar térmica. 2013. www.sedigas.es.

[520] Herrando M, Ramos A, Zabalza I. Cost competitiveness of a novel PVT-based solar combined heating and power system: influence of economic parameters and financial incentives. Energy Convers Manag 2018;166:758–70. https://doi.org/10.1016/j.enconman.2018.04.005.

[521] de Keizer C, Bottse J, De Jong M. PVT Benchmark. An overview of PVT modules on the European market and the barriers and opportunities for the Dutch Market. 2017.

[522] Bellos E, Tzivanidis C, Moschos K, Antonopoulos KA. Energetic and financial evaluation of solar assisted heat pump space heating systems. Energy Convers Manag 2016;120:306–19. https://doi.org/10.1016/J.ENCONMAN.2016.05.004.

[523] Wang G, Quan Z, Zhao Y, Sun C, Deng Y, Tong J. Experimental study on a novel PV/T air dual-heat-source composite heat pump hot water system. Energy Build 2015;108:175–84. https://doi.org/10.1016/j.enbuild.2015.08.016.

[524] Li H, Sun Y. Operational performance study on a photovoltaic loop heat pipe/solar assisted heat pump water heating system. Energy Build 2018;158:861–72. https://doi.org/10.1016/j.enbuild.2017.10.075.

[525] Huide F, Tao Z. Performance analysis of an integrated solar-assisted heat pump system with heat pipe PV/T collectors operating under different weather conditions. Energy Proc 2017;105:1143–8. https://doi.org/10.1016/j.egypro.2017.03.485.

[526] Hobbi A, Siddiqui K. Optimal design of a forced circulation solar water heating system for a residential unit in cold climate using TRNSYS. Sol Energy 2009;83:700–14. https://doi.org/10.1016/j.solener.2008.10.018.

[527] Kim Y, Thu K, Kaur H, Singh C, Choon K. Thermal analysis and performance optimization of a solar hot water plant with economic evaluation. Sol Energy 2012;86:1378–95. https://doi.org/10.1016/j.solener.2012.01.030.

[528] Bazilian MD, Prasad D. A holistic approach to Photovoltaic/thermal/daylight (PV/T/L) cogeneration. Using waste heat and light from PV modules for building energy loads. ISES EUROSUN Conf.; 2000.

[529] Tse K-K, Chow T-T, Su Y. Performance evaluation and economic analysis of a full scale water-based photovoltaic/thermal (PV/T) system in an office building. Energy Build 2016;122:42–52. https://doi.org/10.1016/j.enbuild.2016.04.014.

[530] Cristofari C, Notton G, Poggi P, Louche A. Influence of the flow rate and the tank stratification degree on the performances of a solar flat-plate collector. Int J Therm Sci 2003;42:455–69. https://doi.org/10.1016/S1290-0729(02)00046-7.

[531] del Amo A. Estudio, modelado y simulación de paneles solares híbridos con Cubierta Transparente y Aislante y validación experimental para su aplicación en sistemas de trigeneración. University of Zaragoza; 2015.

[532] de España Gobierno. Orden FOM/1635/2013, de 10 de septiembre, por la que se actualiza el Documento Básico DB-HE «Ahorro de Energía», del Código Técnico de la Edificación, aprobado por Real Decreto 314/2006. de 17 de marzo; 2013.

[533] Kalogirou SA. Solar thermal collectors and applications. Prog Energy Combust Sci 2004;30:231–95. https://doi.org/10.1016/j.pecs.2004.02.001.

[534] Herrando M, Coca-ortegón A, Guedea I, Fueyo N. Solar assisted heat pump systems based on hybrid PVT collectors for the provision of hot water, cooling and electricity in buildings. In: ISES conf. Proc. - eurosun; 2020. p. 2020.

[535] Haurant P, Ménézo C, Gaillard L, Dupeyrat P. A numerical model of a solar domestic hot water system integrating hybrid photovoltaic/thermal collectors. Energy Proc 2015;78:1991–7. https://doi.org/10.1016/j.egypro.2015.11.391.

[536] Tamayo Vera J, Laukkanen T, Sirén K. Multi-objective optimization of hybrid photovoltaic-thermal collectors integrated in a DHW heating system. Energy Build 2014;74:78–90. https://doi.org/10.1016/j.enbuild.2014.01.011.

[537] Guarracino I, Freeman J, Ekins-Daukes N, Markides CN. Performance assessment and comparison of solar ORC and hybrid PVT systems for the combined distributed generation of domestic heat and power. Int Conf Heat Transf Fluid Mech Thermodyn 2016.

[538] Dannemand M, Perers B, Furbo S. Performance of a demonstration solar PVT assisted heat pump system with cold buffer storage and domestic hot water storage tanks. Energy Build 2019;188–189:46–57. https://doi.org/10.1016/j.enbuild.2018.12.042.

[539] Kalogirou SA, Tripanagnostopoulos Y. Industrial application of PV/T solar energy systems. Appl Therm Eng 2007;27:1259–70. https://doi.org/10.1016/j.applthermaleng.2006.11.003.

[540] Hazi A, Hazi G, Grigore R, Vernica S. Opportunity to use PVT systems for water heating in industry. Appl Therm Eng 2014;63:151–7. https://doi.org/10.1016/j.applthermaleng.2013.11.010.

[541] Gang P, Huide F, Jie J, Tin-Tai C, Tao Z. Annual analysis of heat pipe PV/T systems for domestic hot water and electricity production. Energy Convers Manag 2012;56:8–21. https://doi.org/10.1016/j.enconman.2011.11.011.

[542] Boopathi Raja V, Shanmugam V. A review and new approach to minimize the cost of solar assisted absorption cooling system. Renew Sustain Energy Rev 2012;16:6725–31. https://doi.org/10.1016/j.rser.2012.08.004.

[543] Berardi U. Resources, Conservation and Recycling. A cross-country comparison of the building energy consumptions and their trends. Resour Conserv Recycl 2017;123:230–41. https://doi.org/10.1016/j.resconrec.2016.03.014.

[544] Shirazi A, Taylor RA, Morrison GL, White SD. Solar-powered absorption chillers: a comprehensive and critical review. Energy Convers Manag 2018;171:59–81. https://doi.org/10.1016/j.enconman.2018.05.091.

[545] Henning HM. Solar cooling position. 2011. Paper. Technical report. http://task38.iea-shc.org/data/sites/1/publications/IEA-SHC-Solar-Cooling-Position-Paper.pdf. [Accessed 8 August 2020].

[546] Bany Mousa O, Taylor RA, Shirazi A. Multi-objective optimization of solar photovoltaic and solar thermal collectors for industrial rooftop applications. Energy Convers Manag 2019;195:392–408. https://doi.org/10.1016/j.enconman.2019.05.012.

[547] Bany Mousa OM, Taylor RA. A broad comparison of solar photovoltaic and thermal technologies for industrial heating applications. J Sol Energy Eng Trans ASME 2019;141:1–12. https://doi.org/10.1115/1.4040840.

[548] Jordehi AR. Parameter estimation of solar photovoltaic (PV) cells: a review. Renew Sustain Energy Rev 2016;61:354–71. https://doi.org/10.1016/j.rser.2016.03.049.

[549] Shirazi A, Taylor RA, White SD, Morrison GL. Multi-effect absorption chillers powered by the sun: reality or Reverie. In: Energy procedia; 2016. https://doi.org/10.1016/j.egypro.2016.06.251.

[550] Shirazi A, Taylor RA, Morrison GL, White SD. A comprehensive, multi-objective optimization of solar-powered absorption chiller systems for air-conditioning applications. Energy Convers Manag 2017;132. https://doi.org/10.1016/j.enconman.2016.11.039.

[551] Shirazi A, Taylor RA, White SD, Morrison GL. Transient simulation and parametric study of solar-assisted heating and cooling absorption systems: an energetic, economic and environmental (3E) assessment. Renew Energy 2016;86:955–71. https://doi.org/10.1016/J.RENENE.2015.09.014.

[552] Eicker U, Colmenar-Santos A, Teran L, Cotrado M, Borge-Diez D. Economic evaluation of solar thermal and photovoltaic cooling systems through simulation in different climatic conditions: an analysis in three different cities in Europe. Energy Build 2014;70:207–23. https://doi.org/10.1016/J.ENBUILD.2013.11.061.

[553] Fong KF, Chow TT, Lee CK, Lin Z, Chan LS. Comparative study of different solar cooling systems for buildings in subtropical city. Sol Energy 2010;84:227–44. https://doi.org/10.1016/J.SOLENER.2009.11.002.

[554] White S, Sethuvenkatraman S, Peristy M, Pintaldi S, Goldsworthy M, Shirazi A, et al. Design guide for solar cooling with double-effect absorption chillers. In: Sol. Cool. Des. Guid. - case stud. Success. Sol. Air cond. Des. Berlin, Germany: Wilhelm Ernst & Sohn; 2017. p. 99–138. https://doi.org/10.1002/9783433606841.ch5.

[555] Kerme ED, Chafidz A, Agboola OP, Orfi J, Fakeeha AH, Al-fatesh AS. Energetic and exergetic analysis of solar-powered lithium bromide- water absorption cooling system. J Clean Prod 2017;151:60–73. https://doi.org/10.1016/j.jclepro.2017.03.060.

[556] Buonomano A, Calise F, Palombo A. Solar heating and cooling systems by CPVT and ET solar collectors: a novel transient simulation model. Appl Energy 2013;103:588–606. https://doi.org/10.1016/J.APENERGY.2012.10.023.

[557] Calise F, Dentice d'Accadia M, Palombo A, Vanoli L. Dynamic simulation of a novel high-temperature solar trigeneration system based on concentrating photovoltaic/thermal collectors. Energy 2013;61:72–86. https://doi.org/10.1016/j.energy.2012.10.008.

[558] Mittelman G, Kribus A, Dayan A. Solar cooling with concentrating photovoltaic/thermal (CPVT) systems. Energy Convers Manag 2007;48:2481–90. https://doi.org/10.1016/J.ENCONMAN.2007.04.004.

[559] Calise F, Figaj RD, Vanoli L. A novel polygeneration system integrating photovoltaic/thermal collectors, solar assisted heat pump, adsorption chiller and electrical energy storage: dynamic and energy-economic analysis. Energy Convers Manag 2017;149:798–814. https://doi.org/10.1016/J.ENCONMAN.2017.03.027.

[560] Bellos E, Tzivanidis C, Antonopoulos KA. Exergetic, energetic and financial evaluation of a solar driven absorption cooling system with various collector types. Appl Therm Eng 2016;102:749–59. https://doi.org/10.1016/j.applthermaleng.2016.04.032.

[561] Papoutsis EG, Koronaki IP, Papaefthimiou VD. Numerical simulation and parametric study of different types of solar cooling systems under Mediterranean climatic conditions. Energy Build 2017;138:601–11. https://doi.org/10.1016/J.ENBUILD.2016.12.094.

[562] Herrando M, Simón R, Guedea I, Fueyo N. The challenges of solar hybrid PVT systems in the food processing industry. Appl Therm Eng 2020:116235. https://doi.org/10.1016/j.applthermaleng.2020.116235.

[563] Liu XH, Zhang T, Zheng YW, Tu R. Performance investigation and exergy analysis of two-stage desiccant wheel systems. Renew Energy 2016;86:877–88. https://doi.org/10.1016/j.renene.2015.09.025.

[564] Beccali M, Finocchiaro P, Nocke B. Energy and economic assessment of desiccant cooling systems coupled with single glazed air and hybrid PV/thermal solar collectors for applications in hot and humid climate. Sol Energy 2009;83:1828–46. https://doi.org/10.1016/j.solener.2009.06.015.

[565] Saghafifar M, Gadalla M. Performance assessment of integrated PV/T and solid desiccant air-conditioning systems for cooling buildings using Maisotsenko cooling cycle. Sol Energy 2016;127:79–95. https://doi.org/10.1016/j.solener.2015.12.048.

[566] Aneli S, Gagliano A, Tina GM, Gediz Ilis G, Demir H. Effectiveness and constraints of using PV/Thermal collectors for heat-driven chillers. Appl Therm Eng 2022;210:118330. https://doi.org/10.1016/j.applthermaleng.2022.118330.

[567] Goyal P, Baredar P, Mittal A, Siddiqui AR. Adsorption refrigeration technology - an overview of theory and its solar energy applications. Renew Sustain Energy Rev 2016;53:1389–410. https://doi.org/10.1016/j.rser.2015.09.027.

[568] Alelyenai S, Phelan PE, Shahnawaz S. Solar adsorption heat pump and evacuated tube adsorption heat pump and desalination system. 2019. US 2019/0309998 A1.

[569] Gürlich D, Dalibard A, Eicker U. Photovoltaic-thermal hybrid collector performance for direct trigeneration in a European building retrofit case study. Energy Build 2017;152:701–17. https://doi.org/10.1016/j.enbuild.2017.07.081.

[570] Eicker U, Dalibard A. Photovoltaic–thermal collectors for night radiative cooling of buildings. Sol Energy 2011;85:1322–35. https://doi.org/10.1016/j.solener.2011.03.015.

[571] European Commission. Market uptake activities in support of the new heating and cooling strategy. 2016.
[572] Xu Z, Kleinstreuer C. Concentration photovoltaic–thermal energy co-generation system using nanofluids for cooling and heating. Energy Convers Manag 2014;87:504–12. https://doi.org/10.1016/J.ENCONMAN.2014.07.047.
[573] del Amo A. Solar trigeneration: a transitory simulation of HVAC systems using different typologies of hybrid panels. J Sustain Dev Energy, Water Environ Syst 2014;2:1–14. https://doi.org/10.13044/j.sdewes.2014.02.0001.
[574] Herrando M, Ramos A, Zabalza I, Markides CN. Energy performance of a solar trigeneration system based on a novel hybrid PVT panel for residential applications. In: ISES sol. World congr. 2017 - IEA SHC int. Conf. Sol. Heat. Cool. Build. Ind. 2017, proc., Abu Dhabi (UAE); 2017. p. 1090–101.
[575] Ramos A, Chatzopoulou MA, Guarracino I, Freeman J, Markides CN. Hybrid photovoltaic-thermal solar systems for combined heating, cooling and power provision in the urban environment. Energy Convers Manag 2017;150:838–50. https://doi.org/10.1016/j.enconman.2017.03.024.
[576] Herrando M, Elduque D, Javierre C, Fueyo N. Life Cycle Assessment of solar energy systems for the provision of heating, cooling and electricity in buildings: a comparative analysis. Energy Convers Manag 2022;257:115402. https://doi.org/10.1016/j.enconman.2022.115402.
[577] Kong R, Deethayat T, Asanakham A, Kiatsiriroat T. Performance and economic evaluation of a photovoltaic/thermal (PV/T)-cascade heat pump for combined cooling, heat and power in tropical climate area. J Energy Storage 2020;30:101507. https://doi.org/10.1016/j.est.2020.101507.
[578] Buonomano A, Calise F, Palombo A, Vicidomini M. Adsorption chiller operation by recovering low-temperature heat from building integrated photovoltaic thermal collectors: modelling and simulation. Energy Convers Manag 2017;149:1019–36. https://doi.org/10.1016/j.enconman.2017.05.005.
[579] Calise F, Dentice d'Accadia M, Figaj RD, Vanoli L. A novel solar-assisted heat pump driven by photovoltaic/thermal collectors: dynamic simulation and thermoeconomic optimization. Energy 2016;95:346–66. https://doi.org/10.1016/J.ENERGY.2015.11.071.
[580] Giwa A, Fath H, Hasan SW. Humidification–dehumidification desalination process driven by photovoltaic thermal energy recovery (PV-HDH) for small-scale sustainable water and power production. Desalination 2016;377:163–71. https://doi.org/10.1016/j.desal.2015.09.018.
[581] Elsafi AM. Integration of humidification-dehumidification desalination and concentrated photovoltaic-thermal collectors: energy and exergy-costing analysis. Desalination 2017;424:17–26. https://doi.org/10.1016/j.desal.2017.09.022.
[582] Gabrielli P, Gazzani M, Novati N, Sutter L, Simonetti R, Molinaroli L, et al. Combined water desalination and electricity generation through a humidification-dehumidification process integrated with photovoltaic-thermal modules: design, performance analysis and techno-economic assessment. Energy Convers Manag X 2019;1:100004. https://doi.org/10.1016/j.ecmx.2019.100004.
[583] Ong CL, Escher W, Paredes S, Khalil ASG, Michel B. A novel concept of energy reuse from high concentration photovoltaic thermal (HCPVT) system for desalination. Desalination 2012;295:70–81. https://doi.org/10.1016/J.DESAL.2012.04.005.
[584] Krnac A, Araiz M, Rana S, Velardo J, Date A. Investigation of direct contact membrane distillation coupling with a concentrated photovoltaic solar system. Energy Proc 2019;160:246–52. https://doi.org/10.1016/j.egypro.2019.02.143.
[585] Hughes AJ, O'Donovan TS, Mallick TK. Experimental evaluation of a membrane distillation system for integration with concentrated photovoltaic/thermal (CPV/T) energy. Energy Proc 2014;54:725–33. https://doi.org/10.1016/j.egypro.2014.07.313.
[586] Kumar S, Tiwari A. An experimental study of hybrid photovoltaic thermal (PV/T)-active solar still. Int J Energy Res 2008;32:847–58. https://doi.org/10.1002/er.1388.
[587] Singh G, Kumar S, Tiwari GN. Design, fabrication and performance evaluation of a hybrid photovoltaic thermal (PVT) double slope active solar still. Desalination 2011;277:399–406. https://doi.org/10.1016/J.DESAL.2011.04.064.
[588] Singh G, Dwivedi VK, Yadav JK, Tiwari GN. Experimental validation of thermal model of hybrid photovoltaic thermal (HPVT) double slope active solar still. Desalination Water Treat 2012;45:182–90. https://doi.org/10.1080/19443994.2012.692041.
[589] Dev R, Tiwari GN. Characteristic equation of a hybrid (PV-T) active solar still. Desalination 2010;254:126–37. https://doi.org/10.1016/J.DESAL.2009.12.004.
[590] Kumar S, Tiwari GN. Life cycle cost analysis of single slope hybrid (PV/T) active solar still. Appl Energy 2009;86:1995. https://doi.org/10.1016/J.APENERGY.2009.03.005. –2004.
[591] Singh DB, Yadav JK, Dwivedi VK, Kumar S, Tiwari GN, Al-Helal IM. Experimental studies of active solar still integrated with two hybrid PVT collectors. Sol Energy 2016;130:207–23. https://doi.org/10.1016/j.solener.2016.02.024.
[592] Kumar S. Thermal–economic analysis of a hybrid photovoltaic thermal (PVT) active solar distillation system: role of carbon credit. Urban Clim 2013;5:112–24. https://doi.org/10.1016/J.UCLIM.2013.07.001.
[593] Boubekri M, Chaker A, Cheknane A. Modeling and simulation of the continuous production of an improved solar still coupled with a photovoltaic/thermal solar water heater system. Desalination 2013;331:6–15. https://doi.org/10.1016/J.DESAL.2013.09.027.
[594] Naroei M, Sarhaddi F, Sobhnamayan F. Efficiency of a photovoltaic thermal stepped solar still: experimental and numerical analysis. Desalination 2018;441:87–95. https://doi.org/10.1016/j.desal.2018.04.014.
[595] Mittelman G, Kribus A, Mouchtar O, Dayan A. Water desalination with concentrating photovoltaic/thermal (CPVT) systems. Sol Energy 2009;83:1322–34. https://doi.org/10.1016/J.SOLENER.2009.04.003.
[596] Calise F, Dentice d'Accadia M, Piacentino A. A novel solar trigeneration system integrating PVT (photovoltaic/thermal collectors) and SW (seawater) desalination: dynamic simulation and economic assessment. Energy 2014;67:129–48. https://doi.org/10.1016/j.energy.2013.12.060.
[597] An W, Chen L, Liu T, Qin Y. Enhanced solar distillation by nanofluid-based spectral splitting PV/T technique: preliminary experiment. Sol Energy 2018;176:146–56. https://doi.org/10.1016/j.solener.2018.10.029.
[598] An W, Zhang Y, Pang B, Wu J. Synergistic design of an integrated pv/distillation solar system based on nanofluid spectral splitting technique. AIMS Energy 2021;9:534–57. https://doi.org/10.3934/energy.2021026.
[599] Ammous M, Chaabene M. Multi criteria sizing approach for Photovoltaic Thermal collectors supplying desalination plant. Energy Convers Manag 2015;94:365–76. https://doi.org/10.1016/j.enconman.2015.02.004.
[600] Wiesenfarth M, Went J, Bösch A, Dilger A, Kec T, Kroll A, et al. CPV-T mirror dish system combined with water desalination systems. 2016. https://doi.org/10.1063/1.4962076.
[601] Sharma A, Chen CR, Vu Lan N. Solar-energy drying systems: a review. Renew Sustain Energy Rev 2009;13:1185–210. https://doi.org/10.1016/j.rser.2008.08.015.
[602] El-Sebaii AA, Shalaby SM. Solar drying of agricultural products: a review. Renew Sustain Energy Rev 2012;16:37–43. https://doi.org/10.1016/j.rser.2011.07.134.
[603] Rittidech S, Dangeton W, Soponronnarit S. Closed-ended oscillating heat-pipe (CEOHP) air-preheater for energy thrift in a dryer. Appl Energy 2005;81:198–208. https://doi.org/10.1016/j.apenergy.2004.06.003.
[604] Mortezapour H, Ghobadian B, Khoshtaghaza MH, Minaei S. Performance analysis of a two-way hybrid photovoltaic/thermal solar collector. J Agric Sci Technol 2012;12:767–80.
[605] Nayak S, Tiwari GN. Energy and exergy analysis of photovoltaic/thermal integrated with a solar greenhouse. Energy Build 2008;40:2015. https://doi.org/10.1016/J.ENBUILD.2008.05.007. –2021.
[606] Sonneveld PJ, Swinkels GLAM, Campen J, van Tuijl BAJ, Janssen HJJ, Bot GPA. Performance results of a solar greenhouse combining electrical and thermal energy production. Biosyst Eng 2010;106:48–57. https://doi.org/10.1016/J.BIOSYSTEMSENG.2010.02.003.
[607] Sonneveld PJ, Swinkels GLAM, Bot GPA. Design of a solar greenhouse with energy delivery by the conversion of near infrared radiation - Part 1 optics and PV-cells. Acta Hortic 2009:47–54. https://doi.org/10.17660/ActaHortic.2009.807.2.
[608] Othman MY, Yatim B, Sopian K, Zaharim A, Nazari M, Bakar ABU. Studies of A Photovoltaic-Thermal solar drying system for rural applications. In: 2nd WSEAS/IASME int. Conf. Renew. Energy sources; 2008. p. 132–6.
[609] Fterich M, Chouikhi H, Bentaher H, Maalej A. Experimental parametric study of a mixed-mode forced convection solar dryer equipped with a PV/T air collector. Sol Energy 2018;171:751–60. https://doi.org/10.1016/j.solener.2018.06.051.
[610] Barnwal P, Tiwari GN. Grape drying by using hybrid photovoltaic-thermal (PV/T) greenhouse dryer: an experimental study. Sol Energy 2008;82:1131–44. https://doi.org/10.1016/j.solener.2008.05.012.
[611] Tiwari S, Tiwari GN, Al-Helal IM. Performance analysis of photovoltaic–thermal (PVT) mixed mode greenhouse solar dryer. Sol Energy 2016;133:421–8. https://doi.org/10.1016/J.SOLENER.2016.04.033.
[612] Tiwari S, Tiwari GN. Exergoeconomic analysis of photovoltaic-thermal (PVT) mixed mode greenhouse solar dryer. Energy 2016;114:155–64. https://doi.org/10.1016/j.energy.2016.07.132.
[613] Nayak S, Kumar A, Mishra J, Tiwari GN. Drying and testing of mint (Mentha piperita) by a hybrid photovoltaic-thermal (PVT)-Based greenhouse dryer, dry. Technol 2011;29:1002–9. https://doi.org/10.1080/07373937.2010.547265.
[614] Assoa YB, Sauzedde F, Boillot B, Boddaert S. Development of a building integrated solar photovoltaic/thermal hybrid drying system. Energy 2017;128:755–67. https://doi.org/10.1016/j.energy.2017.04.062.
[615] Daghigh R, Shahidian R, Oramipoor H. A multistate investigation of a solar dryer coupled with photovoltaic thermal collector and evacuated tube collector. Sol Energy 2020;199:694–703. https://doi.org/10.1016/j.solener.2020.02.069.
[616] Staffell I, Scamman D, Velazquez Abad A, Balcombe P, Dodds PE, Ekins P, et al. The role of hydrogen and fuel cells in the global energy system. Energy Environ Sci 2019;12:463–91. https://doi.org/10.1039/c8ee01157e.
[617] Zeng K, Zhang D. Recent progress in alkaline water electrolysis for hydrogen production and applications. Prog Energy Combust Sci 2010;36:307–26. https://doi.org/10.1016/j.pecs.2009.11.002.
[618] Janjua MBI, Leroy RL. Electrocatalyst performance in industrial water electrolysers. Int J Hydrogen Energy 1985;10:11–9.
[619] Carmo M, Fritz DL, Mergel J, Stolten D. A comprehensive review on PEM water electrolysis. Int J Hydrogen Energy 2013;38:4901–34. https://doi.org/10.1016/j.ijhydene.2013.01.151.
[620] LeRoy RL, Bowen CT, LeRoy DJ. The thermodynamics of aqueous water electrolysis. J Electrochem Soc 1980;127:1954–62. https://doi.org/10.1149/1.2130044.
[621] Millet P, Grigoriev S. Water electrolysis technologies. In: Gandia LM, Arzamedi G, Diéguez PM, editors. Renew. Hydrog. Technol. Prod. Purification, storage, Appl. Saf. Elsevier; 2013. p. 19–41.
[622] Akrami E, Nemati A, Nami H, Ranjbar F. Exergy and exergoeconomic assessment of hydrogen and cooling production from concentrated PVT equipped with PEM electrolyzer and LiBr-H2O absorption chiller. Int J Hydrogen Energy 2018;43:622–33. https://doi.org/10.1016/j.ijhydene.2017.11.007.
[623] Behzadi A, Habibollahzade A, Ahmadi P, Gholamian E, Houshfar E. Multi-objective design optimization of a solar based system for electricity, cooling, and

hydrogen production. Energy 2019;169:696–709. https://doi.org/10.1016/j.energy.2018.12.047.
[624] Wang H, Li W, Liu T, Liu X, Hu X. Thermodynamic analysis and optimization of photovoltaic/thermal hybrid hydrogen generation system based on complementary combination of photovoltaic cells and proton exchange membrane electrolyzer. Energy Convers Manag 2019;183:97–108. https://doi.org/10.1016/j.enconman.2018.12.106.
[625] Cabeza LF. Advances in thermal energy storage systems: methods and applications. 2nd ed. Elsevier; 2020.
[626] Dinçer I, M. (Marc A.. Rosen. Thermal energy storage systems and applications. Wiley; 2002.
[627] Wang K, Pantaleo AM, Herrando M, Faccia M, Pesmazoglou I, Franchetti BM, et al. Spectral-splitting hybrid PV-thermal (PVT) systems for combined heat and power provision to dairy farms. Renew Energy 2020;159:1047–65. https://doi.org/10.1016/j.renene.2020.05.120.
[628] Zhu T, Li Q. A novel spectrum allocation method in the photovoltaic-thermochemical hybrid solar system. J Power Sources 2021;513:230541. https://doi.org/10.1016/j.jpowsour.2021.230541.
[629] Ling Y, Li W, Jin J, Yu Y, Hao Y, Jin H. A spectral-splitting photovoltaic-thermochemical system for energy storage and solar power generation. Appl Energy 2020;260:113631. https://doi.org/10.1016/j.apenergy.2019.113631.
[630] Tian Y, Zhao CY. A review of solar collectors and thermal energy storage in solar thermal applications. Appl Energy 2013;104:538–53. https://doi.org/10.1016/j.apenergy.2012.11.051.
[631] Leng Guanghui CC, Cao Hui, Peng Hao. The new research progress of thermal energy storage materials. Energy Storage Sci Technol 2017;6:1058–75.
[632] Garg J, Poudel B, Chiesa M, Gordon JB, Ma JJ, Wang JB, et al. Enhanced thermal conductivity and viscosity of copper nanoparticles in ethylene glycol nanofluid. J Appl Phys 2008;103:074301. https://doi.org/10.1063/1.2902483.
[633] Ghazvini M, Akhavan-Behabadi MA, Rasouli E, Raisee M. Heat transfer properties of nanodiamond–engine oil nanofluid in laminar flow. Heat Tran Eng 2012;33:525–32. https://doi.org/10.1080/01457632.2012.624858.
[634] Chang C, Wu Z, Navarro H, Li C, Leng G, Li X, et al. Comparative study of the transient natural convection in an underground water pit thermal storage. Appl Energy 2017;208:1162–73. https://doi:10.1016/J.APENERGY.2017.09.036.
[635] Pang C, Lee JW, Kang YT. Review on combined heat and mass transfer characteristics in nanofluids. Int J Therm Sci 2015;87:49–67. https://doi.org/10.1016/J.IJTHERMALSCI.2014.07.017.
[636] Eastman JA, Choi US, Li S, Thompson LJ, Lee S. Enhanced thermal conductivity through the development of nanofluids. MRS Proc 1996:3.
[637] Shin D, Banerjee D. Enhancement of specific heat capacity of high-temperature silica-nanofluids synthesized in alkali chloride salt eutectics for solar thermal-energy storage applications. Int J Heat Mass Tran 2011;54:1064–70. https://doi.org/10.1016/j.ijheatmasstransfer.2010.11.017.
[638] Dow Dowtherm A. Heat transfer fluid. http://samyangoil.com/new/catalog/1/2_Dow_Chemical/DOWTHERM_A_en.pdf. [Accessed 31 December 2020].
[639] Bauer T, Pfleger N, Laing D, Steinmann WD, Eck M, Kaesche S. High-temperature molten salts for solar power application. In: Molten salts chem. Elsevier Inc.; 2013. p. 415–38. https://doi.org/10.1016/B978-0-12-398538-5.00020-2.
[640] Delpech S. Molten salts for nuclear applications. In: Molten salts chem. Elsevier; 2013. p. 497–520. https://doi.org/10.1016/B978-0-12-398538-5.00024-X.
[641] Goharshadi E, Ahmadzadeh H, Samiee S. Nanofluids for heat transfer enhancement-a review. Phys Chem Res 2013;1:1–33.
[642] Lasfargues M, Geng Q, Cao H, Ding Y. Mechanical dispersion of nanoparticles and its effect on the specific heat capacity of impure binary nitrate salt mixtures. Nanomaterials 2015;5:1136–46. https://doi.org/10.3390/nano5031136.
[643] Lasfargues M, Cao H, Geng Q, Ding Y. Rheological analysis of binary eutectic mixture of sodium and potassium nitrate and the effect of low concentration CuO nanoparticle addition to its viscosity. 2015. p. 5194–204. https://doi.org/10.3390/ma8085194.
[644] Zhang L, Chen X, Wu Y, Lu Y, Ma C. Effect of nanoparticle dispersion on enhancing the specific heat capacity of quaternary nitrate for solar thermal energy storage application. Sol Energy Mater Sol Cells 2016;157:808–13. https://doi.org/10.1016/j.solmat.2016.07.046.
[645] Hu Y, He Y, Zhang Z, Wen D. Effect of Al 2 O 3 nanoparticle dispersion on the specific heat capacity of a eutectic binary nitrate salt for solar power applications. Energy Convers Manag 2017;142:366–73. https://doi.org/10.1016/j.enconman.2017.03.062.
[646] Qiao G, Lasfargues M, Alexiadis A, Ding Y. Simulation and experimental study of the specific heat capacity of molten salt based nanofluids. Appl Therm Eng 2016;111:1517–22. https://doi.org/10.1016/j.applthermaleng.2016.07.159.
[647] Qiao G, Alexiadis A, Ding Y. Simulation study of anomalous thermal properties of molten nitrate salt. Powder Technol 2017;314:660–4. https://doi.org/10.1016/j.powtec.2016.11.019.
[648] Silakhori M, Jafarian M, Arjomandi M, Nathan GJ. Comparing the thermodynamic potential of alternative liquid metal oxides for the storage of solar thermal energy. Sol Energy 2017;157:251–8. https://doi.org/10.1016/j.solener.2017.08.039.
[649] Zhang Q, Liu J. Nano liquid metal as an emerging functional material in energy management, conversion and storage. Nano Energy 2013;2:863–72. https://doi.org/10.1016/J.NANOEN.2013.03.002.
[650] Valkenburg MEV, Vaughn RL, Williams M, Wilkes JS. Thermochemistry of ionic liquid heat-transfer fluids. Thermochim Acta 2005;425:181–8. https://doi.org/10.1016/J.TCA.2004.11.013.
[651] Nieto de Castro CA, Langa E, Morais AL, Lopes MLM, Lourenço MJV, Santos FJV, et al. Studies on the density, heat capacity, surface tension and infinite dilution diffusion with the ionic liquids [C4mim][NTf2], [C4mim][dca], [C2mim][EtOSO3] and [Aliquat][dca]. Fluid Phase Equil 2010;294:157–79. https://doi.org/10.1016/J.FLUID.2010.03.010.
[652] Shin D, Tiznobaik H, Banerjee D. Specific heat mechanism of molten salt nanofluids. Appl Phys Lett 2014;104:121914. https://doi.org/10.1063/1.4868254.
[653] Mehrkesh A, Karunanithi AT. Optimal design of ionic liquids for thermal energy storage. Comput Chem Eng 2016;93:402–12. https://doi.org/10.1016/j.compchemeng.2016.04.008.
[654] Jiang L, Bai L, Zhu J, Chen B. Thermodynamic properties of caprolactam ionic liquids. Chin J Chem Eng 2013;21:766–9. https://doi.org/10.1016/S1004-9541(13)60518-2.
[655] Wu B, Reddy R, R.R.-S. Engineering, U.. Novel ionic liquid thermal storage for solar thermal electric power systems. Proc Int Sol Energy Conf 2001;2001:445–51.
[656] Reddy RG, Zhang Z, Arenas MF, Blake DM. Thermal stability and corrosivity evaluations of ionic liquids as thermal energy storage media. High Temp Mater Process 2003;22:87–94. https://doi.org/10.1515/HTMP.2003.22.2.87.
[657] Li G. Sensible heat thermal storage energy and exergy performance evaluations. Renew Sustain Energy Rev 2016;53:897–923. https://doi.org/10.1016/j.rser.2015.09.006.
[658] Alva G, Lin Y, Fang G. An overview of thermal energy storage systems. Energy 2018;144:341–78. https://doi.org/10.1016/J.ENERGY.2017.12.037.
[659] Grirate H, Zari N, Elamrani I, Couturier R, Elmchaouri A, Belcadi S, et al. Characterization of several Moroccan rocks used as filler material for thermal energy storage in CSP power plants. Energy Proc 2014;49:810–9. https://doi.org/10.1016/J.EGYPRO.2014.03.088.
[660] Calvet N, Gomez JC, Faik A, Roddatis VV, Meffre A, Glatzmaier GC, et al. Compatibility of a post-industrial ceramic with nitrate molten salts for use as filler material in a thermocline storage system. Appl Energy 2013;109:387–93. https://doi.org/10.1016/J.APENERGY.2012.12.078.
[661] Xu Y, Chung DD. Cement of high specific heat and high thermal conductivity, obtained by using silane and silica fume as admixtures. Cement Concr Res 2000;30:1175–8. https://doi.org/10.1016/S0008-8846(00)00296-9.
[662] Khare S, Dell'Amico M, Knight C, McGarry S. Selection of materials for high temperature sensible energy storage. Sol Energy Mater Sol Cells 2013;115:114–22. https://doi.org/10.1016/j.solmat.2013.03.009.
[663] Navarro ME, Martínez M, Gil A, Fernández AI, Cabeza LF, Olives R, et al. Selection and characterization of recycled materials for sensible thermal energy storage. Sol Energy Mater Sol Cells 2012;107:131–5. https://doi.org/10.1016/j.solmat.2012.07.032.
[664] Laing D, Bauer T, Breidenbach N, Hachmann B, Johnson M. Development of high temperature phase-change-material storages. Appl Energy 2013;109:497–504. https://doi.org/10.1016/J.APENERGY.2012.11.063.
[665] Liu M, Saman W, Bruno F. Review on storage materials and thermal performance enhancement techniques for high temperature phase change thermal storage systems. Renew Sustain Energy Rev 2012;16:2118–32. https://doi.org/10.1016/j.rser.2012.01.020.
[666] Mehling H, Cabeza LF. Phase change materials and their basic properties BT. In: Paksoy HÖ, editor. Therm. Energy storage sustain. Energy consum. Dordrecht: Springer Netherlands; 2007. p. 257–77.
[667] Farid MM, Khudhair AM, Razack SAK, Al-Hallaj S. A review on phase change energy storage: materials and applications. Energy Convers Manag 2004;45:1597–615. https://doi.org/10.1016/j.enconman.2003.09.015.
[668] Sharma A, V Tyagi VV, Chen CRR, Buddhi D. Review on thermal energy storage with phase change materials and applications. Renew Sustain Energy Rev 2009;13:318–45. https://doi.org/10.1016/j.rser.2007.10.005.
[669] Agyenim F, Hewitt N, Eames P, Smyth M. A review of materials, heat transfer and phase change problem formulation for latent heat thermal energy storage systems (LHTESS). Renew Sustain Energy Rev 2010;14:615–28. https://doi.org/10.1016/j.rser.2009.10.015.
[670] Ge Z, Ye F, Ding Y. Composite materials for thermal energy storage : enhancing performance through microstructures. 2014. p. 1318–25. https://doi.org/10.1002/cssc.201300878.
[671] Lane GA, Glew DN, Clarke EC, Rossow HE, Quigley SW, Drake SS, et al. Heat of fusion systems for solar energy storage. In: Work. Sol. Energy storage subsystems heat. Cool. Build.; 1975. p. 43–55.
[672] Herrick CS, Golibersuch DC. Qualitative behavior of a new latent heat storage device for solar heating/cooling systems. General Electric Company Corporate Research and Development; 1977.
[673] Ge Z, Huang Y, Ding Y. Eutectic composition-dependence of latent heat of binary carbonates (Na2CO3/Li2CO3). Sol Energy Mater Sol Cells 2018;179:202–6. https://doi.org/10.1016/j.solmat.2017.11.015.
[674] Mohamed SA, Al-Sulaiman FA, Ibrahim NI, Zahir MH, Al-Ahmed A, Saidur R, et al. A review on current status and challenges of inorganic phase change materials for thermal energy storage systems. Renew Sustain Energy Rev 2017;70:1072–89. https://doi.org/10.1016/j.rser.2016.12.012.
[675] Gil A, Medrano M, Martorell I, Lázaro A, Dolado P, Zalba B, et al. State of the art on high temperature thermal energy storage for power generation. Part 1—concepts, materials and modellization. Renew Sustain Energy Rev 2010;14:31–55. https://doi.org/10.1016/j.rser.2009.07.035.
[676] H Abedin A, A Rosen M, Abedin A, Rosen M, Choi JC, Kim SD, et al. A critical review of thermochemical energy storage systems. Open Renew Energy J 2011;4:42–6. https://doi.org/10.2174/1876387101004010042.

[677] Rammelberg HU, Osterland T, Priehs B, Opel O, Ruck WKL. Thermochemical heat storage materials – performance of mixed salt hydrates. Sol Energy 2016;136:571–89. https://doi.org/10.1016/j.solener.2016.07.016.
[678] Chang MH, Huang CM, Liu WH, Chen WC, Cheng JY, Chen W, et al. Design and experimental investigation of calcium looping process for 3-kWth and 1.9-MWth facilities. Chem Eng Technol 2013;36:1525–32. https://doi.org/10.1002/ceat.201300081.
[679] Yu N, Wang RZZ, Wang LWW. Sorption thermal storage for solar energy. Pergamon; 2013.
[680] Scapino L, Zondag HA, Van Bael J, Diriken J, Rindt CCM. Sorption heat storage for long-term low-temperature applications: a review on the advancements at material and prototype scale. Appl Energy 2017;190:920–48. https://doi.org/10.1016/J.APENERGY.2016.12.148.
[681] Gaeini M, Rouws ALL, Salari JWOWO, Zondag HAA, Rindt CCMCM. Characterization of microencapsulated and impregnated porous host materials based on calcium chloride for thermochemical energy storage. Appl Energy 2018;212:1165–77. https://doi.org/10.1016/j.apenergy.2017.12.131.
[682] Cuypers R, de Jong AJ, Eversdijk J, Van 't Spijker H, Oversloot H, Ingenhut BLJ, et al. Microencapsulation of salts for enhanced thermochemical storage materials. 2013.
[683] T. (SE); D. Göran Bolin, K. (SE) Glebov. Salt coated with nanoparticles. 2016. US 9.459,026 B2.
[684] Aneke M, Wang M. Energy storage technologies and real life applications – a state of the art review. Appl Energy 2016;179:350–77. https://doi.org/10.1016/j.apenergy.2016.06.097.
[685] Badescu V. Optimal control of flow in solar collector systems with fully mixed water storage tanks. Energy Convers Manag 2008;49:169–84. https://doi.org/10.1016/j.enconman.2007.06.022.
[686] Badescu V, Budea S, Paulescu M. Empirical versus optimal control of flow in solar domestic hot water systems. J Energy Eng 2016;142. 10.1061/.
[687] Ntsaluba S, Zhu B, Xia X. Optimal flow control of a forced circulation solar water heating system with energy storage units and connecting pipes. Renew Energy 2016;89:108–24. https://doi.org/10.1016/j.renene.2015.11.047.
[688] Kovarik M, Lesse PF. Optimal control of flow in low temperature solar heat collector. Sol Energy 1976;18:431–5. https://doi.org/10.1016/0038-092X(76)90009-8.
[689] Buzás J, Kicsiny R. Transfer functions of solar collectors for dynamical analysis and control design. Renew Energy 2014;68:146–55. https://doi.org/10.1016/j.renene.2014.01.037.
[690] Correa-Jullian C, López Droguett E, Cardemil JM. Operation scheduling in a solar thermal system: a reinforcement learning-based framework. Appl Energy 2020;268:114943. https://doi.org/10.1016/j.apenergy.2020.114943.
[691] Dyson MEH, Borgeson SD, Tabone MD, Callaway DS. Using smart meter data to estimate demand response potential, with application to solar energy integration. Energy Pol 2014;73:607–19. https://doi.org/10.1016/j.enpol.2014.05.053.
[692] Cabeza LF. Advances in thermal energy storage systems: methods and applications. Woodhead Publishing; 2014.
[693] DNV-GL, NERA Economic Consulting. Imperial College London, integration of renewable energy in Europe - final report. 2014.
[694] Jossen A, Garche J, Sauer DU. Operation conditions of batteries in PV applications. Sol Energy 2004;76:759–69. https://doi.org/10.1016/j.solener.2003.12.013.
[695] Parra D, Walker GS, Gillott M. Modeling of PV generation, battery and hydrogen storage to investigate the benefits of energy storage for single dwelling. Sustain Cities Soc 2014;10:1–10. https://doi.org/10.1016/j.scs.2013.04.006.
[696] Puranen P, Kosonen A, Ahola J. Technical feasibility evaluation of a solar PV based off-grid domestic energy system with battery and hydrogen energy storage in northern climates. Sol Energy 2021;213:246–59. https://doi.org/10.1016/j.solener.2020.10.089.
[697] Lokar J, Virtič P. The potential for integration of hydrogen for complete energy self-sufficiency in residential buildings with photovoltaic and battery storage systems. Int J Hydrogen Energy 2020;5. https://doi.org/10.1016/j.ijhydene.2020.04.170.
[698] Bocklisch T, Böttiger M, Paulitschke M. Multi-storage hybrid system approach and experimental investigations. Energy Proc 2014;46:186–93. https://doi.org/10.1016/j.egypro.2014.01.172.
[699] Duffner F, Wentker M, Greenwood M, Leker J. Battery cost modeling: a review and directions for future research. Renew Sustain Energy Rev 2020;127:109872. https://doi.org/10.1016/j.rser.2020.109872.
[700] IRENA. Electricity storage and renewables: costs and markets to 2030. 2017.
[701] Nair N-KC, Garimella N. Battery energy storage systems: assessment for small-scale renewable energy integration. Energy Build 2010;42:2124–30. https://doi.org/10.1016/j.enbuild.2010.07.002.
[702] International Energy Agency. Energy technology perspectives 2020. 2020.
[703] Rogelj J, Den Elzen M, Höhne N, Fransen T, Fekete H, Winkler H, et al. Paris Agreement climate proposals need a boost to keep warming well below 2 °c. Nature 2016;534:631–9. https://doi.org/10.1038/nature18307.
[704] Bany Mousa O, Kara S, Taylor RA. Comparative energy and greenhouse gas assessment of industrial rooftop-integrated PV and solar thermal collectors. Appl Energy 2019;241:113–23. https://doi.org/10.1016/j.apenergy.2019.03.052.
[705] Panwar NL, Kaushik SC, Surendra K. Role of renewable energy sources in environmental protection: a review. Renew Sustain Energy Rev 2011;15:1513–24. https://doi.org/10.1016/J.RSER.2010.11.037.
[706] Alola AA, Yalçiner K, Alola UV, Saint Akadiri S. The role of renewable energy, immigration and real income in environmental sustainability target. Evidence from Europe largest states. Sci Total Environ 2019;674:307–15. https://doi.org/10.1016/j.scitotenv.2019.04.163.
[707] Ivanova D, Barrett J, Wiedenhofer D, Macura B, Callaghan M, Creutzig F. Quantifying the potential for climate change mitigation of consumption options. Environ Res Lett 2020;15. https://doi.org/10.1088/1748-9326/ab8589.
[708] Creutzig F, Agoston P, Goldschmidt JC, Luderer G, Nemet G, Pietzcker RC. The underestimated potential of solar energy to mitigate climate change. Nat Energy 2017;2. https://doi.org/10.1038/nenergy.2017.140.
[709] Nelson J, Gambhir A, Ekins-Daukes N. Solar power for CO2 mitigation. Grantham Inst Clim Change Brief Pap 2014;11:1–16.
[710] Mousa OB, Taylor RA. Global solar technology optimization for factory rooftop emissions mitigation. Environ Res Lett 2020;15. https://doi.org/10.1088/1748-9326/ab702a.
[711] Briner C. The climate change mitigation potential of the solar PV industry: a life cycle perspective. Imperial College London; 2019.
[712] Finnegan S, Jones C, Sharples S. The embodied CO2e of sustainable energy technologies used in buildings: a review article. Energy Build 2018;181:50–61. https://doi.org/10.1016/j.enbuild.2018.09.037.
[713] Osama BM, Robert A. Global embodied emissions assessment of locally manufactured solar technologies global embodied emissions assessment of locally manufactured solar technologies. 2019.
[714] Caldera U, Breyer C. Learning curve for seawater reverse osmosis desalination plants: capital cost trend of the past, present, and future. Water Resour Res 2017;53:10523–38. https://doi.org/10.1002/2017WR021402.
[715] OECD. Investing in climate, investing in growth: a synthesis. 2017. Paris.
[716] International Renewable Energy Agency. Global energy transformation: a roadmap to 2050. 2019.



Name: Professor Christos N. Markides, BA (Hons), MEng, MA, PhD

Affiliation: Professor of Clean Energy Technologies and Head of the Clean Energy Processes (CEP) Laboratory, Imperial College London (UK)

Other roles: Co-Founder and Director of PV-T spin-out company www.solar-flow.co.uk

Editor-in-Chief Applied Thermal Engineering (Elsevier)

Contact details: Email: c.markides@imperial.ac.uk

Web: www.imperial.ac.uk/people/c.markides, www.imperial.ac.uk/cep

Expertise: His research involves fundamental aspects of thermodynamics, fluid flow, heat and mass transfer processes and their applications in a range of components, devices, technologies and systems for energy recovery, conversion and storage, with a particular focus on solar energy and waste heat recovery and utilization. His research covers theoretical, experimental and modelling approaches and the full range of scales from molecules to systems.

Publication record:
h-index (Scopus): 50
Number of citations (Scopus): 7800
Number of publications (Scopus): 302
Google Scholar: https://scholar.google.es/citations?user=YYJ0NjwAAAAJ&hl=en
Scopus ID: 8287822500
ORCID: http://orcid.org/0000-0002-4219-1867



Name: Dr. María Herrando

Affiliation: Project Manager and Juan de la Cierva Fellow at the Aragon Institute of Technology (ITAINNOVA), Zaragoza (Spain)

Other roles: Visiting Researcher at the Clean Energy Processes (CEP) Laboratory, Imperial College London (UK)

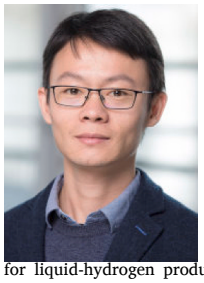
Member of "*Task 60: PVT Systems: Application of PVT Collectors and New Solutions in HVAC Systems*" of the International Energy Agency (IEA), SHC programme

Contact details: Email: mherrando@itainnova.es, mherrando@unizar.es, maria.herrando11@imperial.ac.uk

Web: www.researchgate.net/profile/Maria_Herrando

Expertise: Her research involves the development and validation of models for multi-physics systems and energy efficiency simulation, as well as cost analyses and techcnoeconomic optimization of energy systems. She specializes in modelling, design and outdoor testing of solar hybrid PV-T collectors, as well as in modelling and designing wider solar energy systems for heat, power and/or cooling provision.

Publication record
h-index (Scopus): 12
Number of citations (Scopus): 937
Number of publications (Scopus): 21
Google Scholar: https://scholar.google.es/citations?user=A-L-qA8AAAAJ&hl=en
Scopus ID: 56060197900
ORCID: http://orcid.org/0000-0002-0787-8938



Name: Dr. Kai Wang

Affiliation: Research Professor at the Institute of Refrigeration and Cryogenics, Zhejiang University (China)

Other roles: Visiting Researcher at the Clean Energy Processes (CEP) Laboratory, Imperial College London (UK)

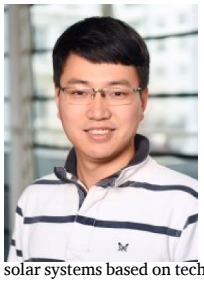
Managing Editor Applied Thermal Engineering (Elsevier)

Contact details: Email: kaiwang19@zju.edu.cn, kai.wang@imperial.ac.uk

Web: www.researchgate.net/profile/Kai_Wang73, https://person.zju.edu.cn/en/kaiwang

Expertise: His research interests focus primarily on high-performance energy technologies, components and systems for liquid-hydrogen production, storage and refuelling, organic Rankine cycles, solar thermal technologies thermoacoustic power generators/coolers, Stirling engines, and co-/trigeneration systems.

Publication record:
h-index (Scopus): 16
Number of citations (Scopus): 1036
Number of publications (Scopus): 60
Google Scholar: https://scholar.google.es/citations?user=GfagTgEAAAAJ&hl=en
Scopus ID: 55547129839
ORCID: https://orcid.org/0000-0002-0581-3858



Name: Dr. Gan Huang

Affiliation: Research group leader at the Institute of Microstructure Technology, Karlsruhe Institute of Technology (Germany)

Other roles: Honorary Research Fellow at the Department of Chemical Engineering, Imperial College London (UK)

Contact details: Email: gan.huang@kit.edu, g.huang@imperial.ac.uk

Web: https://www.imt.kit.edu/1350_3130.php, www.imperial.ac.uk/people/g.huang

Expertise: His current research focusses on next-generation solar technologies, specifically the development of hybrid PV-T solar systems based on technologies of spectral splitting, emissivity control, thin-film semi-transparent solar cells, biomimetic hydrogel, nanofluids, etc., aiming at harvesting solar energy to simultaneously generate electricity and high-temperature heat energy with high efficiencies and low costs

Publication record:
h-index (Scopus): 13
Number of citations (Scopus): 465
Number of publications (Scopus): 34
Google Scholar: https://scholar.google.com/citations?user=FJA6aD4AAAAJ&hl=en
Scopus ID: 57192420291
ORCID: https://orcid.org/0000-0001-7043-8516



kalogirou/?languageId=1

Name: Professor Soteris Kalogirou

Affiliation: Professor at the Department of Mechanical Engineering and Materials Science and Engineering, Cyprus University of Technology (Cyprus)

Other roles: Founding Member of the Cyprus Academy of Sciences, Letters, and Arts

Fellow of the European Academy of Sciences

Member of ISES (International Solar Energy Society)

Editor-in-ChiefRenewable Energy (Elsevier)

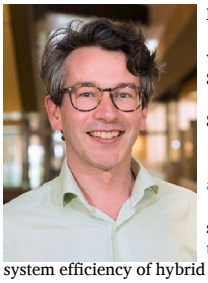
Deputy Editor-in-Chief Energy (Elsevier)

Contact details: Email: soteris.kalogirou@cut.ac.cy

Web: www.cut.ac.cy/faculties/fet/mem/staff/soteris.

Expertise: He is considered an international expert in the field of solar thermal collectors, hybrid PV-T systems and the use of artificial intelligence techniques for the performance prediction of energy and renewable energy systems.

Publication record:
h-index (Scopus): 67
Number of citations (Sc opus): 18600
Number of publications (Scopus): 232
Google Scholar: https://scholar.google.co.uk/citations?user=UNOpofUAAAAJ&hl=en
Scopus ID: 7005998383
ORCID: http://orcid.org/0000-0002-4497-0602



Name: Dr. Ned Ekins-Daukes

Affiliation: Associate Professor in the School of Photovoltaic and Renewable Energy Engineering, University of New South Wales (Australia)

Other roles: Academic Visitor at the Faculty of Natural Sciences, Department of Physics, Imperial College London (UK)

Contact details: Email: nekins@unsw.edu.au

Web: www.qpvgroup.org/ned-ekinsdaukes, https://research.unsw.edu.au/people/associate-professor-nj-ekins-daukes

Expertise: His research aims at increasing the efficiency of solar power conversion, both in terms of improving the electrical efficiency of photovoltaic solar cells and increasing the system efficiency of hybrid PV-T systems. His scientific interests start with the conceptual thermodynamic basis for solar power conversion and continue through to practical demonstration.

Publication record:
h-index (Scopus): 39
Number of citations (Sc opus): 5293
Number of publications (Scopus): 229
Google Scholar: https://scholar.google.co.uk/citations?user=Fd2Y6s8AAAAJ&hl=en
Scopus ID: 6603934588
ORCID: http://orcid.org/0000-0003-1875-9739



-professor-robert-taylor

Name: Associate Professor Robert A. Taylor

Affiliation: Associate Professor in the School of Mechanical and Manufacturing Engineering and in the School of Photovoltaic and Renewable Energy Engineering, University of New South Wales (Australia)

Other Roles: Managing director of Solar and Thermal Energy Solutions

Joint Operating Agent of an IEA Solar Heating and Cooling TCP Task

Editorial Board at Thermopedia

Contact details: Email: robert.taylor@unsw.edu.au

Web: https://research.unsw.edu.au/people/associate

Expertise: His main research aim is to use fundamental knowledge of heat transfer, fluid mechanics, nanotechnology, and thermodynamics to develop new solar energy collectors, compact thermal storage systems, solar concentrators, and high temperature thermal energy systems. He has conducted seminal work on beam splitting nanofluid collector systems and on next-generation, high temperature solar collectors.

Publication record:
h-index (Scopus): 47
Number of citations (Sc opus): 8395
Number of publications (Scopus): 230
Google Scholar: https://scholar.google.com/citations?user=PspJFyoAAAAJ&hl=en
Scopus ID: 55547114594
ORCID: http://orcid.org/0000-0002-1723-3172



Name: Dr. Todd Otanicar, PE

Affiliation: Chair and Associate Professor of Mechanical and Biomedical Engineering, Boise State University (US)

Contact details: Email: toddotanicar@boisestate.edu

Web: www.boisestate.edu/coen-mbe/directory/todd-otanicar

Other roles: Member of Scientific Council International Centre for Heat and Mass Transfer

Co-founder and Chief Scientist, Exaeris Water Innovations LLC

Expertise: His research involves nanoscale heat and energy transport with a particular emphasis on application to energy generation, utilization, and storage. He is one of the leading researchers in the field of nanoparticles for solar thermal energy applications and pioneered the idea of using nanoparticle as spectrally selective absorbers for hybrid solar thermal/photovoltaic systems. Recent efforts have focussed on the advancement of solid particles for use in the concentrating solar power industry.

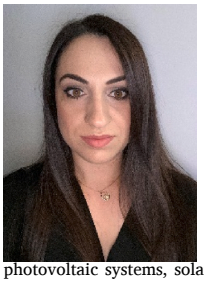
Publication record:
h-index (Scopus): 30
Number of citations (Sc opus): 4154
Number of publications (Scopus): 94
Google Scholar: https://scholar.google.com/citations?user=LdpgdzQAAAAJ&hl=en
Scopus ID: 25960294200
ORCID: http://orcid.org/0000-0002-4579-6183



Name: Professor Yulong Ding FREng FIChemE FRSC
Affiliation: Founding Chamberlian Professor of Chemical Engineering and Director of the Birmingham Centre for Energy Storage, University of Birmingham (UK)
Other roles: Principle Investigator of the Supergen Storage Network Plus (>20 UK investigators)
Member of Net Zero Carbon Panel of The Royal Society
Associate Editor of Energy Storage and Saving (Elsevier)
Associate Editor of Discovery Energy (Springer Nature)
Contact details: Email: y.ding@bham.ac.uk
Web: www.birmingham.ac.uk/staff/profiles/eps/yulong-ding.aspx

Expertise: His research involves energy materials and processes, and currently focusses on developing novel technologies for electrical and thermal energy storage at different scales. He invented liquid air energy storage technology (commercialized by Highview Power), developed composite phase change materials for thermal energy storage and associated large-scale manufacture technologies (currently in large scale commercial applications with a total installation of >300 MW / >1.2 GWh so far), and developed passively cooled container technology (currently on large scale commercial demonstration for cold chain transportation applications).

Publication record:
h-index (Scopus): 61
Number of citations (Sc opus): 20580
Number of publications (Scopus): 455
Google Scholar: https://scholar.google.com/citations?user=p1rD-B0AAAAJ&hl=en
Scopus ID: 26643310400
ORCID: https://orcid.org/0000-0002-7159-5107



Name: Dr. Rafaela Agathokleous
Affiliation: Postdoctoral Research Associate at the Department of Mechanical Engineering and Materials Science Engineering, Cyprus University of Technology (Cyprus)
Other roles: Assistant Editor Energy (Elsevier)
Contact details: Email: rafaela.agathokleous@cut.ac.cy
Web: www.researchgate.net/profile/Rafaela-Agathokleous

Expertise: Her research involves experiments and simulation modelling of the thermal and electrical behaviour of solar energy technologies. She specializes in dynamic and CFD modelling, design, and outdoor testing of building integrated photovoltaic systems, solar collectors for domestic hot water and photovoltaic thermal collectors. She is also specialized in indoor laboratory testing of solar energy technologies with the use of a large scale solar simulator in controlled environmental conditions.

Publication record:
h-index (Scopus): 10
Number of citations (Scopus): 428
Number of publications (Scopus): 23
Google Scholar: https://scholar.google.com/citations?user=Rt8qtuYAAAAJ&hl=en
Scopus ID: 55552252200
ORCID: https://orcid.org/0000-0003-2908-7595



Name: Dr. Osama Bany Mousa
Affiliation: Postdoctoral Research Associate at the School of Mechanical and Manufacturing Engineering, University of New South Wales (Australia)
Other Roles: Joint researcher at IEA Solar Heating and Cooling TCP Task
Contact details: Email: o.banymousa@outlook.com, o.banymousa@unsw.edu.au
Web: www.researchgate.net/profile/Osama-Bany-Mousa-2

Expertise: His research focusses mainly on solar technologies and best practices to exploit solar energy effectively and to enhance overall performance. He is also interested in carbon emission mitigation and how solar energy can help achieve future global emissions targets.

Publication record: h-index (Scopus): 4
Number of citations (Sc opus): 84
Number of publications (Scopus): 4
Google Scholar: https://scholar.google.com.au/citations?user=Ge6P_qwAAAAJ&hl=en
Scopus ID: 57193000434
ORCID: https://orcid.org/0000-0002-1987-2891